INFORMATION TO USERS

This manuscript has been reproduced from the microfilm master. UMI films the text directly from the original or copy submitted. Thus, some thesis and dissertation copies are in typewriter face, while others may be from any type of computer printer.

The quality of this reproduction is dependent upon the quality of the copy submitted. Broken or indistinct print, colored or poor quality illustrations and photographs, print bleedthrough, substandard margins, and improper alignment can adversely affect reproduction.

In the unlikely event that the author did not send UMI a complete manuscript and there are missing pages, these will be noted. Also, if unauthorized copyright material had to be removed, a note will indicate the deletion.

Oversize materials (e.g., maps, drawings, charts) are reproduced by sectioning the original, beginning at the upper left-hand corner and continuing from left to right in equal sections with small overlaps. Each original is also photographed in one exposure and is included in reduced form at the back of the book.

Photographs included in the original manuscript have been reproduced xerographically in this copy. Higher quality 6" x 9" black and white photographic prints are available for any photographs or illustrations appearing in this copy for an additional charge. Contact UMI directly to order.

UMI

A Bell & Howell Information Company
300 North Zeeb Road, Ann Arbor MI 48106-1346 USA
313/761-4700 800/521-0600

FLOW CELLS TO MEASURE ELECTRICAL CONDUCTIVITY: USE IN ESTIMATING GAS HOLDUP IN FLOTATION SYSTEMS.

Francisco Javier Tavera Miranda.

Department of Mining and Metallurgical Engineering
McGill University
November 1996

A Thesis submitted to the
Faculty of Graduate Studies and Research
in partial fulfillment of the requirements for
the degree of
Doctor of Philosophy

This thesis is dedicated to my dear wife Irma,
and my daughters Luz Elisa, Irma Carolina, Adriana, and Ana Cristina,
whose patience made it possible to me to go back to school.

I. ABSTRACT

This thesis has focused on the measurement of gas holdup in flotation systems, a variable not measured reliably to date.

A sensor was designed using so-called flow conductivity cells. Their properties were studied and modelled, and their application in the design, construction, and operation of a gas holdup probe for use in flotation systems described.

A flow cell is defined as one that allows a fluid or dispersion to flow through freely while the electrical conductivity is measured. One of the most important features of a flow cell is the so-called cell constant. Once the cell constant is determined, the cell can be used to measure liquid and dispersion conductivity. The cell constant depends mainly on cell dimensions, and is largely independent of the characteristics of the fluid.

The addition of non conductive bodies to the fluid was studied. It was concluded that the cell constant is not affected by the presence of such bodies. These systems are described by Maxwell's model, which relates the fraction of non conductive phase (holdup) in the system to the conductivity of the continuous phase and the conductivity of the dispersion.

It was demonstrated that the electromagnetic field associated with the flow cells can be solved using the MagNet 5.1 software. Predicted results for cell constant were in good agreement with the experimental. The model holds the potential for design of flow cells for particular applications in mineral processing.

The gas holdup probe developed in this work applies the principle of separation of phases to fulfil the requirements of Maxwell's model. The probe consists of two flow cells. One, the open flow cell, measures the conductivity of the dispersion while the other, the syphon cell, measures the continuum conductivity.

The test work, in both laboratory and industrial flotation columns, demonstrated that the probe gave accurate estimates of gas holdup. The probe satisfied the requirements of an industrial sensor, as it performs in-situ, on-line, in real-time, with no external measurements and no assumptions regarding properties of any phase.

The gas holdup probe was used to explore operating flotation columns. It appears to hold

great promise for diagnosis, readily detecting, for example, differences in gas holdup between sections of baffled columns.

This success may make the probe a candidate sensor for process control, although this will require a significant in-plant effort to realize. As a first step, the probe offers an opportunity to study the relationship between gas holdup and metallurgy, at least in flotation columns.

II. RÉSUMÉ

Cette thèse traite de la charge en gaz des systèmes de flottation, une variable imprécise à date.

Un senseur fut conçu en utilisant ce que l'on appelle des cellules de conductivité. Leurs propriétés furent étudiées et modélisées. On y décrit aussi la planification, la construction et l'utilisation d'une sonde de mesure de charge gazeuse pouvant être utilisée dans des systèmes de flottation.

Une cellule de débit est une cellule qui permet une libre circulation d'un fluide ou d'une dispersion tout en en mesurant la conductivité électrique. La constante de la cellule est une des ses caractéristiques les plus importantes. Une fois cette constante définie, la cellule peut être utilisée pour mesurer la conductivité de fluides et de dispersions. La constante de la cellule ne dépend que de sa dimension et est pratiquement indépendante des caractéristiques du fluide.

On a étudié l'effet de l'addition de corps non conducteurs au système. On en conclu que la constante de la cellule n'est pas affectée par la présence de ces corps. Ces systèmes sont décrits par le modèle de Maxwell qui établit une relation entre: la fraction de la phase non conductive (charge) dans le système à la conductivité de la phase continue et la conductivité de la dispersion.

On y a démontré que le champ électomagnetique associé aux cellules de débit peut être résolu en utilisant le programme pour ordinateur MagNet 5.1. Les valeurs théoriques de la constante de la cellule furent en assez bon accord avec les valeurs mesurées. Le modèle démontre un certain potentiel pour la fabrication de cellules de débit ayant des applications précises pour le traitement des minerais.

La sonde de retenue de charge gazeuse, mise au point par ce travail, met en pratique le principe de séparations des phases pour satisfaire les exigences du modèle de Maxwell. La sonde est faite de deux cellules de débit. L'une, la cellule de débit ouvert, mesure la conductivité de la dispersion tandis que l'autre, la cellule siphon, mesure la conductivité du continuum.

Les tests, utilisant des colonnes de flottation en laboratoire et en usine, démontre que la sonde donne des évaluations précises de la charge gazeuse. La sonde satisfait les exigences d'un capteur industriel parce qu'elle fonctionne in-situ, en direct, en temps réel, sans nécessiter de mesures externes ni de suppositions en ce qui a trait aux propriétés des phases présentes.

On a utilisé la sonde de mesure de charge gazeuse pour explorer des colonnes de flottation

en opération. Elle semble prometteuse, par exemple, pour le diagnostic des variables de charge gazeuse entre deux sections d'une colonne compartimentée.

Ce succès pourrait faire de la sonde un capteur potentiel en contrôle de procédés quoique ceci nécessitera un effort significatif en usine pour le réaliser. Comme première étape, la sonde offre l'opportunité d'étudier la relation entre charge gazeuse et métallurgie, du moins pour les colonnes de flottation.

III. RESUMEN

Esta tésis se ha enfocado a la medición de la fracción de gas en sistemas de flotación, la cual es una variable no medida hasta ahora.

Se diseñó un sensor que emplea celdas de flujo de conductividad. Sus propiedades se estudiaron y modelaron, y se describe sus aplicaciones en el diseño, construcción y operación de una sonda de fracción de gas para uso en sistemas de flotación.

Se define como celda de flujo a aquella que permite que un fluido, o una dispersión, fluya libremente a través de ella mientras que se mide su conductividad eléctrica. Una de las características más importantes de una celda de flujo es la constante de celda. Una vez que se determina la constante de celda, la celda se puede usar para medir la conductividad de un líquido o una dispersión. La constante de celda depende principalmente de las dimensiones de la celda, y es independiente de las características del fluido.

La adición de cuerpos no conductores en el fluido se estudió experimentalmente. Se concluye que la constante de celda no es afectada por la presencia de tales cuerpos. El modelo de Maxwell describe estos sistemas; el modelo relaciona la fracción de la fase no conductora en el sistema con la conductividad de la fase contínua y la conductividad de la dispersión.

Se demostró que el campo electromagnético asociado con las celdas de flujo se puede resolver usando el programa MagNet 5.1. Los resultados de la constante de celda previstos por el programa están de acuerdo con esos medidos experimentalmente. El modelo tiene el potencial para el diseño de celdas de flujo para aplicaciones particulares en procesamiento de minerales.

La sonda de fracción de gas desarrollada en este trabajo aplica el principio de separación de fases para satisfacer los requisitos del modelo de Maxwell. La sonda consiste de dos celdas de flujo. Una de las celdas, llamada celda de flujo abierta, mide la conductividad de la dispersión, mientras que la otra celda, llamada celda sifón, mide la conductividad del continuum.

El trabajo de prueba, en columnas de flotación de laboratorio e industriales, demostró que la sonda da estimaciones precisas de fracción de gas. La sonda satisface los requisitos de un sensor industrial, ya que trabaja in situ, en línea, en tiempo real, sin mediciones externas y sin suposiciones sobre las propiedades de cualquier fase.

La sonda de fracción de gas se usó para explorar la operación de columnas de flotación. La sonda muestra un gran futuro para trabajo de diagnóstico, por ejemplo, detectando de manera veráz diferencias en la fracción de gas entre las secciones de columnas con bafles instalados.

Este éxito podría hacer de la sonda un candidato a sensor para control automático de procesos, aún cuando esto requiera realizar un esfuerzo significante de trabajo en planta. Como primer paso, la sonda ofrece una oportunidad para estudiar la relación entre la fracción de gas y la metalurgia, al menos en columnas de flotación.

IV. ACKNOWLEDGEMENTS

I am indebted specially to two people: Prof. J.A. Finch for his advise, enthusiasm, keen interest and constant support throughout the research program, and Dr. C.O. Gomez for his friendship, his invaluable input and criticism to this work, and for making the most pleasant working atmosphere.

I am also indebted to Dr. S.R. Rao and Prof. Z. Xu for their interest and encouragement throughout this project.

As well, I want to thank all members of the Department of Mining and Metallurgical Engineering, and specially Mr. R. Escudero, Mrs. Y. Shang and Dr. G. Shen for their comradeship, and Mr. M. Knoepfel and Mr. J. Boka for their help in the workshop, and Mr. E. Schneyrinkov for his help in building the electronic systems and during plant experiments. I am also indebted to all my colleagues in the mineral processing group.

I want to express my gratitude to Mr. R. Agnew for his constant support during the plant tests and all the staff and workers of the Matte Separation Plant, INCO Ltd.

V. CONTENTS

VI. LIST OF FIGURES

VII. LIST OF TABLES

VII. LIST OF APPENDICES

CHAPTER 1

INTRODUCTION

Mineral processing systems comprise multiphase dispersions, where the interaction among the phases partly determines process efficiency; therefore, it is important to know the amount, or at least the proportion, of the phases involved in a process.

Mineral processing systems, as in the case of flotation, thickening, filtering, drying, conditioning, fluidisation, conveying, classifying, among others, would benefit from process models. These models can be developed only if the necessary information is available. This information includes: concentration and concentration profiles of the phases, the concentration of components (elements) in those phases, the phase flow rates, and the dispersed phase size distributions. To gather the information requires sensors.

The measurements ideally should be carried out:

- on-line, in-situ,
- with no interruption of the system, nor disturbance of the flow patterns,
- in real-time and,
- with no assumptions regarding properties of any phase,
- or use of measurements external to the system.

Sensors which fulfil these requirements have, to a large degree, still to be developed for mineral processing systems. Some innovative sensing methods are described. Then attention is focussed on measurement of phase, in particular gas, holdup.

Neutron activation technique

Neutron activation (NA) is applied to the analysis of low atomic number elements, which is an advantage over the use of X-rays. The elements that can be analysed include: silicon, aluminium, calcium, magnesium, sodium, hydrogen, phosphorus, fluorine, sulphur, and chlorine.

A portable NA probe was developed and tested in flotation cells [Moudgil et al., 1993]. The

standard deviation of the analysis for calcium and silicon was 0.2% and 0.8% in concentrate, 0.14% and 0.57% in feed, and 0.2% and 0.8% in tailings, respectively. It is claimed that the probe is easy to operate and requires almost no maintenance. No sampling system is involved and the probe can be directly placed in the feed conditioner, tailings and concentrate tanks. It is harmless to the environment. The half live of the elements excited by the neutron source are only a few minutes, therefore, the material does not remain radioactive long after the detection. Also, it was pointed out that the reliability and precision of the probe can be improved by using a high purity germanium detector and a stronger neutron source.

X-ray scattering, X-ray fluorescence, γ-ray absorption

On-line coal slurry ash analysers have been developed using these phenomena [Kawatra, 1993; Watt and Sowerby,1983]. In one case, the instrument determines ash content from measurements of X-ray backscatter, iron K_α fluorescence, and low energy γ-ray absorption. In the results from tests on fine coal slurries, the standard error was 0.72% in a range of composition from 5 to 45% ash.

In this instrument the measurements are made in two stages. The ash sensor uses an annular Cm-244 source and proportional counter to measure backscattered and iron K_α fluorescence X-rays, and a γ-ray transmission cell to sense changes in slurry density using a Gd-153 source and a scintillation detector.

Potentiometric, voltammetric and spectrophotometric sensors

Ultra-violet (UV)-spectroscopic detectors are promising for continuous analysis of flotation pulps. Sensitivity and detection limits depend on the species being detected. With the aid of diode array detectors, a complete spectra in the wavelength (190-800 nm) can be obtained in less than 1/10th of a second. The use for determination of flotation reagents was demonstrated by Jones and Woodcock [1976]. The main limitation of spectroscopic methods is the interference from small amounts of solid particles. This limitation can be overcome, if an automatic system is developed to correct the background absorbance resulting from interference by particles.

Several types of potentiometric methods are used in mineral flotation systems, including: pH electrodes, ion selective electrodes [Lord and Markovic, 1970; Khan and Frolov, 1985], and Eh electrodes for measurements of redox potential [Labonté and Finch, 1989]. Eh measurements in flotation systems are commonly made with a noble metal (Au, Pt) or mineral as the sensing electrode. Potentiometric detectors can be directly used in flotation pulps. Since the redox potential established at the mineral/solution interface is one of the most important parameters controlling flotation, the use of electrodes made from the minerals being floated is attractive; however, a mineral electrode requires more frequent cleaning than metal electrodes due to formation of passivation films on their surface [Gebhardt and Shedd, 1988].

A voltammetric method for detection of xanthate in solution has been proposed by Heimala et al., [1985]. The major advantages of voltammetric detectors are: they can be used for in-stream analysis of flotation pulps, response time is short, the detector can be cleaned directly in the stream, and interference with other species can be reduced to a minimum. These detectors can be used for analysis of complex species and for analysis of multi-component solutions; they are suitable for analysis of multi-redox species.

Tomographic sensing

Williams (1995) recently reviewed tomographic sensing techniques as applied in mineral processing. Tomography provides a means for probing the internal characteristics of a dispersion. The technique provides cross sectional imaging of the contents through one or several planes along a reaction vessel or pipe by using sensors located on the periphery.

Different sensing principles can be applied depending upon the physicochemical characteristics of the dispersion, and from the spatial resolution and image rate required. In general, methods that provide high spatial resolution ($<<$ 5 mm) are slow (less than one frame per minute). Process tomography for on-line measurements requires rapid acquisition of images. In process control applications, data have to be reconstructed and analysed within minutes.

Tomographic techniques can be divided as follows: nucleonic (slow), optical, acoustic, resonance, and electrical. In mineral processing systems electrical resistance tomography (ERT) and

electrical capacitance tomography (ECT) have been applied most frequently.

ERT exploits the dependence of slurry electrical conductivity on the volume fraction of the less conductive phase in two-phase dispersions. This method presents a coarse spatial resolution which cannot detect small individual non conductive phase volumes. ERT has been applied to quantify mixing in different agitated processes, i.e. conditioners, hydrocyclones, and flotation systems, because of the fast measurement and image reconstruction capability [Dicking et al., 1993; Williams et al., 1995 (a) and (b)].

ECT uses the change in dielectric constant to create images in different regions of a system (e.g. a hydrocyclone) to distinguish different types of flow patterns; these images can be obtained at a rate of up to 100 frames per second, which makes it possible to detect oscillations in the flow patterns. This technique has been used to image multiphase-discharge from pressurised vessels [Xie et al., 1995]. ECT can be used to identify flow regimes inside conveying lines for both dilute and dense phase processes [McKee et al., 1995]. Fluidised bed reactors have been monitored with ECT to follow the dynamic interactions between gas and solids under different process conditions [Williams, 1995].

Table 1.1. summarizes the tomographic techniques and their typical industrial applications. Tomographic techniques are expensive and that has restricted their spread as a tool for sensing industrial systems. However, generalised use of these techniques in the near future is predicted.

Holdup measurements

Besides tomographic techniques to determine holdup in multiphase systems (specifically in mineral processing), which are restricted because of cost, other techniques for holdup measurements in mineral processing have been used in laboratory and plant operations. The most relevant methods are presented in the following sections.

Table 1.1. Tomographic techniques for sensing mineral processes [Williams, R.A.,1995].

Tomographic technique	Image reconstruction	Typical ind. application
nucleonic transmision: photon, neutron	direct method: Fourier inversion, filtered back-projection iterative method: algebraic reconstruction (ART)	multiphase flow imaging fluidised bed imaging
nucleonic emission: single photon; positron	positron emision: direct method	nuclear industry particulate flow imaging
nucleonic scattering	solve matrix equation	imaging volume fraction profile of gas-liquid flow
optical transmission	similar to nucleonic transm.	flow study and combustion
optical emission (infrared)	filtered backprojection	temperature imaging; plasma
optical interferometric	ART; series expansion	temperature-flow imaging; mixing
acoustic transmission	similar to nucleonic transm.	bubbly flow imaging
acoustic reflection	back projection	two-phase flow
acoustic time-of-flight (TOF)	back proj.; series expan.; ART; transform methods	imaging: flow void, furnace temp., flow velocity
acoustic diffraction	Fourier inversion	fluid study
microwave diffraction	Fourier inversion	remote thermal sensing
NMR	Fourier inversion	flow velocity imaging
electrical capacitance	backprojection	two-phase flow; fluidised bed
electrical resistivity	filtered backprojection	imaging: hydrocyclone, mixing, geophysics
electrical impedance	back projection	new technique

Pressure method

Measurements of static pressure can be used to estimate holdup. For example, gas holdup in air-water systems is often calculated from pressure measurements taken at two or more locations along the vessel. In a three phase system, the calculation requires the density of the water-solid dispersion [Fan, 1989; Finch and Dobby, 1990]. Gas holdup measurements in laboratory [Banisi et al., 1994; Uribe-Salas et al., 1994], pilot [Gomez et al., 1995] and industrial flotation columns [Gomez et al., 1994] have been made using the pressure technique. The measurements represent the average or overall gas holdup between the points of measurement.

A method based upon static pressure measurement has been developed and tested to estimate on-line gas and solids holdups [Wenge et al., 1995]. The method consisted of measuring the static pressure in the three-phase dispersion followed by interruption of the gas flow, complete gas disengagement, and a second pressure measurement on the resulting two-phase (solid-liquid) slurry. It was claimed the measurement was sufficiently fast that no sedimentation of solids occurred during the second pressure reading. This technique is generally not suited to mineral processing systems, since it requires interruption of the operation.

Electrical conductivity methods

The electrical conductivity of a multiphase dispersion (i.e., air-water, solids-water, air-solids-water) depends on the volume fraction and electrical conductivities of the phases involved. The relation between the conductivity of the dispersion and the concentration of the phases is not linear [Maxwell, 1892]. In many cases of interest, Maxwell's model for a non-conducting dispersed phase has proved suitable for representing the conductivity of the dispersion as a function of composition [Uribe-Salas et al., 1994].

Measurement of conductivity has been used for a long time to monitor process performance in a variety of industries [Fricke, 1925; Tsochatzidis et al., 1992]. The technique has been applied in mineral processing systems for monitoring flotation, sedimentation, and thickening at both laboratory and industrial scale [Begovich and Watson, 1978; Nasr-El-Din et al., 1987; Gomez et al., 1990;

Uribe-Salas et al., 1992, 1994; Banisi et al., 1993, 1995 (a), (b); Paleari et al., 1994; Xu et al., 1994].

A conductivity probe for measurement of solids holdup has been developed and tested in laboratory sedimentation units [Ingham, 1995] and industrial thickeners and clarifiers [Xu et al., 1993; Probst, 1996]. The measurements showed excellent agreement with the actual solids holdup. This type of probe promises accurate measurements of level and solids holdup in thickening operations which may be suitable to determine inventory, and eventually for automatic control.

Summary

The mineral processing industry is in a race to improve productivity and efficiency. Part of the goal is being met by the implementation of automatic process control. To make use of automatic process control there are two basic prerequisites:

- The process must be understood with respect to the relationship between the variables involved; only then, by manipulating such variables, is it possible to control the process
- The variables must be accurately measured; therefore, there is a need for reliable sensors.

Some sensing techniques currently used in other areas, for example in medical diagnosis, are thought to be applicable to mineral processing. An example is tomography. However, at its current stage of development the cost limits its use. Nevertheless, it is anticipated that costs will drop making tomography a candidate technique for sensing and controlling mineral processing systems in the future.

Some methods developed initially for chemical analysis have been proposed as suitable techniques for on-line monitoring. Continuous improvement in these techniques may overcome their present limitations.

Methods based on measurement of electrical conductivity have shown practical application in multiphase dispersions providing a simple, reliable low cost technique. One such technique is pursued in this thesis to measure gas holdup in gas-slurry (flotation) systems.

Objectives of the present work

The electrical conductivity probes currently in commercial use are almost all restricted to measurement of level in a variety of environments. Extending to the estimation of phase holdup depends on having a model of the conductivity of the dispersion.

The Maxwell model has proved adequate in many cases of practical interest. To estimate holdup from Maxwell's model requires knowledge of both the conductivity of the dispersion and of the continuum (with no dispersed phase). For on-line application, the problem lies in the second measurement - the conductivity of the continuum.

This thesis focusses on determination of the gas holdup in flotation systems, in particular flotation columns. The gas holdup is a function of bubble size (which in turns depends of sparger type, frother characteristics and concentration, and air flowrate), slurry flowrate, solids content, and mixing patterns. Gas holdup partly defines flotation kinetics and carrying capacity and is, therefore, an important parameter in flotation. Gas holdup is also useful to diagnose the operation of a flotation system. To now, however, the lack of a reliable on-line sensor for gas holdup has prevented its exploitation in industry.

This work describes the study of electrical conductivity cells, and their application in the design, construction and operation of a gas holdup probe for use in flotation.

CHAPTER 2

ELECTRICAL CONDUCTIVITY AND THE ELECTRIC FIELD

2.1. Introduction

Measurement of electrical conductivity to describe some characteristics of systems of interest in mineral processing has received considerable interest recently [Banisi et al., 1995 (a), (b); Uribe-Salas et al., 1994, 1992; Paleari et al., 1994; Xu et al., 1994]. These works have shown that the procedure is reliable for estimation of solids and gas holdup. To consolidate the technique and increase its industrial acceptance work is required to provide cell designs suited to a particular duty.

Electrical conductivity cells present two concepts of ideality. The first is from the electrical point of view: the ideal cell is one where the equipotential surfaces are parallel to the electrodes surfaces. This implies that the ratio between the surface area used to transfer electric current and the distance between the electrodes is constant whatever is the conductivity of the medium in which the current is transferred. This ideal conductivity cell is formed by the following: two infinite parallel facing plates; two concentric spherical electrodes; or, two infinite concentric cylindrical electrodes. From these geometries, it is clear that such cells are not suitable to industrial applications.

The second concept of ideality is from the point of view of the users: in this case the characteristics of the system should not be disturbed by the presence of the conductivity cell. Since most systems of interest involve flowing (multiphase) systems the conductivity cells will be referred to as "flow cells." The choice of cell shapes and dimensions (i.e. "geometry") and previous knowledge of the system to be measured are important to design flow cells for application in mineral processing systems.

The present Chapter presents the fundamental concepts of electric field theory pertinent to flow conductivity cells. It finishes with a description of a commercial modelling package.

2.2. General background

Electrical conductivity is defined as the ability of a substance to conduct electric current. It has been termed specific conductance [Condon, 1967; Andrews, 1979; Barrow, 1973], specific conductivity [Adamson, 1979; Kasper, 1940], and conductivity [Atkins, 1982; Levine, 1988; Braunstein and Robbins, 1971; Gilmont and Walton, 1956; Lord Rayleigh, 1892; Meredith and Tobias, 1960; Wagner, 1962; Schwab, 1988; Becker, 1964]. The term conductivity and the symbol κ are used in the present work.

The conductivity is the proportionality constant in Ohm's law:

$$i = -\kappa \nabla V \qquad (2.1)$$

where i is the current density (A cm^{-2}), ∇V is the potential gradient (volt cm^{-1}), and κ is the conductivity (S cm^{-1}).

Conductivity is an intensive property that may be thought as of the conductance (or, more precisely, electrical conductance) of a cube of 1 cm edge, assuming the current flux is perpendicular to the opposing faces of the cube.

All substances conduct electricity to some degree, but the magnitude varies widely ranging from very low for insulators to very high for conductors (such as metals). The interest here is the conductivity of dispersions in aqueous electrolyte continuum.

The conduction of electric energy in an electrolyte differes from that of a solid conductor (e.g. a metal). In an electrolyte, conduction is through motion of charged particles of atomic or molecular size, i.e. convective mass transfer takes place, while in a metal the electric current is due to the motion of electrons and no matter is transferred.

Electrolyte conductors are liquid solutions, composed of a solute in a solvent. The solutions are electrically neutral, i.e. they contain equal numbers of positively and negatively charged particles. If a potential gradient is imposed, e.g. by immersing two electrodes (of opposite polarity) in the solution, these charged particles move. These charged particles are known as ions.

Each type of ion moves in an electrolyte solution with a different velocity, therefore each

carries a different fraction of the electric current. This fraction of current for each ion defines the transport number for the solution.

The charge on each ion is equal to the electronic charge or some integral multiple. Thus, one negative univalent ion has a charge equal in magnitude to and of the same sign as a single electron. A bivalent ion has two (negative or positive) electronic charges.

The quantity of an element or aggregate molecule oxidized or reduced by one Avogadro's number of charges is called the electrochemical equivalent of the element or aggregate. In the case of an element which forms univalent ions, the electrochemical equivalent is that of one gram atomic weight, thus the electrochemical equivalent of bivalent ions would be one half gram atomic weight (if the unit of mass is taken as the gram).

Faraday (1833) stated that the chemical power of a current of electricity is in direct proportion to the absolute quantity of electricity which passes. Therefore at the electrode/electrolyte interface, the amount of chemical change (or reaction) in electrochemical equivalents is the same for both electrodes and depends on the quantity of electricity passing through the interface.

In electrolysis there is a definite quantity of electricity that brings about one gram equivalent of chemical reaction in any electrolyte system. This quantity is called the Faraday, and represents an Avogadro's number of charge

$$F = N \times e \qquad (2.2)$$

where N and e are Avogadro's number, and the magnitude of the charge of the electron, respectively (the most comon units of the Faraday is coulombs per gram equivalent).

The measurement of the Faraday by electrochemical methods involves the absolute current, the time, and the mass of material reacted. The value of the Faraday determined by those methods has been accepted as 96 487 coulombs/gram equivalent. Deviations from Faraday's law, as applied to electrochemistry, can be regarded as due to simultaneous electrode reactions, electrolytic reversal of electrode processes, and interaction of the products of one electrode with the products of the other electrode in an electrolytic cell.

The resistance of an electrolyte solution can not be measured using direct current, because

it changes the concentration of the electrolyte and accumulates electrolysis products at the electrodes, thus changing the resistance of the solution. An alternating current of sufficiently high frequency (usually ≥ 1 kHz) is used to avoid these effects.

In a conductivity cell with facing plate electrodes it is assumed that the current flux is at right angles to and constrained to the area of the plates; under this assumption, the resistance of the electrolyte is

$$R = \text{drop of potential/current} = (V_A - V_B)/I \tag{2.3}$$

where V_A and V_B are the potentials on the plate electrodes A and B, respectively, and I is the current in the electric circuit. In the case of a linear conductor, the current density, i, on any equipotential surface is constant, therefore,

$$I = \int_{Acell} i \, d\, A_{cell} = i\, A_{cell} \tag{2.4}$$

$$V_A - V_B = -(V_B - V_A) = -\int_a^b \nabla V \, d\, L = -\nabla V\, (b - a) = -\nabla V\, L \tag{2.5}$$

where A_{cell} is the cross sectional area of the cell, L is the length of the cell, and a and b are the positions of the electrodes A and B, respectively.

Substituting equations (2.1), (2.4) and (2.5) into equation (2.3), yields

$$K = 1/R = I/(V_A - V_B) = -i/(\nabla V)\,(A_{cell}/L) = \kappa\, A_{cell}/L \tag{2.6}$$

where K is the conductance of the electrolyte.

In equation (2.6) the term A_{cell}/L is often referred to as the cell constant (L^{-1}). The conductivity can be calculated from the resistance

$$\kappa = (1/R)\,(L/A_{cell}) \tag{2.7}$$

As was mentioned in Chapter 1, measurement of conductivity to determine holdup in multiphase systems has been applied in different branches of engineering. Several investigations in mineral processing systems have been reported, and it approaches being a standard technique for these applications.

The electrical conductivity of mixtures exhibits a complex relationship as compared to that of pure phases, thus it remains important to study the behaviour of flow cells under different conditions. For example, conductivity measurements are affected by the geometry of the system, i.e. shape, size and separation of electrodes of the conductivity cell.

The underlying principles in modelling the electrical conductivity of dispersions are: the transfer of electrical energy is a linear function of the difference in potential, represented by Ohm's law; and, from the law of conservation of current, the net resultant of the transfer of current is zero. Assuming that the electrical field is homogeneous or, in other words, that the electrical conductivity is constant throughout the medium, these two principles lead to the general formulation of the transfer of electrical energy known as the Laplace equation.

This formulation implies that the path of the current carrying the electric charge is continuous along lines of flux. These lines of flux converge in zones where the conductivity is high and diverge where the conductivity is low.

2.3. Model of the electric field

The concept of electric charge is fundamental in the study of electric fields [Schwab, 1988; Binns and Lawrenson, 1973]. A charge of magnitude q coulombs is considered to emit a total electric flux of q units; therefore, the electric flux q that radiates from any closed surface contains a charge q. The electric flux density at a point is the vector $\underline{D}$, with direction that of the field. Considering a surface of a sphere radius r with its centre at the position of the point charge, the direction of the flux is radially outward, and the density of the flux crossing the surface is

$$D = q/(4\pi r^2) \qquad (2.8)$$

The force on unit charge placed at a point, a distance r from a charge q, is proportional to q/r^2, and to the value of the vector $\underline{D}$ at that point. Therefore, if a vector $\underline{E}$ (electric field strength) is defined to describe the force acting on the unit charge, then $\underline{E}$ is proportional to $\underline{D}$ for a given medium

$$\underline{D} = \epsilon_o \epsilon \underline{E} \qquad (2.9)$$

where ϵ_o and ϵ are the primary electric constant and the relative permittivity of the surrounding medium, respectively. Equations (2.8) and (2.9) lead to $E = q/(4\pi\epsilon_o\epsilon r^2)$, which in free space becomes

$$E = q/(4\pi\epsilon_o r^2) \qquad (2.10)$$

Consider a charge distributed over a volume. As the volume tends to zero, the limit (at a point) of the outward flux per unit volume is called the divergence of the vector $\underline{D}$. Therefore, the divergence of $\underline{D}$ at any point within the volume is equal to the charge density ϱ_c

$$\text{div } D = \varrho_c \qquad (2.11)$$

When charge is uniformly distributed along an infinite straight line, the direction of the flux leaving the charge is everywhere perpendicular to the line, and the flux emitted per unit length of the line is equal to the linear charge density q. At a radius r about the charge, the flux density is

$$D = q/(2\pi r) \qquad (2.12)$$

and $$E = q/(2\pi\epsilon_o\epsilon r) \qquad (2.13)$$

Therefore, the field strength varies inversely as the distance from the line charge. This field is two-dimensional, and a quantity of flux may be represented by a number of flux lines with the same direction as the flux density.

The electric potential, V, which is a scalar quantity, is a point function defined as the work done in moving unit charge from infinity to the point. The work done in moving unit charge a small distance dl by applying the force on unit charge, E, is

$$dV = - E\, dl \qquad (2.14)$$

The negative sign means that the potential decreases in the positive direction of E; therefore, $E = - dV/dl$ expresses that the component of the electric field strength in any direction is equal to the potential gradient in that direction and, expressed as the vector equation, is

$$\underline{E} = - \text{grad } V \qquad (2.15)$$

The work which is done in moving a charge between two points in an electrostatic field is independent of the path followed, and the work done in a closed path (by moving to the initial point) is zero

$$V_2 - V_1 = - \int_c E\, dl = - \int q\, dr/(2\pi\epsilon_o\epsilon r) \qquad (2.16)$$

and the potential difference between two points at radius r_1 and r_2 is

$$\{- q/(2\pi\epsilon_o\epsilon)\}(\log r)_{r1}^{r2} = \{- q/(2\pi\epsilon_o\epsilon)\} \log(r_2/r_1)$$

Since the potential is a point function, it is possible to draw a line which passes through points of the same potential; such a line is called the equipotential line, and when a charge is moved along an equipotential line no work is done. Since no work is done, equipotential lines are perpendicular to flux lines. When equipotential lines and flux lines are drawn together they form a mesh of orthogonal lines or a field map.

Some quantities are defined to facilitate the analysis: a potential function ψ is defined such that the change in this function between any two points is proportional to the change in potential

between them. Its value at any point with respect to the origin of the potential, is a direct measure of the value of the potential at that point, and a line joining points of the same value of potential function is the equipotential line. In a two-electrode system, if on one electrode the potential function is considered to be equal to zero, and on the other electrode is equal to one, then equipotential lines can be drawn in the space between the two electrodes, each representing constant values of the potential function between 0 and 1.

In a similar manner a flux function, φ = constant, defines a flux line. Two flux lines $\varphi = \varphi_o$ and $\varphi = \varphi_o + n$, have n units of flux passing between them.

Since the potential lines and the flux lines are orthogonal, then one function can be derived from the other

$$(dy/dx)_{\varphi=\text{constant}} = - \{1/(dy/dx)_{\psi=\text{constant}}\} \qquad (2.17)$$

The capacitance between two conducting surfaces (electrodes) is given by the ratio of total flux common to the surfaces to the potential difference between them. If ψ_1 and ψ_2 are the potential functions of the two conductors, and φ' and φ'' are the values of the flux functions for the lines bounding the mutual flux, then the capacitance C is

$$C = (\varphi' - \varphi'')/(\psi_1 - \psi_2) \qquad (2.18)$$

This relationship is valid even when more than two conductors are present. If there are only two conductors, one of them may be at infinity, the flux between them is equal to the charge q on either

$$C = q/(\psi_1 - \psi_2) \qquad (2.19)$$

In the case of two charged concentric cylinders the potential function has been shown to vary as $\{[q/(2\pi\epsilon_o\epsilon)]\log r\}$; if the boundaries have radii r_1 and r_2, then the difference in potential function between the boundaries is $\{[q/(2\pi\epsilon_o\epsilon)]\log r_1 - [q/(2\pi\epsilon_o\epsilon)]\log r_2\}$; therefore the capacitance between the cylinders is $q/\{[q/(2\pi\epsilon_o\epsilon)]\log(r_1/r_2)\}$, which can be expressed as

$$C = 2\pi\epsilon_o\epsilon/\log(r_1/r_2) \qquad (2.20)$$

In a region containing charge distributed with uniform density ϱ_c, the divergence of the flux is everywhere equal to ϱ_c, being expressed in terms of $\underline{E}$ as

$$\text{div}\,(\epsilon_o\epsilon\underline{E}) = \varrho_c \qquad (2.21)$$

this expression may be written in terms of potential as div $(-\epsilon_o\epsilon$ grad V) = ϱ_c or

$$\text{div}\,(\text{grad V}) = -\varrho_c/\epsilon_o\epsilon \qquad (2.22)$$

this expression is Poisson's equation. For a region containing no charge $\varrho_c = 0$, then

$$\text{div}\,(\text{grad V}) = 0 \qquad (2.23)$$

which is Laplace's equation.

Deriving these equations in cartesian form considers a small cube with sides of length δx, δy, and δz parallel to the axes x, y, and z. The vector $\underline{D}$, with components Dx, Dy, and Dz, is the flux density at the centre of the cube considering the two faces of the volume elements perpendicular to the axis x. The flux entering the cube through the left hand face is $\{Dx - (1/2)(\partial Dx/\partial x)\delta x\}\,\delta y\,\delta z$, and that leaving the cube through the right-hand face is $\{Dx + (1/2)(\partial Dx/\partial x)\}\,\delta y\,\delta z$. Therefore, the net flux leaving the cube in the x-direction is $(\partial Dx/\partial x)\delta x\,\delta y\,\delta z$.

There are similar expressions for the y- and x-directions, and, therefore, the total flux leaving the cube is

$$\{(\partial Dx/\partial x) + (\partial Dy/\partial y) + (\partial Dz/\partial z)\}\,\delta x\,\delta y\,\delta z$$

and this is equal to the total charge enclosed, $\varrho c\,\delta x\,\delta y\,\delta z$,

$$\{(\partial Dx/\partial x) + (\partial Dy/\partial y) + (\partial Dz/\partial z)\} = \varrho c \qquad (2.24)$$

Taking into consideration the components of the field strength,

$$Dx = \epsilon_o \epsilon Ex,\ Dy = \epsilon_o \epsilon Ey,\ Dz = \epsilon_o \epsilon Ez \qquad (2.25)$$

combining equations (2.24) and (2.25) gives

$$(\partial Ex/\partial x) + (\partial Ey/\partial y) + (\partial Ez/\varrho z) = \varrho c/\epsilon_o \epsilon \qquad (2.26)$$

but recognizing the field strength is equal to the potential gradient means

$$Ex = -(\partial V/\partial x),\ Ey = -(\partial V/\partial y),\ Ez = -(\partial V/\partial z) \qquad (2.27)$$

and thus, combining equations (2.27) and (2.26) gives

$$(\partial^2 V/\partial x^2) + (\partial^2 V/\partial y^2) + (\partial^2 V/\partial z^2) = -\varrho c/\epsilon_o \epsilon \qquad (2.28)$$

which is Poisson's equation in cartesian form, and when $\varrho c = 0$ it becomes Laplace's equation

$$(\partial^2 V/\partial x^2) + (\partial^2 V/\partial y^2) + (\partial^2 V/\partial z^2) = 0 \qquad (2.29)$$

In two dimensional configuration, the variation of potential in one direction is zero, and , therefore, $(\partial^2 V/\partial z^2) = 0$, and in the two dimentional form Laplace's equation is expressed as

$$(\partial^2 V/\partial x^2) + (\partial^2 V/\partial y^2) = 0 \qquad (2.30)$$

All these equations have been expressed in terms of the potential V; nevertheless, they apply equally to the potential function ψ. In cartesian form it is

$$(\partial^2 \psi/\partial x^2) + (\partial^2 \psi/\partial y^2) = 0 \qquad (2.31)$$

(or $\nabla^2\psi = 0$)

and the current density function is

$$i = - \kappa\nabla\psi = - \kappa \{(\partial\psi/\partial x)\underline{i} + (\partial\psi/\partial y)j\} \qquad (2.32)$$

where $\underline{i}$ and j are unitary vectors.

Consider the potential field that builds up in a section of two infinite parallel planes. Replacing the potential field equations by a set of finite difference equations with connect values of the potential function, is the first approach to building a mesh. Assuming that the analysis uses a square mesh distribution; Fig.2.1 represents the elements involved in the finite difference numerical method. In this representation, the mesh length is defined as h. The cathode and anode are presented as the equipotential surfaces $\psi = 0$ and $\psi = 1$, respectively.

The difference equation is developed by expanding the scalar potential ψ at point 0 in Taylor's series and deriving expressions for $(\partial^2\psi/\partial x^2)_o$ and $(\partial^2\psi/\partial y^2)_o$ which are substituted in equation (2.31). At any point x, ψ can be expanded in terms of the ψ at point 0 (i.e. ψ_o) by the use of Taylor's series

$$\psi = \psi_o + (\partial\psi/\partial x)_o (x - x_o) + (1/2!) (\partial^2\psi/\partial x^2)_o (x - x_o)^2 + (1/3!) (\partial^3\psi/\partial x^3)o (x - x_o)^3 + \ldots \qquad (2.33)$$

if $x_1 = x_o + h$ and $x_3 = x_o - h$, then the values of the potential function at points 1 and 3 is

$$\psi_1 = \psi_o + h (\partial\psi/\partial x)_o + (1/2!) h^2 (\partial^2\psi/\partial x^2)_o + (1/3!) h^3 (\partial^3\psi/\partial x^3)o + \ldots \qquad (2.34)$$

and

$$\psi_3 = \psi_o - h (\partial\psi/\partial x)_o + (1/2!) h^2 (\partial^2\psi/\partial x^2)_o - (1/3!) h^3 (\partial^3\psi/\partial x^3)_o + \ldots \qquad (2.35)$$

The addition of equations (2.34) and (2.35) leads to

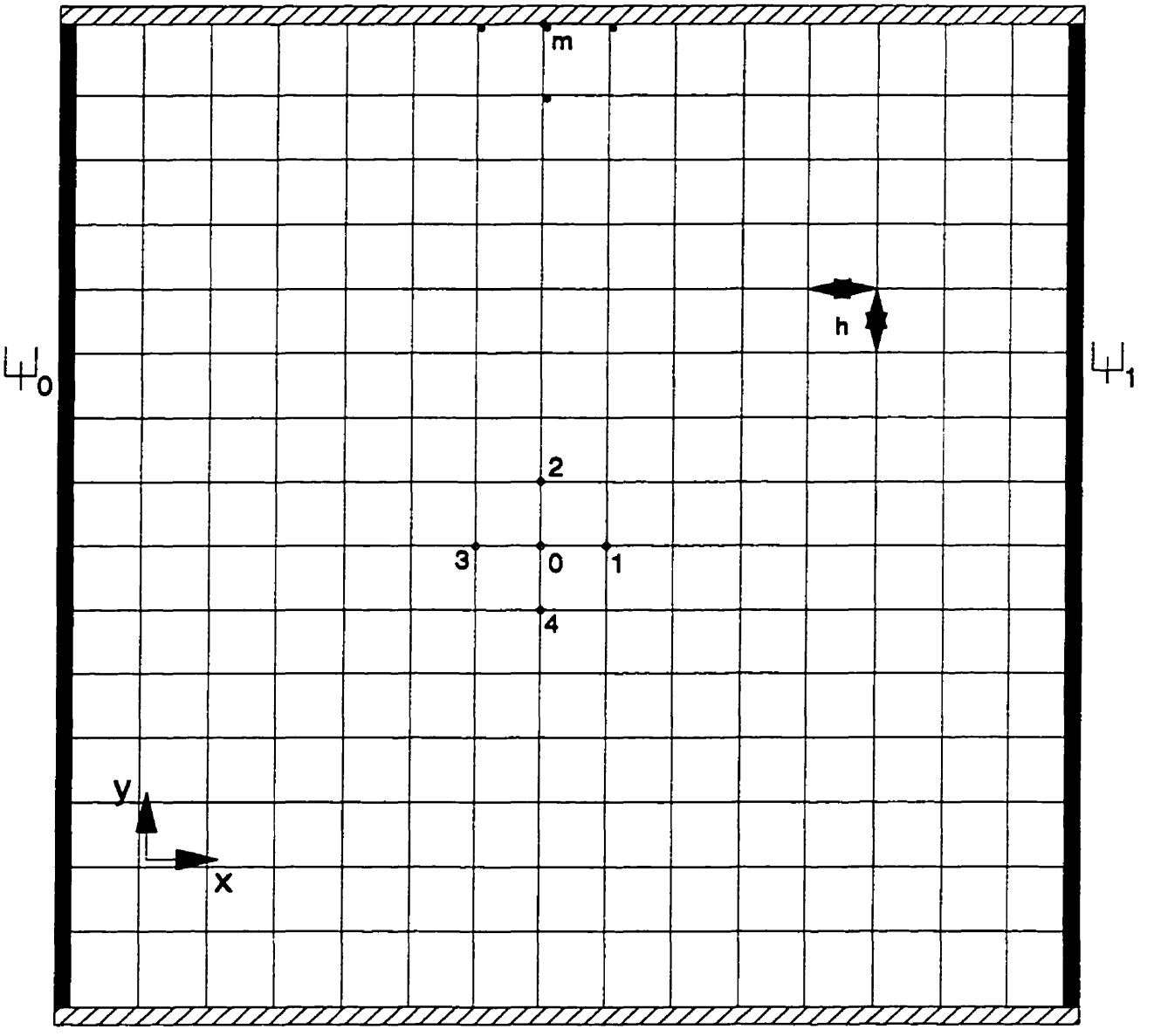

Fig.2.1. Two parallel plate electrodes; nodes distribution with respect to points "0" and "m".

$$\psi_1 + \psi_3 = 2\psi_o + h^2(\partial^2\psi/\partial x^2)_o + h^4(\partial^4\psi/\partial x^4)_o + \ldots \quad (2.36)$$

Neglecting those terms that contain h to the power higher than 3, yields:

$$(\partial^2\psi/\partial x^2)_o = (\psi_1 + \psi_3 - 2\psi_o)/h^2 \quad (2.37)$$

In a similar manner there is an expression for $(\partial^2\psi/\partial y^2)_o$

$$(\partial^2\psi/\partial y^2)_o = (\psi_2 + \psi_4 - \psi_o)/h^2 \quad (2.38)$$

Substituting equations (2.37) and (2.38) in equation (2.31) to represent a point 0 not on a boundary

$$\psi_o = (\psi_1 + \psi_2 + \psi_3 + \psi_4)/4 \quad (2.39)$$

Then, the current density vector i at point 0 is

$$\underline{i}_o = -\kappa\{[(\psi_1 - \psi_3)/2h]\,\underline{i} + [(\psi_2 - \psi_4)/2h]\,\underline{j}\} \quad (2.40)$$

the magnitude of i and its direction θ is

$$i = \kappa\{[(\psi_1 - \psi_3)/2h]^2 + [(\psi_2 - \psi_4)/2h]^2\}^{1/2} \quad (2.41)$$

$$\theta = tg^{-1}\{(\psi_2 - \psi_4)/(\psi_1 - \psi_3)\} \quad (2.42)$$

Considering Fig.2.1, the edges at y=0 and y=b are lines impervious to the flux which represent insulating walls, i.e. $(\partial\psi/\partial y)_{y=0} = 0$, and $(\partial\psi/\partial y)_{y=b} = 0$, since no current is permitted orthogonal to them, i.e. no current crosses those surfaces. Therefore at point m in Fig.2.1,

$$(\psi_2 - \psi_4)/2h = 0, \text{ therefore, } \psi_2 = \psi_4 \qquad (2.43)$$

Considering equation (2.44) for point m,

$$\psi_m = (\psi_1 + \psi_3 + 2\psi_4)/4 \qquad (2.44)$$

Therefore, all the points in the grid are described by a finite difference equation and the computation can be carried out.

2.4. Model computation

The commercial program MagNet 5.1 [Edwards and Freeman, 1995] solves two and three-dimensional electromagnetic field problems. MagNet 5.1 contains two packages, named FastTrack and ToolBox.

FastTrack has three component modules which are activated in sequence: the Describe module; the Solve module; and the Post module. The Describe module allows one to draw the device, assign magnetic materials to regions, and specify coils which form part of a circuit containing current or voltage sources. The result is a complete description of the problem ready for the Solve module, which generates the finite-element mesh and then solves the field equations for the required potential function. The solution generated by Solve is passed to the post-processor module Post, which allows one to inspect and display field quantities such as flux density and permeability, and to calculate global quantities such as energy, force and inductance.

ToolBox gives total control over all phases of the analysis: geometric description, finite-element mesh generation, problem description (material properties and electrical constraints), solution and post processing. It is possible to create macros, known as User Defined Verbs, to control the operation of the modules. It is also possible to automate the operations by supplying command files, or scripts, instead of entering commands through the keyboard.

Thus, the model (Laplace's equation) can be solved for a given device "built" by MagNet 5.1. In this way, flow cell configurations can be simulated. First MagNet 5.1 will be used to compare with

experimental conductivity data, then will be used to simulate flow cells containing two-phase dispersions and compare with holdup predicted by Maxwell's model.

A significant feature in the use of the model here is related to design of flow cells for specific applications in mineral processing; the design of a cell must take into account the cell constant behaviour. The design includes size and geometric characteristics of the cell, and the range of values of operating variables anticipated in real situations, i.e. the conductivity of dispersions to be measured by the flow cell, and the range in holdup.

2.5. Summary

Electrical conductivity is the ability of a substance to conduct electric current, and it can be measured using conductivity cells. In this chapter the so-called "cell constant" is introduced, and its importance in cells is explored in the subsequent chapters of this thesis.

The electric field in a uniform medium is described by Laplace's equation. All physical fields are three dimensional, but for most practical cases analytical solutions are not available, and numerical solutions involve a prohibitive amount of computation. Nevertheless, approximate solutions accurate enough for present purposes can be obtained by using a two-dimensional representation. MagNet 5.1 can be applied to solve the electromagnetic field associated with flow conductivity cells; its application is presented in the following chapters.

CHAPTER 3

FLOW CELLS

3.1. Introduction

A flow cell is defined here as one that allows a fluid or a dispersion to flow through freely while the electrical conductivity is measured. The interest in flow cells in mineral processing is to sense gas-liquid, solids-liquid, and gas-solids-liquid dispersions.

When a flow cell is used to measure the electrical conductivity of a dispersion, the requirement is that the measurement represents that of the dispersion outside the cell. Therefore, from the mineral processing point of view, such a flow cell may be called ideal. (This definition does not imply that the flow cell is ideal from the field theory point of view; indeed, a flow cell cannot behave as an ideal conductivity cell because of the ideality restrictions introduced earlier.)

This Chapter describes the characterisation of flow cells, and presents their most relevant properties for applications in mineral processing systems.

3.2. Experimental

It is important to study the behaviour of flow cells to derive models for their design to meet the variety of situations represented by mineral processing.

Materials, apparatus, experimental procedure, and results are presented in the following sections.

3.2.1. Materials and apparatus

The flow cells studied in this work are cylindrical with internal stainless steel electrodes flush to the cell wall. Because of this geometry the fluid under study can flow relatively freely with little restriction.

The flow cells were made of plexiglas tubing of different internal diameters ranging from 2.5 to 10 cm. Different flow cell designs were tested in a multicell unit referred to as a "fluidisation-flotation" column. The cell electrodes were interchangeable.

The electrodes were made from stainless steel strap, threaded to and flush with the column wall. Three different widths of electrodes were tested; one width was such that its internal area was equal to the cross section area of the column, another was 50% of the cross section area of the column, and the third 25%.

These electrodes were located between column sections of different lengths, to give different separation distances between electrodes.

Five electrodes were used at a time, connected to a conductivity meter (TACUSSEL CD810) through a relay interphase which was connected to a DAS8 board in a IBM compatible computer. Figure 3.1 shows schematically the experimental apparatus described as the fluidisation-flotation column.

Electrolyte solutions were prepared by dissolving known amounts of KCl in water to give the desired conductivity. The conductivity was measured with a portable conductivity meter (Hanna HI8733) as the reference conductivity. The temperature was controlled using a temperature controller/electric heater (Cole Parmer 1266-02).

Some experiments were carried out using a portable flow cell (Fig.3.2) on solutions of different electrolytes under controlled temperature. High purity NaCl, KCl, $CaCl_2$, and $CuSO_4$ (Fisher Scientific) were used in the preparation of the solutions.

Groups of experiments were carried out to study the effect of the addition of non-conductive solids on the conductivity measurements in the flow cells by adding glass beads (boro silicate glass; Fisher Scientific) of different diameter (from 1 mm to 6 mm); these experiments were done under conditions of controlled temperature and conductivity of the electrolyte solution.

3.2.2. Experimental procedure

The fluidisation-flotation column was used to: a) characterize the cell constant, and b) study the response upon addition of fluidized solids.

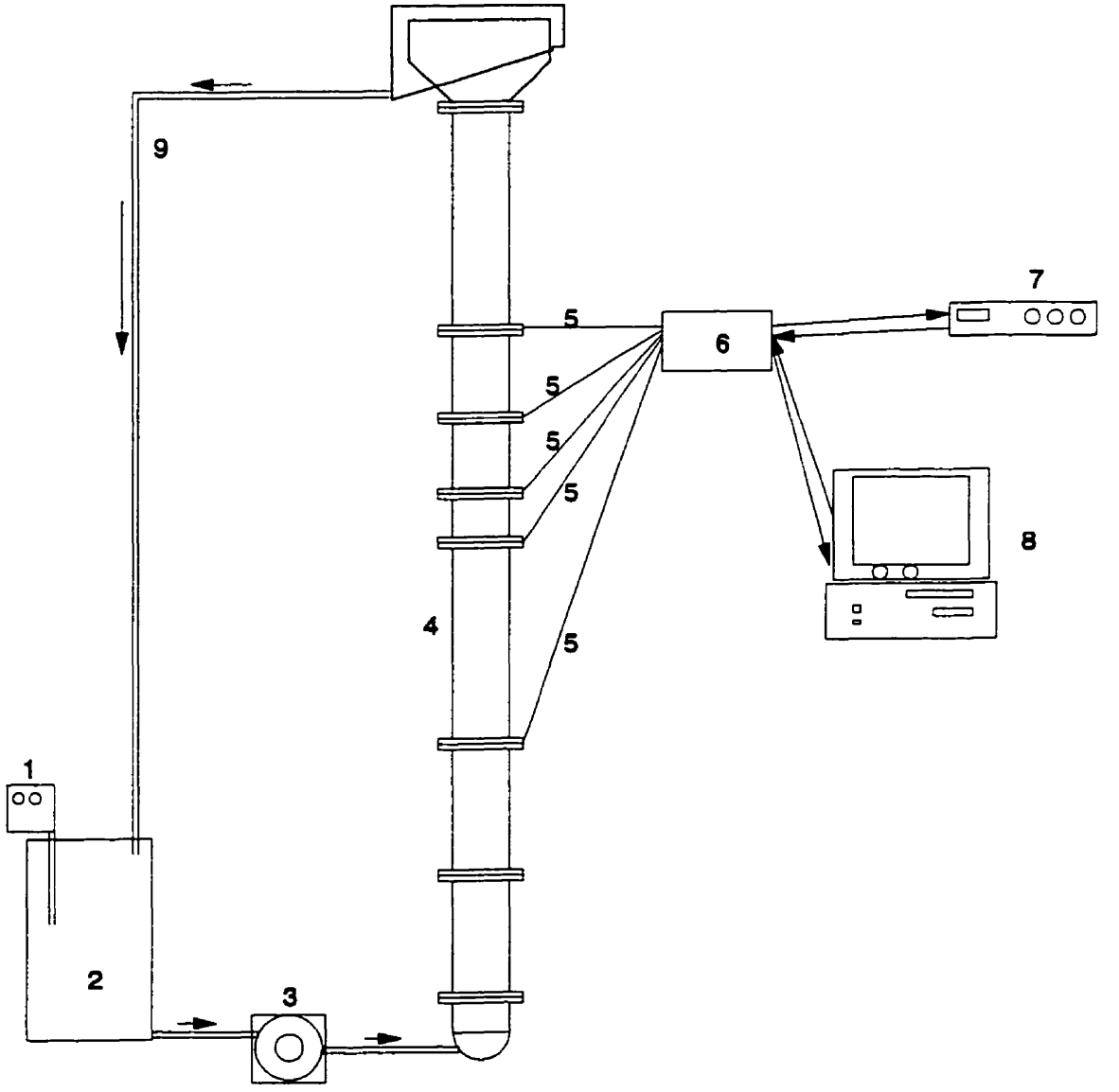

Fig.3.1. Fluidisation-flotation column: 1) temperature controller; 2) solution tank; 3) pump; 4) column; 5) electrodes connection; 6) relays interphase; 7) conductivity meter; 8) computer; 9) overflow.

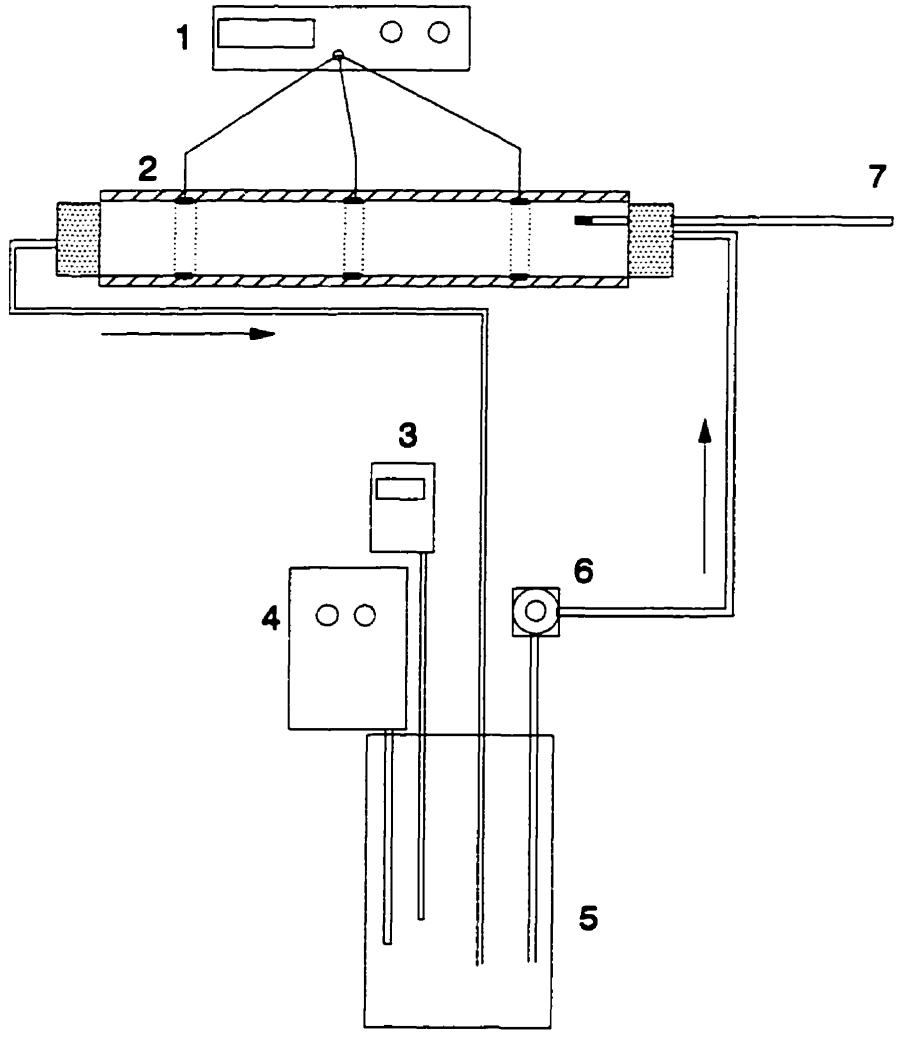

Fig.3.2. Portable flow cell: 1) conductivity meter; 2) flow cell;
3) thermometer; 4) temperature controller; 5) electrolyte solution tank;
6) pump; 7) thermometer.

The experiments were carried out using tap water (the conductivity varied between 0.27 and 0.29 mS cm^{-1} at 298 K during the year) with additions of KCl to give the desired conductivity. These solutions were prepared at a given temperature.

The electrolyte solution was fed into the column through the bottom inlet using a peristaltic pump; once the column was filled, the overflow was collected and returned to the column.

When the temperature was stable, measurements of conductance were taken by connecting pairs of electrodes through the relay board (see Fig.3.1) with a conductivity meter.

In the fluidisation-flotation column there were five electrodes spaced at 10 , 10 , 5 , and 30 cm; therefore, ten different conductivity cell geometries were available by combining selected electrodes in pairs. An additional conductivity cell was formed by connecting three electrodes (separated 10 cm one to the next) with the central electrode held at a different polarity with respect to the other two.

During measurement of the conductance in each cell, the temperature and the conductivity of the electrolyte solution were maintained constant. The conductivity of the solution was altered by adding KCl (to increase it) or water (to decrease it). The procedure was repeated at different temperatures.

The signal from the conductivity meter was collected and saved in a computer (286 IBM compatible Bicmos computer) for subsequent processing.

The experiments in the portable flow cell were carried out in a similar manner to those in the fluidisation-flotation column. In some experiments, the cell was isolated by placing rubber plugs into the cell snug to the outside edge of the two electrodes. In these cases the volume of the cell is constrained to equal the geometrical volume defined by the cross sectional area of the cell and the distance between the electrodes.

The portable unit was used mainly to evaluate the effect of different salts (and their mixtures) on the conductivity measurements. The effect of temperature on the absolute and molar conductivity was analysed in terms of the different electrolyte species.

All measurements of conductance were collected by the conductivity meter every seven seconds twenty times for each electrode arrangement. The range in the results was less than ± 0.5%.

3.3. Results and Discussion

The experimental data are summarised in Appendix 1. The data include the effect on conductivity of temperature, electrolyte species, isolation of the cell, and addition of non-conducting bodies.

In any study of conductivity cells, it is necessary to create criteria to characterise the cells for a particular application. In some instances it may be of importance to define precisely the different electrolyte species and their concentration. However, there are many applications where such information is not entirely necessary it being sufficient to know the conductance measured in the cell.

Also, it is important to identify whether the information reflects the phenomena taking place in the cell or if it is the result of the response of the instruments used to measure the system.

3.3.1. The cell constant behaviour

Equation (2.6), in section 2.1, introduces a term defined by the ratio of the area normal to the flux of electrical energy and the distance between two points. This ratio has been termed the cell constant; in an ideal cell, the cell constant is constant for any value of electrolyte conductivity.

If the electrodes of such ideal cells are in fixed positions, it implies that the area used to transfer the electric energy is constant, and it is equivalent to the area of the electrode plate. This assumption has a physical meaning since the electric current is transfered from the electrode surface by the movement of the ions in the aqueous media; therefore, there must be a relationship between the electrode surface area and the effective area normal to the transport of current in the cell. In the case of a simple geometric representation of an ideal cell, the cell constant is equal to the cross sectional area of the cell divided by the distance between the electrodes.

The values of the effective cell constant, which describes the transfer of electric energy in a cell, and the geometric cell constant estimated from the dimensions of the cell, become increasingly different as the geometry of the cell becomes less and less simple. These differences can be regarded as a deviation from the ideal case, resulting from the nature of the transfer of energy in real systems.

As first approximation, in simple configurations the cell constant remains constant. The cell

constant can be estimated by measuring the conductance in the cell with electrolyte solutions of known conductivity.

Figs.3.3 and 3.4 show the experimental cell constants for various dimensions of cells as a function of the conductivity of the electrolyte; it can be seen that the cell constant decreases with increasing separation between the electrodes and with decreasing electrode surface area. This behaviour is as expected (from the definition of cell constant: A_{cell}/L).

The behaviour of the cell constant with respect to the conductivity of the electrolyte suggests one of the following:

1. Electrical energy flows between the electrodes such that the distance is equal to the geometric separation of the electrodes but the flux follows an annular path in such a manner that the full cross section area of the cell (normal to the flux) is not used. Consequently, the ratio between the area and the distance between the electrodes is lower than the geometric cell constant.
2. The full area of the cell normal to the flux of energy is used for transferring electric energy but, there is an extended volume of electric field beyond the edges of the electrodes in the cell, with the net effect of producing an apparent increase in the distance. Consequently, the ratio of the area to the effective distance for transfer of energy decreases.

To understand the observed behaviour of the cell constant in these flow cells a number of experiments were conducted by isolating the conductivity cell using rubber bungs. The purpose was to ascertain which of the two proposed paths (or neither) was correct. If the first path is correct, the cell constant should not change; if the second path is correct, the measured cell constant should have the same value as the geometric cell constant.

The cell constant as a function of electrolyte conductivity in the isolated flow cell is shown in Fig.3.5. It can be seen that the cell constant is equal to the geometric cell constant.

These results suggest that the electric field is enclosed in the isolated flow cell because the available space for the transfer of energy is restrained to the volume of the cell in between the electrodes. Therefore, from these results the second path appears to be followed. This implies that the isopotential planes formed between the electrodes are not parallel to the cross section area of the cell but are concave, consequently producing an electric field that extends beyond the edges of the electrodes.

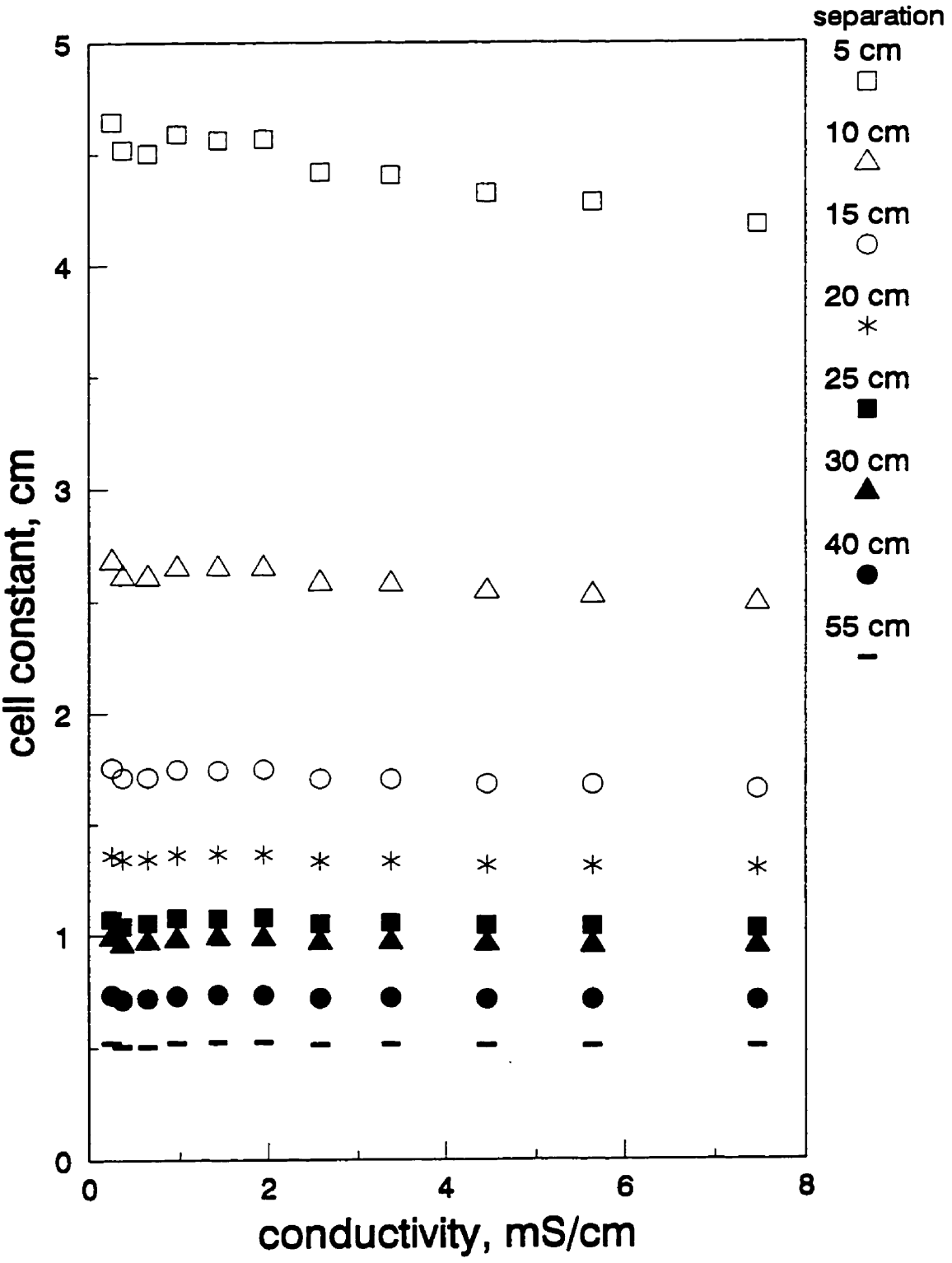

Fig.3.3. Cell constant in flow cells of 6.3 cm i.d.; 1.6 cm width; effect of different separation between electrodes.

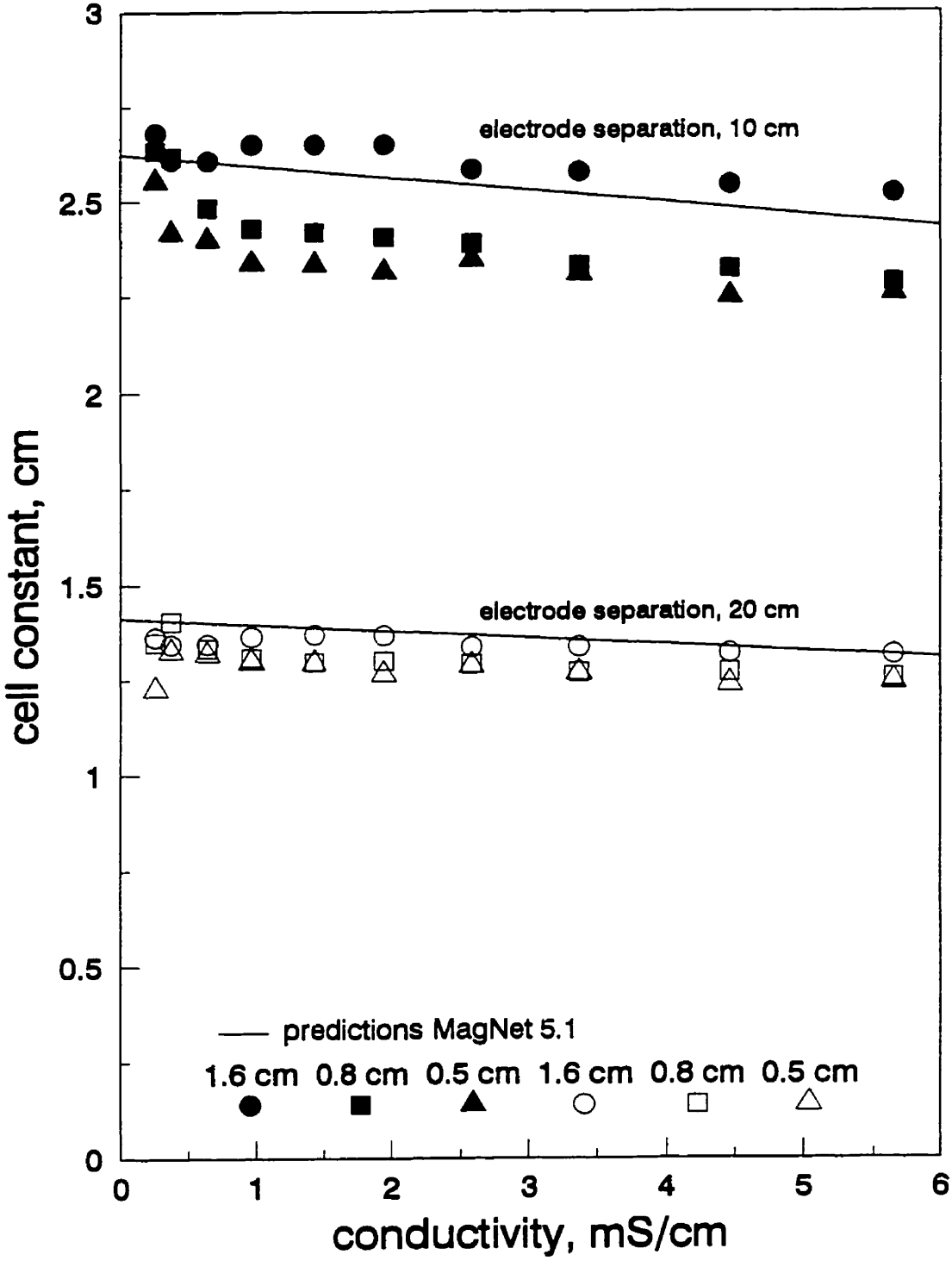

Fig.3.4. Experimental cell constant values and model predictions; cell diameter = 6.3 cm; two-electrodes arrangement in each cell; effect of electrode width and electrode separation; data collected at 298 K.

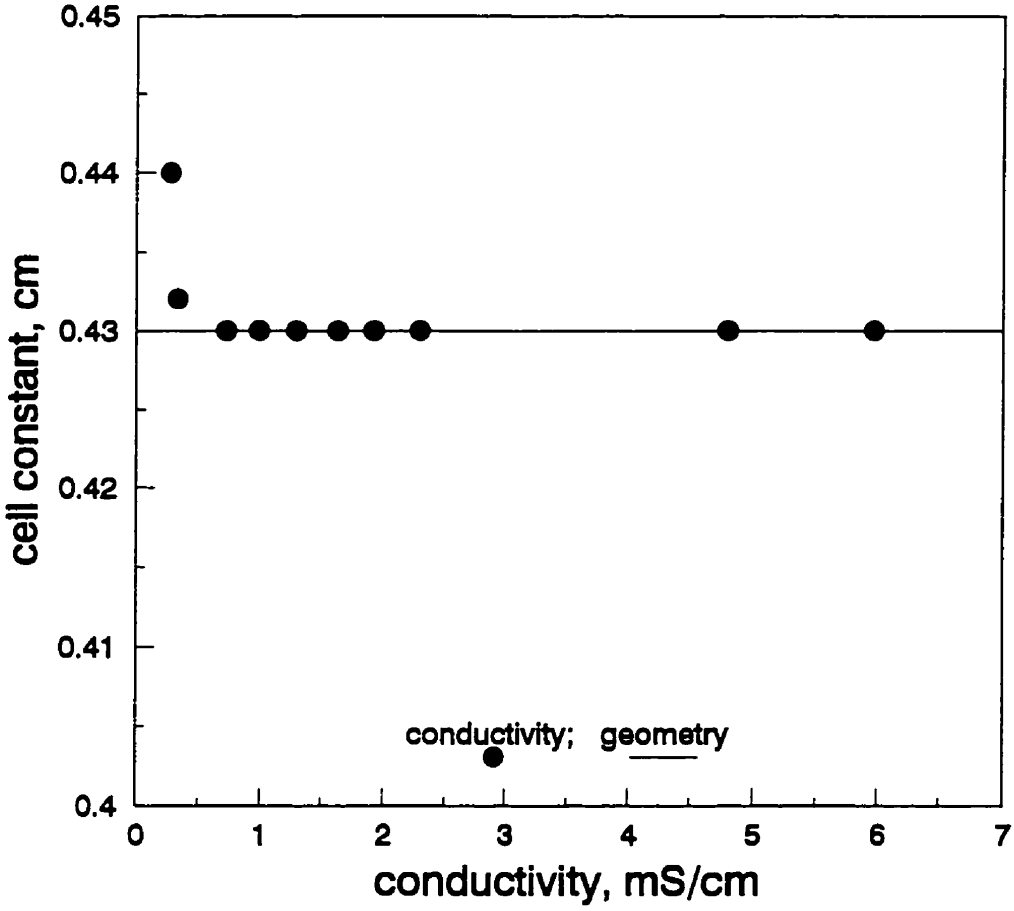

Fig.3.5. Estimated cell constant from geometric characteristics of the cell and from conductivity measurements as a function of the conductivity of the electrolyte solution. The cell is "isolated," i.e. rubber bungs are inserted up to the edge of the electrodes.

The experimental data from the open flow cells imply that this extension of the electric field increases with increasing conductivity of the aqueous media, as reflected in the decrease of the cell constant.

From these observations it is apparent that the cell constant, for the present flow cell configurations, depends on the dimension of the electrodes, the geometric characteristics of the cell, and the properties of the media.

The process of characterizing the cell constant, in terms of the relationship between the measured conductance and the conductivity of the fluid constitutes calibration of the cell. Once the flow cell is calibrated it can be used to "interrogate" the conductivity of the fluid flowing through it.

3.3.2. Effect of electrolyte concentration

The effect of electrolyte concentration of several electrolyte species was analysed. The measurements of conductance (mS) and conductivity (mS cm^{-1}) appear to be unaffected by the nature of the solute (as expected, Fig.3.6). The cell constant values are plotted in Fig.3.7. In describing an electrolyte solution in the flow cell, it is convenient to represent the conductance (and conductivity) relative to the concentration of solute.

The equivalent conductivity, Λ, is defined as

$$\Lambda = \kappa/E \qquad (3.1)$$

where E is the number of equivalents per cubic centimeter. Consequently, it is necessary to know how the electrolyte solution ionises, i.e. whether the solute ionises simply or not, otherwise the equivalent weight of the solute can not be estimated.

If the manner of ionisation is unknown, then molar conductivity can be used. This quantity can be symbolised as

$$\Lambda_m = 1000\ \kappa/m \qquad (3.2)$$

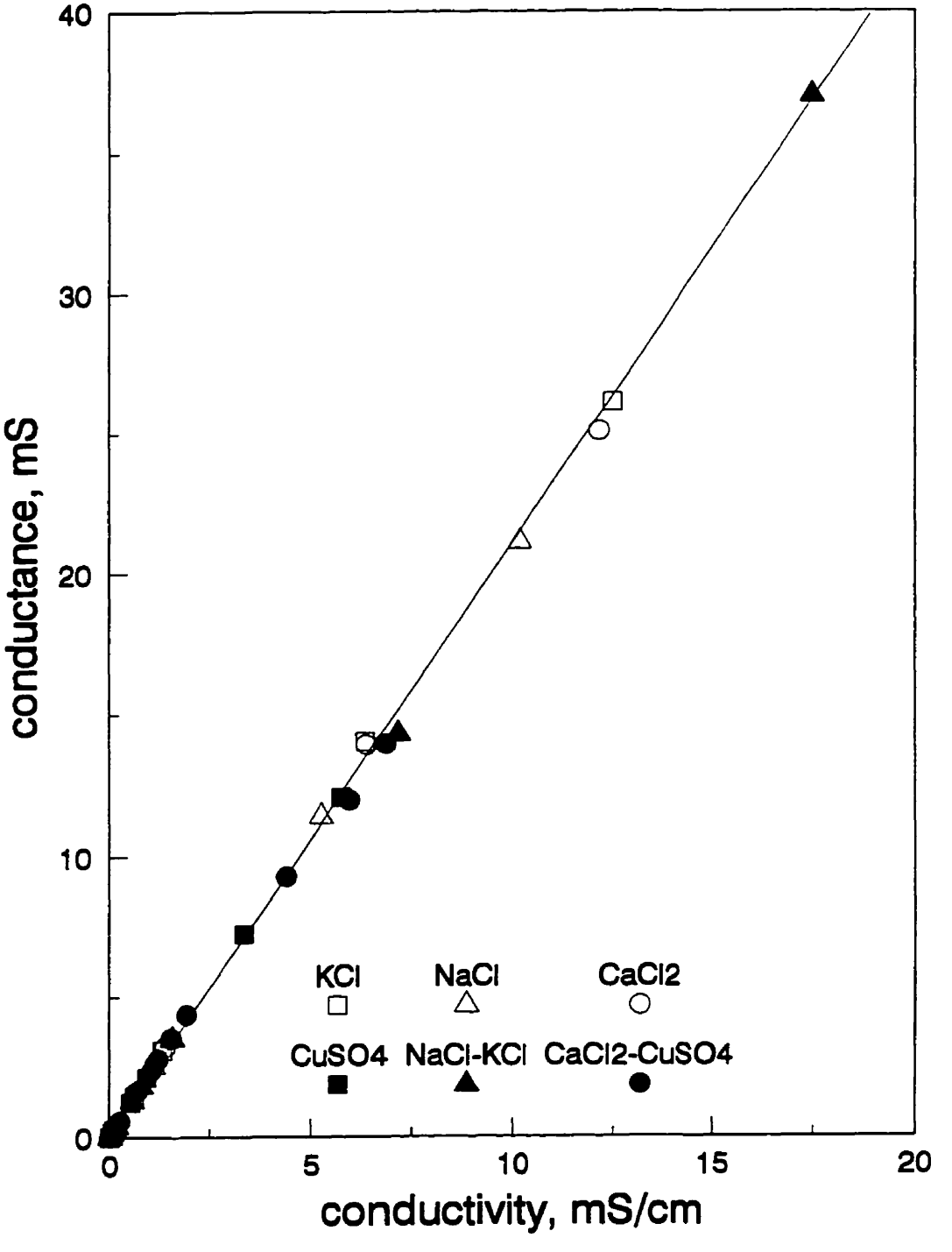

Fig.3.6. Conductance as a function of conductivity: different electrolytes at different concentration; 298 K.

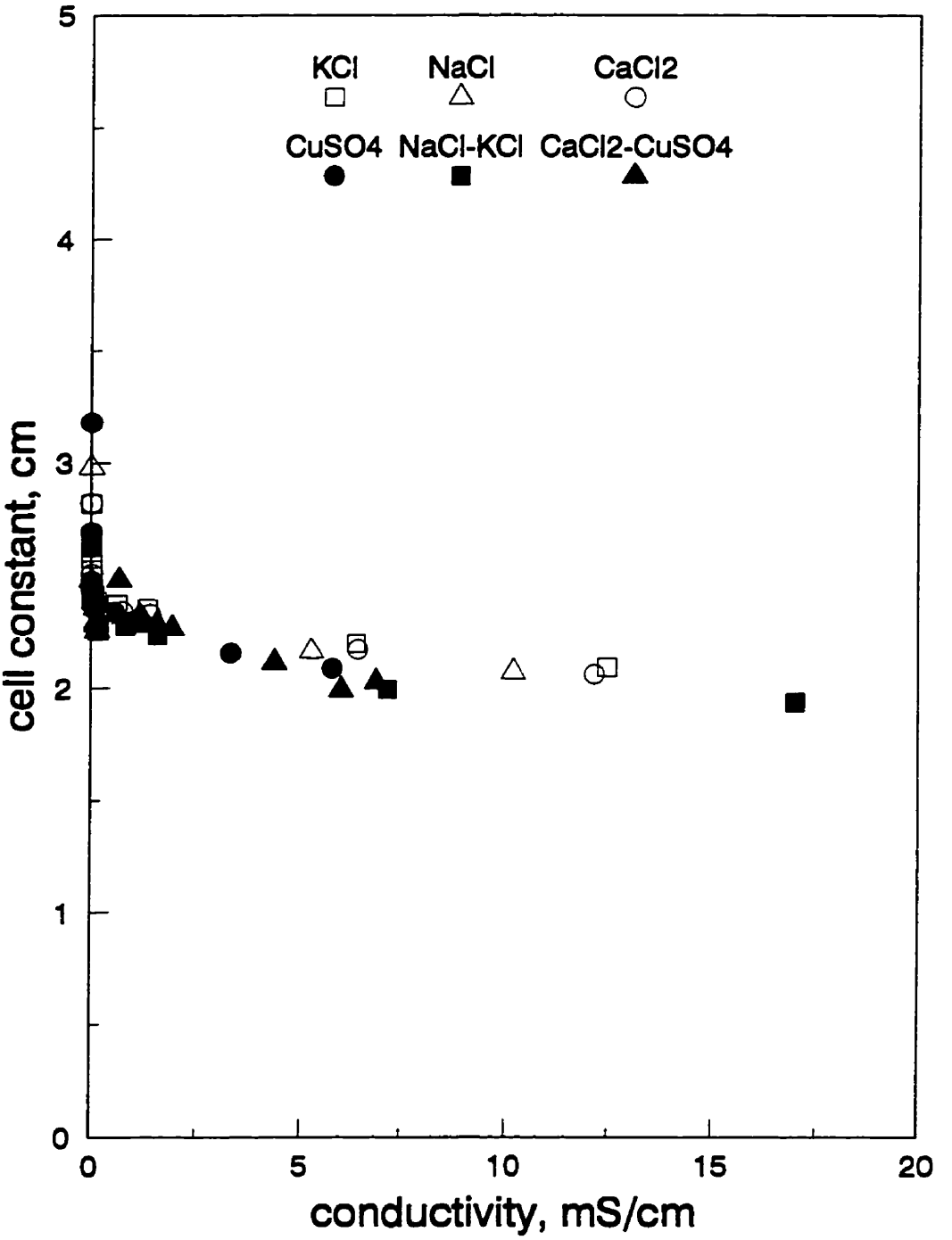

Fig.3.7. Cell constant as a function of conductivity for data in Fig.3.6.

where m is the gram moles of solute dissolved in 1000 cubic centimeter of solvent.

The relation between the equivalent conductivity and the molar conductivity is given by

$$\Lambda_m = \nu_+ z_+ \Lambda = \nu_- z_- \Lambda = \nu z \Lambda \qquad (3.3)$$

where ν_+ is the number of positive ions of charge z_+ formed by the dissociation of one molecule of solute, and ν_- is the corresponding number of negative ions. Since $\nu_+ z_+ = \nu_- z_-$, it can be designated just as νz, with the product of quantities with like signs implied.

These relative conductivity quantities increase on dilution, and approach a limiting value Λ° at infinite dilution. The experimental data for a flow cell for different electrolyte systems, in terms of relative conductivity, are presented in Appendix 2.

3.3.3. Effect of temperature

If ions behave ideally at infinite dilution they have no influence on each other, and their motion will depend only on their nature, and that of the electric field and solvent. Walden's rule states that the product of the limiting molar (or equivalent) conductivity and the viscosity of the solvent for a particular solute should be a constant at a given temperature [Walden, 1929]. This rule can be represented in terms of Stokes's law as

$$\Lambda^\circ \eta = \{zeF/(6\pi r)\} = \text{constant} \times (1/r) \qquad (3.4)$$

where the force on an ion is given by the product zeF, and η is the viscosity of the media.

The viscosity of the media can be represented in terms of Eyring's theory [Eyring, 1936] as follows

$$\eta = (Nh/V) \exp(E/RT) \qquad (3.5)$$

where V is the molal volume of solute species.

Therefore, the molar conductivity of these systems can be represented in terms of Eyring's theory as the Arrhenius relationship

$$\Lambda_m = A \exp(-E/RT) \qquad (3.6)$$

where the constant A contains the properties of the solute, i.e. molal volume, hydrated ionic radii, and the electric field acting on the ion.

Experiments in this work were conducted at controlled temperatures between 288 K and 333 K. The electrolyte species added into the system were KCl, NaCl, $CaCl_2$, and $CuSO_4$, in molar concentrations of 0.001, 0.01, and 0.1.

The experimental data show the conductivity increases with increasing temperature, which is the expected effect since specie mobility increases (Fig.3.8).

The data on the effect of temperature on molar conductivity are given in Appendix 3.

3.3.4 Effect of presence of non conducting bodies

In Chapter 1, it was pointed out that Maxwell's model can be used to estimate the holdup in two-phase dispersions. A form of the model appropriate to the case of a dispersion with a non conducting dispersed phase is

$$\varepsilon = \{1 - (\kappa_d/\kappa_l)\}/\{1 + 0.5(\kappa_d/\kappa_l)\} \qquad (3.7)$$

where ε, κ_d and κ_l are, respectively, the non-conducting phase holdup (i.e. volumetric fraction), the conductivity of the dispersion, and the conductivity of the continuous phase (aqueous electrolyte solution in the present situation).

All the conductivity values in equation (3.7) are estimated from the conductance measurements using a calibrated cell. This means that Maxwell's model as represented in equation (3.7) contains the cell constant characteristics.

In this work, different quantities of monosized glass beads were added into a flow cell

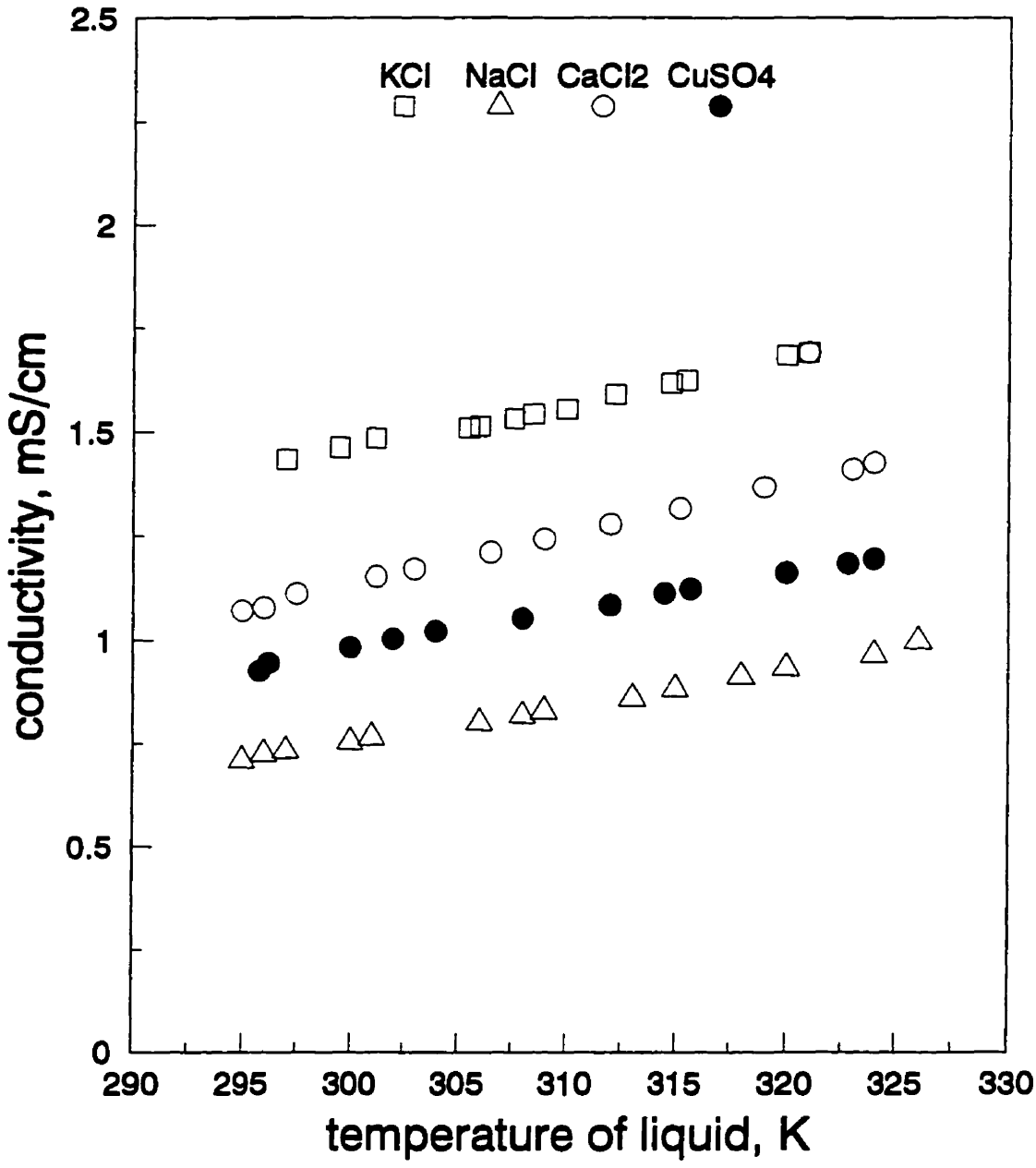

Fig.3.8. Effect of temperature on the conductivity of electrolyte solutions: electrolyte concentration, 0.01 Molar.

containing KCl electrolyte solutions, at 298 K; these amounts were weighed to give the actual holdup of the beads (by knowing their density).

For each increment of beads added, the conductance was measured for different known values of electrolyte conductivity and, knowing the cell constant of the flow cell, the conductivity of the solids-liquid dispersion was estimated. In this manner, equation (3.7) was solved to estimate the glass beads holdup, which was compared to the actual holdup.

Fig.3.9 shows the estimated solids holdup from conductivity as a function of the actual holdup (also, predictions made with MagNet 5.1 are included). Clearly, there is good agreement between the two values. A further representation of these data is in Fig. 3.10 which shows the estimated cell constant as a function of the solids holdup. The information presented in Figs. 3.9 and 3.10 show the importance of knowing the cell constant to be able to use flow cells.

3.4. Application of MagNet 5.1 for design

The software MagNet 5.1 has been described in Chapter 2. Some of its multiple applications with regard to flow cells are further explored in this section.

A cylindrical flow cell of 7.6 cm diameter was "built" using MagNet 5.1. The cell had a non conducting shell (simulating PVC), containing three electrodes in such a manner that the outer electrodes are at one polarity and the central electrode at the opposite polarity. The separation between the edges of the electrodes was 10 cm, and the width of the electrodes, 1.9 cm. A real flow cell with these characteristics was analysed experimentally. The MagNet 5.1 predictions and the experimental measurements are presented in Fig.3.11 (as cell constant vs the conductivity of the media). It can be seen that there is good agreement.

Two cells were "built" in MagNet 5.1 to have different dimensions but the same cell constant. One of the cells was 3.8 cm diameter with electrodes separated 1 cm, and 0.95 cm width; the other cell was 10 cm diameter, with 10 cm electrode separation, and 2.55 cm electrode width. MagNet 5.1 gave a cell constant of 11.27 cm for the first flow cell and of 11.25 cm for the second cell. The predicted behaviour of these cells is presented in Fig.3.12 as conductance vs conductivity. Included in the Figure is experimental data for the second cell which shows close agreement with the predicted

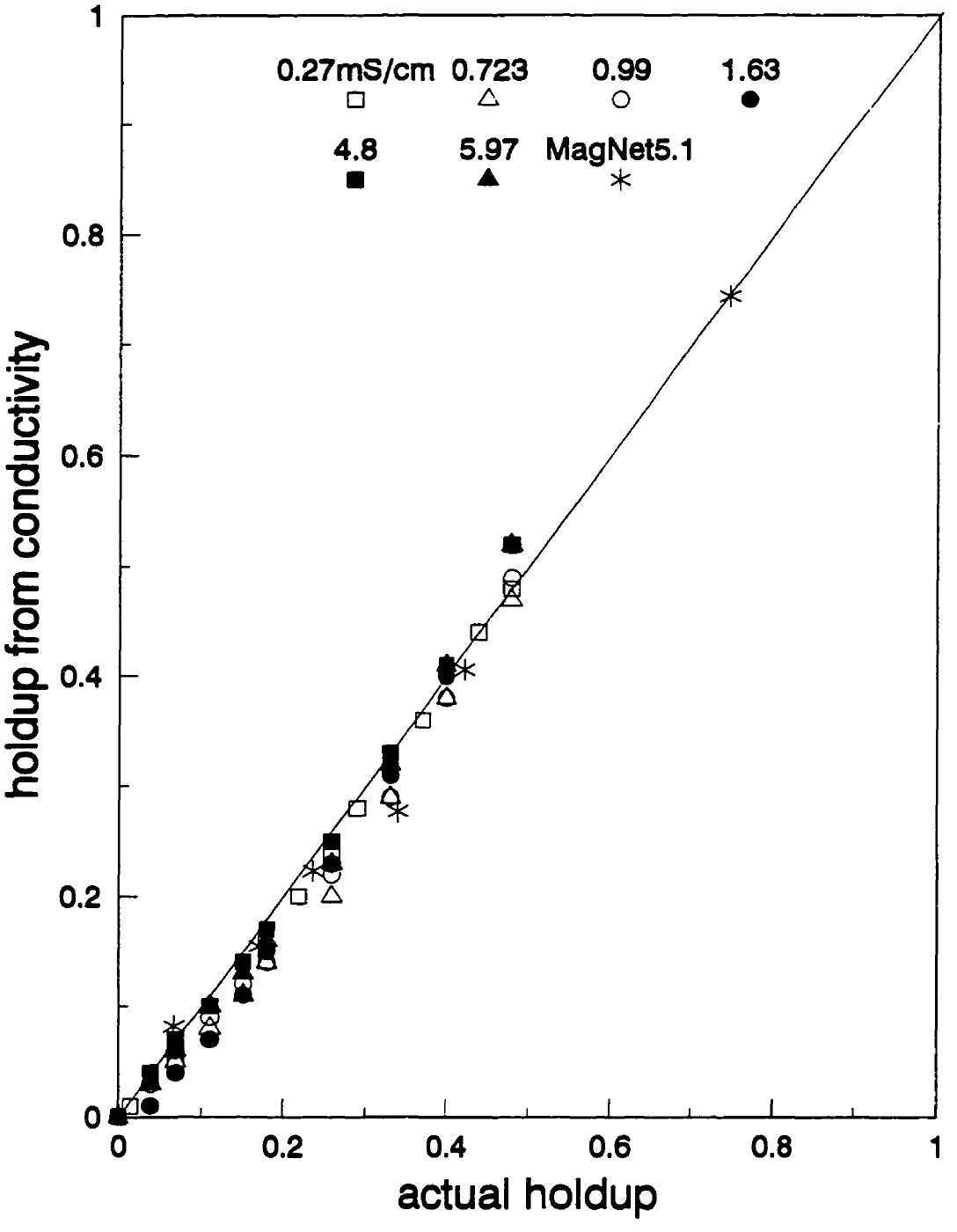

Fig.3.9. Holdup estimated from conductivity vs the actual holdup (measured by weighing the beads and converting to volume knowing the density) for different electrolyte conductivities. Also given is the prediction from MagNet 5.1.

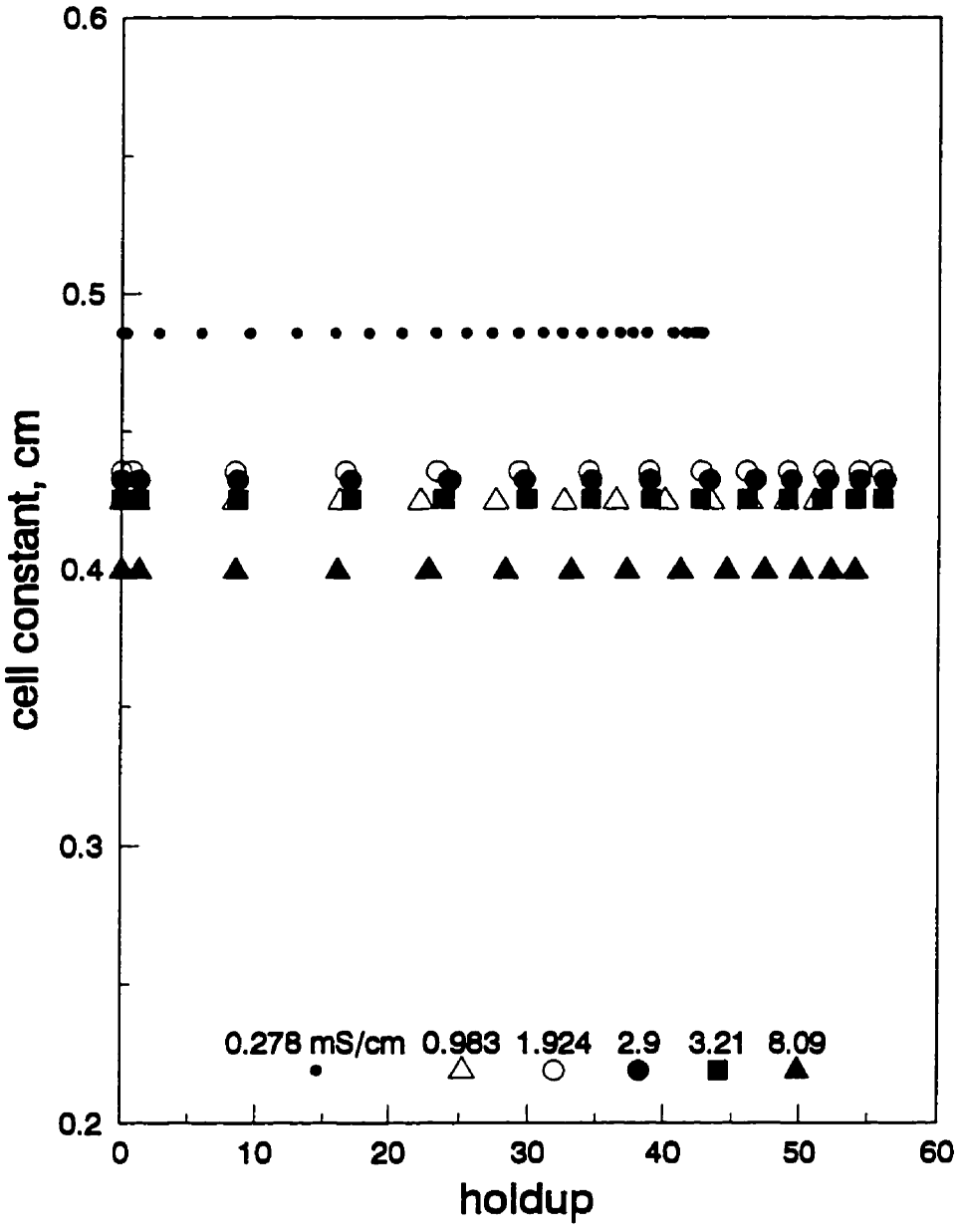

Fig.3.10. Estimated cell constant vs holdup (of glass beads). The plot shows the effect of the conductivity of different electrolyte solutions.
All measurements are at 298 K.

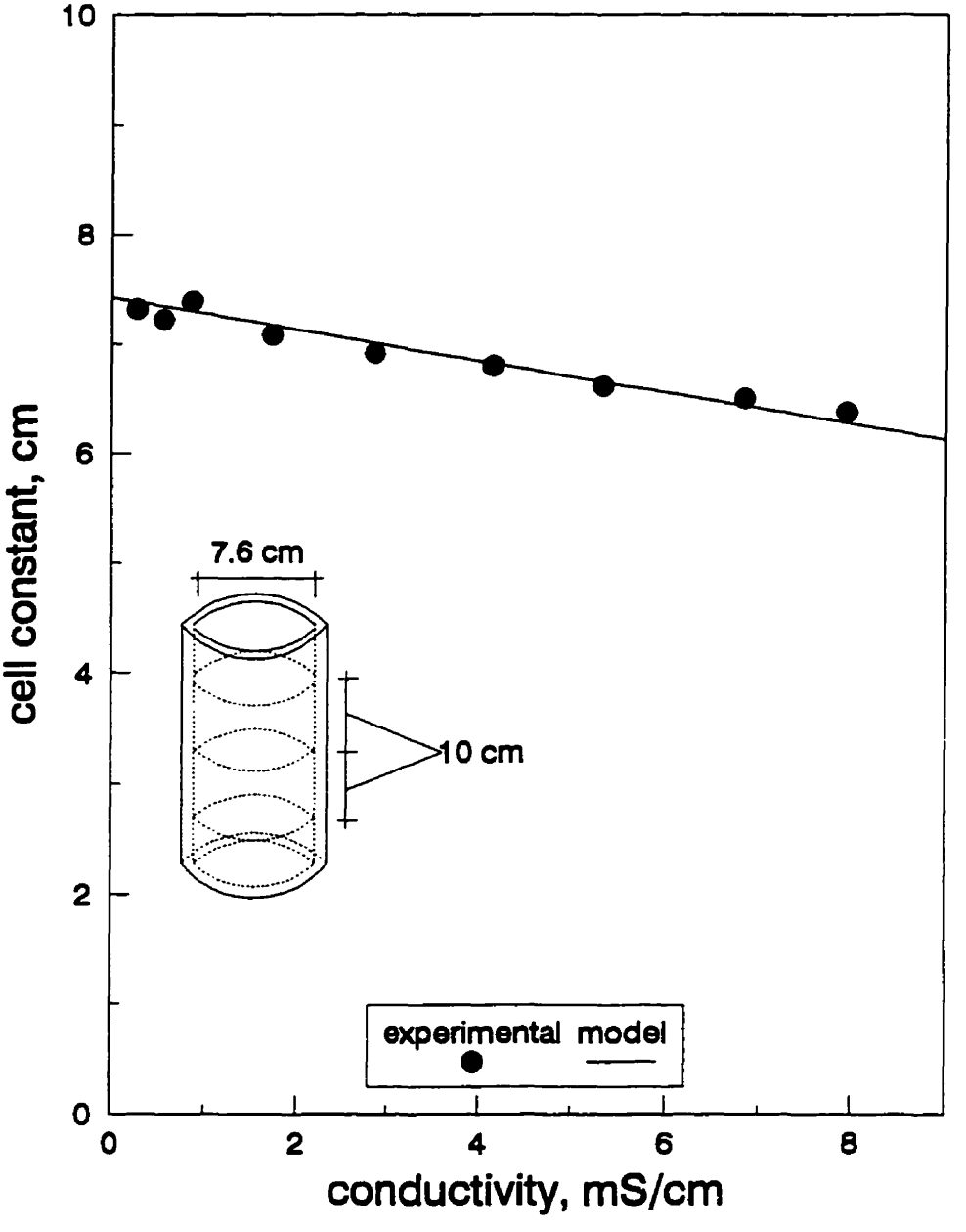

Fig.3.11. Flow cell with three ring electrodes flush to the internal wall: electrode diameter 7.6 cm; electrode width 1.9 cm; end electrodes separation to the central electrode 10 cm. Experimental and predicted cell constant values.

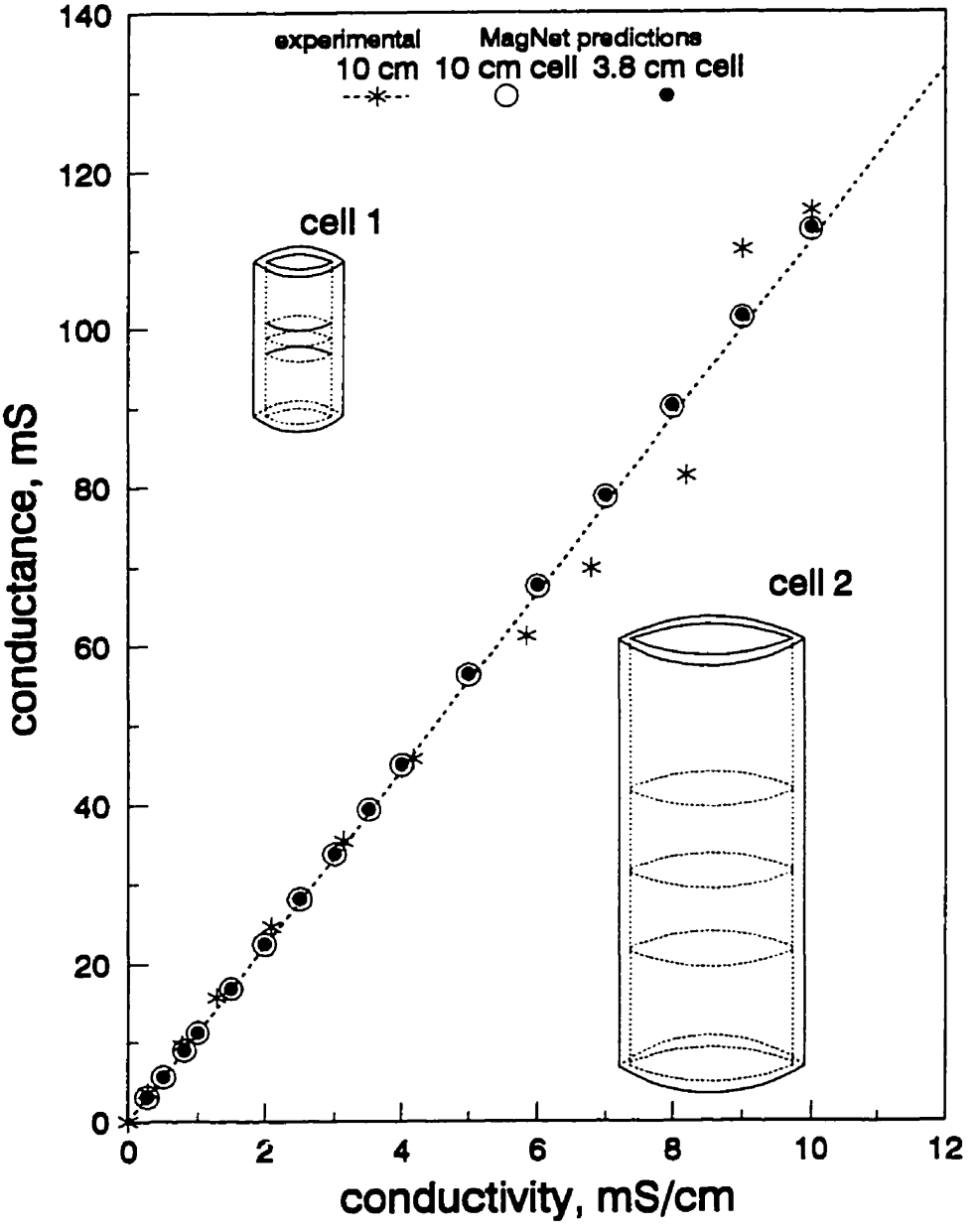

Fig.3.12. Illustration of use of MagNet 5.1 to design two flow cells of different dimension but the same cell constant:

Cell	Diameter	Electrode separation	Electrode width
1	3.8 cm	1.0 cm	0.95 cm
2	10.0	10.0	2.55

Cell constant: 11.27 cm.

relationship.

In many circumstances, the characteristics of the system to be assessed with a flow cell, and the working range of the instrument used to measure the conductance, mean it is useful to carefully select the cell. MagNet 5.1 can help in the selection. As an example, suppose that the conductivity meter to be used is a Bailey industrial type, with three ranges, and for some reason the diameter of the flow cell has been specified. Then, by varying the electrode configuration it is possible to design a flow cell with the appropriate cell constant to work under the conditions of the industrial system without the need to change the range on the meter. Fig. 3.13 presents the predictions for a 3.8 cm diameter flow cell with 1 cm width electrodes. If the flow cell is required to work in the conductivity range from 1.0 to 7.0 mS/cm and the conductivity meter can measure conductance up to 200 mS, then, from Fig.3.13 the suitable flow cell should have electrodes separated 1 cm.

3.5. Summary

One of the most important features of a flow cell is the so-called cell constant. The cell constant has been defined as the ratio between the effective surface area used to transfer electrical energy (which is normal to the flux of electric current), and the distance between two points where the electrical energy is transferred.

The cell constant of a flow cell is determined by using MagNet 5.1 or by calibration against electrolyte solutions of known conductivity.

The cell constant depends mainly on cell dimensions; the experimental observations suggest that the cell constant is independent of the type of electrolyte.

The effect of addition of non conductive bodies in the flow cells has been experimentally analysed. From these observations it is concluded that the cell constant is not affected by the presence of these bodies. The systems are described by Maxwell's model for a dispersion of non-conducting phase in a conducting medium; Maxwell's model relates the fraction of non-conductive phase (holdup) in the system to the conductivity of the continuous phase and the conductivity of the dispersion.

It has been demonstrated that the electromagnetic field associated with the flow cells can be solved by using MagNet 5.1. Predicted cell constants were in good agreement with experimental

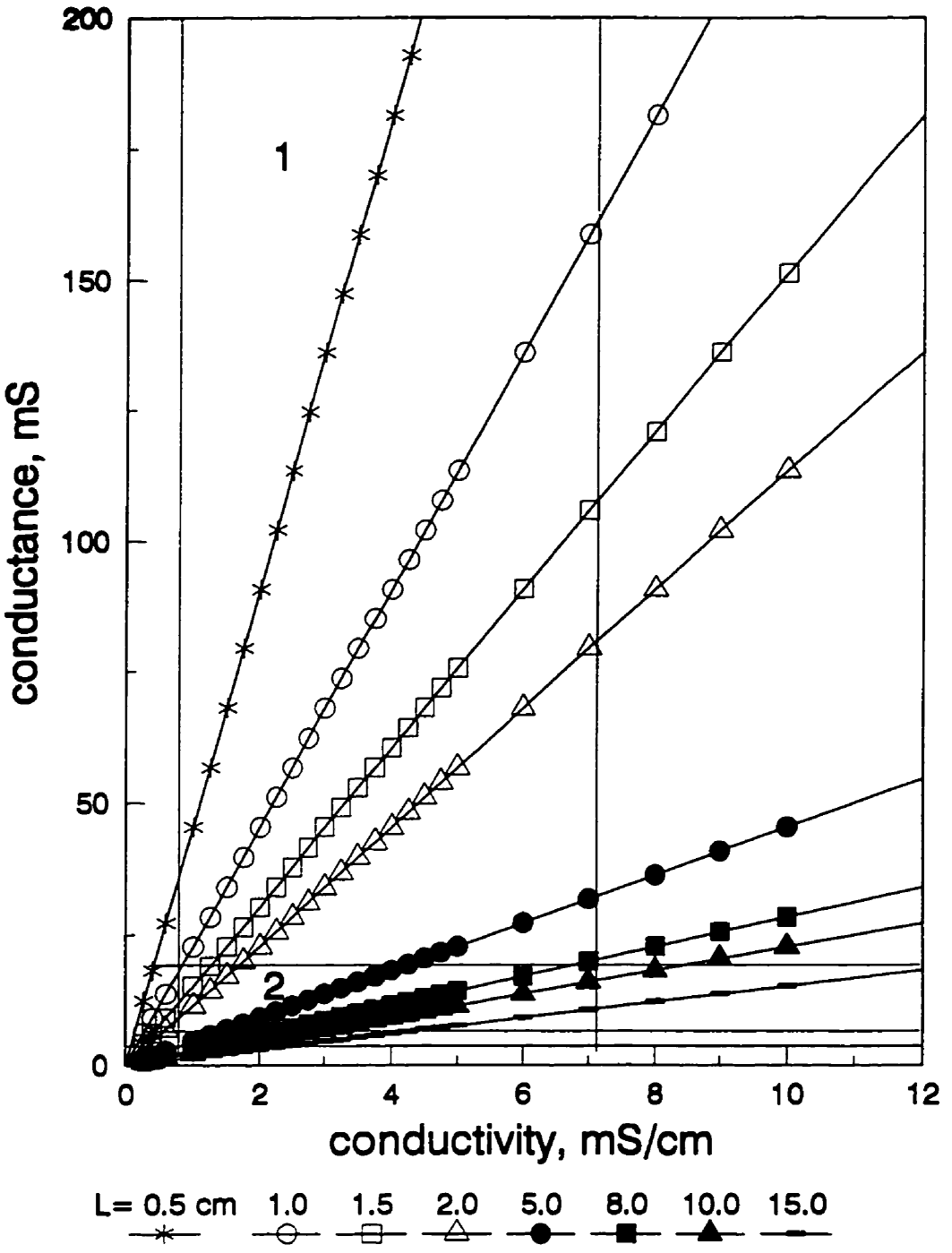

Fig.3.13. Conductance-conductivity predictions (MagNet 5.1) for a 3.8 cm diameter flow cell; estimations are done for different electrode separations varying from 0.5 cm to 15.0 cm; the electrode width is 1 cm in all cases.

results. The model appears to hold the potential for design of flow cells for particular applications in mineral processing systems.

CHAPTER 4

FLOW CELLS AND HOLDUP IN DISPERSIONS

4.1. Introduction

As introduced, a flow cell is one which allows a fluid or dispersion to flow freely through while the electrical conductance is being measured by an electrode arrangement. This Chapter describes the application of flow cells to estimate holdup from conductance measurements in multiphase fluids.

4.2. Maxwell's model to estimate holdup

Maxwell's model, as represented by equation (3.7), gives a relationship between the holdup and the conductivity of the continuum and the dispersed phase in a two-phase system. This representation of the model is also suitable for application in a multiphase system provided it can be represented as a two-phase system. In this sense, previous experimental work [Probst, 1996; Banisi et al., 1995 (a) and (b), 1994, 1993; Uribe-Salas et al., 1994, 1992; Paleari et al., 1994; Xu et al., 1993] have demonstrated the applicability of the model.

In order to apply Maxwell's model, Equation (3.7), to estimate the holdup, there are two requirements: the conductivity of both the dispersion and the continuum must be measured, and the conductivity of the dispersed phase must be zero. The latter requirement is met in the case of bubbles. Therefore, to apply Maxwell's model a technique must be developed to measure the two conductivities. The difficulty lies in measuring the continuum (i.e. bubble-free) conductivity. The technique described in this thesis is based on what is termed the "phase separation" method.

4.3. The phase separation method

A version of the phase separation method to determine the continuum conductivity has been

used extensively in laboratory studies, namely to measure the conductivity of the dispersion on-line and in-situ, while external to the system the conductivity of the continuous phase is measured. In this manner, the required information is collected to estimate holdup.

Estimations of gas holdup by conductivity using this phase separation technique have been compared with those from pressure, volumetric displacement, and sampling of isolated sections of a column [Banisi et al., 1995(a), (b); Shen, 1994; Uribe-Salas et al., 1994].The estimations have been shown to be reliable.

As a test, flow cells were used to measure solids-water dispersion conductivity with water conductivity being measured separately. Two cases are analysed: water-glass beads, and water-silica. Experiments were carried out in the fluidisation-flotation column. The experimental procedure followed was similar to that described in Chapter 3.

Fig.4.1 shows the measurements on glass beads fluidized by water. The data are presented as the conductivity of the solids-water dispersion, and the water only conductivity, as a function of the solids holdup. It is clear that the conductivity of the dispersion decreases as the fraction of the non conductive phase increases, while the conductivity of the continuous phase remains at the same value. When the glass beads were replaced by silica the the results were similar (Fig. 4.2).

Fig. 4.3 shows the comparison between the solids holdup estimated from the conductivity measurements and the actual solids holdup calculated from the weight of solids added into the system. It can be seen that there is good agreement between the experimental results for both silica and glass beads.

This phase separation method, using measurements on the continuum external to the system, is not suitable for measurements in industrial systems, since external measurements may not be relevant to the conditions inside the reactor.

4.4. Summary

The experimental data in the present work, as well as from previous investigations, have shown that the Maxwell model applies to dispersions encountered in mineral processing and gives accurate estimations of holdup.

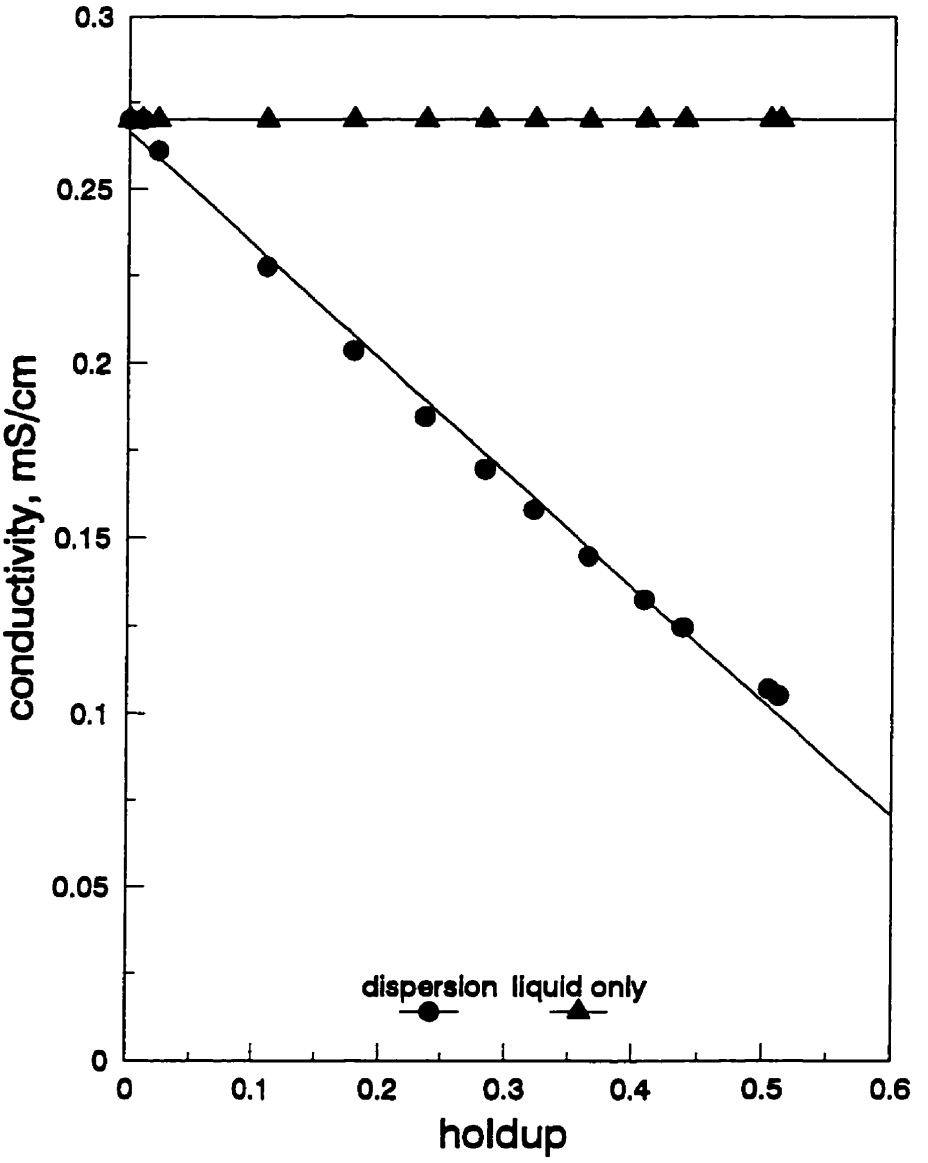

Fig.4.1. Experimental measurements in the fluidisation-flotation column; 3 mm glass beads in fluidised bed in the column; holdup is estimated by applying the phase separation method; liquid only conductivity is measured externally to the column.

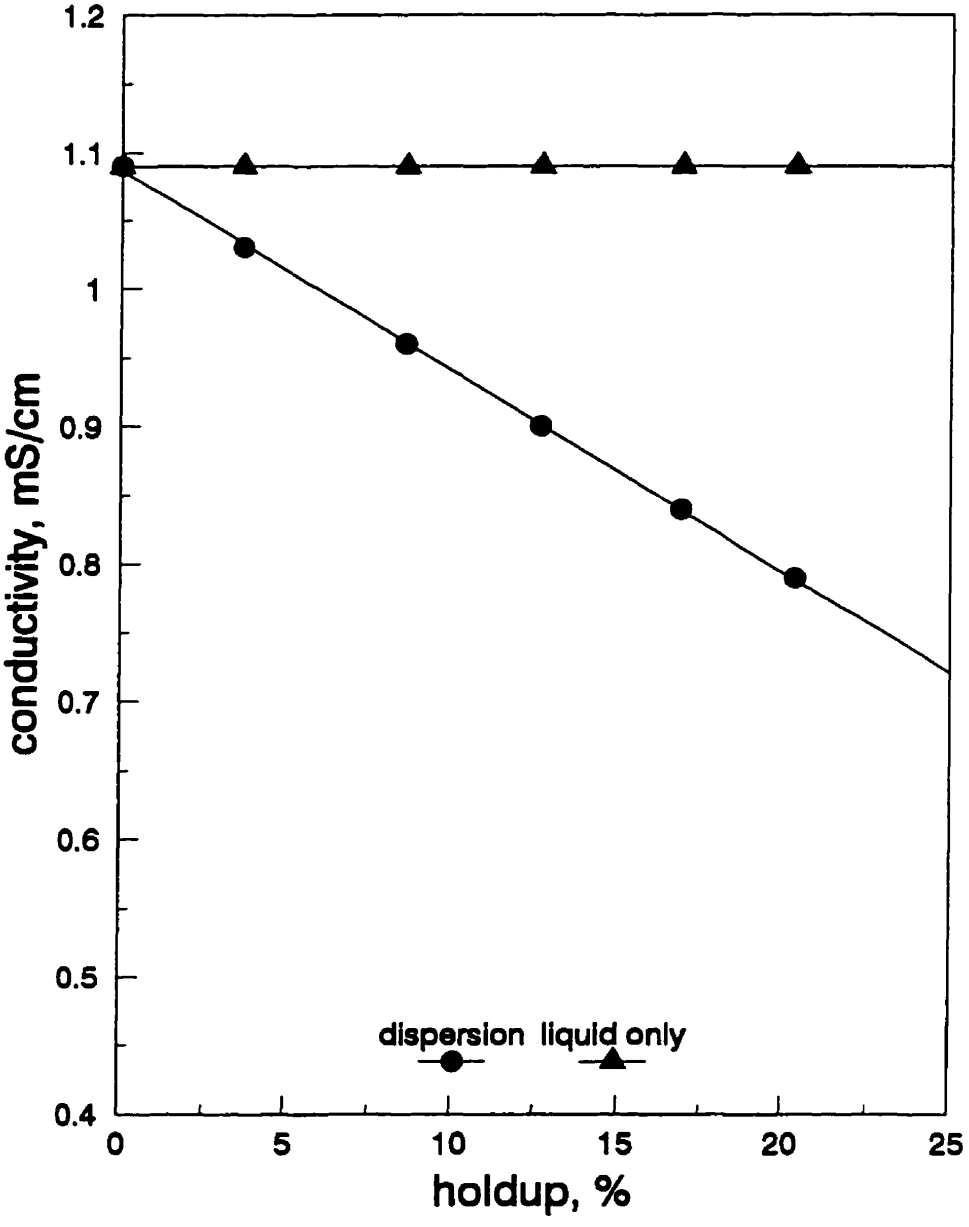

Fig.4.2. Silica-water slurry in a vertical flow cell; phase separation method to measure holdup; the silica was minus 150 um.

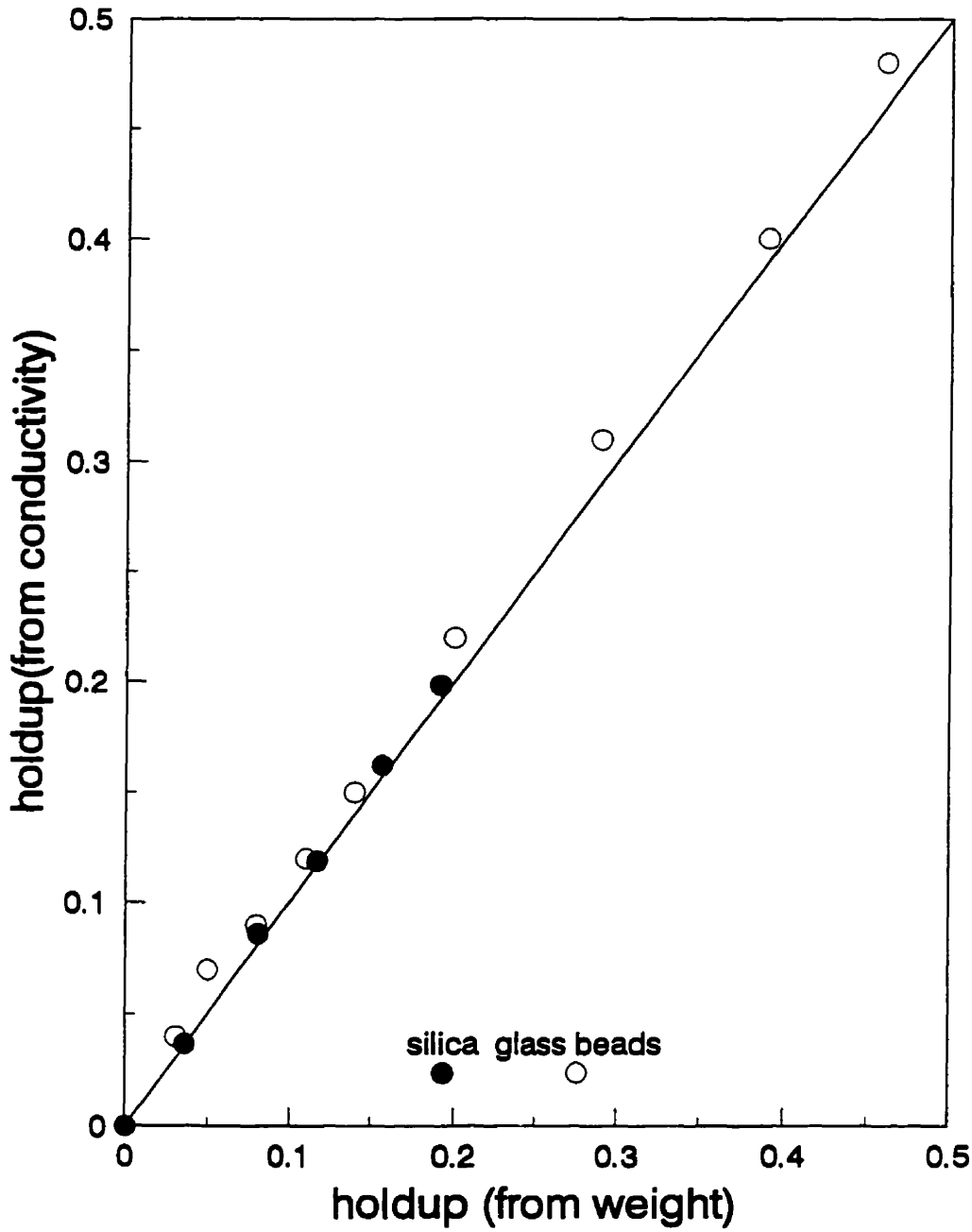

Fig.4.3. Experimental determination of solids holdup by conductivity and that determined by weight of solids; comparison between the addition of silica and glass beads.

The approach using Maxwell's model is presented. The phase separation method has been shown to give reliable holdup estimates by comparison with direct measurements. The plan is to try to exploit the technique for monitoring streams on-line, in-situ, and in real time. The use of flow cells in this endeavour appears appropriate.

CHAPTER 5

DEVELOPMENT OF A GAS HOLDUP PROBE

It has been shown that flow cells can be used to measure liquid and dispersion conductivity. Also, it was shown that the phase separation technique combined with Maxwell's model, can give accurate estimates of holdup. This chapter is devoted to the task of designing a probe to measure gas holdup in gas-slurry dispersions.

5.1. The phase separation method

5.1.1. The open flow cell

In a flotation machine, e.g. a flotation column, the conductivity of the dispersion can be measured by a flow cell open at both ends, such that the dispersion flows through with minimum disturbance. This is called an "open" flow cell.

Initially, the open flow cell had an arrangement of two stainless steel electrodes flush to the internal wall of the cell. But, measurement of the dispersion conductivity was not reliable apparently because the electric flux followed two paths between the electrodes: one through the cell (as desired), and another outside of the cell (Fig.5.1.(A)). Consequently, the cell constant was not stable because the outside path changed depending on the conductivity of the dispersion.

To resolve this, the electrode arrangement was changed to three electrodes, a central one at one polarity with the two outer electrodes at opposite polarity. With this design, the current flux was constrained to flow only through the cell and the cell constant was stable (Fig.5.1(B)). In fact the cell constant approached the geometric value. Therefore, the open cell with three electrodes was adopted.

The next problem was to design a method of measuring the continuum in the absence of the dispersed gas phase.

(A) (B)

Fig.5.1. MagNet 5.1 solution of an open flow cell with (A) two electrodes, and (B) with three electrodes (the central one at different polarity as the two outer electrodes); the representation shows the equipotential lines.

5.1.2. The syphon flow cell

Guiding principle: When a swarm of air bubbles passes through a column of water, the bubble-water dispersion presents a lower (dispersion) density relative to that of water with no air bubbles.

This difference in density was exploited to develop a technique to separate the continuous phase (water, in two-phase systems; slurry in three-phase systems) from the dispersion in order to measure its conductivity. The separation is accomplished in a flow cell which is open at the top, but closed at the bottom, except for a small side orifice. Because the cell is closed at the bottom, it does not allow the ascending air bubbles to enter the cell; therefore, the cell becomes filled with liquid (slurry) without air, creating a hydrostatic pressure difference across the orifice at the bottom of the cell which causes the liquid to flow out. When this happens, continuous replenishment of fresh liquid takes place from the top of the cell creating, in the end, a syphon effect.

Equiping the "syphon" cell with the same three electrode arrangement, the conductivity of the continuous phase can be measured. Successful operation requires that the liquid velocity in the downward direction be lower than the rise velocity of the air bubbles outside the cell, otherwise air bubbles could be drawn into the cell at the top. Also, in the case of three-phase systems, the velocity of the slurry in the syphon cell must be higher than the particle settling velocity to avoid particles settling at the bottom of the cell, and eventually obstructing the orifice.

The required velocity range in the syphon cell depends on the dimensions of the cell, and the size of the discharge orifice. The velocity range can be estimated using Bernoulli's equation, employing a so-called orifice discharge coefficient, coupled with knowledge of bubble swarm velocity and solid settling velocities.

Use of Bernoulli's equation in design of syphon cell: A fluid flowing in a conduit has kinetic energy by virtue of its mass and motion. If the fluid flows at an angle to the horizontal, the potential energy of the fluid varies in the flow direction, and the friction arising from the shear stress exerted on the fluid by the conduit walls converts mechanical energy to thermal energy.

For a fluid flowing through a section of pipe between two locations defined by two planes, 1 and 2, let the static pressure at those points be P_1 and P_2. The fluid enters the pipe (at 1) with velocity v_1 and leaves (at 2) with a flow velocity v_2. The fluid entering the pipe is being pushed by the

fluid behind it, and the work done per unit mass is P_1V, where $V = 1/\rho$ is the volume per unit mass of the fluid (and the work done on the fluid is P_1/ρ). Similarly, the fluid leaving the pipe is pushing the fluid in front of it and the work done on unit mass of fluid leaving is P_2V (or P_2/ρ). The difference between these two is the flow work done on the fluid.

The kinetic energy for the fluid entering the pipe at 1 is $E_k = (1/2)\, m\, v_1^2$ which per unit mass, is $(1/2)\, v_1^2$. Similarly the kinetic energy per unit mass at 2 is $(1/2)\, v_2^2$. The potential energy of the fluid entering the pipe is $E_P = m\, g\, Z_1$ where Z_1 is the height with respect to point 2; in terms of unit mass $E_P = g\, Z_1$; similarly, the potential energy per unit of mass at 2 is $E_P = g\, Z_2$.

The conservation of energy between points 1 and 2, requires that the flow work done on the fluid equals the sum of the change in kinetic energy plus the change in potential energy:

$$(P_1/\rho) - (P_2/\rho) = (1/2)\,(v_2^2 - v_1^2) + g\,(Z_2 - Z_1) \qquad (5.1)$$

which is Bernoulli's equation. If the fluid is inviscid, the local fluid velocities at points 1 and 2 are independent of the position in the cross section area. Therefore, the mass flow rate in the tube is $M = \rho\, A_1\, v_1 = \rho\, A_2\, v_2$. If the fluid is not inviscid, the local flow velocity at any position along the tube is a function of the radial position. In this case $M = \int \rho\, v\, dA$ and the rate at which kinetic energy enters at point 1 is (kinetic energy/mass)×(mass/unit time) $= (1/2)\, v_1^2 \times M$, therefore, kinetic energy entering in unit time is $(1/2) \int \rho\, v_1^3\, dA$, or for an incompressible fluid flowing in a tube, the kinetic energy in unit of time is $(1/2)\, 2\pi\, \rho \int r\, v_1^3\, dr$.

For horizontal laminar flow in a tube of radius R, $v_x = (\Delta P/L)\,\{(R^2 - r^2)/4\eta\}$ derived by substituting in the previous expression, the kinetic energy entering in unit time can be represented as $\pi\, \rho(\Delta P/L)^3\, (1/4\eta)^3 \times \int (R^6 - 3R^4r^2 + 3R^2r^4 - r^6)r\, dr = \pi\, \rho\, (\Delta P/L)^3\, (1/4\eta)^3\, R^8/8$, which is equal to $\pi\, \rho\, (\Delta P/L)^3\, (R^2/8\eta)^3\, R^2$, and the average flow velocity is $\underline{v}_x = (\Delta P/L)\, (R^2/8\eta)$, therefore, the energy entering in unit time is $\pi\, \rho\, \underline{v}_1^3\, R^2 = \rho\, A\, \underline{v}_1^3 = (\rho A \underline{v}_1)\, \underline{v}_1^2$, and the mas flow rate is $\int \rho\, v\, dA = \rho\, A\, \underline{v}$, and the kinetic energy entering in unit time is $M\, \underline{v}_1^2$ or per unit mass $= \underline{v}_1^2$.

Similarly, the kinetic energy leaving per unit mass at plane 2 is $= \underline{v}_2^2$.

If fluid flow is fully turbulent, the kinetic energy per unit of mass would be as approximately $(1/2)\underline{v}^2$. Both laminar and turbulent flow are accommodated by the equation: kinetic energy per unit

mass = $(\underline{v}^2/2\beta)$; where $\beta = 0.5$ for laminar flow and $\beta = 1$ for turbulent. Substituting in equation (5.1), leads to

$$(P_1/\rho) - (P_2/\rho) = (\underline{v}_2^2/2\beta_2) - (\underline{v}_1^2/2\beta_1) + g\,(Z_2 - Z_1) \qquad (5.2)$$

with units $\{(\text{kg m/s}^2)\text{m}\}(1/\text{kg}) = \text{J/kg}$.

Equation (5.2) must be satisfied to account for the dissipation of energy caused by the viscous drag on the flowing fluid by the tube wall. This quantity is termed friction loss, E_f, and the energy balance becomes:

flow work done on the fluid = (increase in the kinetic energy) + (increase in the potential energy) + (friction loss)

If between locations 1 and 2, heat Q is added to unit mass of the fluid and work ω is done on unit mass of the fluid, the energy balance becomes

$$\text{flow work} + Q + \omega = \Delta E_k + \Delta E_p + E_f$$

or $$\{(P_2/\rho) - (P_1/\rho) + \{(v_2^2/2\beta_2) - (v_1^2/2\beta_1) + g\,(Z_1 - Z_2) - Q - \omega + E_f = 0 \qquad (5.3)$$

which is called the modified Bernoulli equation.

As the fluid at both points 1 and 2 is in contact with the dispersion, $P_1 \approx P_2$. From mass balance considerations, the volume flow rate through the orifice equals that through the syphon tube,

$$\underline{v}_1\,\pi\,D^2/4 = \underline{v}_2\,\pi\,d^2/4;\ \underline{v}_1 D^2 = \underline{v}_2\,d^2;\ \underline{v}_1 = \underline{v}_2(d/D)^2,$$

such that if $d \ll D$, then $\underline{v}_1 \ll \underline{v}_2$; therefore, $E_f = 2\,f\,(h/D)\,\underline{v}_1^2 + (1/2)\,e_f\,\underline{v}_2^2$, and neglecting the term which contains $\underline{v}_1$;

$$\underline{v}_2^2/2\ \beta_2 + g\ (Z_2 - Z_2) + (1/2)\ e_f\ \underline{v}_2^2 = 0$$

$$\underline{v}_2^2\ \{1/(2\beta_2) + (1/2)\ e_f\} = g\ (Z_1 - Z_2);\ \text{and}\ Z_1 - Z_2 = h;$$

$$\underline{v}_2 = (2\ g\ h)^{1/2}/\{(1/\beta_2) + e_f\}^{1/2};$$

In this representation, the term containing the friction factors, β_2 and e_f, is termed the discharge coefficient of the orifice, C_D, and is represented as

$$C_D = \{(1/\beta_2) + e_f\}^{-1/2},$$

Therefore,

$$\underline{v}_2 = C_D\ (2\ g\ h)^{1/2} \qquad (4.4)$$

which relates the velocity of the fluid at the discharge orifice with the length of the syphon tube.

The determination of the discharge coefficient was done by fixing the column of liquid inside the tube at a given height (at constant temperature, i.e. 298 K), and measuring the liquid flow rate discharging from the tube. Different orifice diameters were tested to give the corresponding discharge coefficient and liquid flow rate through the tube. By choosing the appropriate orifice diameter it is possible to meet the working requirements of the syphon tube, in terms of the bubble swarm velocity, and, in the case of a solids-gas-liquid dispersion, the solids settling velocity. Fig.5.2 represents the syphon flow cell.

Fig.5.3 presents the measurements of liquid velocity at the orifice as a function of the height of the column of liquid inside the syphon tube, and the estimated value of the discharge coefficient. Fig. 5.4 presents the velocity of the liquid inside of the syphon tube as a function of the height of the column of liquid for each orifice diameter.

Bubble swarm velocities have been measured [Shen, 1994] in air-water systems under different conditions of frother concentration and air superficial velocities. It was found that at a

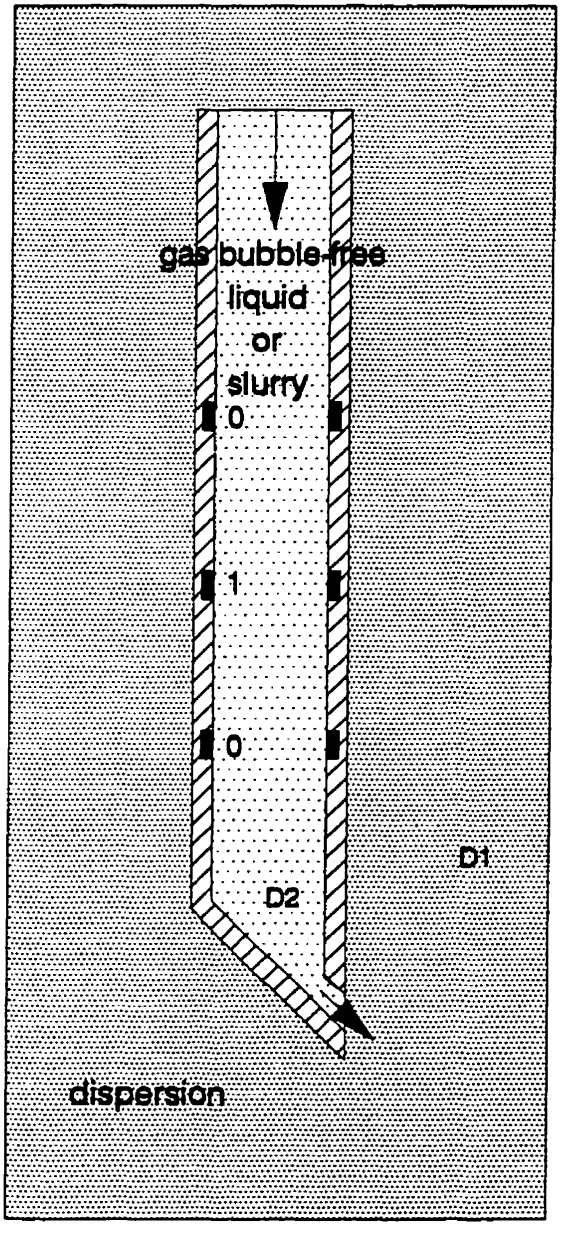

Fig.5.2. Schematic representation of the syphon flow cell in an air-liquid dispersion; the three ring electrode arrangement is shown; bubble-free continuous phase with density D2 is created in the cell; density D2 is greater than the dispersion density D1; arrows show the direction of the continuous phase motion through the cell.

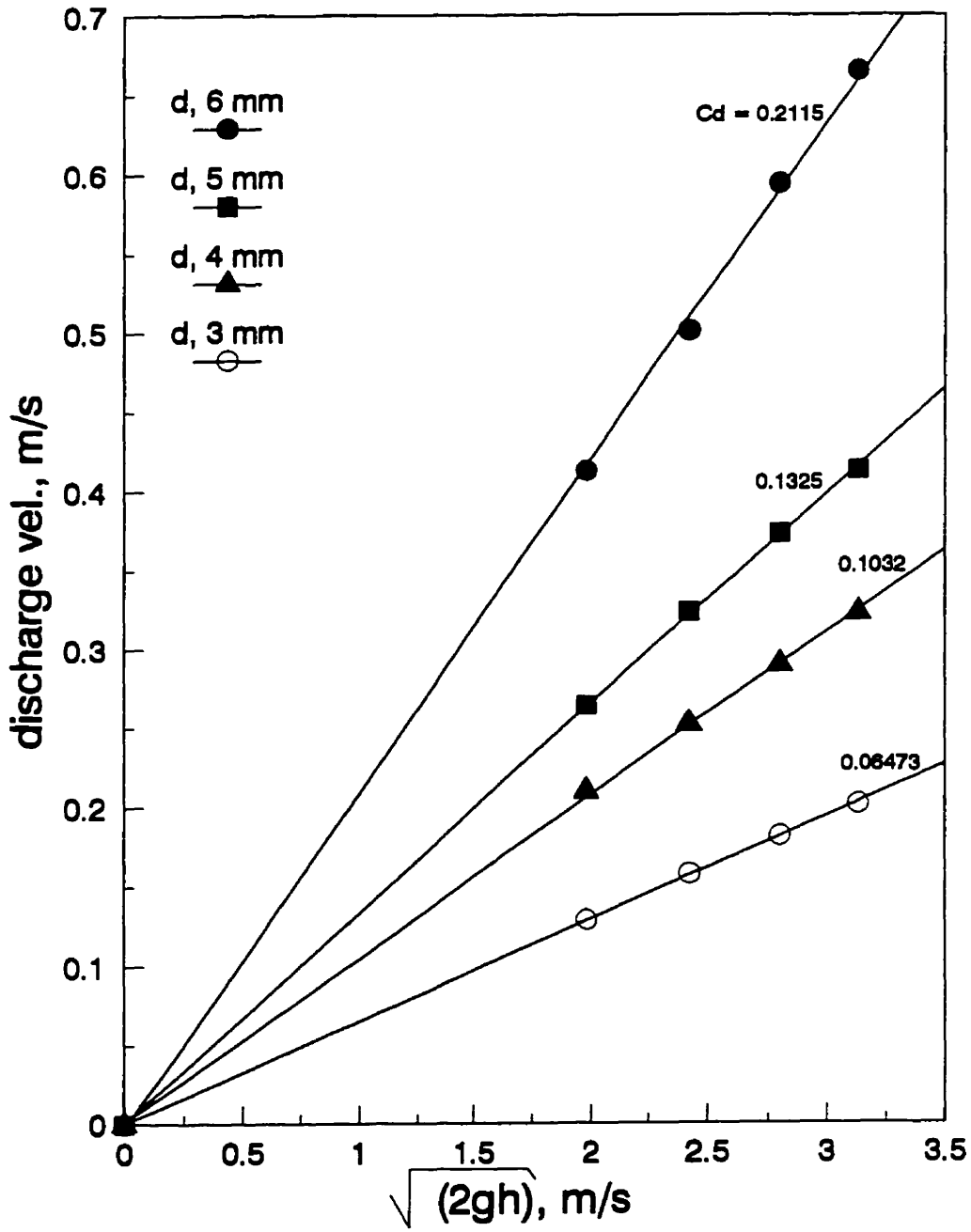

Fig.5.3. Determination of discharge coefficient in the syphon cell for orifice diameters between 3 and 6 mm.

superficial gas velocity of 1.25 cm/s bubble swarm velocities were 12 cm/s, 7.8 cm/s, and 6.9 cm/s in water with no frother, 10 ppm Dowfroth 250, and 20 ppm Dowfroth 250, respectively. The presence of solids may increase the bubble swarm velocities [Banisi et al., 1995, (a) and (b)].

Settling velocities of silica for particles 75μm, 150μm, and 300μm, are approximately 0.0045 cm/s, 0.018 cm/s, and 0.07287 cm/s, respectively [Heiskanen, 1993].

Therefore, by comparing the liquid velocities in the syphon tube with these velocities of rising bubbles and settling solids, the dimensions of syphon flow cell for a given duty can be assigned. In the present design the syphon cell was 44 cm long, 3.8 cm diameter, with a 6 mm orifice diameter (which presents a discharge velocity at the orifice of 0.65 m/s; and a liquid velocity in the tube of 1.6 cm/s) that ensure that no air bubbles enter the cell, and that solids are swept out of the cell through the discharge orifice.

5.1.3. The probe: proof of concept

The last two sections have introduced the use of an open flow cell to determine the conductivity of an air-liquid (slurry) dispersion, and the use of a syphon cell to measure the continuous phase. As explained, these two flow cells contain three electrodes to restrain the electrical field to the volume of the cell (in between the top and bottom electrode rings).

The assembly of the open and syphon flow cells together is referred to as the probe. A prototype, with dimensions and construction details, is shown in Fig.5.5.

The prototype was subjected to two types of experiments:

- To characterize the cell constants for the two cells
- To assess gas holdup estimates.

These experiments were run in a laboratory column 50 cm in diameter and 4 m high. The column was run batch using water-electrolyte solutions (with and without frother).

Air was dispersed through 8 cylindrical spargers (10 cm in diameter and 16.5 cm long) installed vertically and equally spaced in a ring of diameter at 35 cm. The column had four pressure taps each separated by 1 m with the first stationed 50 cm from the top. The probe was placed and

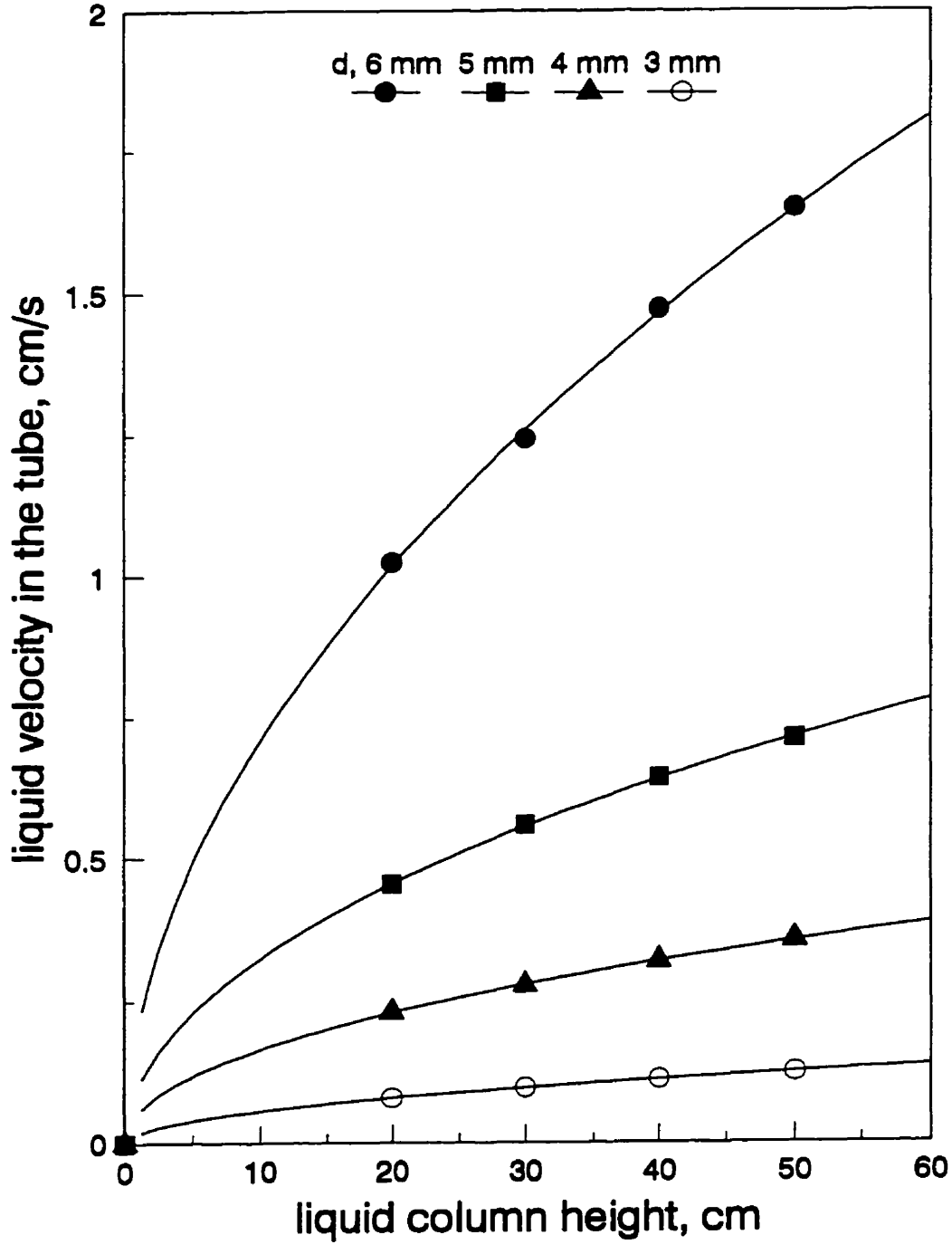

Fig.5.4. Liquid velocity in the syphon tube as a function of the length of the tube. Bubble swarm velocities typically vary from 7 to 12 cm/s in water-frother systems [Shen, 1994], and solid settling velocities from 0.0045 cm/s to 0.07 cm/s [Heiskanen, 1993].

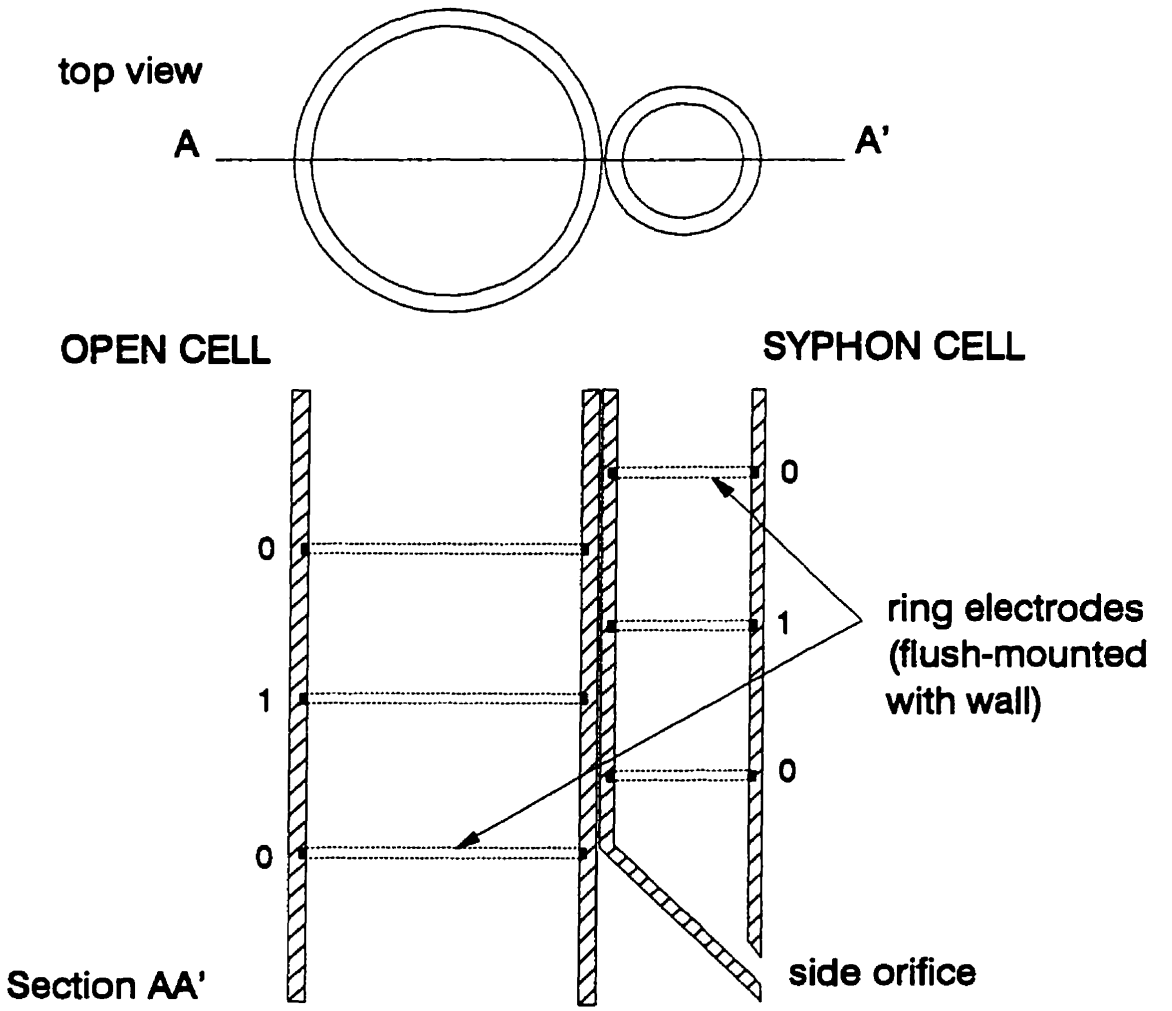

Fig.5.5. The combination of the open and syphon flow cells to form the probe. For the probe described in the text the open cell is 10 cm in diameter and the syphon cell is 3.8 cm in diameter; electrodes are separated 10 cm.

maintained at the centre of the column between the second and the third pressure taps (2 m from the top). Fig.5.6 illustrates the set-up.

In the tests to characterize the cell constant, the two cells were calibrated using KCl electrolyte solutions of known conductivity (with no air); the conductance in each cell was measured with a conductivity meter (Tacussel CD816, and Tacussel CDVR62). The conductivity was varied between 0.27 and 10 mS/cm.

The results of calibration are summarised in Fig.5.7 where the conductance measured in each cell is plotted as a function of the conductivity of the electrolyte solution. The slope equals the cell constant. The flow cells with the present geometry are not ideal, as the numerical value of the cell constant varies with the conductivity of the fluid. The relationship was fitted by a polynomial.

The test to assess the probe performance consisted in simultaneous collection of pressure and conductance values at several air flowrates, with the column run with water only (with and without frother). The air flowrate was monitored and controlled using a thermal based mass flow controller (MKS, model 1562).

When the system contains no solids, the gas holdup can be accurately measured from pressure difference, which provides a standard to compare against the gas holdup measured with the conductivity probe. Gas holdup in this case is estimated from pressure using the equation:

$$\varepsilon_g = 1 - \Delta P/\Delta L \qquad (5.5)$$

where ΔP is the pressure difference between two points separated a vertical distance ΔL. A differential pressure transmitter (Bailey, model PTSD) was connected to the second and the third pressure taps, to record the pressure difference. The probe cells were connected to the conductivity meters (Tacussel models CD810, and CDRV 62). The analog outputs of both conductivity meters and the pressure transmitter were processed in a A/D converter and transmitted to the computer using serial communication.

The ability of the probe to measure gas holdup depends entirely on the performance of the syphon flow cell which must separate the air bubbles from the continuous phase under all conditions.

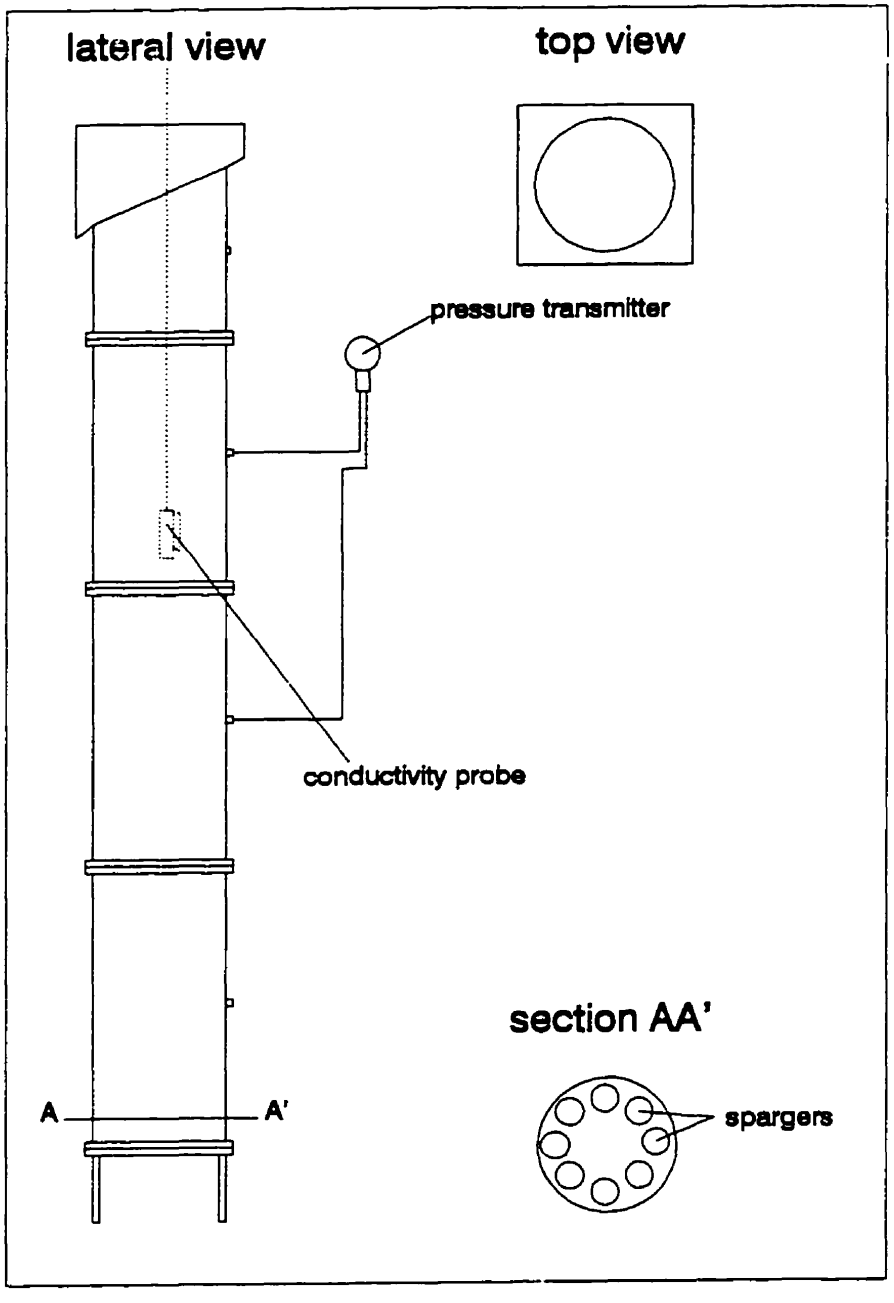

Fig.5.6. General set-up for laboratory tests. The column is 4 m high, and 0.5 m in diameter.

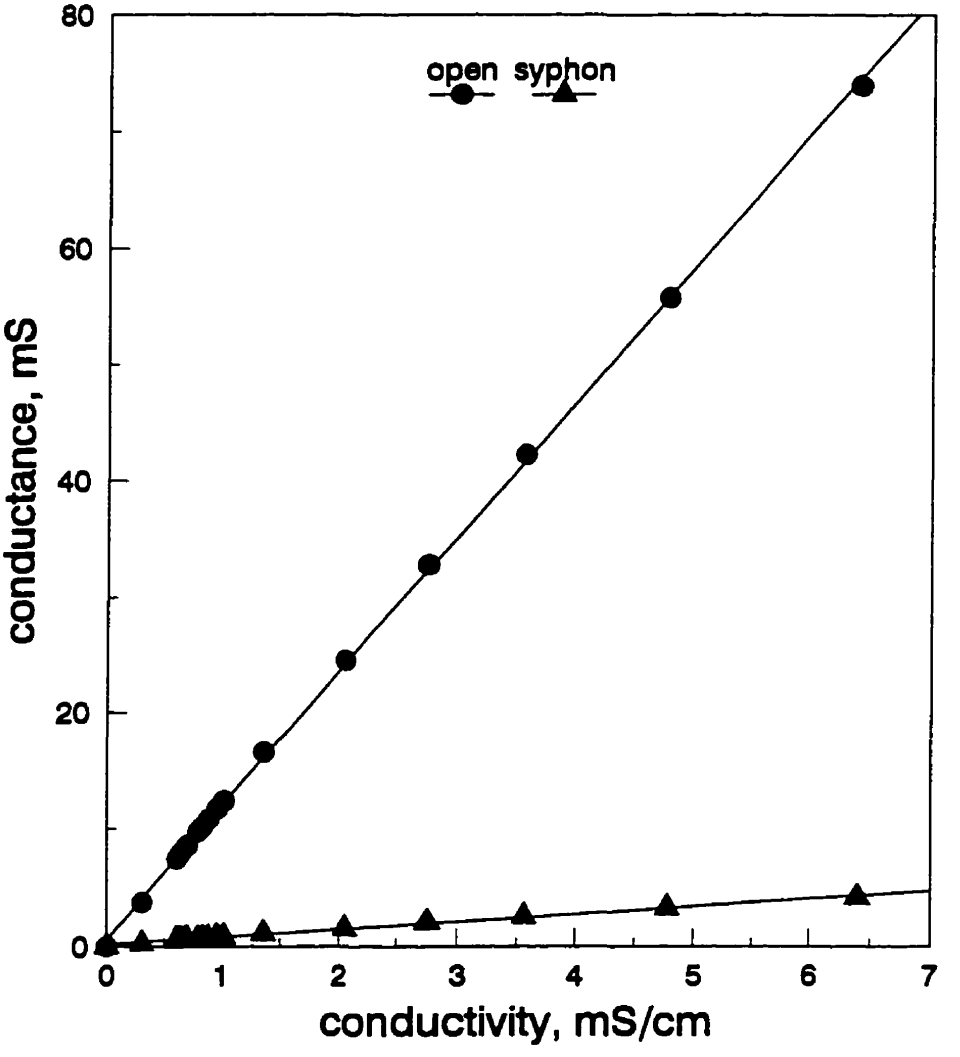

Fig.5.7. Calibration of the open and syphon flow cells in the probe.

Results of tests are presented in Fig.5.8 where the conductivity of the dispersion and the continuous phases, measured with the open and the syphon flow cells, respectively, are given as a function of the air velocity in the column. It is observed that the conductivity of the continuous phase, measured with the syphon flow cell, remains constant regardless of air flowrate and equal to the value measured independently; this result proves that no air bubbles enter the syphon flow cell.

In contrast, the conductivity measured with the open flow cell decreased as gas rate was increased, indicating an increase in gas content.

At this point, the probe has satisfied the conditions required by Maxwell's model to estimate gas holdup. Several probes with cells of different sizes were made. Fig.5.9 compares gas holdups calculated from conductivity and pressure measurements for two probes. The agreement is good under all conditions tested.

5.2. Summary

The main limitation to the use of electrical conductivity for on-line measurement of gas holdup in flotation systems is the measurement of the conductivity of the air-free slurry. This was achieved by using a syphon flow cell. The open and syphon cells were equipped with three ring electrodes, the two outer electrodes held at a different polarity from the middle one. This ensured the electrical field was restricted to the volume in between the bottom and the top rings.

The assembly of open and syphon flow cells forms the gas holdup probe. Estimates of the gas holdup using measurements from the probe and applying Maxwell's model gave results in good agreement with independent estimates.

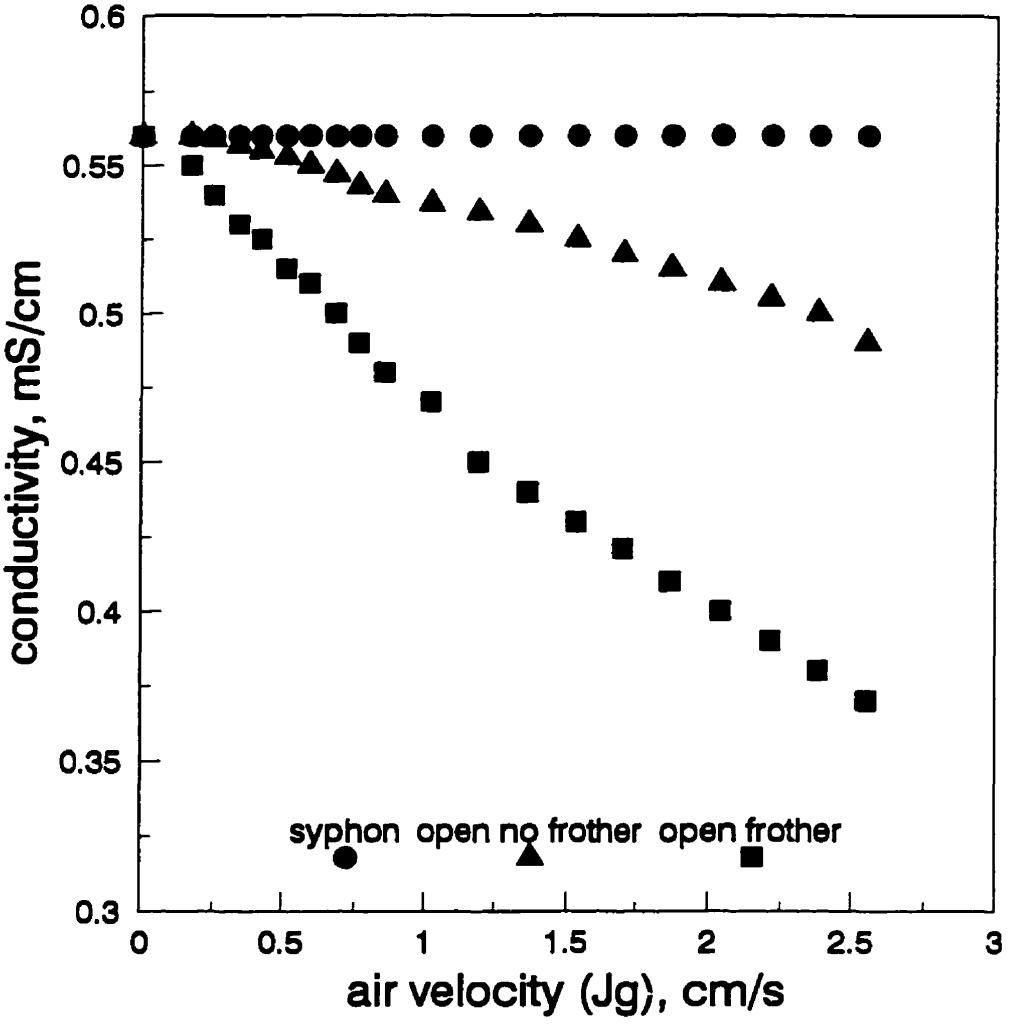

Fig.5.8. Conductivity measured in the syphon and open flow cells. Water-air system, with no frother and with 20 ppm frother.

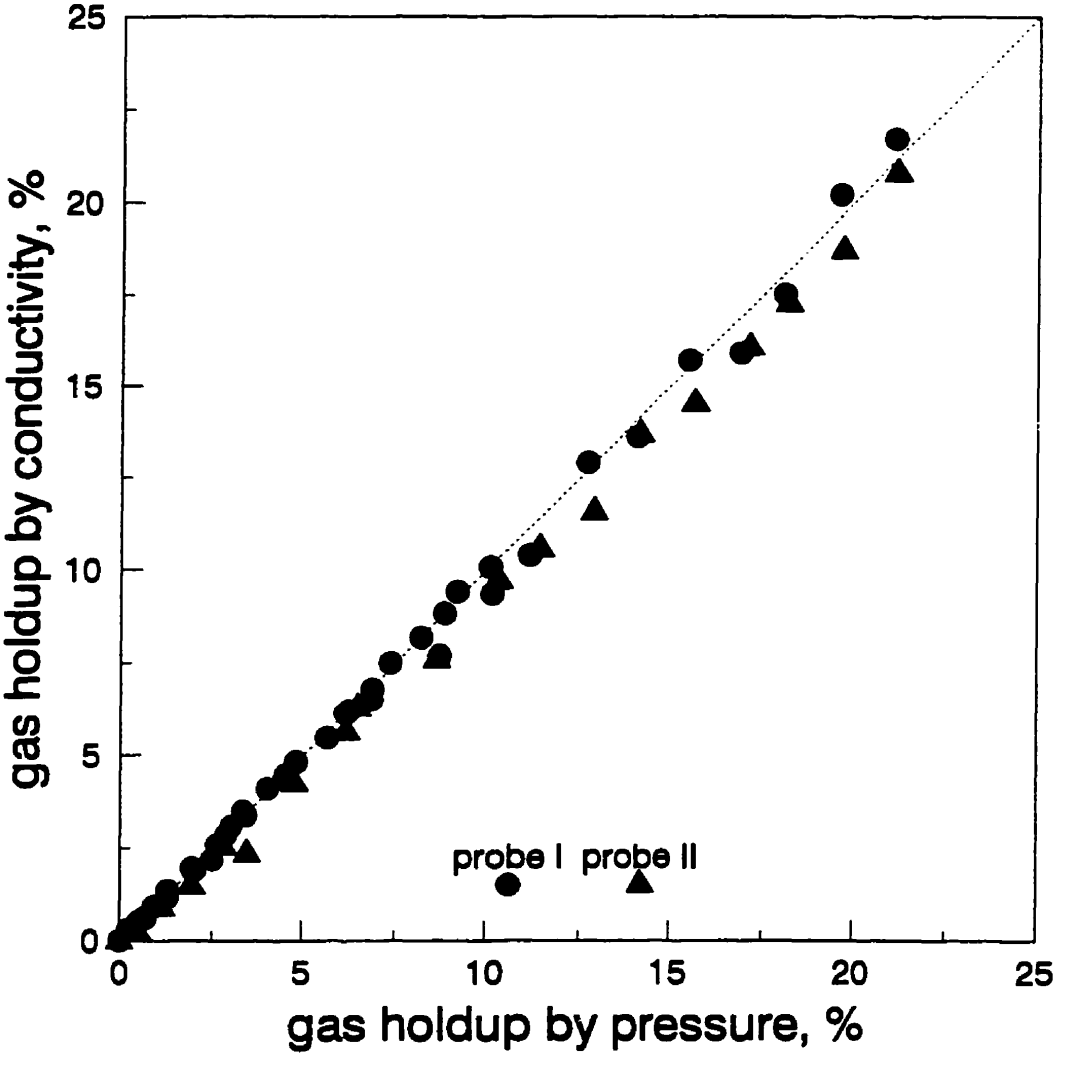

Fig.5.9. Gas holdup in water-air system. Comparison between measurements of conductivity and pressure; two probes are used; probe I has an open cell 10 cm in diameter while probe II has an open cell 5 cm in diameter.

CHAPTER 6

GAS HOLDUP MEASUREMENTS IN LABORATORY FLOTATION COLUMNS

Gas holdup is a variable which affects flotation performance. Because of the lack of a reliable technique for measuring gas holdup on-line, in real time in the industrial environment, it has been considered as an unmeasured variable. However, as shown in the previous chapter, there is a possibility to measure gas holdup by using an electrical conductivity probe. This probe is evaluated in the present chapter.

6.1. Two phase air-water system

The gas holdup probe was tested in air-water systems. Experiments were conducted in columns of 10 cm, 16 cm, and 50 cm diameter. The experiments consisted in injecting air into water through porous spargers (porous metal and filter cloth). The conductivity of the dispersion and the continuous phases were measured using the probe. Gas holdup was estimated using Maxwell's model and compared to that estimated from pressure difference.

Some experiments were conducted under batch-water conditions, others were carried out with water circulating through the column. Tests were conducted to determine the effect of changes in air flowrate, distribution of air and wash water (i.e. water added at the top of the column) and frother addition. Lastly, experiments were conducted to compare baffled and unbaffled columns.

6.1.1. Comparison of the gas holdup measured with the probe and by pressure

Experiments were conducted in batch-water as a function of air flowrate in the 50 cm laboratory flotation column. The tests were carried out in the presence of frother (20 ppm Dowfroth 250).

Two probes were used: probe I (with an open flow cell of 10 cm diameter), and probe II (open flow cell of 5 cm diameter). Table 6.1 presents characteristics of several probes used during

this work.

Table 6.1. Characteristics of several gas holdup probes (the probes are made of PVC).

Description	Probe I	Probe II	Probe III	Probe IV
Open cell length	45 cm	44 cm	44 cm	44 cm
Open cell diameter	10 cm	5.8 cm	7.3 cm	7.3 cm
Open cell separation between electrodes	10 cm	10 cm	10 cm	10 cm
Open cell calibration	$\kappa = K11.732 + 0.198$	$\kappa = K3.639 + 0.57$	$\kappa = K4.861 + 0.478$	$\kappa = K5.827 + 1.842$
Syphon cell length	45 cm	44 cm	44 cm	44 cm
Syphon cell diameter	2.5 cm	1.5 cm	3.8 cm	3.8 cm
Orifice diameter	5 mm	5 mm	6 mm	6 mm
Syphon cell separation between electrodes	10 cm	10 cm	10 cm	5 cm
Syphon cell calibration	$\kappa = K0.664 + 0.133$	$\kappa = K0.245 + 0.0093$	$\kappa = K1.643 + 0.056$	$\kappa = K3.083 + 2.182$

The gas holdup estimates from conductivity compared well with those from pressure (Fig.6.1). The Figure shows some scatter. One source of scatter is related to the fact that the gas holdup estimated from pressure is an average value over the volume contained between the two tapping points, while measurement with the conductivity probe is more localised. Therefore, differences can be expected if the gas holdup is not evenly distributed radially in the column.

The radial distribution of gas holdup was checked by placing probes at three radial positions

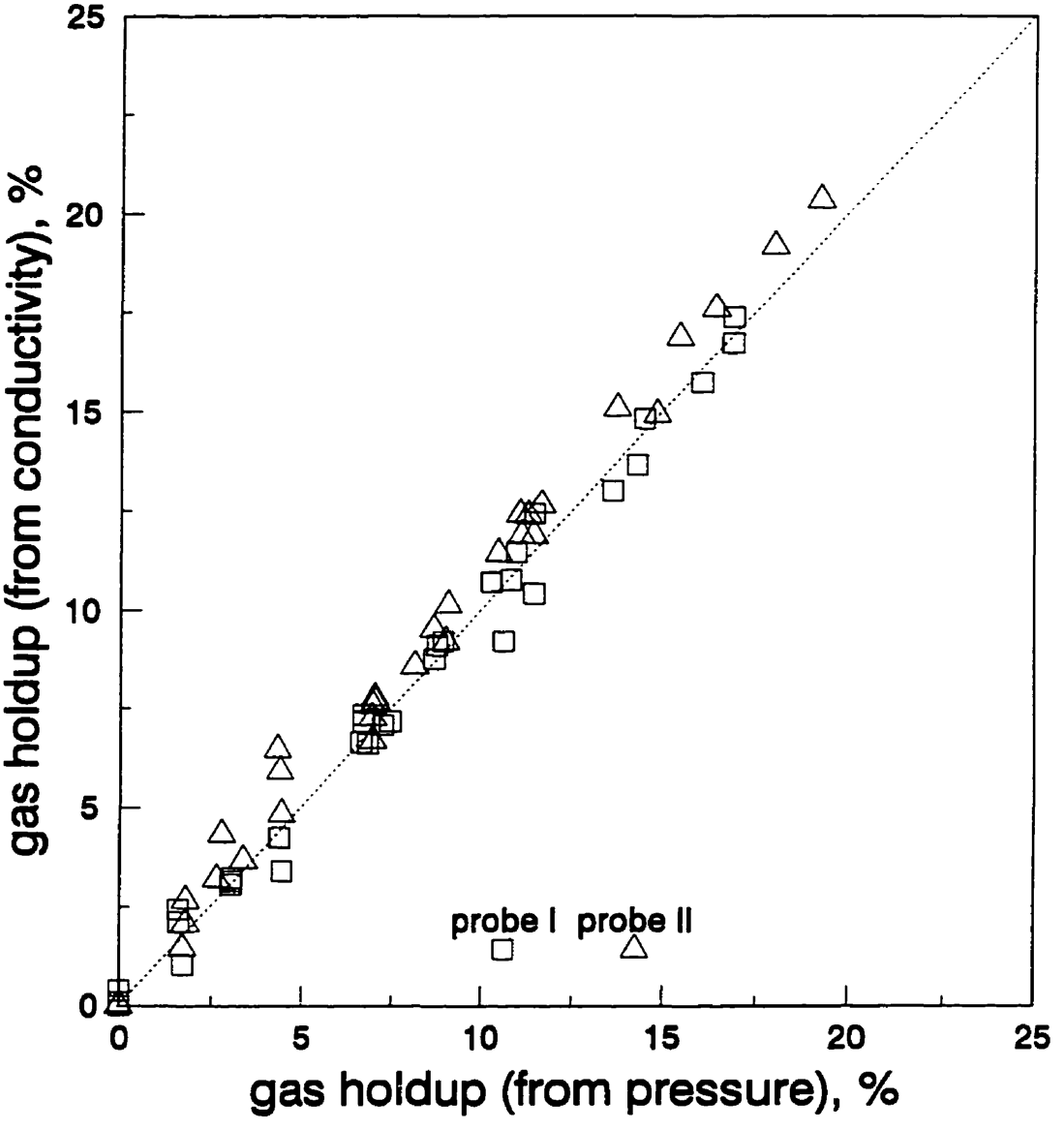

Fig.6.1. Gas holdup estimates from conductivity and pressure measurements; two probes (I and II) are tested in the 50 cm diameter column.

in the column, i.e. in the centre, mid-way between the centre and the wall, and at the wall of the column, along a line mid-way between the position of the two tapping points. The experimental set-up is that in Fig.5.6. The column had eight vertical filter cloth spargers in a ring arrangement at the bottom of the column. Therefore, air enters as an annular "curtain". The results (Fig.6.2.(a), (b)), show the gas holdup is higher at the centre of the column than at the wall. The results with probes I and II were similar further confirming this radial pattern in gas holdup. In the tests the gas holdup determined from pressure fell in between the values determined from conductivity.

Tests were also conducted in systems containing no frother. The results are presented in Fig.6.3.(a), (b). These data consistently show that the gas holdup is highest mid-way between the wall and the centre of the column.

The gas holdup is higher with frother (compare Figs. 6.2 and 6.3), as expected since the bubbles are smaller and rise velocity lower. The radial distribution appears to be different when frother is present. This implies that the hydrodynamic behaviour of the system is modified by the bubble size [Finch and Dobby, 1990].

The probe was also used to detect variations in gas holdup along the axial direction of the 4 m high × 50 cm diameter column. The measurements were made at three different depths in the column and different air flowrates. Fig. 6.4 shows that the gas holdup increases with the column height. This behaviour becomes more evident as the air flowrate is increased. These results are in agreement with measurements in laboratory and pilot columns with gas holdup estimated using pressure [Gomez et al., 1995].

The so-called buoyancy velocity of a bubble swarm [Nicklin, 1962] was also measured using the technique of Shen and Finch [1995]. As anticipated, the buoyancy velocity decreased as gas holdup increased. It was also found that there was a radial profile in the buoyancy velocity which reflects the radial distribution of gas holdup (Fig.6.5).

The gas holdup measured locally with the probe showed these probes are sufficiently sensitive to consistently detect changes in bubble swarm characteristics which are reflected in the gas holdup; therefore, the gas holdup probe has great potential in analysis of system hydrodynamics.

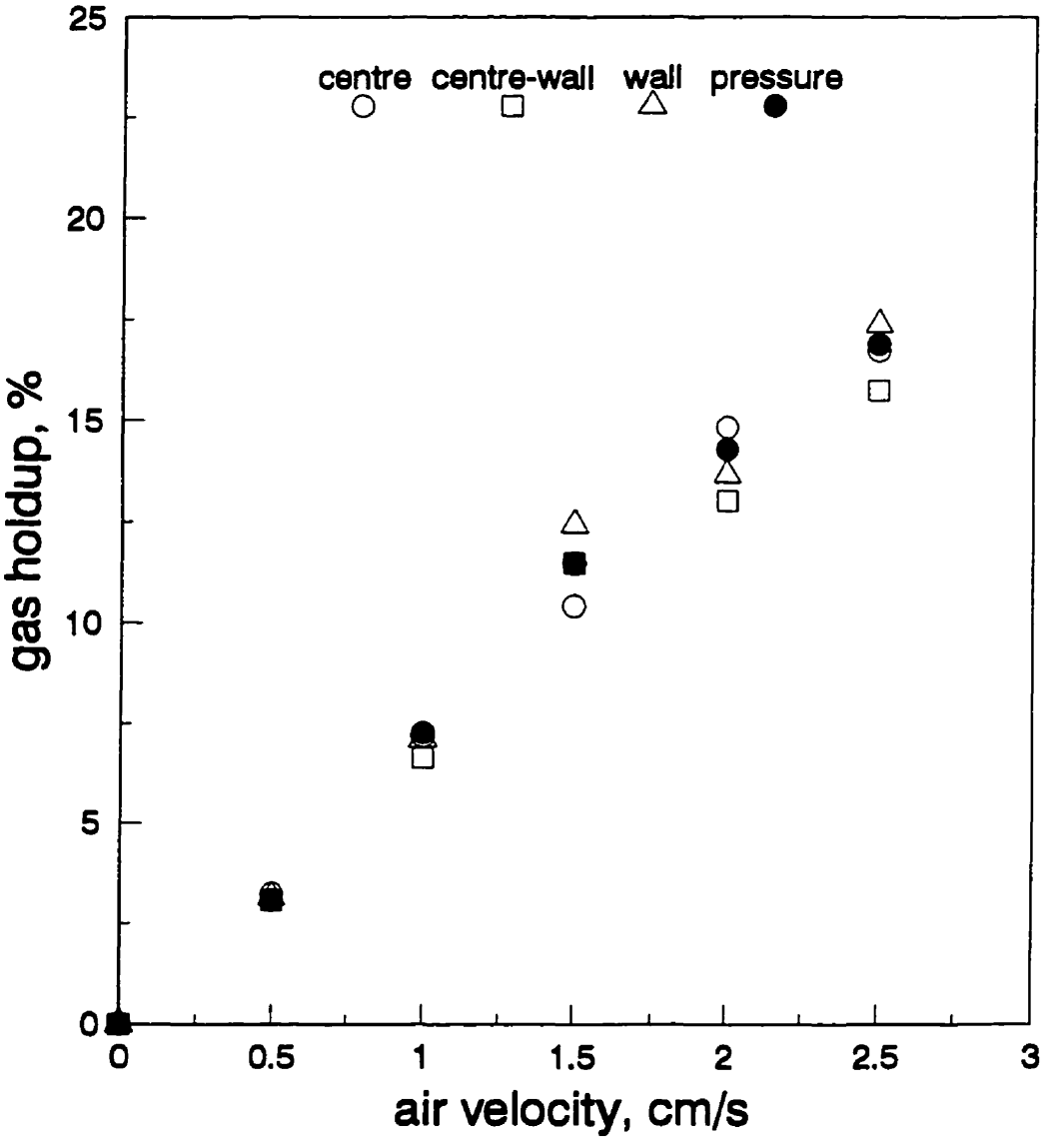

Fig.6.2.(a). Gas holdup vs air velocity in 50 cm diameter laboratory column: probe I used in three radial positions; 20 ppm Dowfroth 250; gas holdup from pressure is also presented.

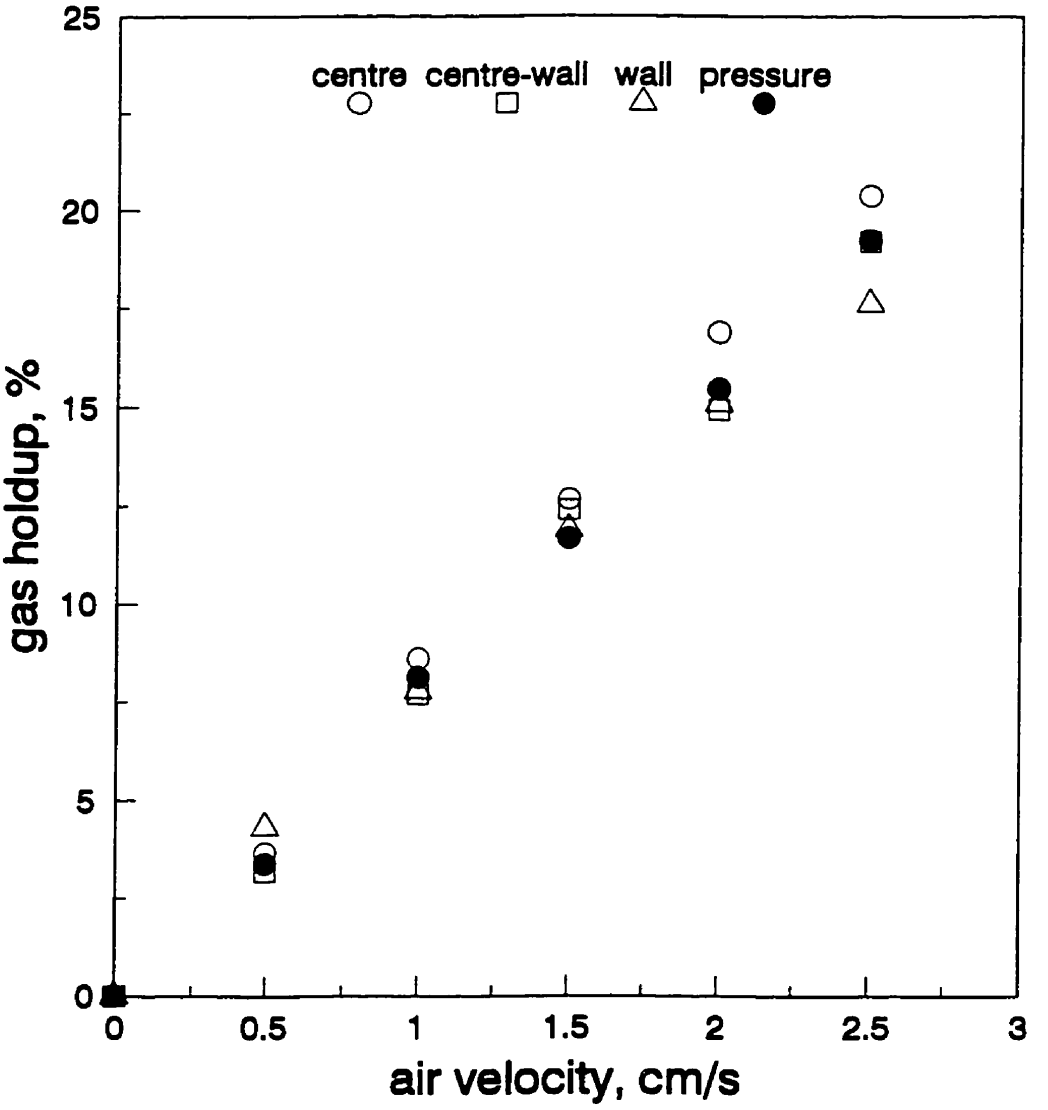

Fig.6.2.(b). Gas holdup vs air velocity in 50 cm laboratory column; probe II used in three radial positions; 20 ppm Dowfroth 250; gas holdup from pressure is also presented.

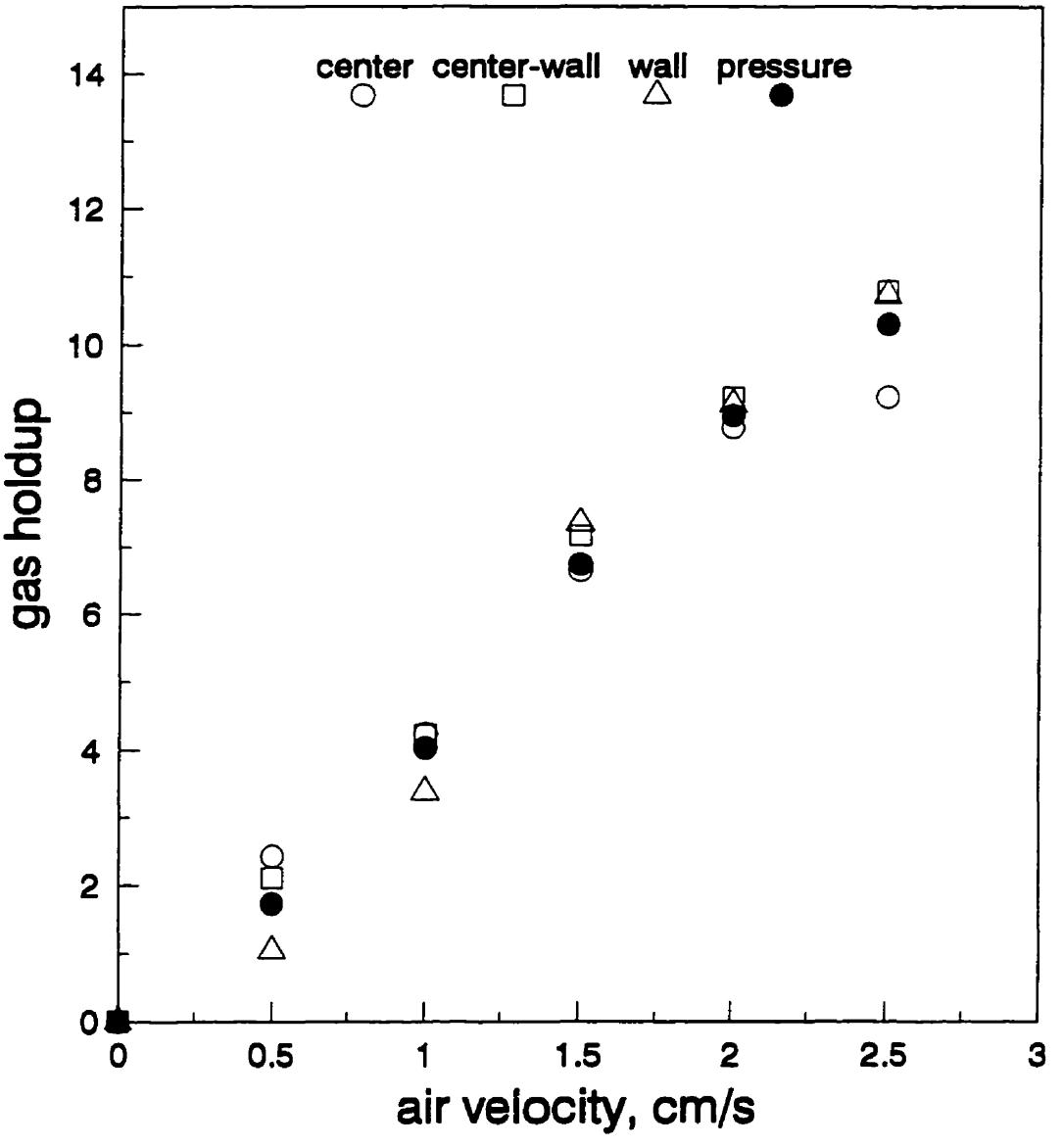

Fig.6.3.(a). Gas holdup vs air velocity in 50 cm diameter laboratory column; probe I used in three radial positions; no frother; holdup from pressure (average) included.

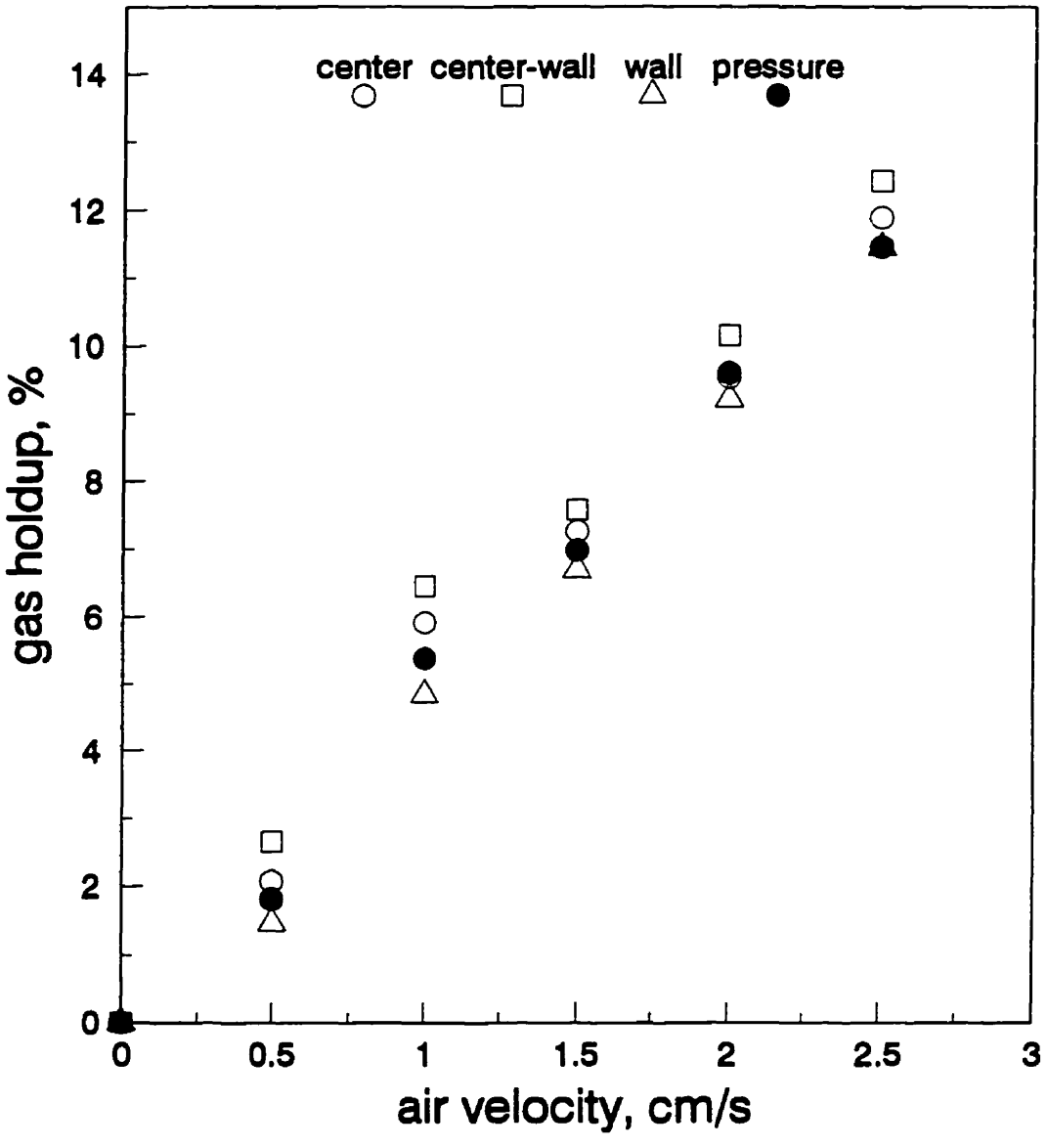

Fig.6.3.(b). Gas holdup vs air velocity in 50 cm diameter laboratory column; probe II used in three radial positions; no frother; holdup from pressure (average) included.

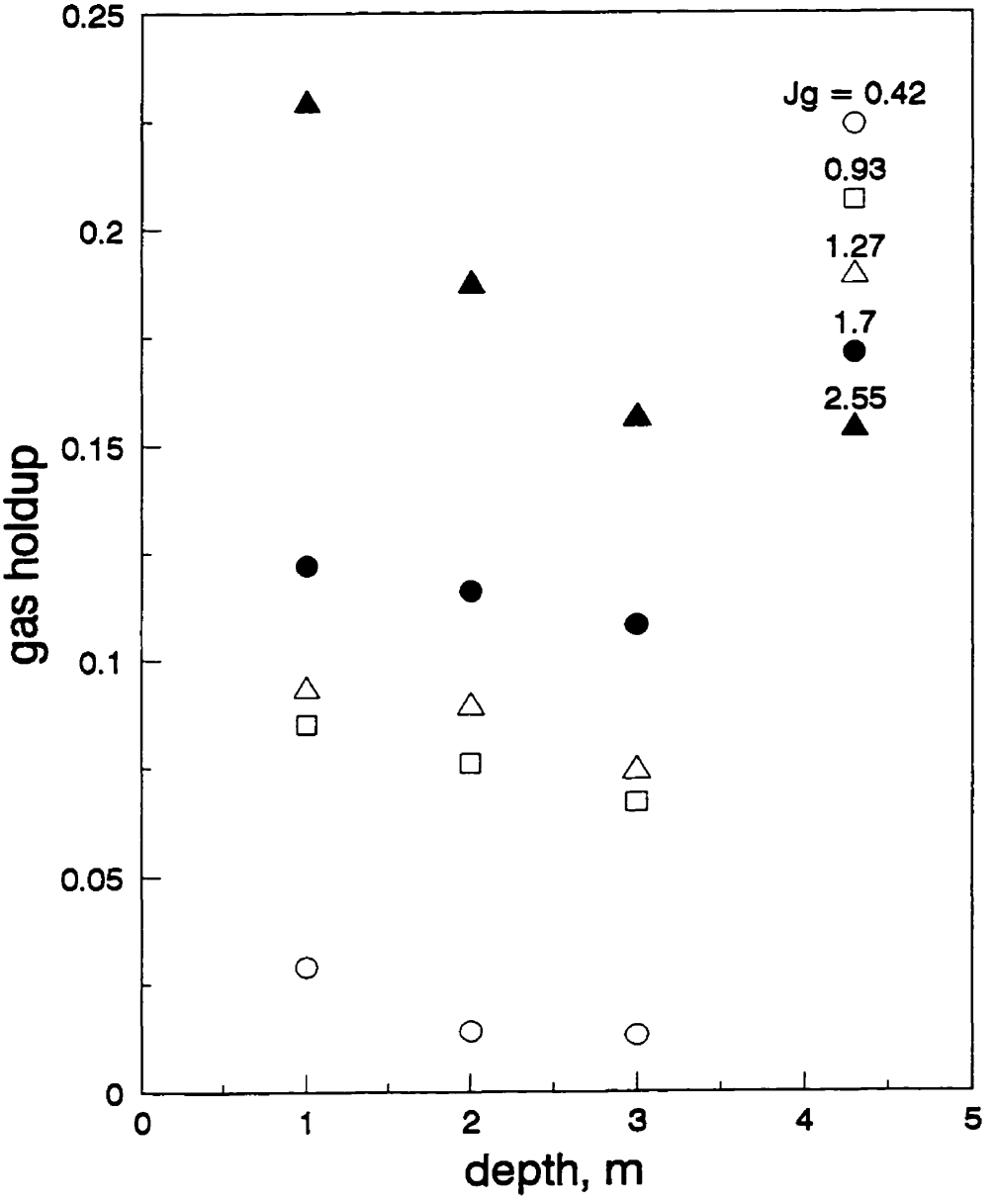

Fig.6.4. Gas holdup as a function of depth in 50 cm column; probe I used.

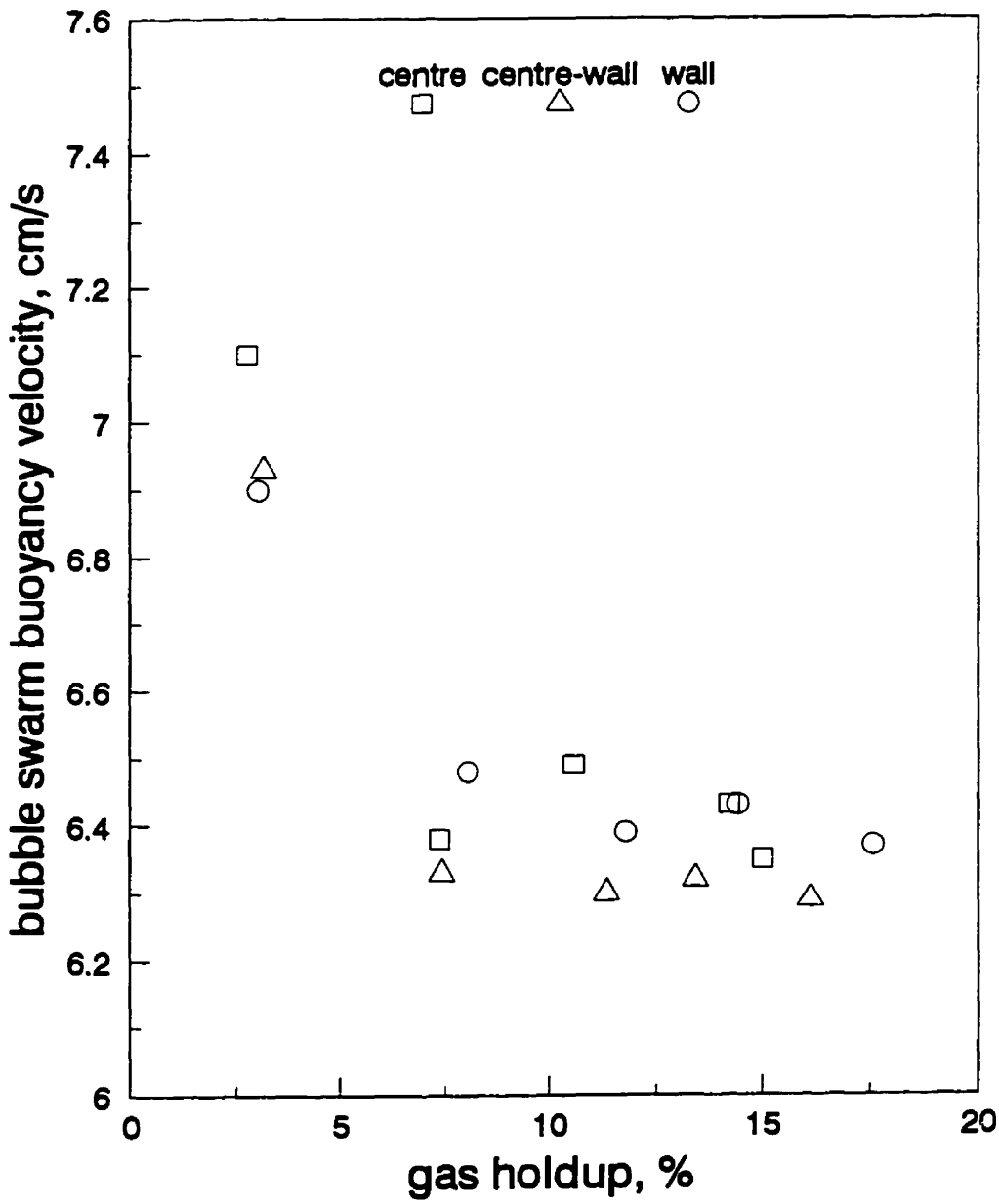

Fig.6.5. Bubble swarm buoyancy velocity as a function of gas holdup in 50 cm laboratory column; no frother.

6.1.2. Measurements in baffled and unbaffled columns

Large diameter unbaffled flotation columns are well-mixed [Finch et al., 1995]. It has been recommended that columns greater than 1 m diameter be baffled to reduce axial mixing. However, some researchers have found that baffles enhanced rather than dampened mixing. The reason was a "pumping" action between the baffled section if slurry and gas are not well distributed and differences in bulk density are generated. In a laboratory column mixing was only reliably reduced when the baffle was raised so that its top was above the level of the froth-slurry interface which stopped the "pumping" action [Moys et al., 1991].

In the present work, a number of tests were conducted to assess if the probe could detect differences in gas holdup between sections of the 50 cm diameter laboratory column after introducing baffles. Three m long cruciform baffles were installed vertically in the column and held 50 cm above the spargers and 50 cm below the lip. In this manner, the column was divided into four quadrants such that below each quadrant there were two vertical filter cloth spargers.

Fig.6.6 shows the data collected in the presence of frother (20 ppm Dowfroth 250). This shows a consistent but minor difference in holdup between sections. Pressure measurements confirmed the gas holdup values.

6.1.3. Effect of gas maldistribution on gas holdup

The above results show a radial distribution in gas holdup and hint at differences between baffled sections. Every effort was made to ensure an even injection of gas among the spargers. In practice this may not always be the case. To test, maldistribution of gas was simulated by switching off selected spargers in the 50 cm column.

Fig.6.7 shows the gas holdup estimates with one sparger switched off. Measurements were made along the diameter passing through the switched off sparger. It can be seen that there is a decrease in gas holdup in the region above the switched off sparger.

Fig.6.8 shows that the drop in gas holdup increases slightly when two neighbouring spargers are switched off. There is a change in gas holdup distribution compared to the case of one switched

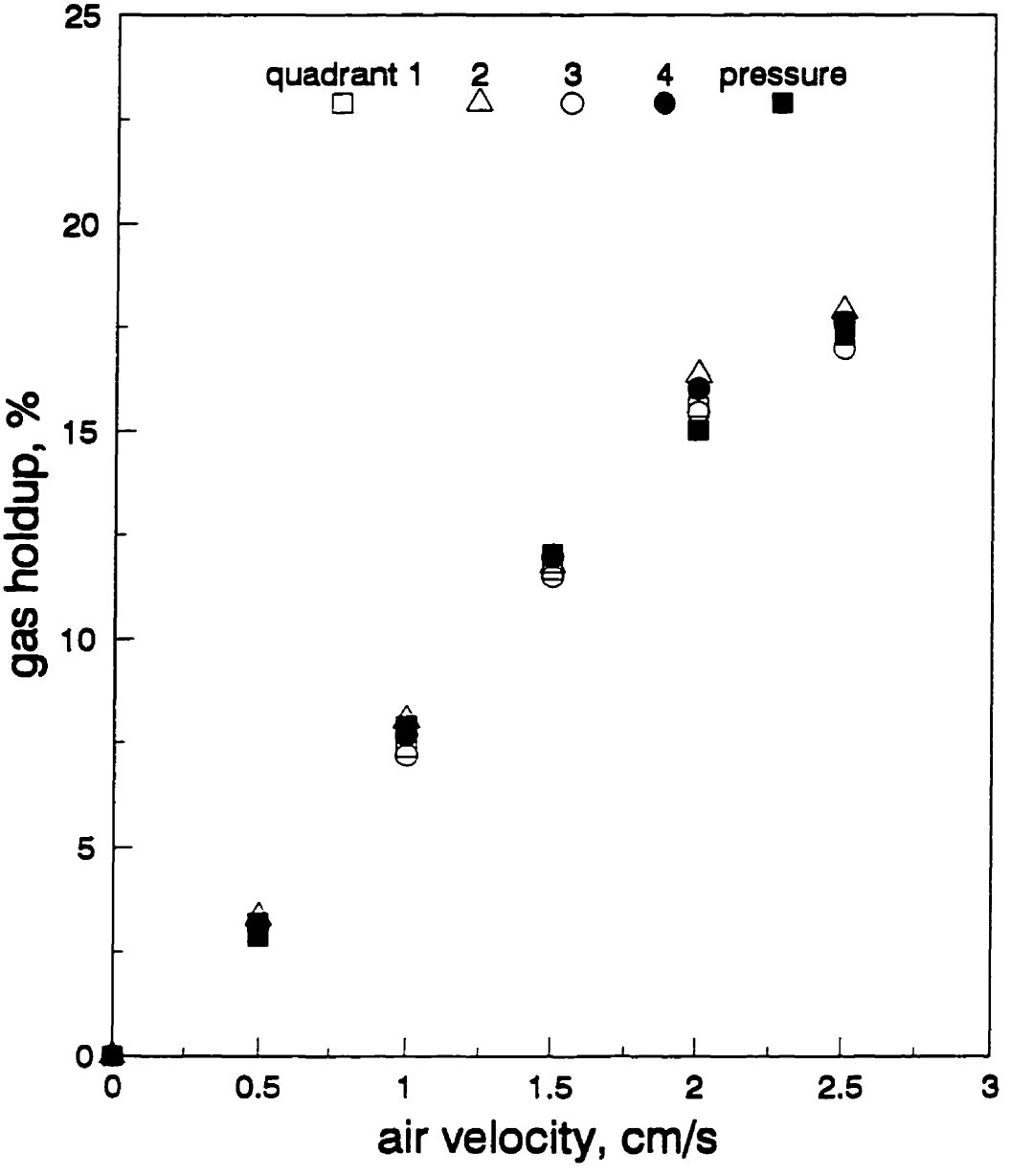

Fig.6.6. Gas holdup vs air velocity in 50 cm laboratory column with baffles: column is divided into four quadrants; probe I used in each quadrant; 20 ppm Dowfroth 250.

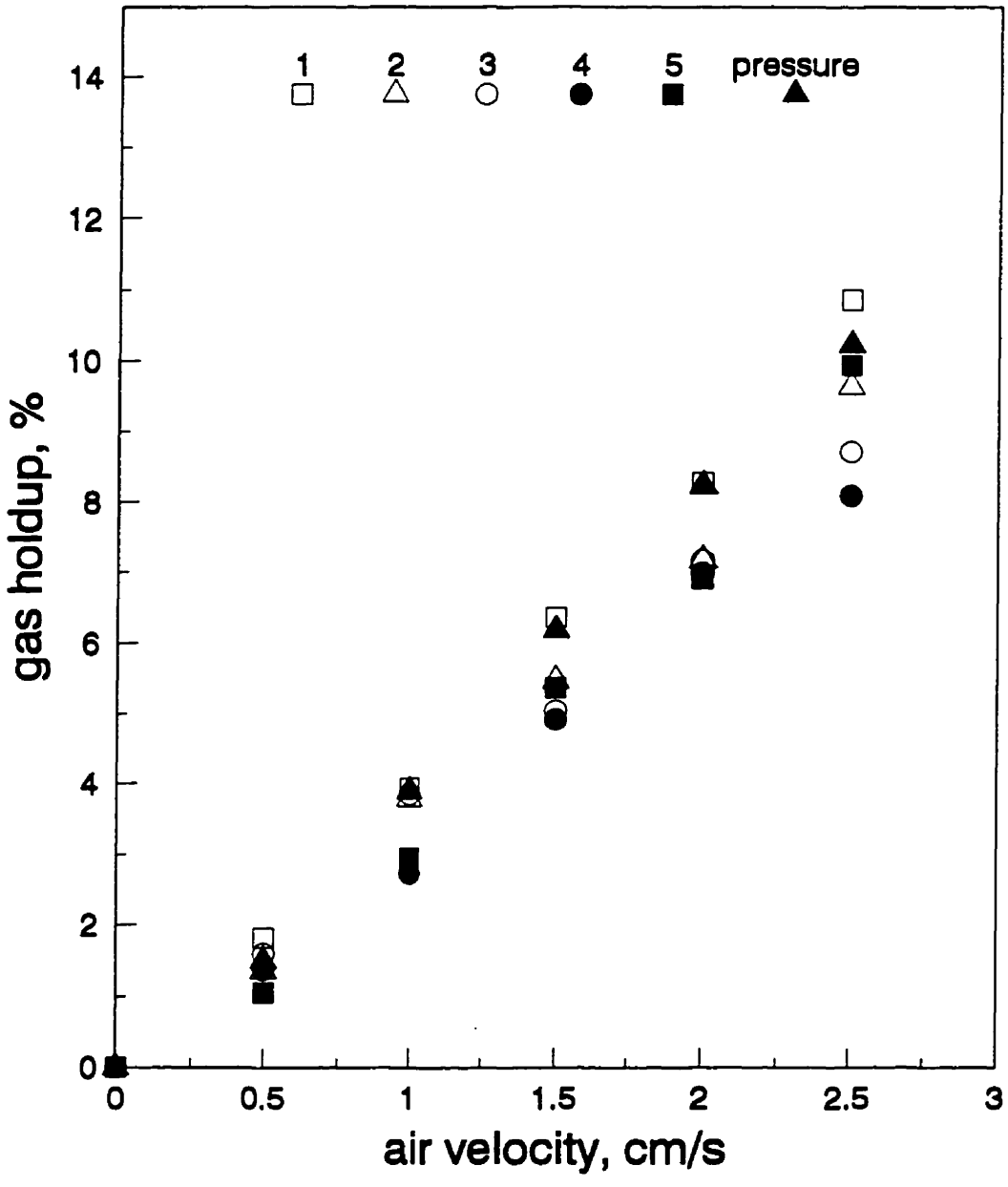

Fig.6.7. Gas holdup vs air velocity in 50 cm column: one sparger is switched off; no frother: 1 the probe is on the wall opposite to switched off sparger; 2 the probe is between position 1 and the column centre; 3 the probe is at the column centre; 4 the probe is between the centre and the wall above the switched off sparger; 5 the probe is on the wall above the switched off sparger.

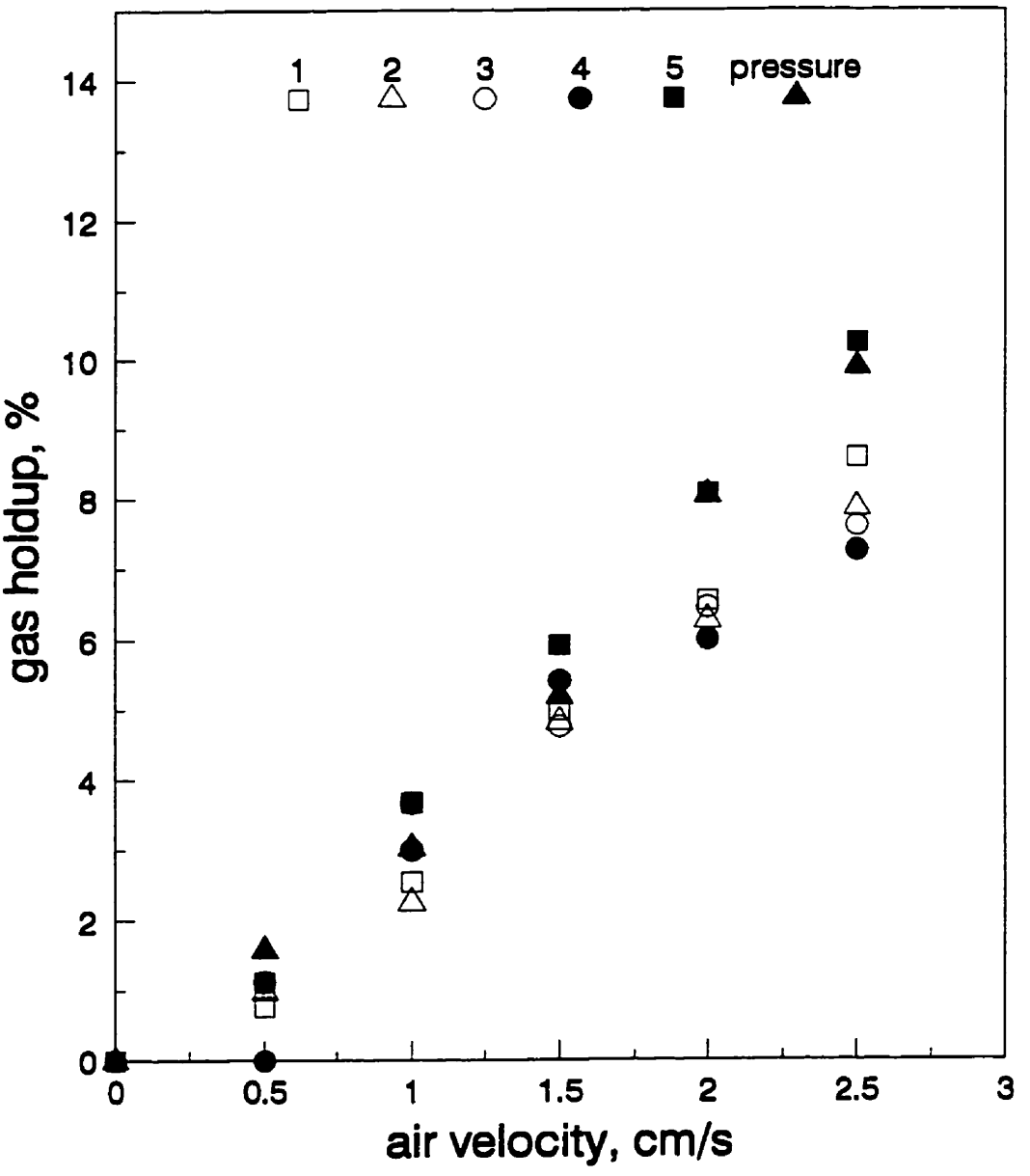

Fig.6.8. Gas holdup vs air velocity in 50 cm laboratory column; two neighbouring spargers switched off; gas holdup probe positions (1 to 5) are the same as in Fig.6.7; no frother.

off sparger, implying a different circulation pattern.

Fig.6.9 repeats Fig.6.8 but in the presence of 20 ppm frother (Dowfroth 250). The presence of small bubbles appears to bring the column more into balance, minimising the effect of gas maldistribution.

Fig.6.10 shows the results for a baffled column. It can be seen that gas holdup is lower in quadrant 1, above the "failed" spargers, and highest in quadrant 3, which is on the side opposite to quadrant 1; quadrants 2 and 4 presented intermediate values.

It can be seen that the probe has proven useful for detecting differences in gas holdup due to non uniform distribution of air into the column.

6.1.4. Effect of wash water distribution on the gas holdup

Variables other than gas injection could produce an effect on gas holdup in a flotation column. An important parameter is wash water, because it acts to reject entrained slurry (and hydrophilic gangue) from the froth. An interesting question is: Does wash water and its distribution have any effect on the gas holdup in the collection zone of a column?

Tests were carried out in a 16 cm diameter (1.5 m height) plexiglas flotation column. The column had a single vertical porous metal sparger and was operated on water only with the underflow being recirculated as wash water. A baffle was placed in a vertical position at the middle of the column. In this way, the column was divided into two sections starting 15 cm above the sparger to 30 cm below the lip.

Gas holdup probe II was placed in one of the baffled sections. The wash water was placed first on one and then on the other side of the baffle to observe the effect of uneven wash water distribution on the gas holdup. Conductivity readings were carried out in the section receiving wash water and the one not. The results are presented in Fig.6.11. It can be seen that gas holdup is higher in the section receiving wash water (the "in" results). This suggests that the downward flow of water retards the bubble swarm in that section, and thus increases the gas holdup as compared with the section with no wash water. Based on these observations, it may be anticipated that an uneven distribution of wash water would be a disturbance to the hydrodynamics in the column.

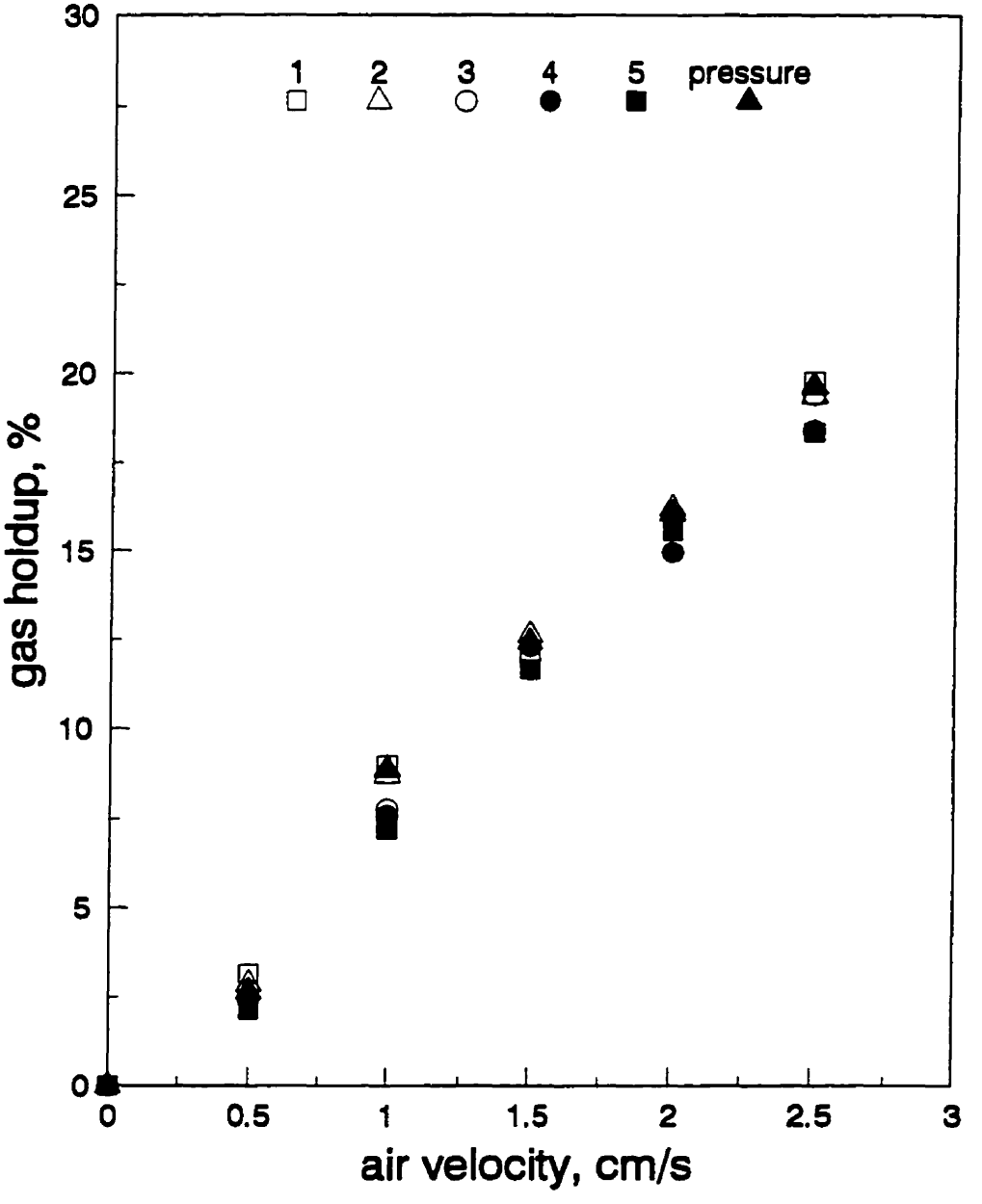

Fig.6.9. Gas holdup vs air velocity in 50 cm laboratory column; two spargers are switched off; gas holdup probe positions are the same as in Fig.6.7; 20 ppm Dowfroth 250.

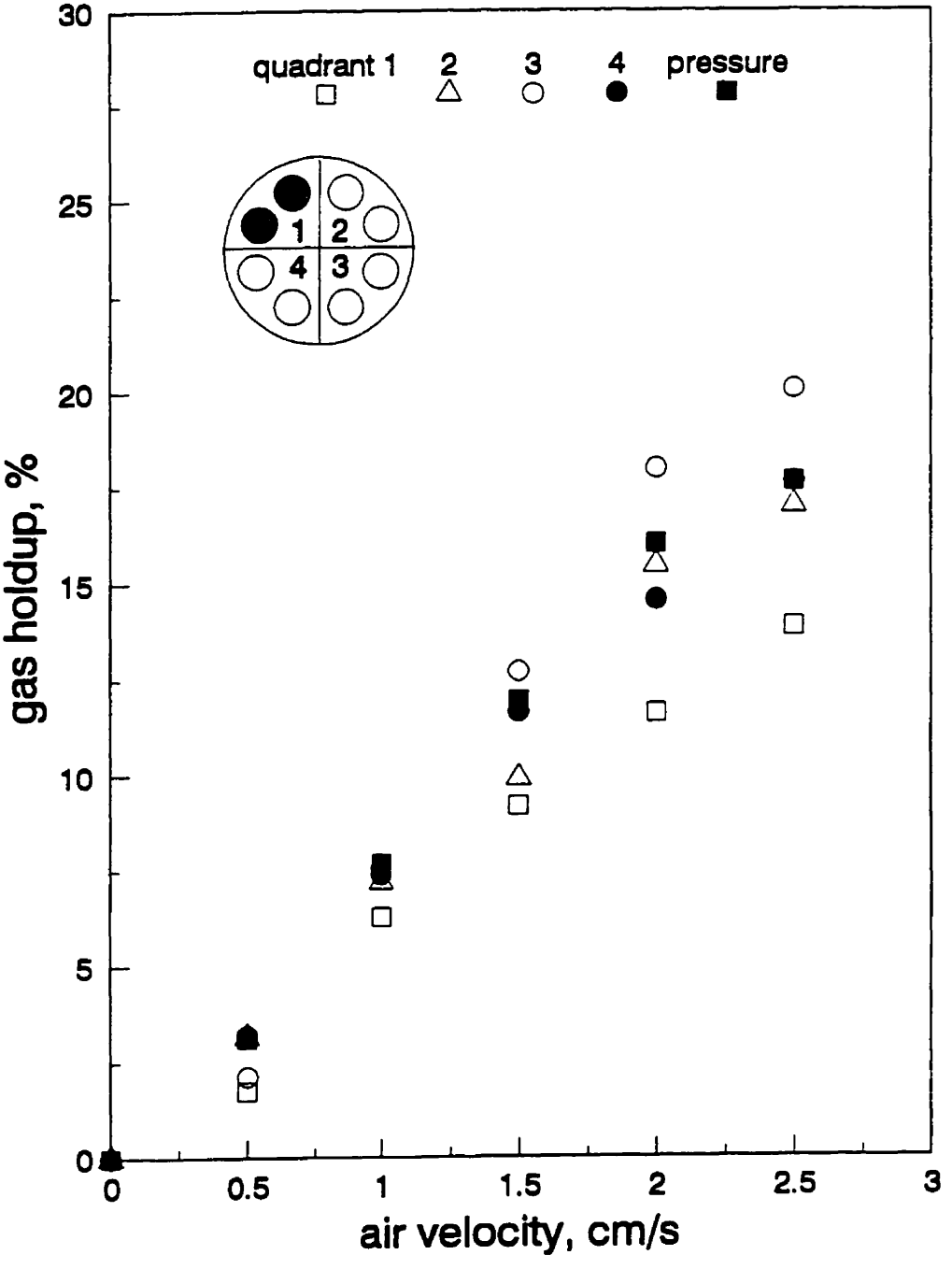

Fig.6.10. Gas holdup vs air velocity in baffled 50 cm laboratory column; two spargers are switched off in quadrant 1; the gas holdup probe is placed in each quadrant at 2 m from the column lip; 20 ppm Dowfroth 250.

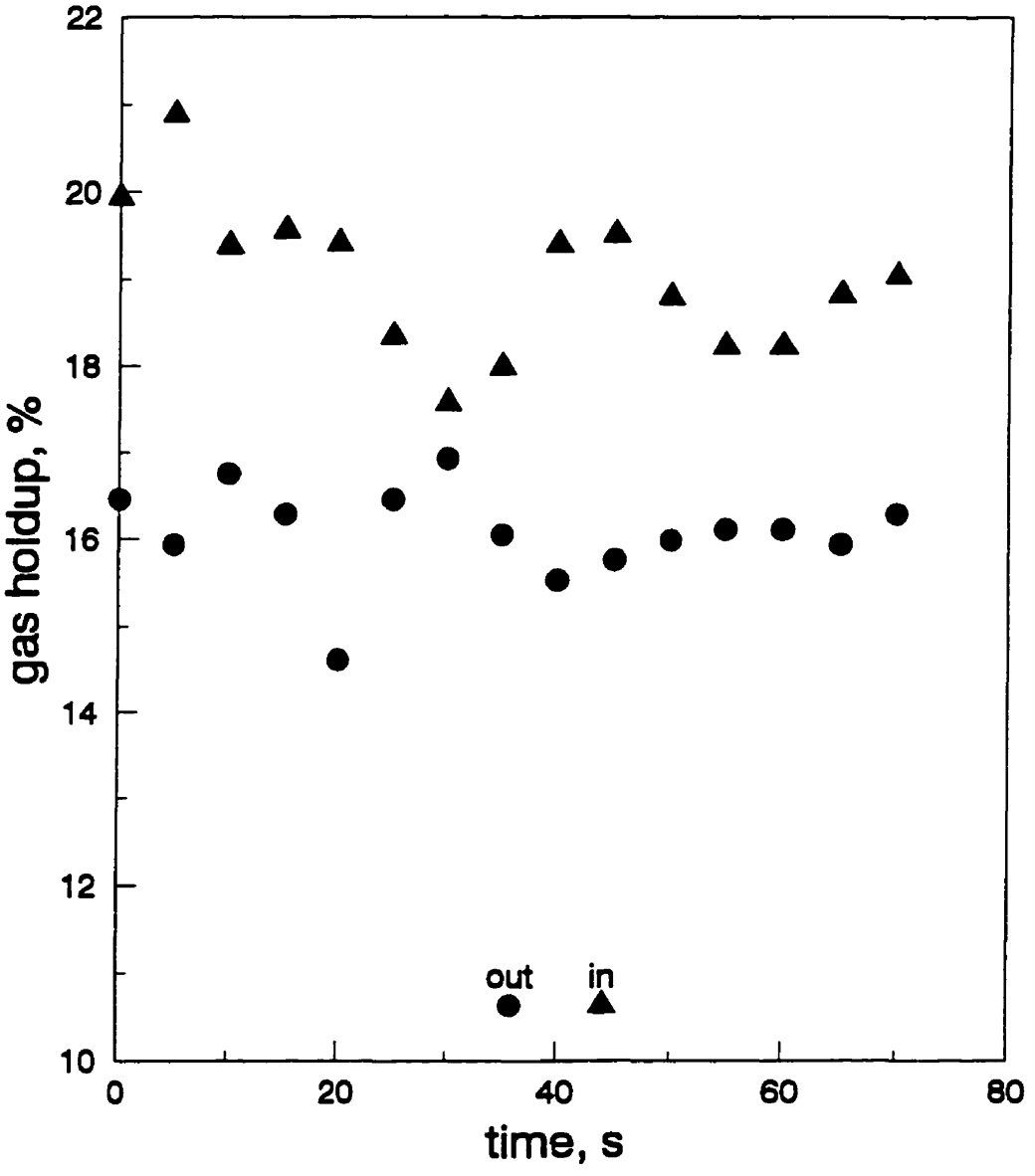

Fig.6.11. Gas holdup over time in 16 cm laboratory column with one vertical baffle; wash water enters one half of the column (designated "in"); 20 ppm Dowfroth 250.

6.2. Three phase (air-water-solids) systems

The application of Maxwell's model to gas holdup in a flotation system assumes that the slurry acts as an homogeneous continuous phase. Under this assumption the conductivity technique has been proved valid in three phase systems [Shen et al., 1995; Banisi et al., 1995 (a) and (b); Uribe-Salas et al., 1994]. The gas holdup probe must be proven suitable in the present context also.

6.2.1. Comparison of gas holdup from probe and slurry displacement.

Tests on three-phase systems were conducted in a 10 cm diameter (plexiglas) column. Two systems were analysed: air-silica-water, and air-carbon-water.

The experimental technique consisted in mixing solids in a tank to the desired slurry composition (percent solids). The slurry was fed to the column at the top (with a pump) and the underflow and overflow were pumped back to the tank, i.e. the slurry was circulated continuously through the column. By controlling the pump speed slurry level was kept constant at the lip of the column. The slurry flowrate was maintained low enough to avoid sedimentation of solids at the bottom of the column.

Gas holdup probe II was located in the middle of the column. Air was introduced, and simultaneously the pumps were switched off. The slurry displaced from the column by the air was collected in a container as a measure of gas holdup. Once the displacement of slurry terminated (no additional slurry was collected from the column), the pumps were switched on to reestablish the circulation. The gas holdup probe was working continuously during this period. The gas holdup value remained virtually constant throughout.

The test data are presented in Figs.6.12 and 6.13 where the gas holdup estimated from conductivity is compared with the gas holdup from slurry displacement for the carbon and silica tests, respectively. The solids percent (% v/v) varied between 5% and 30%. The results show the two estimates are in good agreement; therefore, it can be said that the gas holdup probe appears to be suitable for flotation systems.

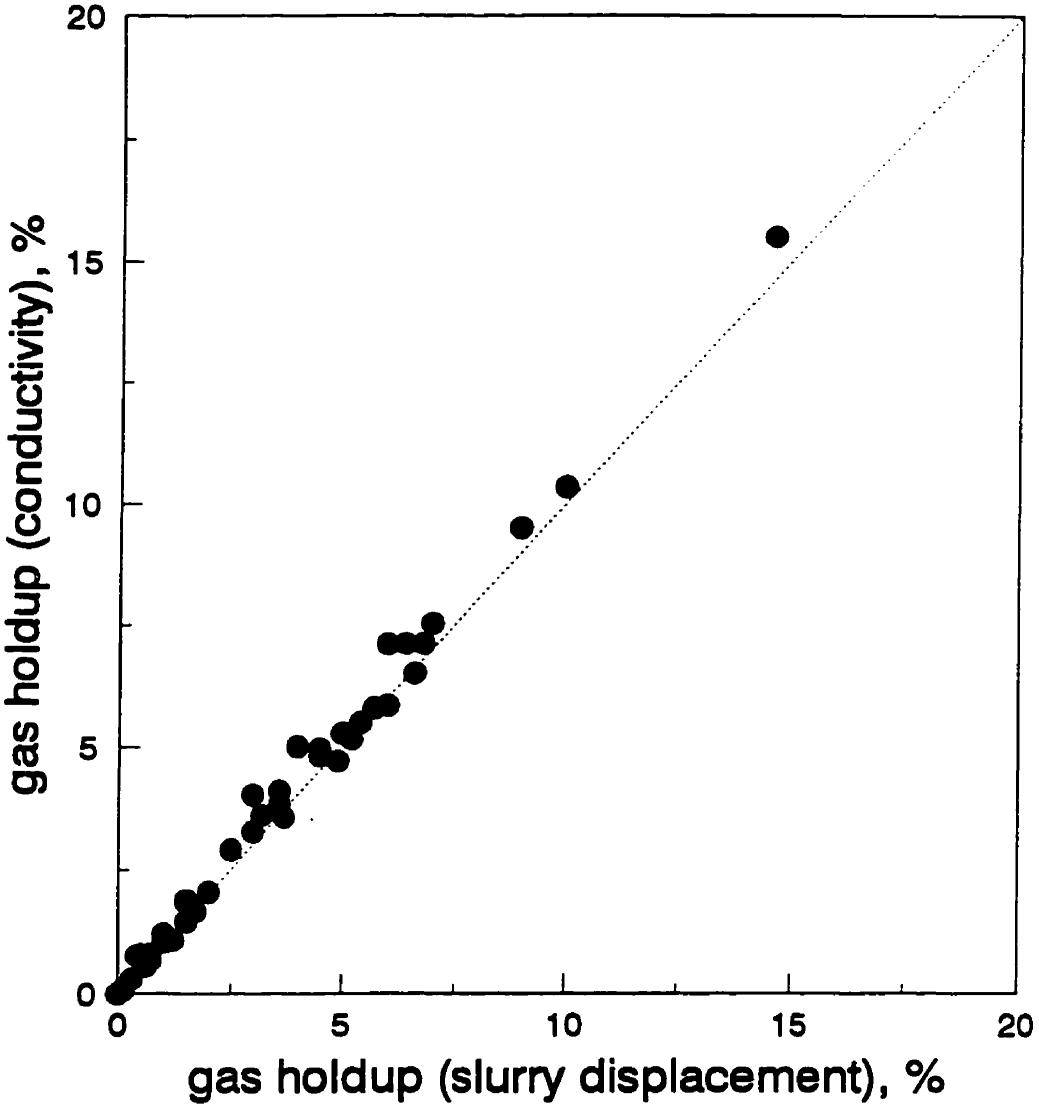

Fig.6.12. Comparison between gas holdup values estimated from conductivity measurements and slurry displacement in air-carbon-water system; 10 cm diameter laboratory column; probe II.

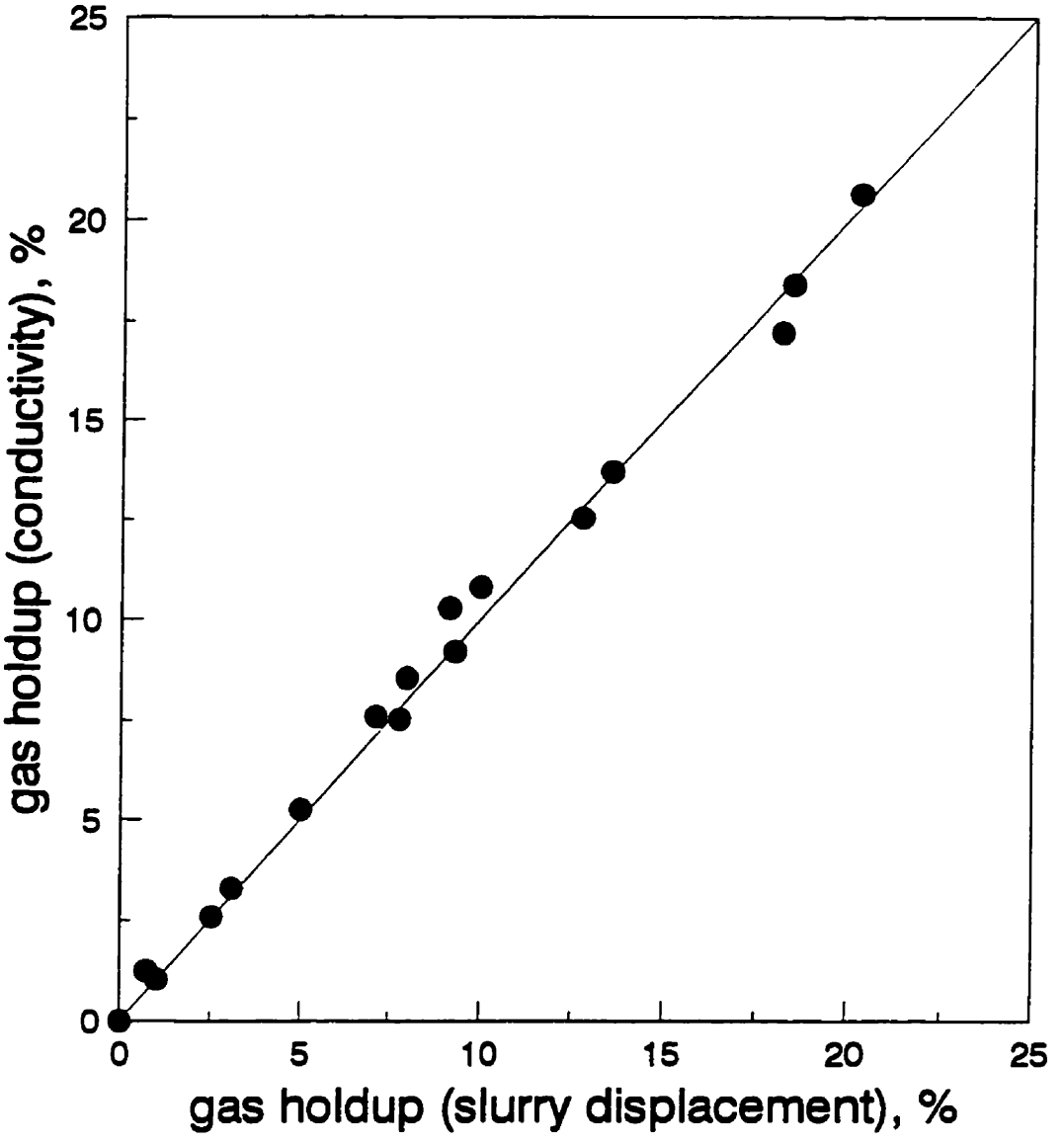

Fig.6.13. Comparison between gas holdup estimated from conductivity and slurry displacement measurements; 16 cm laboratory column; air-silica-water system; probe II.

6.2.2. Effect of solids and measurements in co- and counter-current systems

The literature on three-phase bubble columns gives conflicting evidence on the effect of solids on the gas holdup. In flotation column tests, some authors claim the presence of solids decreases the gas holdup [Shen et al., 1995; Banisi et al., 1995 (a) and (b)], while Ityokumbul et al. [1995] claim there is no effect.

Tests were carried out to determine if the probe could detect an effect of solids on gas holdup. Slurries were made by adding coal (85% -75 μm, +38 μm), or silica (80% -75 μm +53 μm), to give percent solids between 5% and 30% v/v.

Fig. 6.14 shows gas holdup vs air velocity. It can be seen that the gas holdup always decreased upon addition of coal and for silica up to 5%. Above 5% silica the gas holdup increased. The results, therefore, partly agree with those of Banisi et al. [1995 (a) and (b)] and Shen et al. [1995].

Figure 6.15 presents the effect of co-current vs counter-current flow in two-phase air-water and in three-phase air-carbon-water systems. These data show that in both cases, gas holdup was lower in co-current compared with counter-current as expected [Finch and Dobby, 1990]. For either system gas holdup decreased in the presence of solids, more for carbon than silica. It is possible that carbon, being hydrophobic, caused bubble coalescence [Van Weert, 1995].

6.3. Summary

Experiments have been carried out on laboratory columns to test the gas holdup probe under a variety of conditions. The results show the following:

- The gas holdup estimates using the probe are in good agreement with those determined by independent methods; i.e. pressure in two-phase systems, and slurry displacement in three-phase systems;
- the probe was able to detect radial and axial distribution in gas holdup, and to detect differences in gas holdup between sections of a baffled column;
- sparger performance, including sparger failure, can be assessed using the probe,

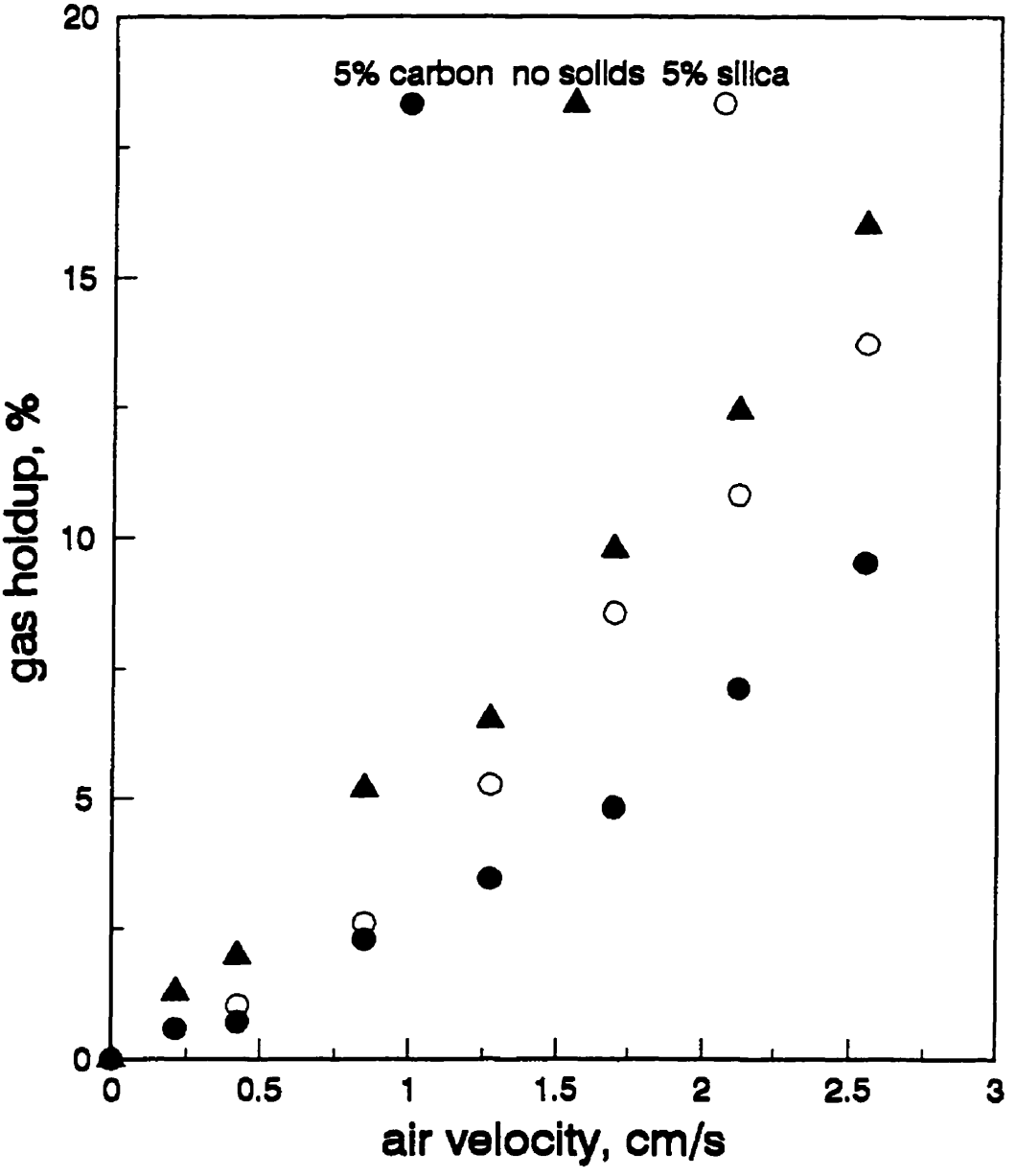

Fig.6.14. Comparison of gas holdup between two-phase and three-phase systems; no frother added; 5% v/v solids; 10 cm diameter laboratory column; probe II.

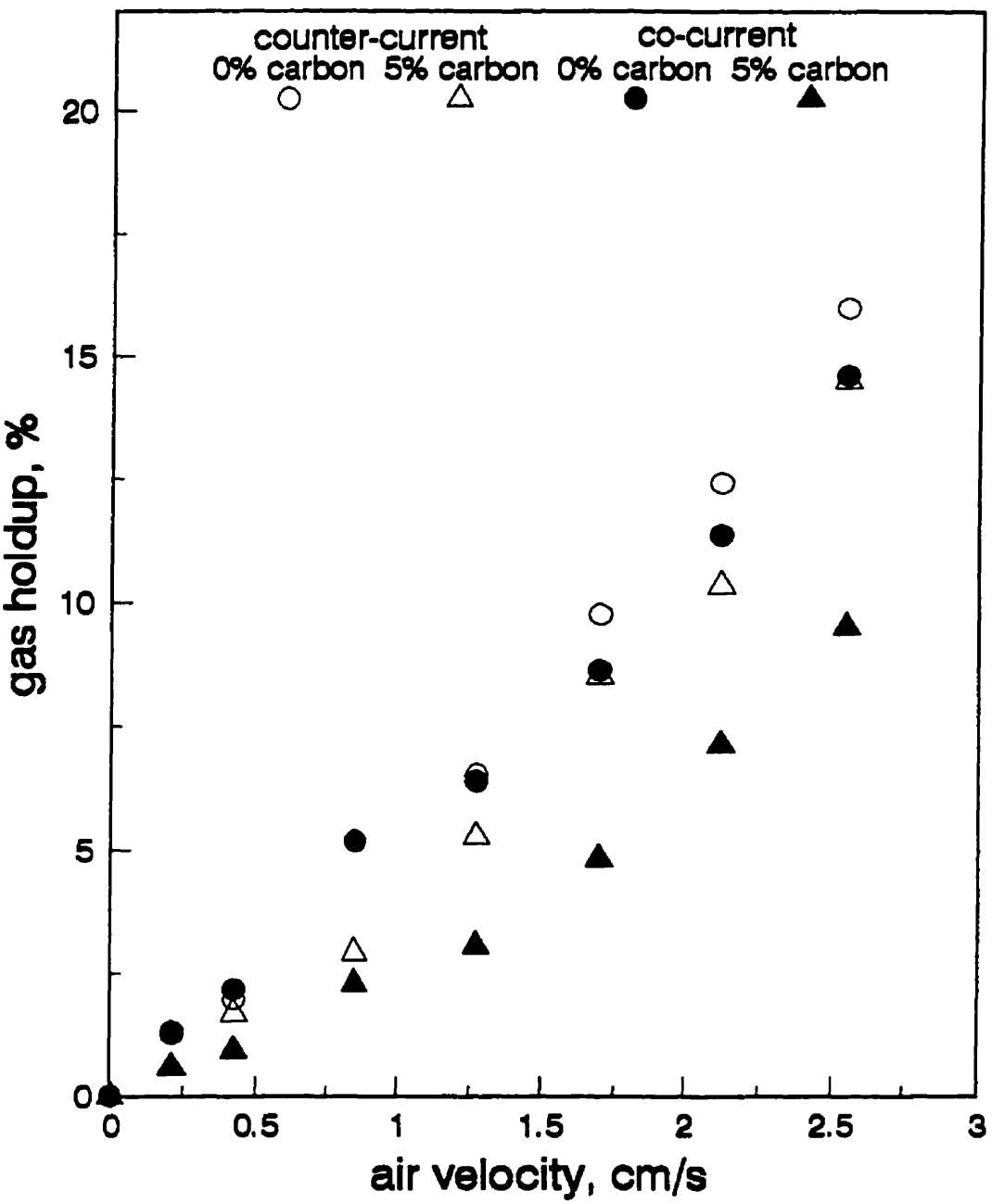

Fig.6.15. Gas holdup as a function of air velocity in systems with and without solids: effect of co-current and counter-current flows in the 10 cm laboratory column; probe II.

- variations in gas holdup could be detected due to changes in operating conditions; i.e. wash water distribution, and co-current and counter-current flow;
- the effect of addition of solids on the gas holdup could be detected. With carbon and silica up to 5% v/v, gas holdup estimates using the probe are in agreement with recent experimental work which showed the gas holdup decreased in the presence of solids.

In conclusion, the gas holdup probe gives reliable measurements in air-slurry (flotation) systems and appears to be a useful tool to diagnose gas holdup-related issues in flotation columns.

The probe meets all the requirements established at the outset: measurements are made in real time, on-line, in-situ, and without any measurements external to the system.

CHAPTER 7

GAS HOLDUP MEASUREMENTS IN INDUSTRIAL FLOTATION COLUMNS

It has been shown that the probe gave accurate estimates of gas holdup in two and three-phase dispersions in laboratory columns. In this chapter, the gas holdup probe is tested at an industrial site, the Matte Separation Plant, INCO Ltd. (Copper Cliff, ON).

7.1 Experience at INCO's Matte Separation Plant

In the Matte Separation Plant nickel-copper matte (produced at the smelter) is cooled, comminuted and separated by flotation into copper sulphide and nickel sulphide products which are sent for extraction of metals. There are four flotation columns in the plant. A description of the columns, and the data obtained with the gas holdup probe follows.

7.1.1. Description of the Matte Separation Plant flotation columns

These flotation columns are designated by numbers. All the tests were carried out in columns 2, 3 and 4. The general characteristics of the columns are presented in Table 7.1.

Column 2 is used to float copper sulphide, while columns 3 and 4 are used as scavenger units to produce nickel sulphide concentrate. The columns have a wash water distribution system (unless otherwise specified), consisting of a series of horizontal PVC perforated pipes (2" inside diameter), through which wash water is fed to the column. The pipe array is placed at the top of the columns about 10 cm below the column lip, which ensures wash water goes into the froth rather than short-circuiting to the overflow.

Table 7.1. INCO Matte Separation Plant: some column characteristics.

Description	Column 2	Column 3	Column 4
Column diameter, m	1.77	1.77	2
Column height, m	12	12	12
Baffled	Yes	No	Yes
Sparger type	Horizontal perforated rubber	Minnovex variable gap, 4 spargers	Horizontal perforated rubber
Jg, cm/s (*)	3.5	2.4	3.4

(*) Gas flow rate under "normal operation" at the time of the test.

The feed system consists of a horizontal 4" steel pipe located about 3 m from the column lip, which extends horizontally to the centre of the column, where it has a 90° elbow which directs the feed upwards. Above the feed there is a deflecting steel plate to distribute the feed around the column.

Columns 2 and 4 were baffled by vertical steel plates in a cruciform fashion such that they are divided into four quadrants. The baffles are located just below the feed pipe, and extend down to about 1 m above the sparger line. The sparger line is situated about 1 m above the bottom of the column where the underflow port is located.

The gas holdup probe was tested under two regimes: batch-water in order to repeat some of the laboratory tests in an industrial size column, and under normal operating conditions.

7.1.2. Gas holdup/pressure measurements in air-water systems

Verification tests

Tests on two-phase air-water systems were performed in columns 3 and 4. Two portable pressure transmiters (Omega, model PX429; Druck, model PX234) together with the probe were used. The pressure transmiters were fixed to the probe support frame, one 0.5 m above, the other 0.5 m below the probe. Therefore, simultaneous measurements of pressure and conductivity were made at the same approximate location. In this way the estimated gas holdup from pressure can be

compared with those estimates from conductivity.

Fig.7.1 presents the results. The data were collected at different air flow rates and at different depths (at the centre of the column) to give a wide range of gas holdup values. It can be seen that there is good agreement between the estimates over the whole range of conditions used. This finding is similar to that in the air-water laboratory column tests. From this it can be concluded that the probe functions well in commercial scale flotation columns.

Exploratory tests

Experiments were conducted to observe the effect of air flow rate on the gas holdup in column 3. Fig.7.2 presents the data collected at different depths below the column lip, and with air flowrates ranging from 0.8 to 3 cm/s.

As anticipated, gas holdup increased steadily with decreasing depth. The gas holdup increase is almost 100% from near the bottom to the top of the column for all air flow rates. This is in agreement with previous observations [Gomez et al., 1995].

Tests were performed in column 3 to measure the gas holdup as a function of radial position (Fig.7.3). It can be seen that gas holdup is higher at the centre of the column than at the wall. This suggests that gas is concentrated at the center of the column. (This column has four Minnovex variable gap spargers, set about 1 m from the bottom of the column, which inject gas horizontally from all sides. With this configuration the spargers may concentrate air in the centre of the column.)

Tests were carried out in column 4 which is baffled. Fig.7.4 shows gas holdup as a function of gas flow rate. In these tests, probe I was placed about 5.5 m from the column lip in two opposing quadrants (quadrants 1 and 3). It can be seen that gas holdup in quadrant 1 is lower than in quadrant 3 for air velocities between 0.8 cm/s and 3.0 cm/s; but at an air velocity of 3.8 cm/s it became higher in quadrant 1. Because gas is the only fluid being injected it can be concluded that there is an uneven distribution of air in the column, which is reflected in differences of gas holdup among the quadrants.

The results of the measurements in industrial flotation columns under batch-water conditions presented in this section confirm the gas holdup probe give reliable results. Differences in estimates of gas holdup between conductivity and pressure were similar in magnitude to those encountered in the laboratory columns. The response in gas holdup to changes in operating conditions for both

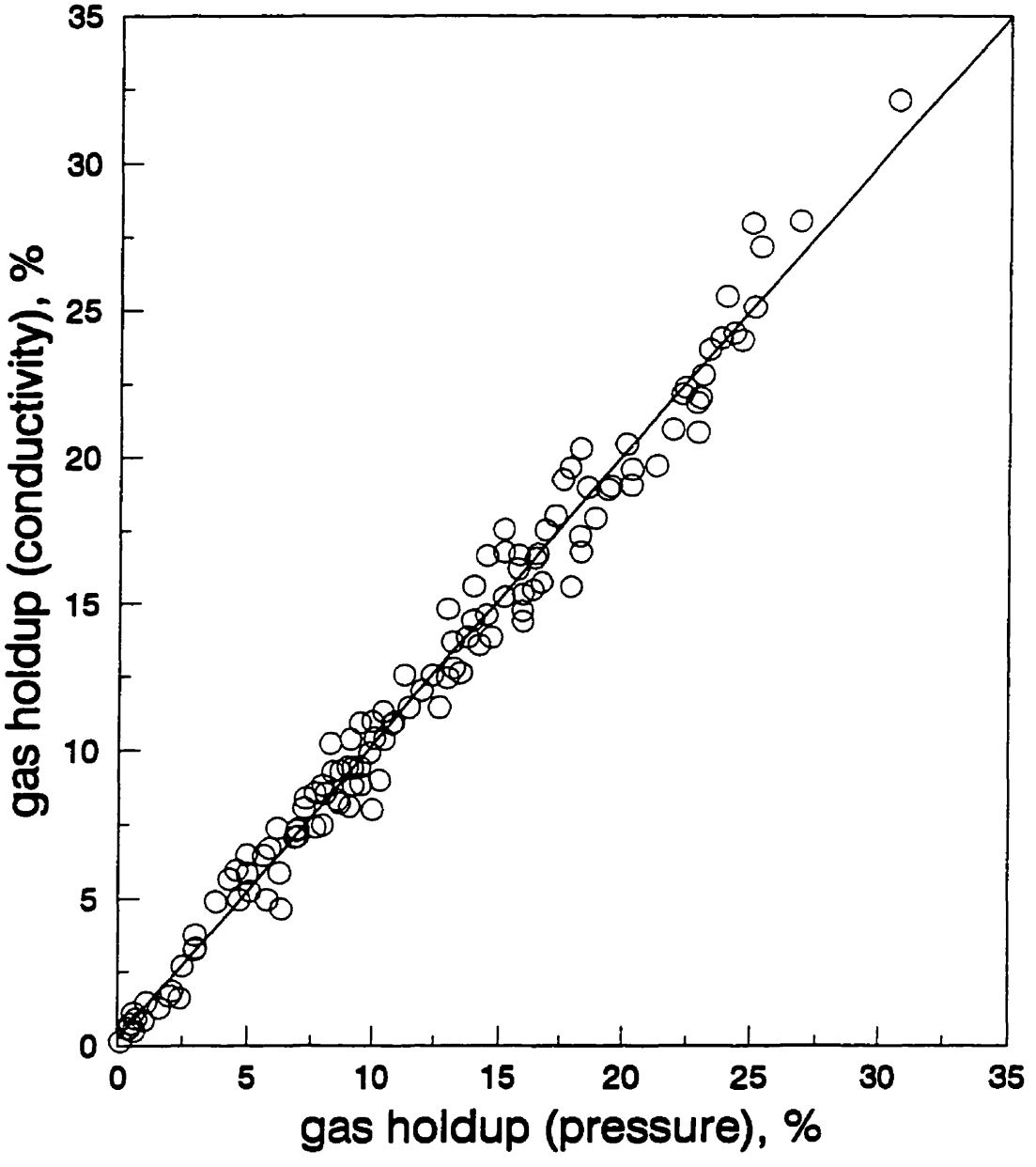

Fig.7.1. Comparison of gas holdup estimates in INCO column 3: unbaffled; probe I located at different depths in centre of column; different air flow rate (Jg: 0.8 to 3.0 cm/s); batch water (with frother).

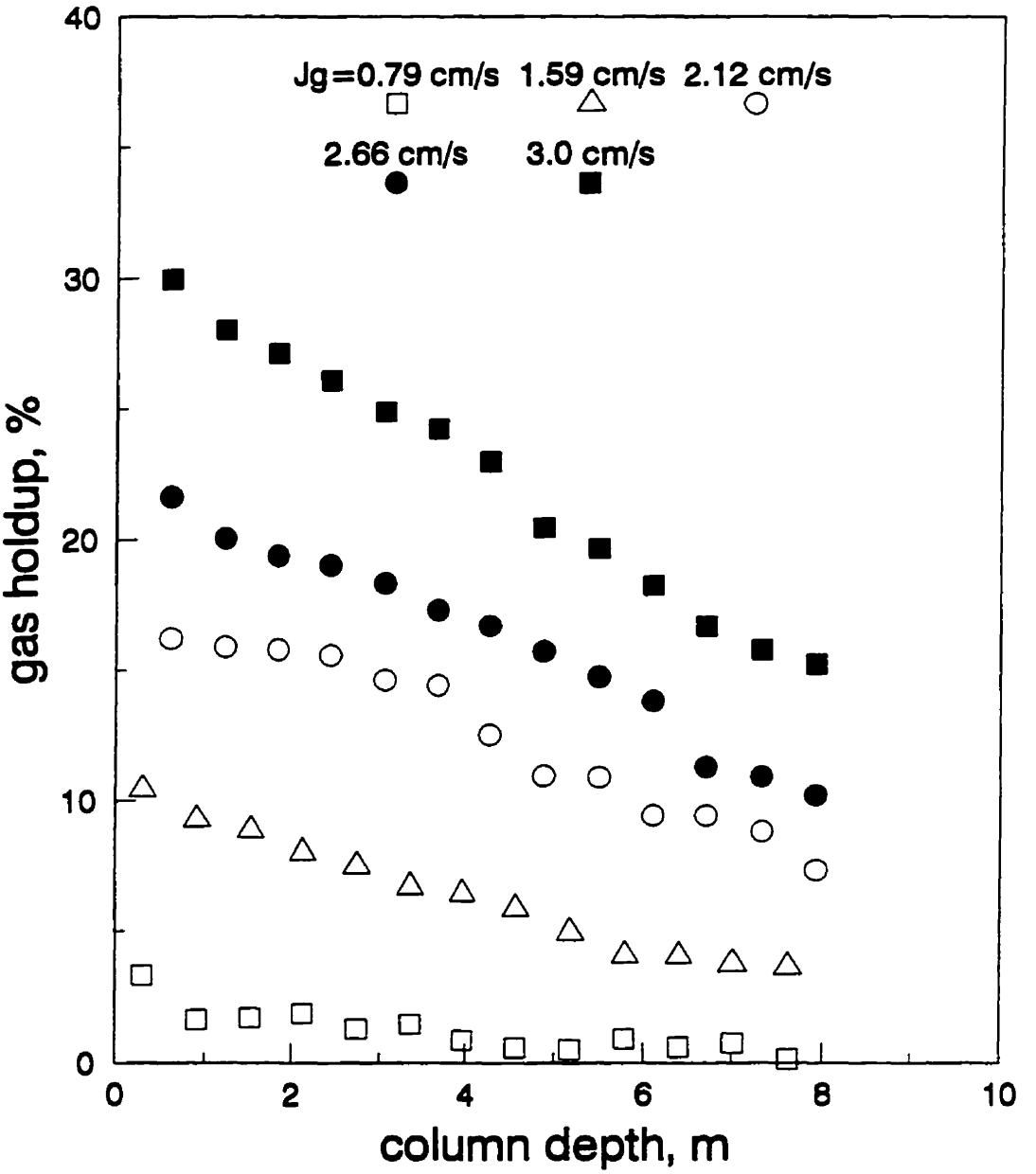

Fig.7.2. Gas holdup vs depth in INCO column 3: unbaffled; probe I in centre; batch water (with frother); various air flow rates.

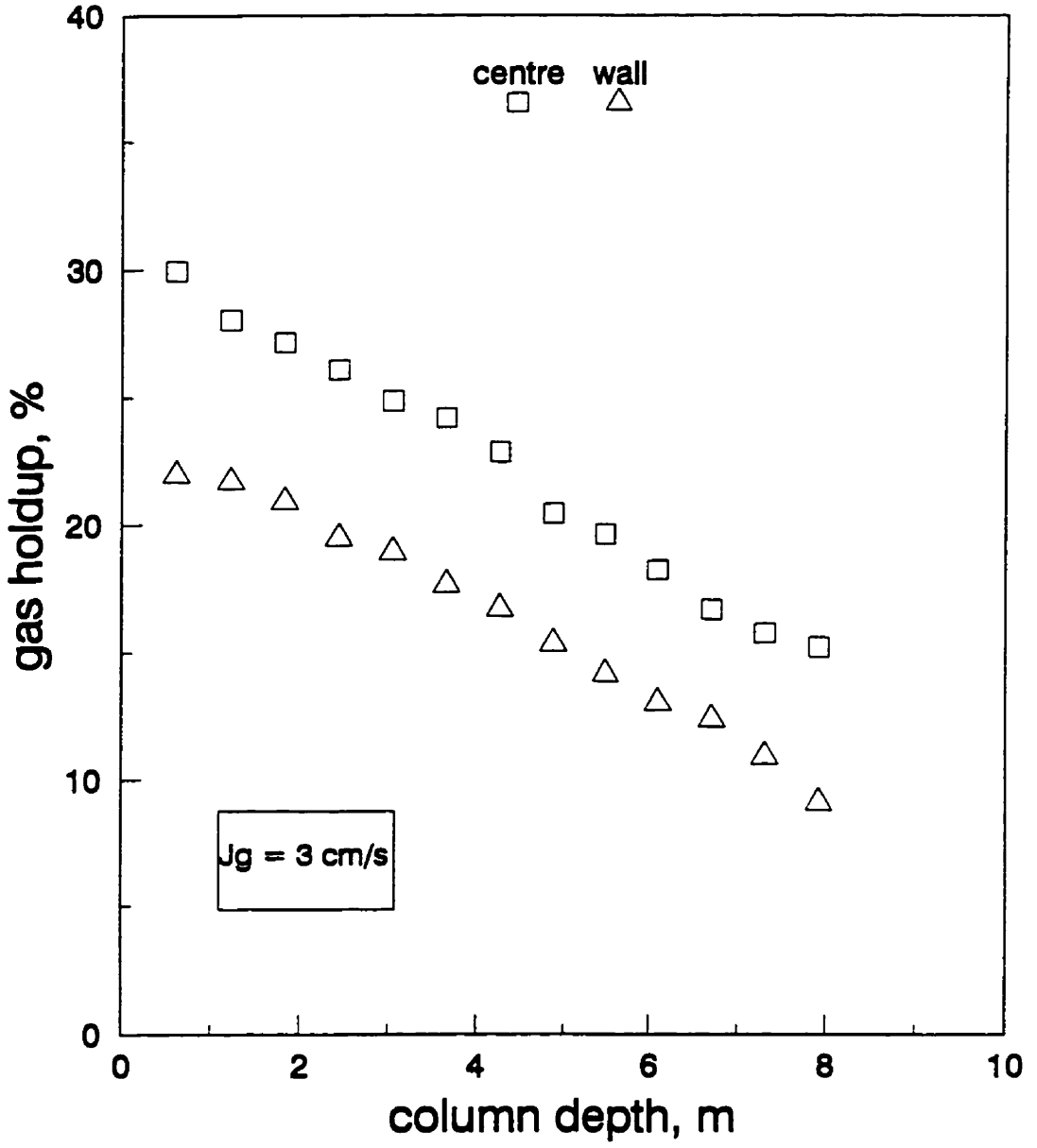

Fig.7.3. Gas holdup vs depth in INCO column 3: unbaffled; probe I located at two radial positions along the column; batch water (with frother).

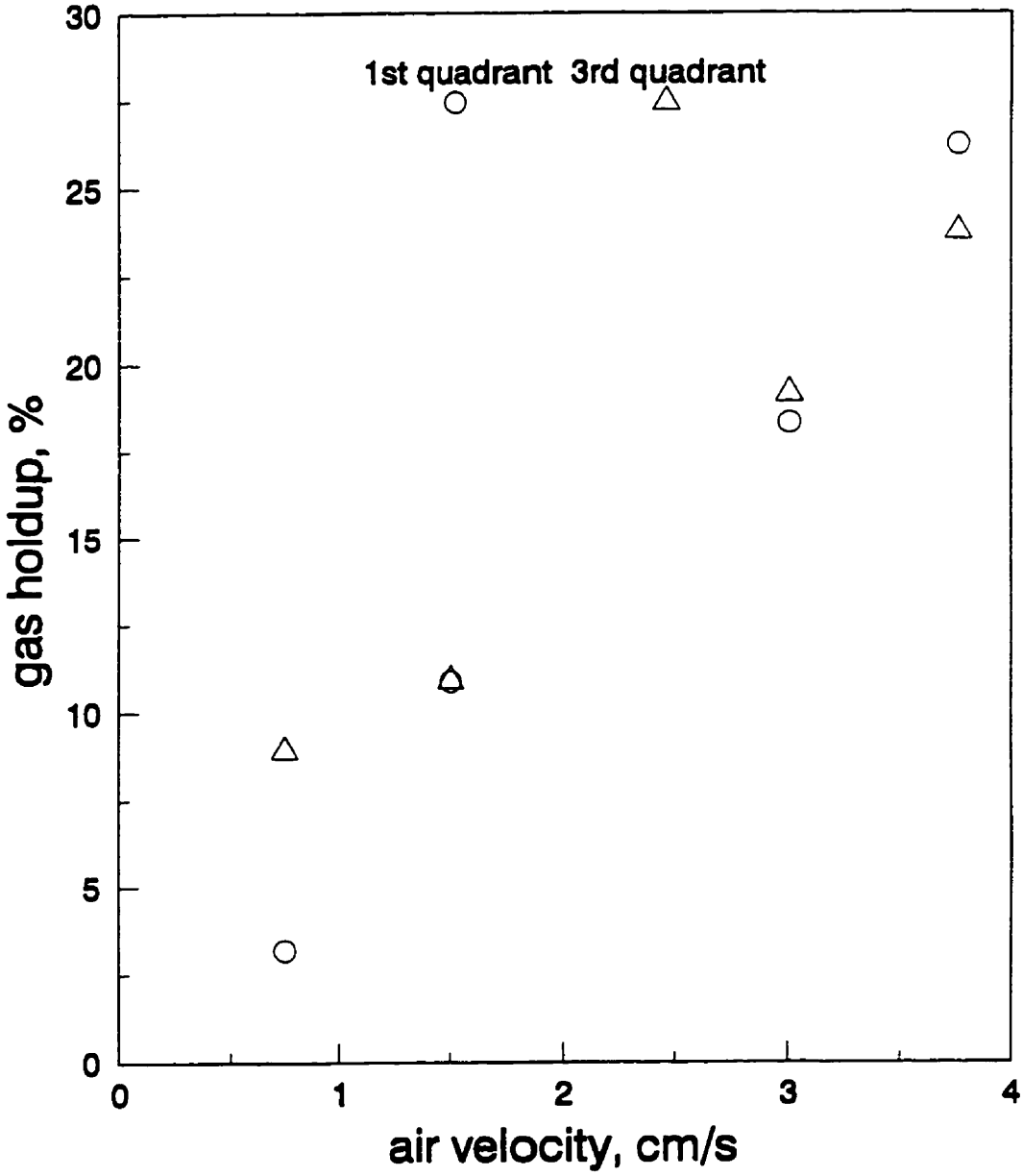

Fig.7.4. Gas holdup vs air velocity in INCO column 4: batch water (frother); probe I in two opposite quadrants 5.5 m from the column lip.

baffled and unbaffled columns also resembled those found in laboratory studies.

Therefore, up to this point the probe appears to be suitable to estimate gas holdup under plant conditions.

7.1.3. Testing column 2 under plant operating conditions

The probe was evaluated in column 2 under (normal) operating conditions. In these tests the air flowrate was fixed (in the control room) at 314 m^3/h, equivalent to an air superficial velocity of 2.8 cm/s.

Tests consisted in placing the probe in each quadrant of the baffled section of the column, and measuring the conductivity of the dispersion (with the open cell) and the slurry (with the syphon cell) every 0.5 m from a depth of 8.5 m to the column lip. Therefore axial gas holdup profiles were obtained along each quadrant, and continued above the top of the baffles.

Fig.7.5.(a) shows the raw conductivity data collected in the third and the second quadrants, and Fig.7.5.(b) gives the estimated gas holdup. The gas holdup was higher by about 25% in quadrant 2 throughout the baffled section of the column; however, once the probe reached the top of the baffles, the gas holdup above the second quadrant dropped to approach the same value as that above the third quadrant. The differences between these positions remained minimal as the probe approached the top of the column.

Radial differences in gas holdup in a flotation column can have several origins as shown in Chapter 6. An uneven distribution of air, wash water, feed slurry, or a combination may induce differences which may be intensified when baffles are installed. The data do not allow any definitive judgment to be made regarding the origin of the differences in gas holdup among the quadrants in column 2.

One approach to resolving the origin of gas holdup variations may be to consider the actual values of the conductivity of the slurry and of the dispersion. As presented in Fig.7.5.(a), it can be

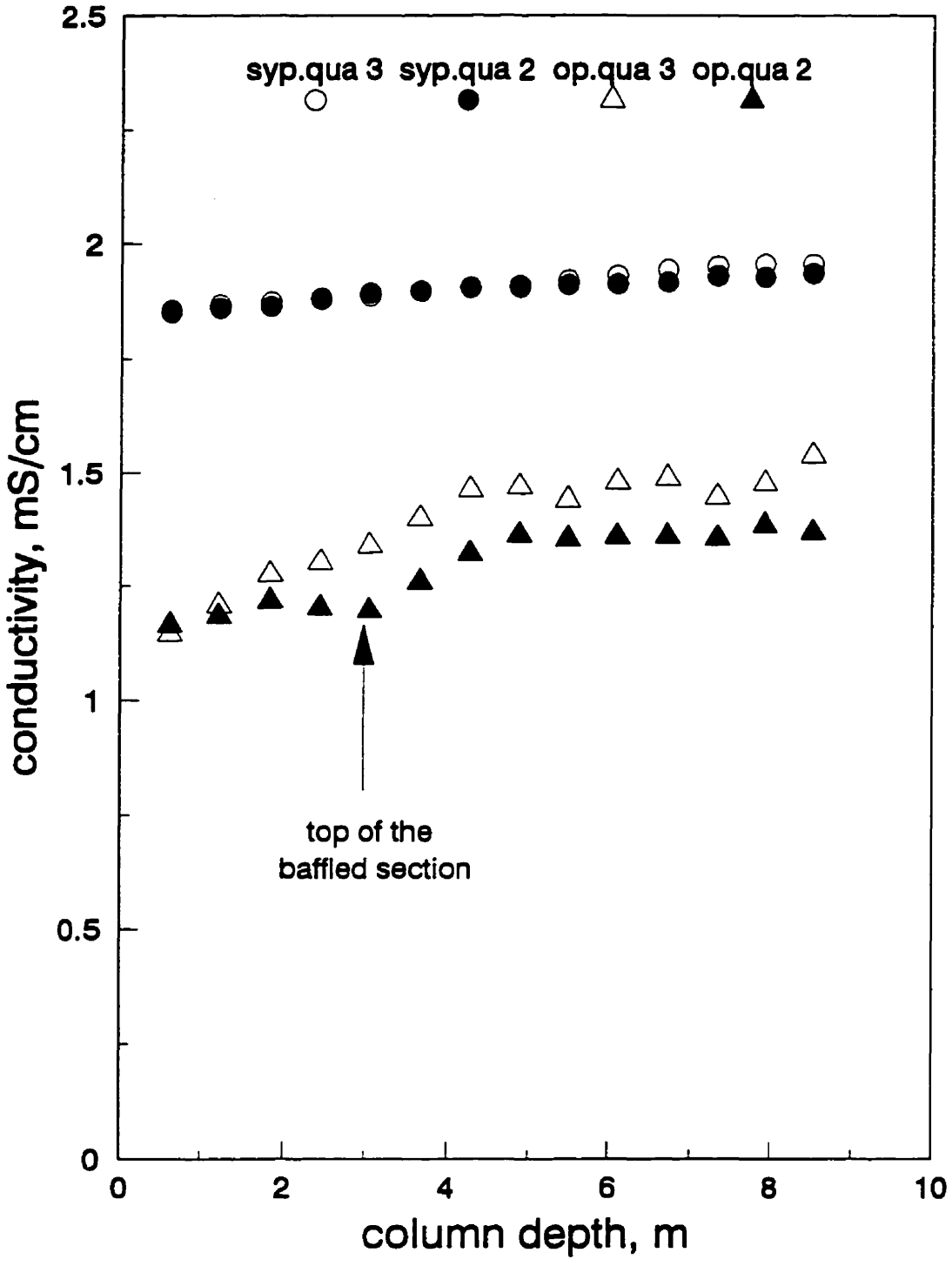

Fig.7.5.(a). Conductivity vs depth in INCO column 2: conductivity of the slurry, and conductivity of the dispersion (air-slurry) inside two quadrants and above the baffled section; normal operating conditions (Jg = 2.8 cm/s).
(Note: syp = syphon cell; op = open cell; qua = quadrant)

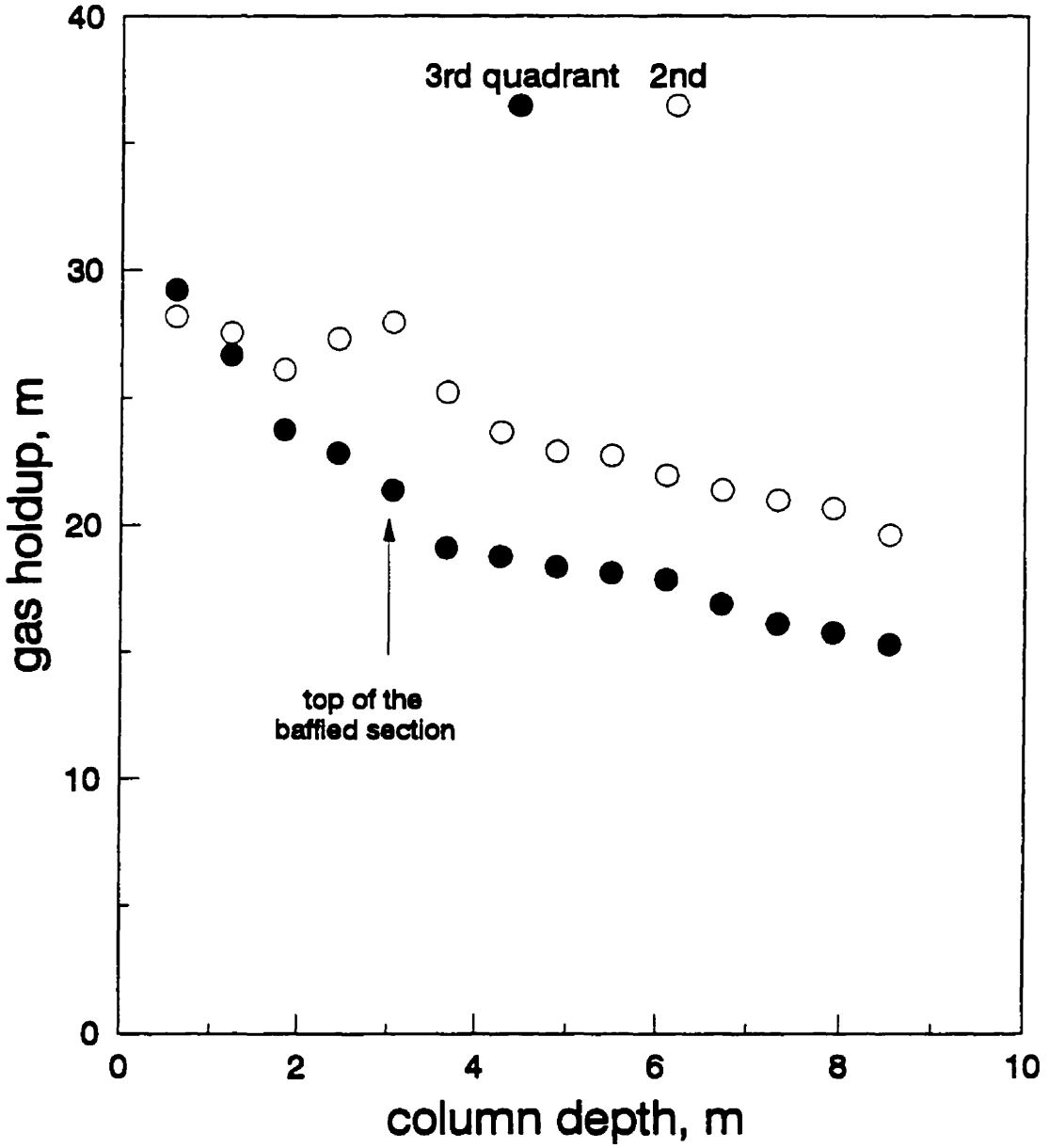

Fig.7.5.(b). Gas holdup vs depth in INCO column 2: probe II; normal operating conditions; the probe placed in different quadrants and moved up and down.

seen that the conductivity of the slurry is the same in both quadrants, and above the baffled section of the column, which implies that both the feed and wash water are uniformly distributed. (The differences in dispersion conductivity, of course, reflect the difference in gas holdup reported in Figure 7.5 (b)). Based on this, it seems that the origin of the difference in gas holdup is an uneven distribution of air.

A repeat test was carried out in column 2, at the same air flow rate (314 m^3/h; or Jg = 2.8 cm/s), 48 hours later. It was found that the gas holdup was different. Fig.7.6.(a) compares the data in and above the second quadrant, at the same axial and radial positions. It can be seen that the general pattern in the gas holdup behaviour does not change, but the gas holdup during the second test is markedly higher than in the first. Fig.7.6.(b) shows that the conductivity of the slurry in the first test is lower (by about 1 mS/cm) than in the second test.

This information suggests there were changes in the feed characteristics. The data could mean that in the test performed 48 hours later the feed solids content was lower which caused the increase in the conductivity of the slurry.

7.1.4. Testing column 3 under normal operating conditions

Column 3 is an unbaffled (or "open") flotation column, with dimensions similar to those of column 2 but using a different sparger system. The gas holdup probe was placed at three radial positions in the column: at the centre, in the middle between the centre and the wall, and at the column wall, and moved vertically.

In Fig.7.7 it is observed that there is a radial gas holdup profile, similar to that observed in the batch-water system, where the gas holdup is highest at the centre, and lowest at the column wall. This supports the notion that the sparger type and arrangement concentrates the air in the centre of the column.

Fig.7.8 presents the data as the raw conductivity data. The conductivity of the slurry does not vary significantly from the centre to the mid-way position but clearly increases at the column wall.

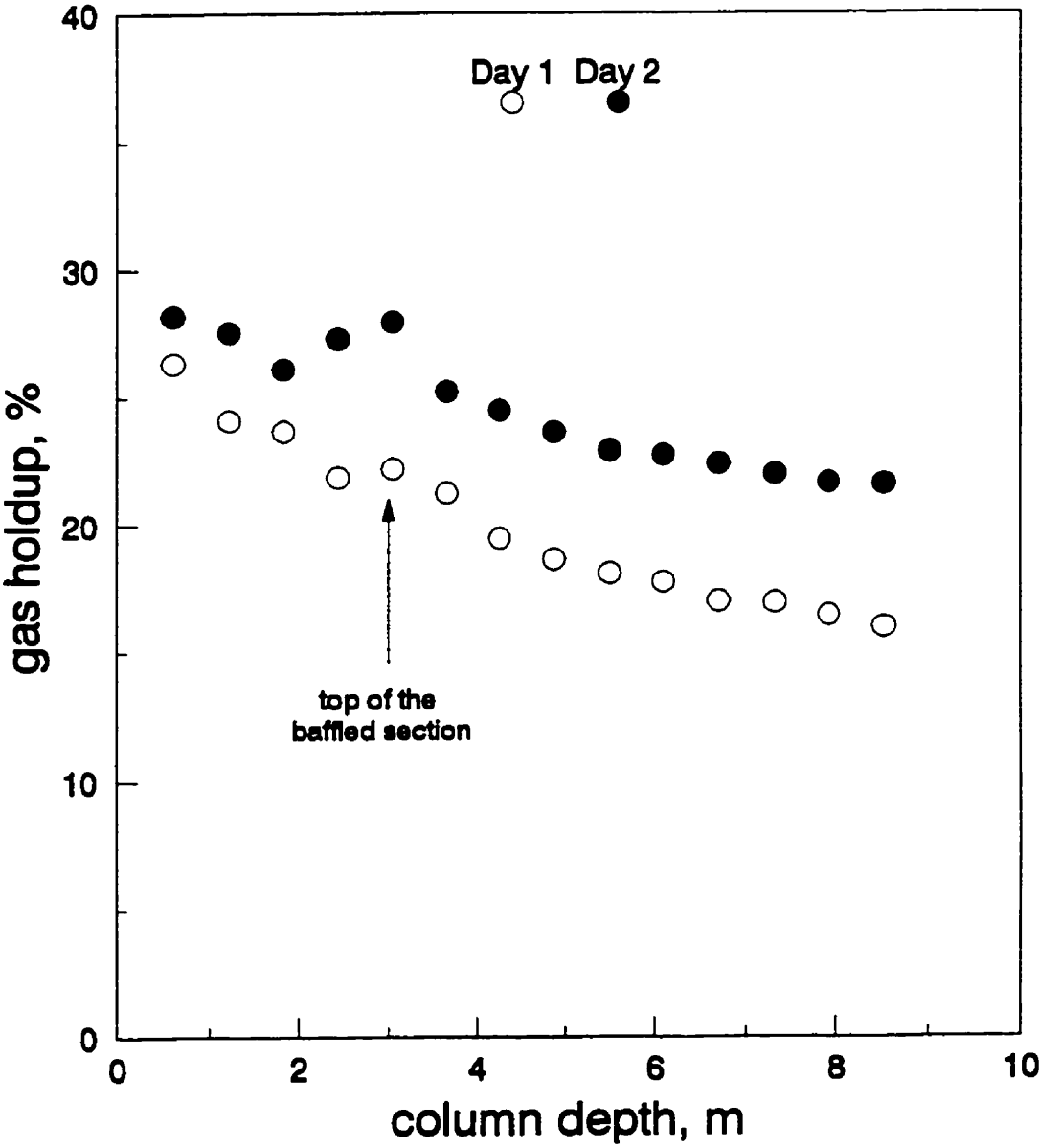

Fig.7.6.(a). Gas holdup vs depth in INCO column 2: probe II in same quadrant; measurements done 48 hours apart; normal operating conditions.

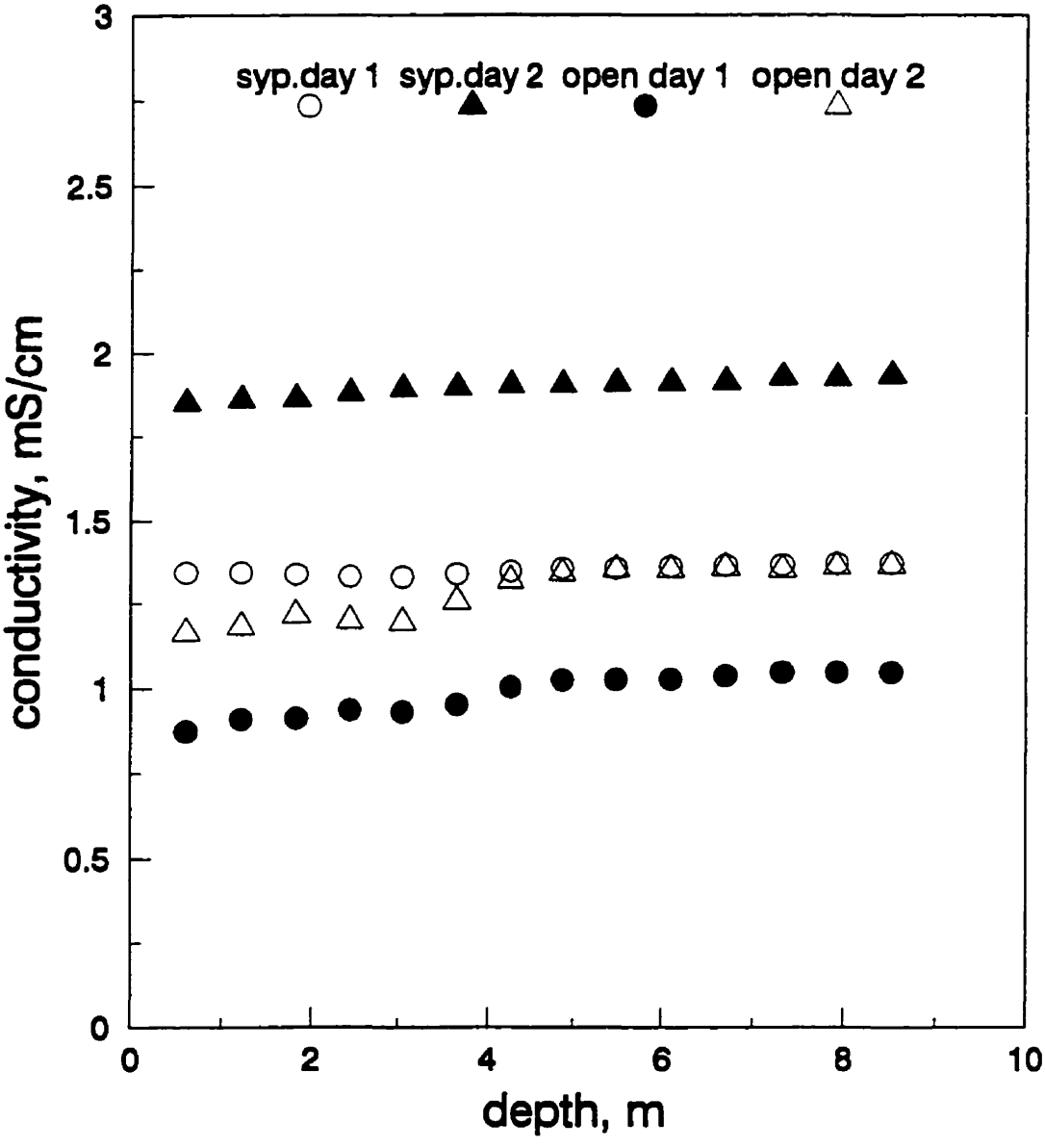

Fig.7.6.(b). Conductivity vs depth in INCO column 2; normal operating conditions; measurements 48 hours apart.

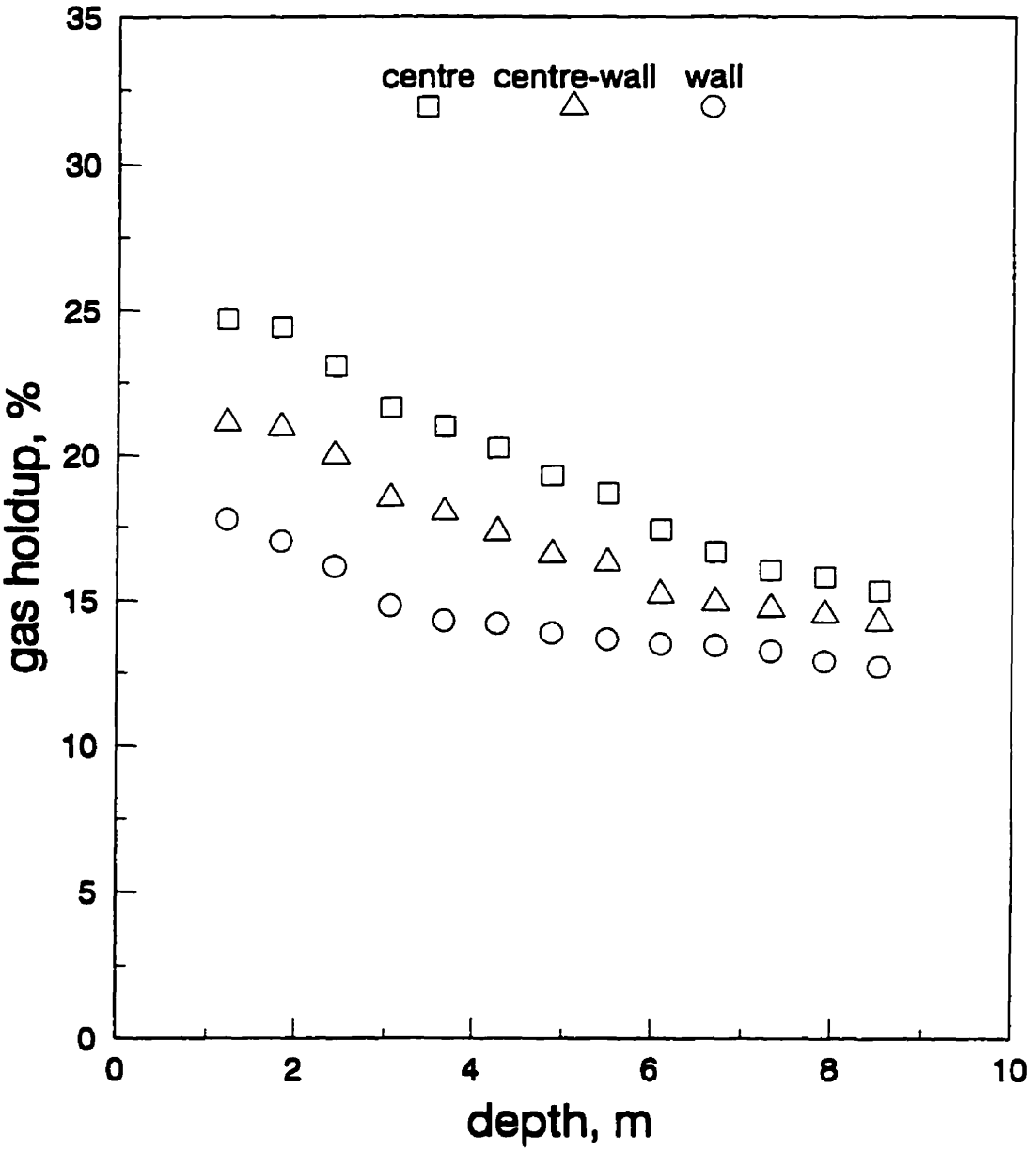

Fig.7.7. Gas holdup vs depth in INCO column 3: normal operating conditions; probe I in three radial positions; Jg = 2.4 cm/s.

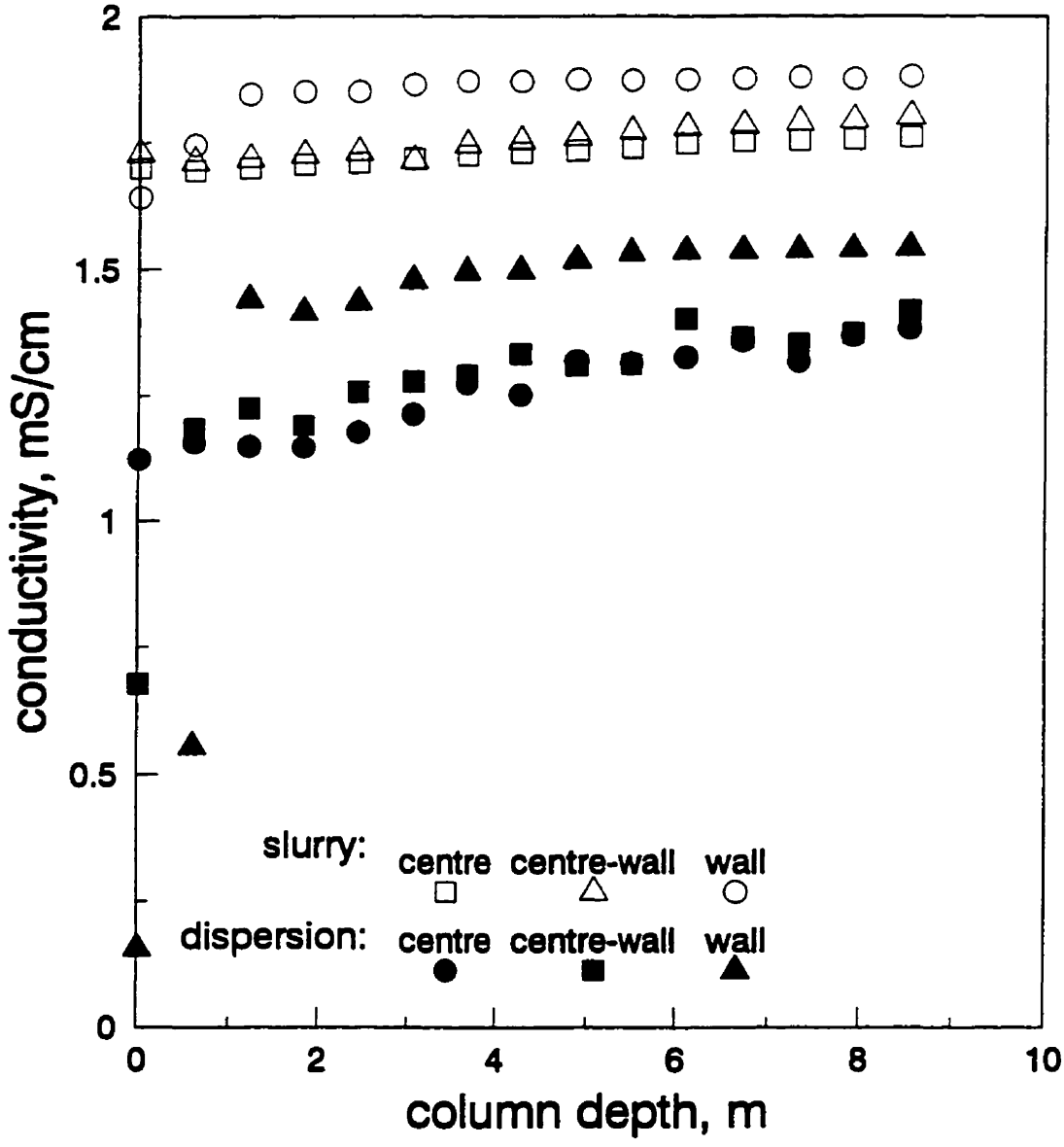

Fig.7.8. Slurry only conductivity and dispersion conductivity at three radial positions as a function of depth; INCO column 3; normal operating conditions.

This suggests that the slurry near the column wall may contain a lower amount of solids as compared with the slurry elsewhere. These observations suggest that mixing produces a distribution of solids in the collection zone of this flotation column.

To further explore this, solids holdup was estimated from the slurry only conductivity, and the conductivity of the clear liquid measured in a sample taken from the column (using a "Noranda sampler"); the conductivity of the clear liquid was 2.5 mS/cm. The solids holdup estimation was done by applying Maxwell's model. The results (Fig.7.9) show that solids holdup appears to be higher at the centre of the column than at the wall. These estimates, however, must be regarded as preliminary, because they are partly based on measurements external to the process (namely liquid conductivity).

7.1.5. Testing column 4 under operating conditions

Column 4, is the largest column, and used as a scavenger for nickel sulphide. The column has vertical baffles which extend from the feed level to about 1 m above the spargers. The spargers are horizontal perforated rubber. The feed line is 3 m below the column lip.

As shown previously (Fig.7.4), column 4 appears to have an uneven distribution of air. A test was conducted placing two probes in opposite quadrants to measure the conductivity of the dispersion and the slurry phases down the column to a depth of 8.5 m. The gas holdup was estimated at each position. Measurements were repeated at each time by interchanging probes I and II. The readings from the two probes were similar for the same position in the column. The advantage of using two probes, is that the two quadrants can be examined simultaneously which ensures similarity of conditions (gas rate, feed rate, etc.).

Fig.7.10 presents gas holdup as a function of depth. It is observed that gas holdup is larger in the first quadrant; however, when the probe is located above the baffled section, the gas holdups become similar. Above the baffled section of the column, mixing tends to equilibrate conditions.

A test was performed by placing the probes simultaneously 5 m from the lip of the column, then at 2 m. Results from these measurements (Fig.7.11) showed that the gas holdup in the first quadrant remained almost the same whether in or above the baffled section. But, the gas holdup in the third quadrant increased abruptly above the baffled section, becoming even higher than that above

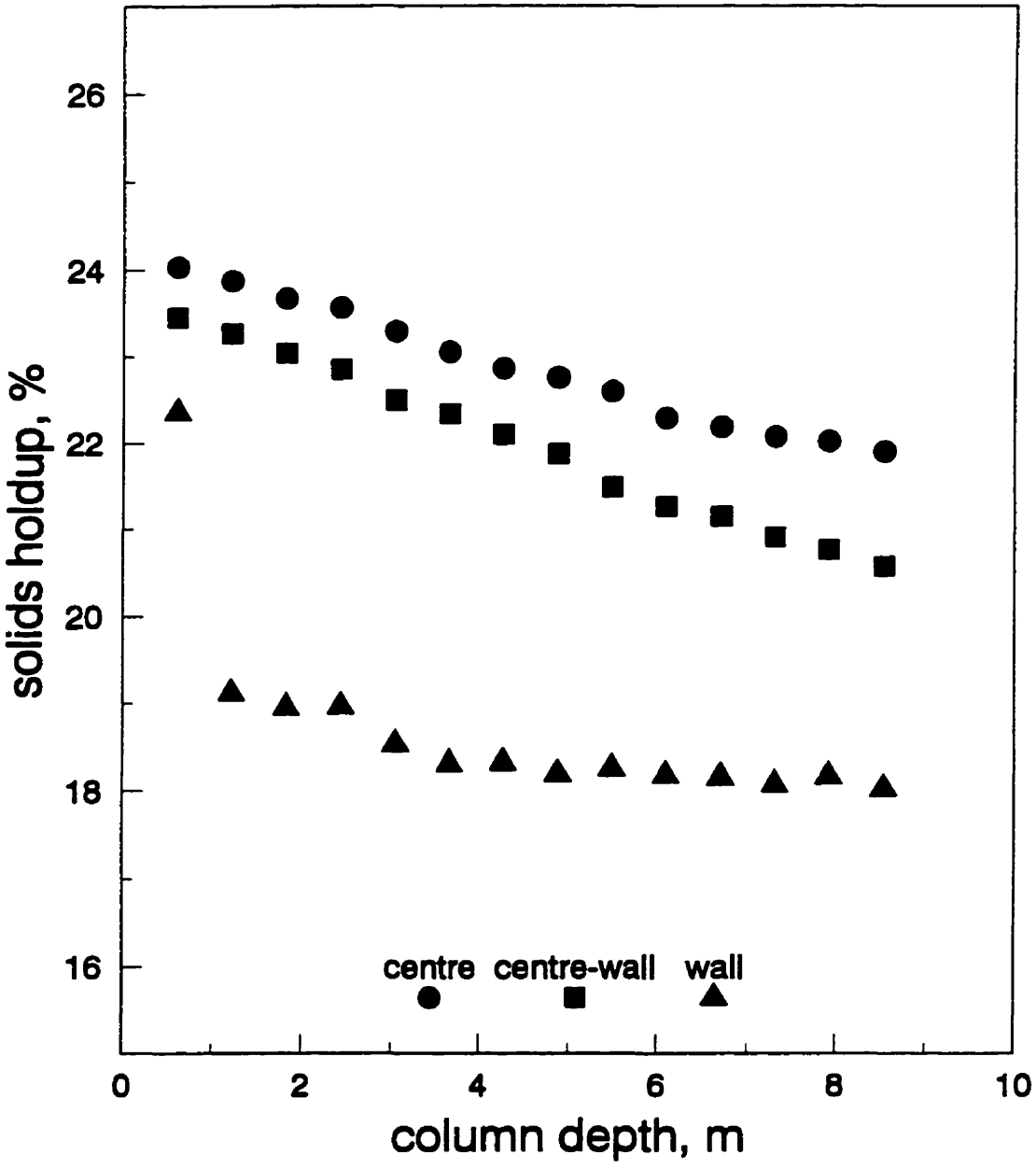

Fig.7.9. Solids holdup vs depth in INCO column 3: estimated solids holdup in three radial positions, from the slurry only conductivity and the conductivity of the clear liquid (2.5 mS/cm) using Maxwell's model.

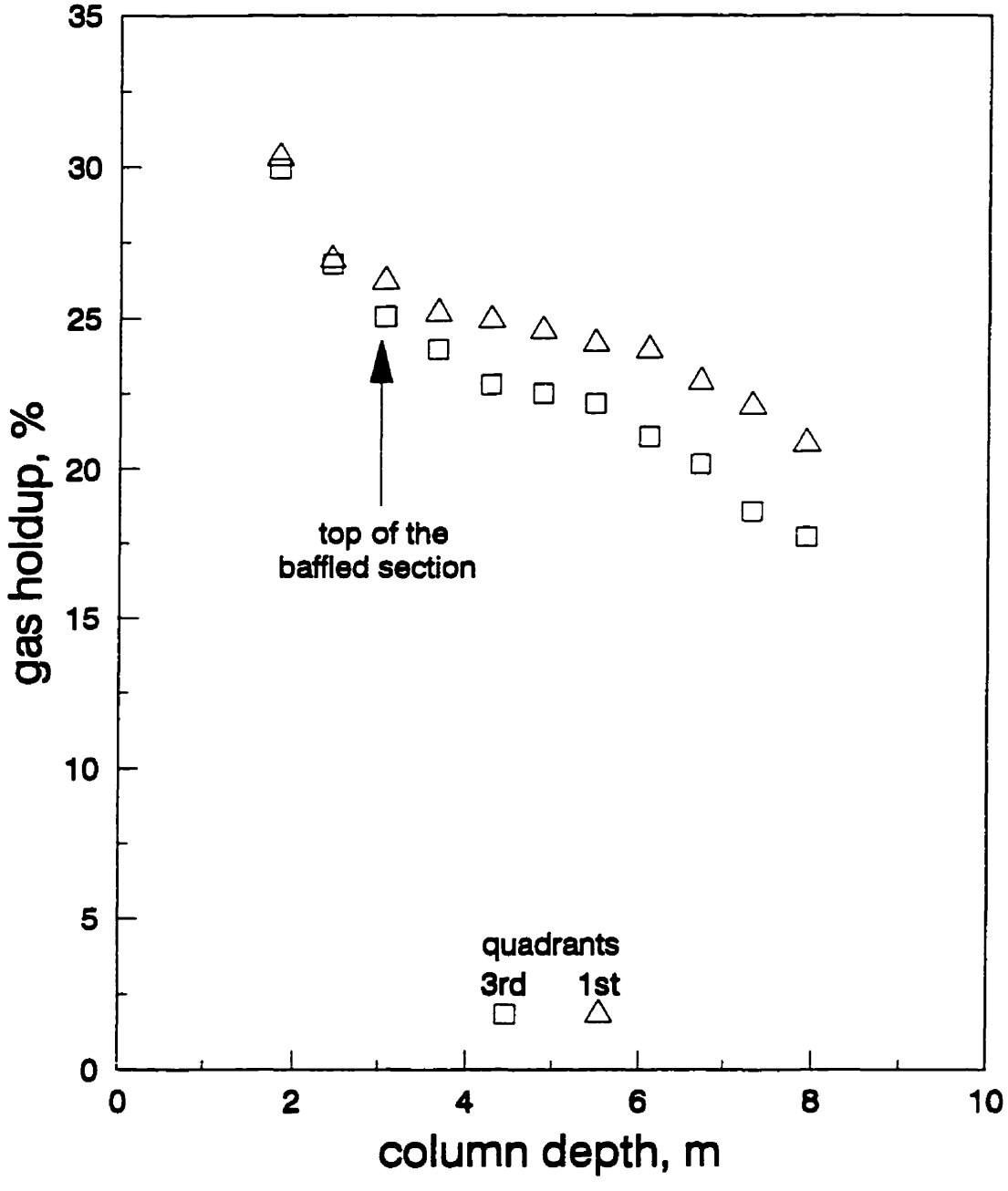

Fig.7.10. Gas holdup vs depth in INCO column 4: normal operating conditions; probe in different quadrants.

the first quadrant.

These data, do not reveal the possible origin in the gas holdup behaviour (nor whether this is significant for metallurgy). Therefore, it is necessary to "look" inside the flotation column process, perhaps through analysis of the conductivity data rather than just the data after processing to give gas holdup.

The conductivity data are presented in Fig.7.12 as a function of time. The slurry conductivity was found to be lower in the first quadrant than in the third quadrant (at a depth of 5m); however, the conductivity of the slurry above the baffles in the first quadrant increased noticeably approaching the values of the slurry conductivity associated with the third quadrant. This implies the percent solids is higher inside the 1st quadrant than the 3rd. At this stage, this does not correspond to expectations regarding the gas holdup behaviour.

7.2. Summary

The gas holdup probe has been tested in flotation columns at the INCO Matte Separation Plant, Sudbury District, ON.

Groups of tests were carried out under batch water conditions, by varying the air flow rate. The aim was to reproduce (to some extent) the tests carried out in laboratory flotation columns. The tests confirmed the accuracy of the gas holdup estimates using the probe.

The gas holdup probe detected radial and axial gas holdup profiles and differences between baffled sections. By analysing the slurry only conductivity it was possible to offer some insight into the role of gas, slurry and wash water distribution on gas holdup. Overall, the results indicate the gas holdup probe is a powerful new tool to diagnose flotation column operation.

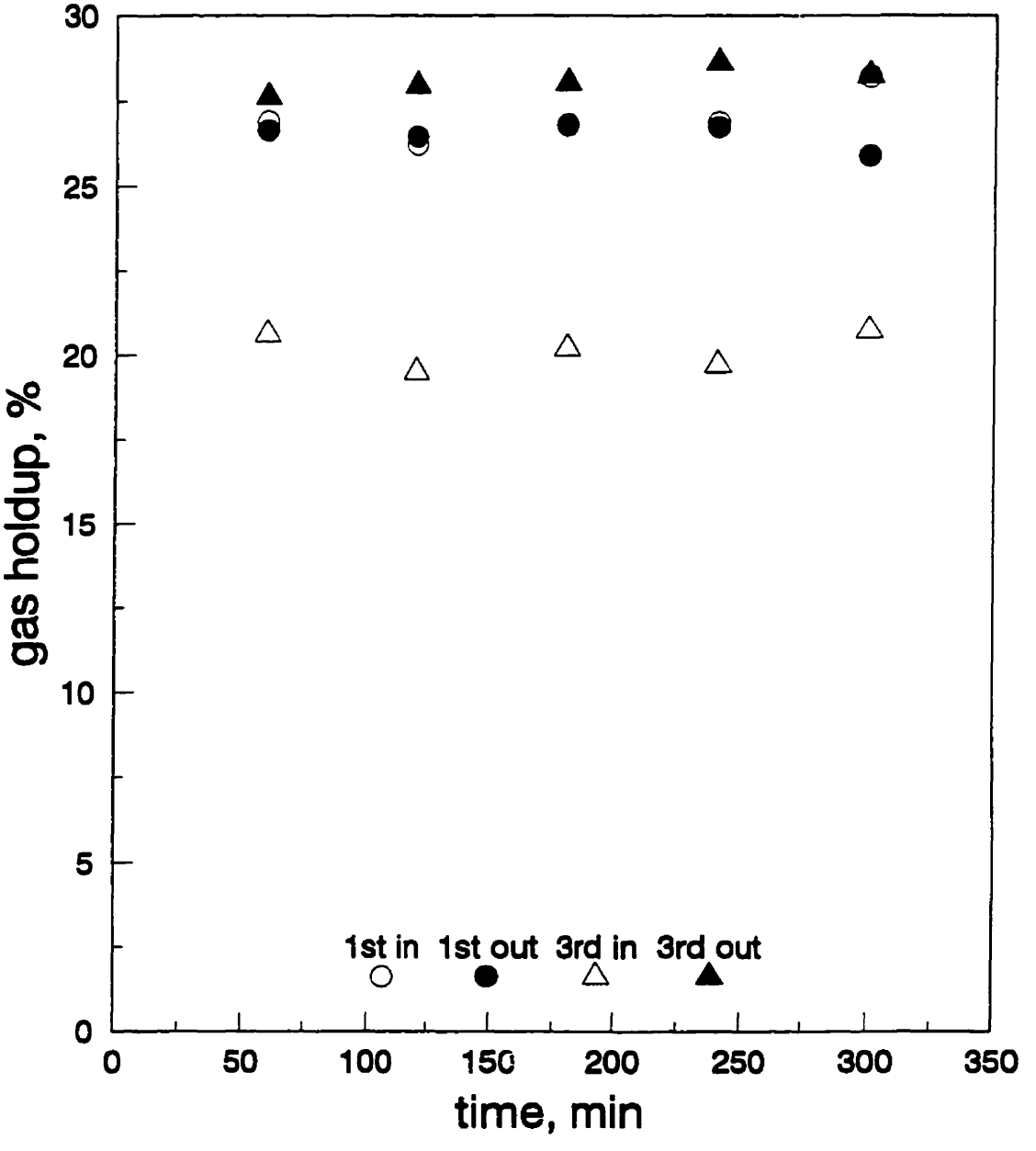

Fig.7.11. Gas holdup over time in INCO column 4: Gas holdup in 1st and 3rd quadrants in the baffled section at 5 m from the column lip ("in"), and above the baffled section at 2 m from the column lip ("out"); probe I; normal operating conditions.

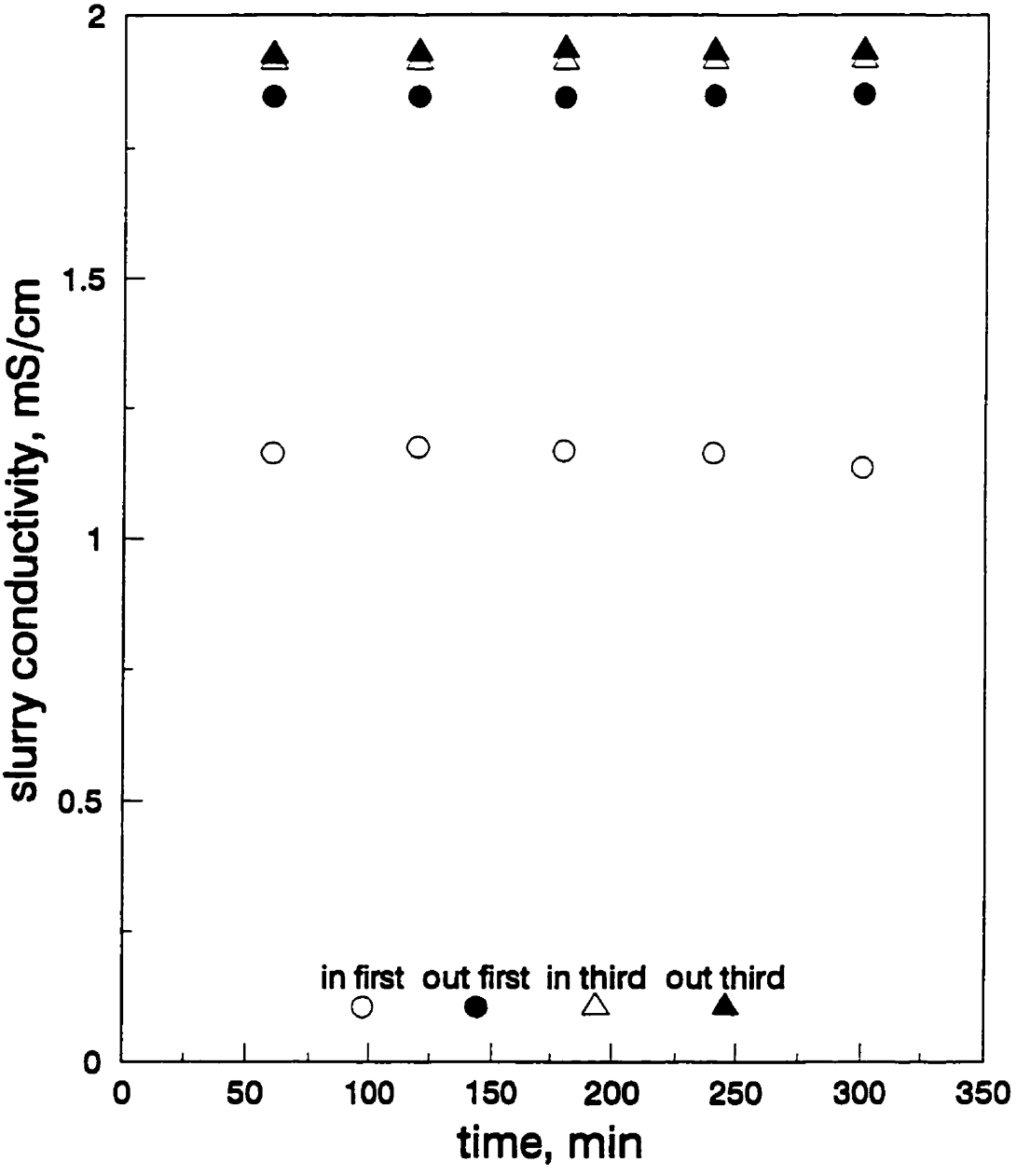

Fig.7.12. Slurry conductivity over time in INCO column 4: slurry conductivity in 1st and 3rd quadrants; normal operating conditions; the conductivity is measured in different quadrants in two positions, i.e. in the baffled section (5 m from the column lip), and above the baffles (2 m from the column lip).

CHAPTER 8

CONCLUSIONS AND FUTURE WORK

CONCLUSIONS

The mineral processing industry is in a race to improve productivity. This goal is being attained largely by implementation of automatic process control. This in turn demands better understanding of the relationship between the variables involved in the process, and accurate measurement of those variables. This thesis has focused on the measurement of gas holdup in flotation systems, a variable not measured reliably to date.

Measurements to be of use in plant should be carried out: on-line, in-situ, with no interruption of the system, or disturbance to the flow patterns, in real-time and, and with no assumptions regarding properties of any phase, or measurements external to the system. These were the objectives set.

A sensor was designed using so-called flow conductivity cells. Their properties were studied and modelled, and their application in the design, construction, and operation of a gas holdup probe for use in flotation systems described.

The following conclusions were drawn from the work.

8.1. Flow conductivity cells

A flow cell is defined as one that allows a fluid or dispersion to flow through relatively freely while the electrical conductivity is measured.

One of the most important features of a flow cell is the so-called cell constant. The cell constant has been defined as the ratio between the effective surface area used to transfer electrical energy, and the distance between two points between which the electrical energy is transferred. Once the cell constant is determined through calibration, the cell can be used to measure liquid and dispersion conductivity.

The cell constant depends mainly on cell dimensions, and is largely independent of the characteristics of the fluid. That is, absolute values of conductance (S) and conductivity (SL^{-1}) measured in a given cell are independent of the type of electrolyte.

The addition of non conductive bodies to the fluid was experimentally analysed. It was concluded that the cell constant is not affected by the presence of such bodies. These systems are described by Maxwell's model for a dispersion of non-conducting phase in a conducting medium; Maxwell's model relates the fraction of non conductive phase (holdup) in the system to the conductivity of the continuous phase and the conductivity of the dispersion.

It was demonstrated that the electromagnetic field associated with the flow cells can be solved using the MagNet 5.1 software. Predicted results for cell constant were in good agreement with the experimental. The model holds the potential for design of flow cells for particular applications in mineral processing.

8.2. The gas holdup probe

The gas holdup probe developed in this work applies the principle of separation of phases to fulfil the requirements of Maxwell's model. The key to this approach consists of using two flow cells to assess the required properties of the system.

One of the cells, named the open flow cell, measures the conductivity of the dispersion while the other, the syphon cell, measures the continuum conductivity. The syphon cell is open at the top, and closed at the bottom save for a small side orifice. This geometry excludes air bubbles from entering. Consequently the liquid (slurry) with no air bubbles in the cell has a larger density than the dispersion outside the cell, and this induces a flow of liquid (slurry) out of the cell through the side orifice. The liquid (slurry) is continuously replenished by liquid (slurry) flowing into the cell at the top, hence the name "syphon cell". Provided this flow is not sufficient to carry air bubbles in, the cell becomes filled with bubble-free liquid (slurry).

In both the open and syphon cells three ring electrodes are used, the outer two of the opposite polarity to the middle one. In this way the electrical field is constrained inside the cell.

The assembly of these two cells is called the gas holdup probe. It measures simultaneously

the conductivity of the dispersion and the conductivity of the continuous (conductive) phase at close to the same point in the system.

The test work, in both laboratory and industrial flotation columns, demonstrated that the probe gave accurate estimates of gas holdup. The probe satisfied the requirements of an industrial sensor, as it performs in-situ, on-line, in real-time, with no external measurements and no assumptions regarding properties of any phase.

The gas holdup probe was used to explore operating flotation columns. It appears to hold great promise for diagnosis, readily detecting, for example, differences in gas holdup between sections of a baffled column.

This success may make the probe a candidate sensor for automatic control process, although this will require a significant in-plant effort to realize. As a first step, the probe offers an opportunity to study the relationship between gas holdup and metallurgy, at least in flotation columns.

SUGGESTIONS FOR FUTURE WORK

8.3.1. Relationship between gas holdup and metallurgy

The results from plant demonstrated that the gas holdup probe is accurate enough to detect gas holdup changes during operation. Work has to be conducted to develop several units which can be maintained in operation for extended periods of time; the purpose is to detect gas holdup changes and to relate these changes to operating conditions and/or metallurgical performance.

8.3.2. Simultaneous gas and solids holdup measurement in flotation systems

To achieve such measurements, a probe using conductivity as the basis combined with the phase separation method used in this thesis and with the standard addition method proposed by Pérez [1996] and described by Gomez et al. [1995(b)] could be conceived. Alternatively, a probe could be based on a combination of conductivity and pressure measurements.

For example, the syphon cell may contain two flow cells (Fig.8.1.(a)): one, as currently

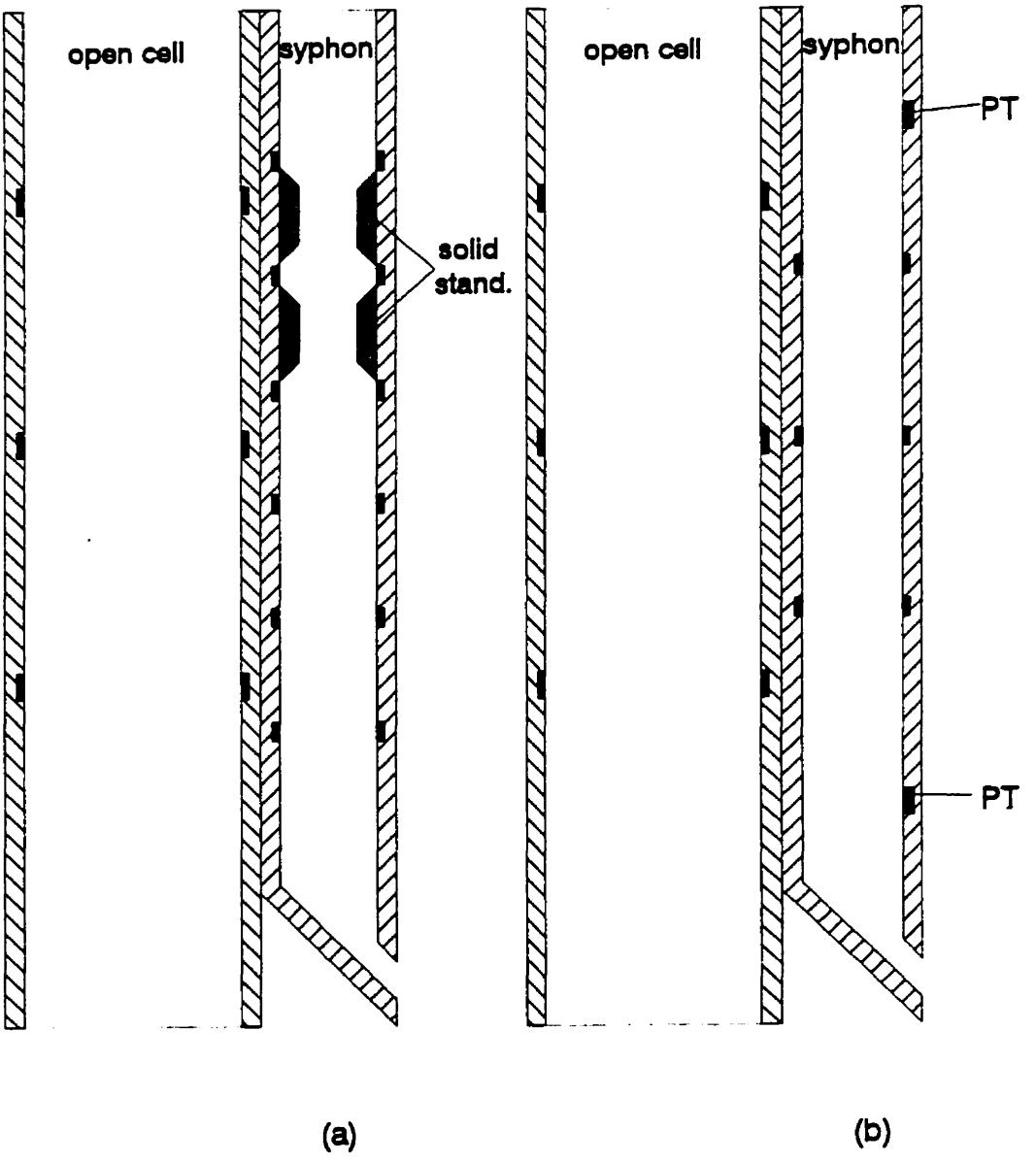

Fig.8.1. Schematic representation of two possible probes for simultaneous gas and solids holdup measurements:
(a). Syphon with two cells; one is with added solids "standard".
(b). Syphon with electrodes and pressure transmitters (PT).

designed and a second containing a solid standard to determine (in combination with the first) the solids content . Or alternatively the conductivity cell may be used in conjunction with two pressure transmiters to measure the pressure drop between two points inside the syphon cell (Fig.8.1.(b)). Therefore, Maxwell's model may be used to determine gas holdup from the conductivity measured with the open cell and the conductivity of the solids-liquid conductivity (slurry only conductivity) measured with the syphon flow cell, and to determine the solids holdup from the combined cells in the syphon tube, or from pressure measurement.

Experimental work on modelling of flow cells by using the standard addition technique and combined conductivity-pressure is required to design an overall holdup probe.

8.3.3. Probe modification to rotate the open cell

The gas holdup probe could be modified to rotate the open cell at different angles with respect to the original vertical position in order to detect radial components in the gas-slurry dispersions in flotation systems. At the actual stage of the gas holdup probe, it is thought that the bubble-slurry dispersion flows in the axial direction and the sample of the dispersion represents that of the place of measurement.

8.3.4. Measurement of bubble size.

The gas holdup probe offers a unique opportunity to estimate bubble size in flotation column operations, as a tool for gas holdup measurement, to relate flotation rate constant to bubble size, bubble surface area flux, particle collection efficiency, and superficial gas velocity [Gorain et al., 1996].

8.3.5. Applications in other fields of engineering

In mineral processing the measurement of conductivity has been applied in different areas such as thickening, filtering and flotation. There is a growing interest in other fields of engineering.

Wherever there exist differences in conductivity between phases involved in a process, the technique may be applied (provided suitable materials are available to build conductivity probes). Some examples are:

- Hydrometallurgy: solvent extraction; agitated leach tanks; precipitation processes;
- pyrometallurgy: molten salt processes; metal-slag-gas systems;
- chemical engineering: percent solids in pipes; liquid fraction in pipes; bubble column reactors; liquid-liquid reaction systems; liquid-solid reaction systems; crystallisation processes; food industry; water deoiling systems; paper recycling; etc.

8.4. Claims for original research

1. Flow cells for measuring conductivity have been used to assess properties of dispersions in mineral flotation systems. The technique to characterize the cell constant in flow cells was identified. The appropriate methodology to generate the conductivity data was determined. MagNet 5.1 software was used to solve the electromagnetic field associated with the flow cells. The potential of this software for design of flow cells for applications in mineral processing was demonstrated.

2. A conductivity probe to measure gas holdup in the collection zone of flotation columns was conceived, developed and verified. The probe developed in this work applies the principle of separation of phases to fulfil the requirements of Maxwell's model. The probe carries out the measurements on-line, in-situ, with no interruption of the system, nor disturbance of the flow patterns, in real-time, with no assumptions regarding properties of any phase, and with no measurements external to the system. Therefore, the probe could be described as ideal from the point of view of the mineral processing engineer. The probe was shown to be suitable to diagnose flotation columns operation.

REFERENCES

Agar, G.E., Khan, F., Markovich, B., Mukherjee, A., Shea, B., Kelly, C., Robertson, G.E. and Stratton-Crawley, R., 1996. "Laboratory flotation separation of INCO "bulk" matte," 28th Annual Meeting of the Canadian Mineral Processors, CIM, Paper No. 20, pp. 289-304.

Banisi, S., Finch, J.A. and Laplante, A.R., 1993. "Electrical conductivity of dispersions," Minerals Eng., Vol. 6, No. 4, pp. 369- 385.

Banisi, S., Finch, J.A. and Laplante, A.R., 1994. "On-line gas and solids holdup estimation in solid-liquid-gas systems," Minerals Eng., Vol. 7, No. 9, pp. 1099-1113.

Banisi, S., Finch, J.A., Laplante, A.R. and Weber, M.E., 1995 (a). "Effect of solid particles on gas holdup in flotation columns - I. Measurements," Chem. Eng. Sci., Vol. 50, No. 14, pp. 2329-2334.

Banisi, S., Finch, J.A., Laplante, A.R. and Weber, M.E., 1995 (b). "Effect of solid particles on gas holdup in flotation columns - II. Investigation of mechanisms of gas holdup reduction in presence of solids," Chem. Eng. Sci., Vol. 50, No. 14, pp. 2335-2342.

Begovich, J.M. and Watson, J.S., 1978. "An electroconductivity technique for measurement of axial variation of holdups in three-phase fluidized beds," AIChE Journal, Vol. 24, No. 2, pp. 351-354.

Binns, K.J. and Lawrenson, P.J., 1973. Analysis and computation of electric and magnetic field problems, second edition, Pergamon Press, Oxford.

Dickin, F.J., Williams, R.A. and Beck, M.S., 1993. "Determination of composition and motion of multicomponent mixtures in process vessels using electrical impedance tomography," Chem. Eng. Sci., Vol. 48, pp.1883-1897.

Dobby, G.S., Yianatos, J.B. and Finch, J.A., 1988. "Estimation of bubble diameter in flotation columns from Drift flux analysis," Can. Met. Quart., Vol. 27, No. 2, pp. 85- 90.

Edwards, J.D. and Freeman, E.M., 1995. MagNet 5.1 User Guide, Infolytica Corporation, Montreal.

Eyring, H., 1936. "Viscosity, plasticity and diffusion as examples of absolute reaction rates," Journal of Chemical Physics, Vol. 4, pp. 283-293.

Fan, L.S., 1989. Gas-Liquid-Solid Fluidization Engineering. Chapter 2. Butterworth Publishers.

Finch, J.A. and Dobby, G.S., 1990. Column Flotation, Pergamon Press, Oxford.

Fricke, H., 1925. "A mathematical treatment of electric conductivity and capacity of dispersed systems, II," Phys. Rev., Vol. 26, pp 678-687.

Gebhart, J.E. and Shedd, K.N., 1988. 173rd Meeting of the Electrochemical Society, Atlanta, GA, May 15-20, 17 pp.

Gomez, C.O., Uribe-Salas, A., Finch, J.A. and Huls, B.J., 1990. "A calibration probe for level detection systems in flotation columns," CIM Bulletin, Vol. 83, No. 935, pp. 118-121.

Gomez, C.O., Uribe-Salas, A., Finch, J.A. and Huls, B.J., 1995. "Axial gas holdup profiles in the collection zones of flotation columns," Minerals and Metal. Processing, Feb., pp. 16-23.

Gomez, C.O., Tavera, F., Finch, J.A., Perez, R. and del Villar, R., 1995(b). "Continuous gas holdup measurements in flotation columns," in Flotation. Proc. IVth Meeting of the southern hemisphere on mineral technology, Castro S. and Alvarez J. eds. (Concepción, Chile: University of Concepción, 1994), pp. 123-136.

Gorain, B.K., Manlapig, E.V. and Franzidis, J.-P., 1996. "The effect of gas dispersion properties on the kinetics of flotation," in COLUMN'96, Proc. of the International Symposium on Column Flotation, C.O. Gomez and J.A. Finch ed., the Metallurgical Society of the Canadian Institute of Mining, Metallurgy and Petroleum (Montreal, Quebec, Canada), pp. 299-313.

Heimala, S., Jounela, S., Rantpuska, S. and Saari, M., 1985. Proc. XIV International Mineral Processing Congress, Gedim (France), Vol. 3, pp. 88-98.

Heinrich, G.W., Wells, P.F., Whittaker, P.J. and Kelebek, S., 1995. "Copper-nickel separation pilot plant evaluation of flowsheet options," 27th Annual Meeting of the Canadian Mineral Processors, CIM, Paper No. 7, pp. 101-118.

Heiskanen, K., 1993. Particle Classification, Powder Technology Series, Chapman & Hall, London.

Ingham, S., 1995. Report, Department of Mining and Metallurgical Eng., McGill University, Sept.

Israelachvili, J.N., 1992. Intermolecular and surface forces, Academic Press Limited, London.

Ityokumbul, M.T., Kosaric, N. and Bulani, W., 1995. "Effect of fine solids and frother on gas hold-up and liquid mixing in a flotation column," Minerals Engineering, Vol. 8, No. 11, pp. 1369-1380.

Jones, M.H. and Woodcock, J.T., 1976. Analytical Chimica Acta, Vol. 87, pp. 463-471.

Kawatra, S.K., 1993. in Emerging Computer Techniques for the Mineral Industry. Scheiner, B.J., Stanley, D.A. and Karr, C.L. eds., AIME, pp. 259-270.

Khan, G.A. and Frolov, Y.M., 1985. Tsvetn, Met, No. 1, pp. 90-94.

Labonté, G. and Finch, J.A., 1989. SME Annual Meeting, Las Vegas, Feb 27-March 2.

Lord, J.A. and Markovic, s., 1970. Proc. 9th Int. Mineral Process. Congr., Prague, Vol. 1, pp. 259-269.

Maxwell, J.C., 1892. A Treatise of Electricity and Magnetism, 3rd Edition, Vol. 1, Part II, Chapter IX, Oxford University Press, London, pp. 435-449.

McKee, S.L., Bell, T., Dyakowski, T., Williams, R.A., Davies, R. and Allen, T., 1995. "Solids flow imaging and attrition studies in a pneumatic conveyor," Powder Technology, Vol. 82, pp. 105-113.

Moudgil, B.M., Zhu, S.L. and Pinault, J.L., 1993. in Emerging Computer Techniques for the Mineral Industry. Scheiner, B.J., Stanley, D.A. and Karr, C.L. eds., AIME, pp. 251-258.

Moys, M.H., Engelbrecht, J. and Terblanche, N., 1991. "Design of baffles to reduce axial mixing in flotation columns," Column'91, Proceedings of an International Conference on Column Flotation, Vol. 1, (Agar, G.E., Huls, B.J. and Hyma, D.B., eds.), MITEC, CIM, CMP, Sudbury, Ontario, June 2-6, pp. 275-288.

Nasr-El-Din, H., Shook, C.A. and Colwell, J., 1987. "A conductivity probe for measuring local concentrations in slurry systems," Int. J. Multiphase Flow, Vol. 13, No. 3, pp. 365-378.

Nichols, T.L., Jung, S.J., Wu, G.L. and Priesbrey, K., 1993. in Emerging Computer Techniques for the Mineral Industry. Scheiner, B.J., Stainley, D.A. and Karr, C.L. eds., AIME, pp. 251-258.

Nicklin, D.J., 1962. "Two-phase bubble flow," Chem. Eng. Sci., Vol. 17, pp. 693-702.

Paleari, F.T., Xu, M. and Finch, J.A., 1994. "Radial gas holdup profiles: the influence of sparger systems," Minerals and Metal. Proc. (SME/AIME), May, pp. 111-117.

Pérez, R., 1996. Ph.D. Thesis, Laval University, Quebec.

Probst, A., 1996. Graduate Seminar, Department of Mining and Metallurgical Eng., McGill University, March.

Shen, G., 1994. Ph.D. Thesis, McGill University, Montreal.

Shen, G., Nawfal, H., Watson, J., Banisi, S. and Finch, J.A., 1995. "Measurement of bubble swarm buoyancy velocity in three-phase system," CAMI'95: 3rd Canadian Conference on Computer Applications in the Mineral Industry, Montreal, Quebec, Oct. 22-25, pp. 1-8.

Stephanopoulos, G., 1984. Chemical Process Control, an Introduction to Theory and Practice, Prentice-Hall, Inc., N.J.

Tsai, T.H., Lane, J.W. and Lin, C.S., 1986. Modern Control Techniques for the Process Industries, Marcel Decker, Inc., New York.

Tsochatzidis, N.A., Karapantsios, T.D., Kostoglou, M.V. and Karabelas, A.J., 1992. "A conductance probe for measuring liquid fraction in pipes and packed beds," Multiphase Flow, Vol. 18, No. 5, pp. 653-667.

Uribe-Salas, A., Vermet, F. and Finch, J.A., 1992. "Apparatus and technique to measure settling velocity and holdup of solids in water slurries," Chem. Eng. Sci., Vol. 48, No. 4, pp. 815-819.

Uribe-Salas, A., Gomez, C.O. and Finch, J.A., 1994. "A conductivity technique for gas and solids holdup determination in three-phase reactors," Chem. Eng. Sci., Vol. 49, No. 1, pp. 1-10.

Walden, P., 1929. Salts, acids and bases, McGraw-Hill, New York.

Watt, J.S. and Sowerby, B.D., 1983. in Whitmore R. (Ed.), Proc. 2nd Aust. Coal Prep. Conference, 6A, pp. 263-290.

Wenge, F., Chisti, Y. and Moo-Young, M., 1995. Ind. Eng. Chem. Res., Vol. 34, No. 3, pp. 928-935.

Williams, R.A., 1995. "A journey inside mineral separation processes," Minerals Eng., Vol. 8, No.7, pp. 721-737.

Williams, R.A., Llyas, O.M. and Dyakowski, T., 1995 (a). "Air core imaging in cyclonic separators using electrical impedance tomography," Coal Preparation, in press.

Williams, R.A., Dyakowski, T., Xie, C.G., Luke, S.P., Gregory, P.J., Edwards, R.B., Dickin, F.J. and Gate, L.F., 1995 (b). "Industrial measurement and control of particulate processes using electrical impedance tomography," Proc. European Concerted Action in Proc. Tomography, ECAPT'95, Bergen (UMIST: EU Brite Euram, Manchester) 13.

Xie, C.G., Reinecke, N., Beck, M.S., Mewes, D. and Williams, R.A., 1995. "Electrical tomography for process engineering applications," Chem. Eng. J., Vol. 56, pp. 127-133.

Xu, M., Probst, A. and Finch, J.A., 1993. Proc. of the International Symposium on Modelling, Simulation and Control of Hydrometallurgical Processes, Papangelakis, V.G. and Demopoulos, G.P. editors, The Metallurgical Soc. of CIM, pp.261-270.

Xu, M., Probst, A. and Finch, J.A., 1994. "Level and solids profile detection in thickeners using conductivity," CIM Bull., Vol. 87, No. 985, pp. 46-52.

APPENDICES

APPENDIX 1

Table 1.1. Experimental data from fluidisation-flotation column: conductance (K) is given in mS, and coonductivity of the liquid (κ_l) is in mS/cm. The digits at the top of each column represent the connected electrodes. The separation between the electrodes were: 1 -2, 10 cm; 1 - 3, 20 cm; 1 - 4, 25 cm; 1 - 5, 55 cm; 2 - 3, 10 cm; 2 - 4, 15 cm; 2 - 5, 45 cm; 3 - 4, 5 cm; 3 - 5, 35 cm; 4 - 5, 30 cm; and the arrangement 2,4 - 3, 10 cm (to the central electrode). Electrodes are 10.1 cm i.d., and three different width of electrodes are presented.

Temperature is 298 K.

2.55cm	width										
1 - 2	1 - 3	1 - 4	1 - 5	2 - 3	2 - 4	2 - 5	3 - 4	3 - 5	4 - 5	1, 3 - 2	κ_l
1.87	0.978	0.766	0.3794	1.884	1.23	0.47	3.072	0.61	0.738	3.612	0.28
5.04	2.646	2.076	1.036	5.08	3.328	1.276	8.24	1.654	1.998	9.64	0.769
8.26	4.36	3.422	1.714	8.56	5.48	2.108	13.48	2.734	3.302	15.76	1.287
13.1	6.94	5.44	2.734	13.24	8.7	3.364	21.18	4.34	5.24	24.72	2.1
18.96	10.12	7.96	4.0	18.16	12.64	. 4.92	30.4	6.36	7.66	35.42	3.13
24.78	13.28	10.46	5.28	25.02	16.58	6.48	39.34	8.38	10.1	45.8	4.18
33.58	18.16	14.32	7.26	33.92	22.6	8.92	52.8	11.52	13.86	61.2	5.84
38.54	20.9	16.52	8.38	38.86	26.0	10.3	60.0	13.28	16.00	69.8	6.79
45.6	24.9	19.7	10.06	56.0	30.9	12.34	70.6	15.88	19.1	81.4	8.2
1.27 cm	width										
1.724	0.938	0.75	0.3664	1.738	1.186	0.454	2.79	0.582	0.692	3.204	0.271
5.34	2.932	2.354	1.174	5.36	3.708	1.434	8.5	1.836	2.18	9.8	0.875
8.68	4.78	3.858	1.93	8.68	6.02	2.354	13.64	3.016	3.584	15.78	1.452
12.12	6.74	5.42	2.722	12.16	8.48	3.322	18.16	4.26	5.06	21.88	2.09
18.4	10.34	8.36	4.22	18.48	12.96	5.14	28.88	6.56	7.8	32.8	3.28
23.64	13.42	10.84	5.48	23.9	16.78	6.68	37.42	8.94	10.14	41.2	4.3
31.04	17.82	14.4	7.32	31.36	22.16	8.9	48.4	11.38	13.48	53.6	5.79

39.76	23.02	18.66	9.52	39.8	28.4	11.56	61.4	14.78	17.5	67.2	7.6
47.8	28.16	22.84	11.7	48.4	34.8	14.22	74.0	18.16	21.46	81.0	9.4
0.5 cm	width										
1.79	1.026	0.836	0.414	1.794	1.284	0.5	2.762	0.632	0.736	3.16	0.292
5.58	3.256	2.66	1.332	5.66	4.06	1.622	8.84	2.066	2.396	9.8	0.951
8.84	5.24	4.28	2.154	8.98	6.5	2.602	13.88	3.302	3.83	15.46	1.545
13.7	8.16	6.68	3.374	13.94	10.12	4.08	21.34	5.16	5.98	23.62	2.47
18.26	10.9	8.94	4.52	18.56	13.5	5.46	28.14	6.92	8.0	30.52	3.33
23.72	14.16	11.62	5.9	24.06	17.56	7.12	36.12	9.0	11.6	40.0	4.36
28.74	17.24	14.16	7.22	29.22	21.36	8.7	43.2	10.98	12.7	48.6	5.36
33.6	20.38	16.78	8.56	34.44	25.24	10.34	50.4	13.02	15.04	56.2	6.4
37.66	22.7	18.7	9.56	38.22	28.08	11.54	55.6	14.5	16.76	62.6	7.17

Table 1.2. Experimental data from fluidisation-flotation column. Units of conductance and conductivity, and separation between electrodes are the same as those in Table 1.1. Electrodes are 7.6 cm i.d.

Temperature is 298 K.

1.9 cm	width										
1 - 2	1 - 3	1 - 4	1 - 5	2 - 3	2 - 4	2 - 5	3 - 4	3 - 5	4 - 5	1, 3 - 2	κ_l
1.346	0.692	0.542	0.256	1.328	0.862	0.306	2.174	0.3934	0.474	2.538	0.279
3.29	1.71	1.344	0.656	3.304	2.166	0.806	5.54	1.044	1.252	6.34	0.858
6.34	3.302	2.6	1.274	6.36	4.18	1.564	10.62	2.024	2.426	12.18	1.72
10.38	5.42	4.26	2.1	10.4	6.86	2.58	17.24	3.336	4.0	19.7	2.85
14.92	7.84	6.18	3.048	14.98	9.9	3.742	24.6	4.84	5.8	28.16	4.14
18.92	9.98	7.88	3.892	18.96	12.56	4.78	30.88	6.16	7.4	35.32	5.34
23.88	12.68	10.0	4.96	23.92	15.92	6.08	38.66	7.86	9.42	44.4	6.83
27.6	14.62	11.58	5.76	27.52	18.36	7.04	44.2	9.1	10.9	50.6	7.94
1.0 cm	width										

1.036	0.554	0.442	0.214	1.038	0.702	0.2584	1.716	0.3324	0.3902	1.954	0.267
3.786	2.046	1.63	0.798	3.81	2.58	0.976	6.22	1.252	1.478	8.54	1.031
7.2	3.922	3.128	1.54	7.26	4.94	1.88	11.76	2.416	2.848	13.38	1.986
10.82	4.94	4.74	2.342	10.92	7.46	2.862	17.64	3.674	4.32	19.78	3.07
14.28	7.9	6.32	3.13	14.44	9.9	3.816	23.2	4.9	5.78	26.02	4.13
18.4	10.24	8.22	4.08	18.62	12.84	4.96	29.9	6.38	7.52	33.16	5.39
22.26	12.48	10.02	4.98	22.6	15.64	6.08	36.04	7.8	9.18	39.8	6.64
25.2	14.2	11.4	5.7	25.66	17.8	6.94	40.6	8.9	10.48	44.6	7.6
2.118	1.136	0.906	0.442	2.124	1.442	0.54	3.508	0.692	0.818	3.982	0.551
0.5 cm	width										
1.028	0.56	0.452	0.2164	1.024	0.712	0.2628	1.646	0.3298	0.384	1.89	0.274
3.114	1.71	1.378	0.68	3.084	2.156	0.826	4.66	1.048	1.228	5.58	0.857
4.56	2.586	2.042	1.012	4.46	3.17	1.228	6.66	1.552	1.818	8.12	1.271
7.94	4.4	3.606	1.806	7.66	5.52	2.19	10.98	2.758	3.224	13.9	2.32
10.78	6.0	4.94	2.504	10.28	7.54	3.036	14.38	3.8	4.44	18.64	3.22
14.18	7.86	6.56	3.352	13.26	9.98	4.06	18.12	5.02	5.9	24.08	4.4
17.24	9.56	8.04	4.14	15.88	12.16	5.0	21.5	6.16	7.26	28.88	5.45
20.52	11.36	9.68	4.98	18.62	14.54	6.04	24.88	7.38	8.74	32.92	6.61
24.54	13.56	11.7	6.06	21.96	17.5	7.32	29.14	8.88	10.56	39.96	8.07

Table 1.3. Experimental data from the fluidisation-flotation column. Conductance and conductivity units are the same as in Table 1.1. The separation between electrodes are: 1 - 2, 5 cm; 1 - 3, 15 cm; 1 - 4, 25 cm; 1 - 5, 55 cm; 2 - 3, 10 cm; 2 - 4, 20 cm; 2 - 5, 50 cm; 3 - 4, 20 cm; 3 - 5, 40 cm; 4 - 5, 30 cm. The electrodes are 6.3 cm i.d. and three different width. Temperature is 298 K.

1.6 cm	width										
1 - 2	1 - 3	1 - 4	1 - 5	2 - 3	2 - 4	2 - 5	3 - 4	3 - 5	4 - 5	2, 4 - 3	K_1
1.176	0.444	0.2714	0.1318	0.678	0.3444	0.1472	0.68	0.1856	0.2504	1.332	0.253
1.664	0.63	0.3834	0.1862	0.96	0.494	0.21	0.962	0.2618	0.3526	1.86	0.368

2.91	1.106	0.682	0.3256	1.684	0.868	0.363	1.688	0.464	0.626	3.284	0.646
4.44	1.69	1.042	0.504	2.562	1.318	0.56	2.556	0.704	0.948	4.94	0.967
6.5	2.482	1.534	0.744	3.772	1.948	0.83	3.776	1.046	1.41	7.32	1.424
8.9	3.406	2.106	1.02	5.160	2.66	1.132	5.14	1.426	1.92	9.9	1.948
11.4	4.4	2.718	1.322	6.66	3.444	1.474	6.66	1.85	2.494	12.82	2.58
14.84	5.74	3.56	1.732	8.68	4.5	1.924	8.68	2.426	3.262	16.58	3.37
19.28	7.5	4.66	2.27	11.34	5.88	2.528	11.32	3.18	4.28	21.6	4.46
24 18	9.48	5.88	2.866	14.24	7.42	3.184	14.2	4.02	5.38	26.9	5.65
31.26	12.38	7.7	3.774	18.6	9.74	4.2	18.54	5.28	7.1	34.92	7.48
0.8 cm	width										
1.154	0.458	0.2772	0.1366	0.674	0.345	0.1514	0.676	0.1882	0.249	1.276	0.256
3.476	1.41	0.886	0.532	2.06	1.104	0.478	2.046	0.596	0.794	3.806	0.787
6.26	2.552	1.602	0.782	3.722	1.998	0.866	3.684	1.08	1.434	6.9	1.499
8.36	3.424	2.15	1.048	4.98	2.68	1.16	4.92	1.446	1.924	9.18	2.05
10.26	4.2	2.64	1.29	6.12	3.28	1.428	6.04	1.78	2.364	11.26	2.53
13.88	5.72	3.606	1.764	8.3	4.48	1.954	8.2	2.434	3.232	15.1	3.45
17.0	7.06	4.44	2.182	10.22	5.52	2.416	10.06	3.01	3.994	18.78	4.28
22.94	9.62	6.08	2.994	13.84	7.54	3.304	13.62	4.1	5.44	24.88	5.94
27.14	11.46	7.26	3.59	16.46	9.0	3.966	16.16	4.92	6.5	29.42	7.09
30.76	13.08	8.3	4.1	18.74	10.28	4.54	18.36	5.62	7.42	33.22	8.2
0.5 cm	width										
1.148	0.48	0.267	0.139	0.692	0.332	0.1546	0.694	0.1904	0.2426	1.292	0.271
3.776	1.644	1.042	0.51	2.358	1.292	0.564	2.34	0.702	0.922	4.12	0.975
6.02	2.766	1.756	0.86	3.96	2.172	0.95	3.894	1.18	1.548	6.88	1.65
7.92	3.522	2.234	1.088	4.98	2.762	1.2	4.84	1.48	1.956	8.8	2.13
10.66	4.68	3.006	1.466	6.7	3.716	1.618	6.48	2.008	2.624	11.98	2.87
13.12	5.76	3.686	1.798	8.24	4.5	1.982	7.98	2.46	3.21	14.5	3.56
16.4	7.24	4.58	2.262	10.32	5.66	2.496	9.96	3.096	3.96	18.34	4.4
19.4	8.62	5.46	2.698	12.28	6.74	2.974	11.82	3.668	4.7	21.46	5.32
23.44	10.5	6.66	3.298	14.92	8.22	3.632	14.36	4.46	5.7	26.26	6.64
25.84	11.58	7.36	3.636	16.44	9.06	3.98	15.9	4.92	6.3	28.62	7.29

Table 1.4. Experimental data from the fluidisation-flotation column. Conductance and conductivity units, and separation between electrodes are similar as those presented in Table .1. The electrodes are 5.1 cm i.d.; trhee different electrodes width are presented. Temperature is 298 K.

1.25 cm	width										
1 - 2	1 - 3	1 - 4	1 - 5	2 - 3	2 - 4	2 - 5	3 - 4	3 - 5	4 - 5	1, 3 - 2	K_1
0.53	0.2678	0.2114	0.1016	0.534	0.3432	0.1248	0.94	0.1608	0.1924	1.046	0.28
0.932	0.478	0.3678	0.1774	0.934	0.614	0.2178	1.644	0.281	0.3362	1.816	0.502
1.886	0.968	0.764	0.3568	1.89	1.242	0.448	3.298	0.578	0.688	3.684	1.022
3.064	1.58	1.248	0.598	3.078	2.026	0.732	5.34	0.944	1.124	5.96	1.672
5.42	2.8	2.21	1.062	5.44	3.582	1.3	9.36	1.676	1.998	10.52	3.04
7.66	3.962	3.13	1.504	7.68	5.06	1.84	13.12	2.376	2.832	14.72	4.35
9.84	5.1	4.04	1.944	9.88	6.52	2.38	16.78	3.072	3.662	18.92	5.65
10.9	6.2	4.9	2.356	11.94	7.9	2.888	20.18	3.718	4.44	22.66	6.88
13.66	7.12	5.62	2.718	13.72	9.08	3.328	23.08	4.28	5.1	26.0	7.95
0.65 cm	width										
0.494	0.2428	0.1964	0.0952	0.504	0.3124	0.1162	0.868	0.1472	0.1636	0.954	0.266
1.18	0.628	0.5	0.2166	1.18	0.798	0.255	1.976	0.218	0.3644	2.224	0.67
2.274	1.214	0.962	0.462	2.264	1.522	0.562	3.66	0.718	0.834	4.22	1.299
3.284	1.742	1.374	0.66	3.27	2.178	0.802	5.02	1.02	1.182	6.1	1.855
5.24	2.782	2.188	1.05	5.18	2.456	1.274	7.76	1.612	1.862	9.82	3.02
6.8	3.61	2.838	1.36	6.7	4.42	1.648	9.94	2.082	2.396	12.62	3.98
8.32	4.42	3.48	1.67	8.22	5.44	2.022	12.16	2.556	2.938	15.52	4.88
10.32	5.48	4.3	2.07	10.18	6.72	2.506	14.9	3.168	3.634	19.02	6.07
12.78	6.82	5.36	2.58	12.62	8.36	3.122	18.38	3.938	4.36	23.6	7.64
0.4 cm	width										
0.378	0.2322	0.1988	0.0982	0.3498	0.2816	0.115	0.854	0.1438	0.1712	0.948	0.28
1.23	0.668	0.536	0.2336	1.218	0.846	0.2602	2.0	0.4	0.468	2.254	0.712
2.95	1.64	1.33	0.648	2.86	2.046	0.782	4.0	0.98	1.162	4.74	1.795
4.36	2.52	2.118	1.038	3.94	3.222	1.246	4.78	1.572	1.846	7.04	2.94
5.84	3.542	2.922	1.438	5.22	4.18	1.722	7.5	2.162	2.548	9.38	4.09
7.52	4.38	3.754	1.85	6.68	5.36	2.216	9.48	2.776	3.27	12.0	5.33
9.1	5.28	4.46	2.232	8.22	6.54	2.682	11.72	3.358	3.944	14.96	6.39

10.5	6.06	5.08	2.544	9.58	7.54	3.06	13.82	3.828	4.36	17.22	7.37
11.86	6.84	5.76	2.878	10.98	8.6	3.466	16.0	4.2	4.94	19.86	8.38

Table 1.5. Experimental data from the fluidisation-flotation column. Conductance and conductivity units are the same as in Table 1.1. Separation between electrodes is: 1 - 2, 5 cm; 1 - 3, 15 cm; 1 - 4, 25 cm; 1 - 5, 55 cm; 2 - 3, 10 cm; 2 - 4, 20 cm; 2 - 5, 50 cm; 3 - 4, 10 cm; 3 - 5, 40 cm; 4 - 5, 30 cm. Three different electrode width are presented. Electrodes are 3.8 cm i.d.

Temperature is 298 K.

1.0 cm	width										
1 - 2	1 - 3	1 - 4	1 - 5	2 - 3	2 - 4	2 - 5	3 - 4	3 - 5	4 - 5	2, 4 - 3	K_l
0.554	0.2028	0.124	0.058	0.3074	0.1566	0.0642	0.3056	0.0802	0.1068	0.608	0.268
1.23	0.458	0.277	0.1306	0.698	0.3512	0.1452	0.698	0.182	0.2432	1.372	0.639
2.532	0.944	0.578	0.2686	1.438	0.732	0.2982	1.438	0.3748	0.506	2.81	1.321
4.66	1.744	1.07	0.504	2.652	1.356	0.56	2.652	0.702	0.936	5.18	2.49
6.66	2.508	1.54	0.726	3.812	1.95	0.806	3.814	1.01	1.348	7.42	3.6
8.56	3.232	1.988	0.936	4.92	2.518	1.04	4.92	1.302	1.74	9.56	4.67
11.42	4.34	2.668	1.26	6.58	3.38	1.4	6.6	1.754	2.342	12.74	6.33
13.34	5.08	3.13	1.48	7.7	3.96	1.642	7.72	2.058	2.746	14.92	7.44
0.5 cm	width										
0.572	0.216	0.1332	0.0622	0.3224	0.1674	0.069	0.3216	0.086	0.1138	0.63	0.274
1.176	0.45	0.2746	0.1282	0.674	0.3458	0.1432	0.674	0.179	0.2372	1.292	0.602
2.644	1.014	0.626	0.291	1.52	0.79	0.3226	1.52	0.406	0.538	2.93	1.368
3.984	1.494	0.924	0.434	2.234	1.162	0.48	2.232	0.598	0.794	4.26	2.06
5.9	2.278	1.41	0.662	3.404	1.774	0.734	3.404	0.914	1.212	6.52	3.18
7.5	2.914	1.804	0.848	4.34	2.268	0.838	4.34	1.17	1.55	8.3	4.08
9.28	3.612	2.24	1.052	5.38	2.812	1.164	5.38	1.452	1.924	10.28	5.12
12.24	4.8	2.98	1.4	6.12	3.734	1.552	7.12	1.932	2.558	13.54	6.8
13.44	5.38	2.276	1.542	7.82	4.1	1.704	7.82	2.122	2.81	14.82	7.6

0.3 cm	width										
0.442	0.211	0.1312	0.0614	0.3102	0.164	0.0676	0.31	0.084	0.1108	0.598	0.279
2.282	0.902	0.562	0.2604	1.332	0.702	0.2872	1.332	0.3568	0.476	2.514	1.235
2.854	1.13	0.702	0.323	1.664	0.878	0.3586	1.664	0.45	0.594	3.158	1.544
3.762	1.492	0.928	0.434	2.192	1.162	0.48	2.196	0.596	0.786	4.16	2.08
5.52	2.202	1.372	0.642	3.236	1.712	0.708	3.24	0.88	1.162	6.12	3.09
6.94	2.798	1.744	0.818	4.1	2.174	0.902	4.1	1.12	1.476	7.74	3.94
9.76	3.938	2.458	1.156	5.78	3.066	1.274	5.76	1.582	2.086	10.86	5.59
11.74	4.76	2.972	1.398	6.96	3.706	1.542	6.96	1.914	2.522	13.02	6.77
13.5	5.5	3.438	1.618	8.02	4.28	1.782	8.02	2.212	2.914	15.0	7.84

Table 1.6. Experimental data from the fluidisation-flotation column. Conductance and conductivity units are the same as in Table 1.1. Electrodes separation is: 1 - 2, 30 cm; 1 - 3, 35 cm; 1 - 4, 45 cm; 1 - 5, 55 cm; 2 - 3, 5 cm; 2 - 4, 15 cm; 2 - 5, 25 cm; 3 - 4, 10 cm; 3 - 5, 20 cm; 4 - 5, 10 cm. Three different electrodes width are presented. Electrodes are 2.5 cm i.d.

Temperature is 298 K.

0.65 cm	width										
1 - 2	1 - 3	1 - 4	1 - 5	2 - 3	2 - 4	2 - 5	3 - 4	3 - 5	4 - 5	3, 5 - 4	K_1
0.0452	0.0384	0.0298	0.02472	0.2366	0.0856	0.0522	0.1298	0.0658	0.1288	0.2544	0.275
0.097	0.0822	0.064	0.0522	0.524	0.1814	0.1108	0.2754	0.1402	0.2724	0.556	0.603
0.1954	0.166	0.1288	0.1054	1.052	0.3616	0.2222	0.572	0.281	0.57	1.118	1.224
0.3546	0.3016	0.2348	0.192	1.898	0.686	0.418	1.038	0.526	1.034	2.024	2.27
0.498	0.422	0.3224	0.2636	2.598	0.94	0.574	1.426	0.722	1.416	2.77	3.13
0.682	0.58	0.45	0.3628	3.556	1.29	0.786	1.958	0.994	1.946	3.794	4.32
0.888	0.754	0.586	0.478	4.6	1.678	1.024	2.546	1.294	2.532	4.92	5.63
0.97	0.822	0.64	0.522	5.02	1.832	1.118	2.776	1.408	2.756	5.38	6.14
1.194	1.014	0.798	0.644	6.16	2.254	1.376	3.414	1.734	3.39	^.62	7.6
0.35 cm	width										

0.0458	0.039	0.0304	0.025	0.2262	0.0858	0.0528	0.1248	0.0656	0.121	0.2322	0.28
0.0872	0.074	0.0578	0.0472	0.462	0.162	0.0996	0.2346	0.123	0.2236	0.484	0.542
0.2126	0.181	0.1412	0.115	1.13	0.418	0.2394	0.62	0.2926	0.612	1.19	1.35
0.3188	0.2718	0.2132	0.1734	1.706	0.63	0.359	0.932	0.484	0.932	1.83	2.13
0.49	0.418	0.312	0.2542	2.51	0.932	0.572	1.38	0.714	1.364	2.644	3.07
0.692	0.59	0.46	0.3572	3.538	1.318	0.808	1.946	1 01	1.926	3.688	4.35
0.878	0.748	0.584	0.478	4.42	1.664	1.024	2.46	1.28	2.442	4.68	5.55
1.01	0.862	0.672	0.55	5.1	1.916	1.18	2.83	1.474	2.808	5.34	6.35
1.154	0.984	0.768	0.63	5.8	2.19	1.35	3.23	1.686	3.206	6.12	7.31
0.2 cm	width										
0.045	0.0388	0.0304	0.025	0.2254	0.0864	0.0534	0.1264	0.0664	0.1254	0.24	0.27
0.101	0.086	0.068	0.056	0.528	0.192	0.12	0.28	0.148	0.278	0.552	0.648
0.1612	0.138	0.1086	0.0894	0.838	0.316	0.1892	0.466	0.2366	0.464	0.892	1.039
0.304	0.264	0.208	0.17	1.604	0.608	0.258	0.896	0.468	0.88	1.684	2.04
0.486	0.416	0.326	0.268	2.436	0.92	0.574	1.268	0.718	1.36	2.602	3.17
0.66	0.566	0.442	0.352	3.284	1.26	0.778	1.848	0.97	1.834	3.478	4.29
0.81	0.696	0.546	0.448	4.0	1.548	0.958	2.27	1.194	2.252	4.26	5.29
0.942	0.806	0.632	0.52	4.6	1.79	1.11	2.626	1.384	2.604	4.9	6.14
1.13	0.968	0.758	0.624	5.48	2.144	1.332	3.142	1.66	3.116	5.88	7.39

Table 1.7. Experimental data from two isolated flow cells with similar dimensions. The geometric cell constant ($A_{cell}/L_{electrodes}$) is 0.43 cm.

κ (cell 1), mS/cm	K (cell 1), mS	κ (cell 2), mS/cm	K (cell 2), mS
0.28	0.13	0.27	0.12
0.49	0.22	0.72	0.31
0.98	0.42	0.99	0.42
1.92	0.84	1.3	0.56
2.05	0.93	1.63	0.7
2.9	1.25	1.92	0.83

3.21	1.37	2.29	0.98
8.09	3.2	4.8	2.06
		5.97	2.57

APPENDIX 2

Table 2.1. Conductivity data at 298 K. Addition of salts in water.

KCl

Molar concentration	κ, mS/cm	K, mS	Cell constant, cm
0.00001	0.0028	0.0079	2.821428
0.00005	0.0083	0.0214	2.578313
0.0001	0.014	0.0354	2.528571
0.0005	0.0678	0.1634	2.410029
0.001	0.1209	0.2886	2.387096
0.005	0.609	1.446	2.374384
0.01	1.322	3.112	2.354009
0.05	6.39	14.04	2.197183
0.1	12.49	26.14	2.092874

NaCl

Molar concentration	κ, mS/cm	K, mS	Cell constant, cm
0.00001	0.0021	0.00626	2.980952
0.0001	0.0128	0.03176	2.48125
0.0005	0.059	0.1408	2.38644
0.001	0.1154	0.2722	2.358752
0.005	0.562	1.302	2.316725
0.01	1.102	2.538	2.303085
0.05	5.28	11.42	2.162878

0.1	10.2	21.14	2.072549

$Ca\ Cl_2$

Molar concentration	κ, mS/cm	K, mS	Cell constant, cm
0.00001	0.0025	0.00706	2.824
0.00006	0.0096	0.0241	2.510416
0.0001	0.0157	0.03844	2.448407
0.0005	0.0774	0.1854	2.395348
0.001	0.1521	0.3608	2.372123
0.005	0.722	1.69	2.34072
0.01	1.395	3.248	2.328315
0.05	6.42	13.94	2.171339
0.1	12.17	25.1	2.062448

$CuSO_4$

Molar concentration	κ, mS/cm	K, mS	Cell constant, cm
0.000002	0.0011	0.0035	3.181818
0.000012	0.0027	0.00728	2.696296
0.000053	0.0088	0.02182	2.479545
0.000111	0.0179	0.0436	2.435754
0.000535	0.078	0.1834	2.351282
0.005	0.531	1.242	2.338983
0.01	0.934	2.144	2.295503
0.05	3.35	7.22	2.155223
0.1	5.79	12.08	2.086355

Table 2.2. Conductivity data on mixtures of salts in water at 298 K.

NaCl - KCl

NaCl Molar C.	KCl Molar C.	κ, mS/cm	K, mS	Cell const., cm
0.00001	0.00001	0.0041	0.00668	1.629268
0.0001	0.0001	0.0205	0.049	2.390243
0.001	0.001	0.1656	0.3732	2.253623
0.005	0.005	0.8	1.82	2.275
0.01	0.01	1.571	3.508	2.232972
0.05	0.05	7.18	14.32	1.994428
0.1	0.1	21.3	37	1.737089

$CaCl_2$ - Cu SO_4; $CaCl_2$ 0.01 Molar.

$CuSO_4$ Molar C.	κ, mS/cm	K, mS	Cell constant, cm.
0.000001	1.12	2.596	2.327857
0.00001	1.125	2.596	2.307555
0.0001	1.132	2.612	2.30742
0.0005	1.17	2.7	2.307692
0.001	1.216	2.802	2.304276
0.005	1.548	3.538	2.285529
0.01	1.923	4.36	2.26729
0.05	4.39	9.28	2.113895
0.1	6.89	13.98	2.029027

$CaCl_2$ - $CuSO_4$; $CaCl_2$ 0.001 Molar

$CuSO_4$ Molar C.	κ, mS/cm	K, mS	Cell const., cm
0.000001	0.1191	0.2736	2.297229
0.00001	0.1232	0.2814	2.28409
0.0001	0.137	0.309	2.255474
0.0005	0.1866	0.442	2.368703
0.001	0.25	0.582	2.328
0.005	0.649	1.61	2.480739
0.01	1.049	2.392	2.280266
0.1	6.01	11.98	1.993344

APPENDIX 3

Table 3.1. Experimental data on conductivity of water. Effect of temperature.

Temperature, K	κ, mS/cm	K, mS	Cell const., cm
299.5	0.0008	0.0034	4.25
304.5	0.002	0.00614	3.07
305.3	0.0023	0.0069	3
306	0.0024	0.00712	2.966666
307	0.0025	0.00752	3.008
310	0.0027	0.00816	3.022222
312	0.00287	0.00866	3.017421
313	0.00293	0.009	3.071672
314	0.0031	0.0094	3.032258
316	0.0032	0.01002	3.13125
317.3	0.0034	0.0106	3.117647
319	0.0035	0.0112	3.2
320	0.0037	0.0118	3.189189
321	0.0038	0.01202	3.163157
322	0.0039	0.0122	3.128205
323	0.004	0.013	3.25
324	0.0041	0.0134	3.268292
325	0.0042	0.0136	3.238095

Table 3.2. Experimental data on conductivity of KCl - water solutions. Effect of temperature.

KCl; 0.001 Molar

Temperature, K	κ, mS/cm	K, mS	Cell const., cm
291	0.1138	0.252	2.214411
292	0.1144	0.254	2.220279
294	0.118	0.268	2.271186
295	0.1188	0.274	2.306397
298	0.1226	0.292	2.381729
300	0.1248	0.302	2.419871
301	0.1267	0.31	2.446724
303	0.1289	0.322	2.49806
305	0.1308	0.33	2.522935
306.2	0.1328	0.342	2.575301
308	0.1345	0.348	2.58736
309	0.1363	0.358	2.626559
311	0.1382	0.366	2.648335
313	0.1463	0.394	2.693096
316	0.1513	0.416	2.749504
320.5	0.1607	0.46	2.862476
323.2	0.1674	0.486	2.903225

KCl; 0.01 Molar

Temperature, K	κ, mS/cm	K, mS	Cell const., cm
297	1.435	3.308	2.305226
299.5	1.463	3.444	2.354066
301.2	1.485	3.566	2.411346

305.5	1.51	3.78	2.503311
306	1.514	3.8	2.509907
307.6	1.532	3.9	2.545691
308.5	1.543	3.98	2.57939
310	1.555	4.04	2.59807
312.2	1.589	4.2	2.643171
314.8	1.617	4.34	2.683982
315.5	1.624	4.4	2.709359
320	1.683	4.68	2.780748
321	1.69	4.74	2.804733

KCl; 0.1 Molar

Temperature, K	κ, mS/cm	K, mS	Cell const., cm
295	13.15	26.4	2.007604
296.5	13.44	27.36	2.035714
302	14.02	30.04	2.142653
303	14.14	30.58	2.162659
305	14.33	31.24	2.180041
306	14.46	31.9	2.206085
308	14.56	32.78	2.251373
310	14.68	33.9	2.309264
312.3	15.38	35.3	2.295188
313	15.54	35.94	2.312741
320	16.6	39.28	2.366265

Table 3.3. Experimental data on conductivity of NaCl - water solutions. Effect of temperature.

NaCl; 0.001 Molar

Temperature, K	κ, mS/cm	K, mS	Cell const., cm
297	0.0761	0.1766	2.32063
300	0.079	0.1892	2.394936
301	0.0794	0.1916	2.413098
302	0.0806	0.1964	2.436724
303	0.0816	0.201	2.463235
306	0.0842	0.213	2.529691
308	0.0851	0.2186	2.568742
311	0.0877	0.2294	2.615735
312	0.0886	0.2354	2.656884
313	0.0897	0.2402	2.677814
315.5	0.0917	0.2488	2.713195
316.5	0.0931	0.2546	2.734693
319	0.0953	0.2644	2.774396
322	0.0983	0.2784	2.832146
325	0.1015	0.2916	2.872906

NaCl; 0.01 Molar

Temperature, K	κ, mS/cm	K, mS	Cell const., cm
295	0.711	1.64	2.30661
296	0.725	1.656	2.284137
297	0.733	1.688	2.302864
300	0.755	1.802	2.386754
301	0.765	1.838	2.402614

306	0.801	2.006	2.504369
308	0.818	2.08	2.542787
309	0.829	2.13	2.56936
313	0.859	2.27	2.642607
315	0.882	2.366	2.682539
318	0.912	2.492	2.732456
320	0.933	2.578	2.763129
324	0.965	2.714	2.812435
326	0.998	2.834	2.839679

NaCl; 0.1 Molar

Temperature, K	κ, mS/cm	K, mS	Cell const., cm
298	6.88	14.12	2.052325
300	7.13	14.84	2.081346
304.5	7.45	16.22	2.177181
307	7.58	16.66	2.197889
310	7.81	17.48	2.238156
312	7.97	18.12	2.273525
315	8.2	18.96	2.312195
318.6	8.48	20.06	2.365566
323	8.82	21.28	2.412698
324	8.95	21.76	2.431284
325.5	9.07	22.2	2.447629

Table 3.4. Experimental data on conductivity of $CaCl_2$ - water solutions. Effect of temperature.

$CaCl_2$; 0.001 Molar

Temperature, K	κ, mS/cm	K, mS	Cell const., cm
298	0.1172	0.2624	2.238907
298.5	0.1192	0.2806	2.354026
299	0.1201	0.2844	2.368026
301	0.1221	0.2934	2.402948
304	0.1261	0.3112	2.467882
307	0.1295	0.3272	2.52664
310	0.1338	0.3462	2.587443
313.2	0.1384	0.3772	2.725433
316.5	0.1428	0.3864	2.705882
320	0.1479	0.424	2.866801
323	0.1527	0.446	2.920759

$CaCl_2$; 0.01 Molar

Temperature, K	κ, mS/cm	K, mS	Cell const., cm
295	1.072	2.404	2.242537
296	1.079	2.46	2.279888
297.5	1.112	2.546	2.289568
301.2	1.154	2.74	2.37435
303	1.172	2.83	2.414675
306.5	1.213	3.022	2.491343
309	1.244	3.158	2.538585
312	1.28	3.32	2.59375
315.2	1.317	3.49	2.649962

319	1.368	3.722	2.72076
323	1.411	3.914	2.773919
324	1.426	3.978	2.789621

$CaCl_2$; 0.1 Molar

Temperature, K	κ, mS/cm	K, mS	Cell const., cm
298	9.52	18.96	1.991596
299.5	9.66	19.22	1.989648
301	9.91	20.04	2.022199
304	10.13	20.82	2.055281
307	10.39	21.82	2.1
310.5	10.77	23.16	2.150417
313.5	11.07	24.24	2.189701
317	11.39	25.38	2.22827
320.5	11.82	26.88	2.274111

Table 3.5. Experimental data on conductivity of $CuSO_4$ - water solutions. Effect of temperature.

CuSO4; 0.001 Molar

Temperature, K	κ, mS/cm	K, mS	Cell const., cm
293	0.137	0.219	1.59854
301	0.1421	0.3384	2.381421

303.1	0.1462	0.355	2.42818
307.7	0.1525	0.3836	2.515409
312	0.1602	0.438	2.734082
316	0.1652	0.462	2.79661
319	0.1704	0.486	2.852112
321	0.1735	0.504	2.904899
322.1	0.1758	0.514	2.923777
324	0.1786	0.528	2.956326

$CuSO_4$; 0.01 Molar

Temperature, K	κ, mS/cm	K, mS	Cell const., cm
295.8	0.925	2.154	2.328648
296	0.944	2.166	2.294491
300	0.983	2.334	2.374364
302	1.004	2.42	2.410358
304	1.023	2.51	2.453567
308	1.054	2.662	2.525616
312	1.086	2.834	2.609576
314.5	1.114	2.946	2.644524
315.7	1.125	2.99	2.657777
320	1.163	3.164	2.72055
322.8	1.185	3.274	2.762869
324	1.195	3.318	2.776569

$CuSO_4$; 0.1 Molar

Temperature, K	κ, mS/cm	K, mS	Cell const., cm
297.6	6.04	12.34	2.043046

298	6.05	12.4	2.049586
299	6.12	12.6	2.058823
300.8	6.2	12.94	2.087096
303.1	6.32	13.48	2.132911
307	6.43	14.1	2.192846
309	6.54	14.64	2.238532
313	6.7	15.46	2.307462
314.5	6.76	15.72	2.325443
317	6.87	16.3	2.372634
321.5	7.03	17.08	2.429587
322.9	7.1	17.4	2.450704
328.5	7.31	18.64	2.549931

APPENDIX 4

Table 4.1. Effect of addition of non conducting solids in a flow conductivity cell. Glass beads (0.6 cm d) are used. The flow cell (2.54 cm d) has ring electrodes with 1 cm width and are separated 9.85 cm. The volume of the flow cell is 60.04 cm^3. KCl - water solutions are used. Holdup (ε) is estimated from weight of the glass beads and from conductivity with Maxwell's model.

κ solution; 0.278 mS/cm

K, mS	ε, actual (%)	ε, conductivity (%)	Cell const., cm
0.135	0	0	0.485
0.1349	1.88	0.05	0.485
0.1343	3.77	0.35	0.485
0.1295	5.65	2.75	0.485
0.1233	7.53	5.95	0.485
0.1166	9.42	9.52	0.485
0.1104	11.3	12.93	0.485
0.1053	13.18	15.83	0.485
0.1009	15.07	18.39	0.485
0.0968	16.95	20.83	0.485
0.0928	18.84	23.26	0.485
0.0894	20.72	25.38	0.485
0.0864	22.6	27.27	0.485
0.0834	24.49	29.2	0.485
0.0807	26.37	30.97	0.485

0.0785	28.25	32.42	0.485
0.0764	30.14	33.83	0.485
0.0742	32.02	35.33	0.485
0.0723	33.9	36.63	0.485
0.0709	35.79	37.61	0.485
0.0694	37.67	38.66	0.485
0.0667	39.55	40.57	0.485
0.0654	41.44	41.5	0.485
0.0645	43.32	42.15	0.485
0.0637	45.21	42.73	0.485
0.0639	47.09	42.59	0.485
0.0641	48.97	42.44	0.485

κ solution; 0.494 mS/cm

0.2226	0	0	0.4506
0.221	0.77	0.48	0.4506
0.1957	7.53	8.39	0.4506
0.1737	13.67	15.8	0.4506
0.1552	20.09	22.45	0.4506
0.1413	25	27.72	0.4506
0.1293	31.37	32.48	0.4506
0.1195	35.1	36.51	0.4506
0.1122	37.87	39.61	0.4506
0.1043	42.9	43.06	0.4506
0.0979	44.3	45.92	0.4506
0.0926	47	48.35	0.4506
0.0845	51.21	52.14	0.4506

κ solution; 0.983 mS/cm

0.4173	0	0	0.4245
0.4099	0.97	1.19	0.4245
0.3665	7.94	8.46	0.4245
0.3235	15.27	16.2	0.4245
0.2923	20.05	22.18	0.4245
0.2657	24.82	27.56	0.4245
0.242	31.87	32.57	0.4245
0.2246	35.37	36.39	0.4245
0.2085	38.35	40.03	0.4245
0.1942	43.12	43.37	0.4245
0.1824	45.98	46.19	0.4245
0.1713	47.56	48.91	0.4245
0.1624	50.1	51.13	0.4245

κ solution; 1.159 mS/cm

0.4757	0	0	0.4104
0.4673	0.77	1.18	0.4104
0.4221	7.53	7.8	0.4104
0.373	14.3	15.51	0.4104
0.3367	19.07	21.58	0.4104
0.3056	26.84	27.07	0.4104
0.278	32.6	32.16	0.4104
0.2558	36.37	36.43	0.4104
0.2383	38.14	39.91	0.4104
0.2212	42.9	43.41	0.4104

0.2079	45.67	46.2	0.4104
0.1957	47.44	48.82	0.4104
0.1847	50.21	51.23	0.4104
0.1768	50.97	52.99	0.4104

κ solution; 1.924 mS/cm

0.838	0	0	0.4355
0.828	0.77	0.8	0.4355
0.736	7.79	8.46	0.4355
0.645	15.8	16.63	0.4355
0.575	21.13	23.37	0.4355
0.517	27.06	29.27	0.4355
0.469	31.8	34.41	0.4355
0.429	36.42	38.86	0.4355
0.396	41	42.66	0.4355
0.368	44.5	45.99	0.4355
0.343	46.37	49.03	0.4355
0.321	47.56	51.78	0.4355
0.301	48.7	54.32	0.4355
0.289	49.97	55.88	0.4355

κ solution; 2.05 mS/cm

0.927	0	0	0.4521
0.906	1.2	1.52	0.4521
0.808	7.53	8.94	0.4521
0.7	15.78	17.78	0.4521
0.628	22.2	24.09	0.4521

0.559	28.04	30.5	0.4521
0.507	33.7	35.58	0.4521
0.465	38.01	39.84	0.4521
0.43	40.2	43.52	0.4521
0.399	44.3	46.48	0.4521
0.372	45	49.87	0.4521
0.348	46.5	52.59	0.4521
0.328	48.7	54.9	0.4521
0.311	49.97	56.91	0.4521

κ solution; 2.9 mS/cm

1.254	0	0	0.4324
1.229	1.87	1.34	0.4324
1.098	7.53	8.65	0.4324
0.959	16	17.02	0.4324
0.848	21.3	24.2	0.4324
0.768	27.4	29.67	0.4324
0.699	32.3	34.61	0.4324
0.641	37.21	38.93	0.4324
0.585	40.89	43.26	0.4324
0.543	43.2	46.61	0.4324
0.51	45	49.3	0.4324
0.477	46.5	52.06	0.4324
0.45	48	54.36	0.4324
0.429	49	56.18	0.4324

κ solution; 3.21 mS/cm

1.366	0	0	0.4255
1.339	2.77	1.33	0.4255
1.196	7.6	8.66	0.4255
1.044	15.2	17.06	0.4255
0.93	20.1	23.81	0.4255
0.834	26.4	29.84	0.4255
0.762	32.1	34.57	0.4255
0.697	47.3	39.02	0.4255
0.646	40.58	42.63	0.4255
0.599	44.2	46.05	0.4255
0.559	46.5	49.04	0.4255
0.525	47	51.64	0.4255
0.494	48.9	54.06	0.4255
0.469	49.5	56.04	0.4255

κ solution; 8.09 mS/cm

3.231	0	0	0.3993
3.167	2.7	1.33	0.3993
2.835	7.5	8.52	0.3993
2.511	15	16.05	0.3993
2.24	20.96	22.78	0.3993
2.029	26.5	28.31	0.3993
1.854	31	33.12	0.3993
1.71	34.8	37.22	0.3993
1.577	39.2	41.15	0.3993
1.465	42.28	44.56	0.3993

1.376	45.3	47.33	0.3993
1.291	46.4	50.05	0.3993
1.221	48.7	52.32	0.3993
1.169	49.9	54.04	0.3993

Table 4.2. Experimental data on the fluidisation - flotation column. Solids holdup determination from conductivity. Addition of glass beads (1 mm d).

κ liquid, mS/cm	κ dispersion, mS/cm	ε, conductivity	ε, beads
0.27	0.27	0	0
0.27	0.2609	0.0226	0.02
0.27	0.2276	0.1101	0.12
0.27	0.2036	0.1785	0.19
0.27	0.1845	0.235	0.24
0.27	0.1696	0.283	0.29
0.27	0.1579	0.321	0.33
0.27	0.1449	0.365	0.38
0.27	0.1324	0.4089	0.42
0.27	0.1245	0.4377	0.45
0.723	0.723	0	0
0.723	0.719	0.368	1

0.723	0.6497	6.98	7
0.723	0.5676	15.43	16
0.723	0.5124	21.5	22
0.723	0.4657	0.269	0.28
0.723	0.4011	0.348	0.36
0.723	0.3481	0.417	0.42
0.723	0.3126	0.466	0.47

0.99	0.99	0	0
0.99	0.9794	0.007119	0.01
0.99	0.8766	0.0793	0.08
0.99	0.8024	0.1347	0.14
0.99	0.728	0.1934	0.20
0.99	0.6374	0.2693	0.27
0.99	0.5407	0.3564	0.36
0.99	0.4817	0.4128	0.42
0.99	0.4225	0.4723	0.48

1.298	1.298	0	0
1.298	1.268	0.0154	0.02
1.298	1.1322	0.0888	0.09
1.298	0.9919	0.1706	0.17
1.298	0.886	0.2366	0.24
1.298	0.8054	0.2895	0.29
1.298	0.695	0.3664	0.37

1.298	0.5845	0.4486	0.46

1.634	1.634	0	0
1.634	1.6269	0.00289	0.002
1.634	1.4972	0.05739	0.06
1.634	1.2921	0.1499	0.15
1.634	1.1577	0.2152	0.22
1.634	1.0351	0.2783	0.28
1.634	0.8676	0.3705	0.38
1.634	0.7498	0.4401	0.44
1.634	0.6672	0.4913	0.49

1.921	1.921	0	0
1.921	1.8588	0.0218	0.02
1.921	1.6607	0.0946	0.09
1.921	1.4925	0.1606	0.16
1.921	1.3405	0.224	0.22
1.921	1.2069	0.2828	0.29
1.921	1.0134	0.3738	0.38
1.921	0.8798	0.4409	0.45
1.921	0.7877	0.4895	0.49

2.29	2.29	0	0
2.29	2.2275	0.0183	0.02

2.29	2.0067	0.086	0.09
2.29	1.8	0.1534	0.15
2.29	1.637	0.21	0.20
2.29	1.4282	0.2868	0.29
2.29	1.205	0.3751	0.38
2.29	1.0465	0.4419	0.43
2.29	0.9409	0.4886	0.49

4.8	4.8	0	0
4.8	4.6938	0.0148	0.01
4.8	4.1802	0.0899	0.09
4.8	3.7061	0.1644	0.17
4.8	3.3185	0.2293	0.24
4.8	2.9901	0.2875	0.3
4.8	2.5209	0.376	0.38
4.8	2.1827	0.4442	0.44
4.8	1.9728	0.4885	0.49

5.97	5.97	0	0
5.97	5.9003	0.0078	0.01
5.97	5.2262	0.0866	0.09
5.97	4.7138	0.1508	0.15
5.97	4.1765	0.2225	0.23
5.97	3.8257	0.272	0.28
5.97	3.1914	0.3672	0.37

5.97	2.8034	0.4295	0.43
5.97	2.5123	0.4784	0.48

Table 4.3. Experimental data on solids holdup. Effect of addition of silica (80% 425 μm). Experiments carried out in the fluidisation - flotation column. Temperature is 298 K. The technique used here is the phase separation method.

κ liquid, mS/cm	κ slurry, mS/cm	ε conductivity, %	ε actual, %
1.09	1.09	0	0
1.09	1.03	3.67	3.55
1.09	0.96	8.6	8.1
1.09	0.9	12.66	11.7
1.09	0.84	16.88	15.7
1.09	0.79	20.36	19.2

Table 4.4. Experimental data on solids holdup. Measurements in the fluidisation - flotation column. Silica slurries. Comparison between solids holdup estimated by the phase separation method and the "standard addition" method *, with solids holdup determined by density. The "standard solid" added is 44 % v/v. Temperature is 298 K.

κ liquid mS/cm	κ open cell, mS/cm	κ stand. cell, mS/cm *	ε, from open, %	ε, stand. cell, % *	ε, weight, %
0.305	0.305	0.2434	0	0	0
0.305	0.2985	0.1351	1.41	1.42	1.5
0.305	0.2944	0.1333	2.32	2.007	2
0.305	0.2878	0.128	3.83	3.77	3.5
0.305	0.2543	0.1052	11.71	11.68	11
0.305	0.2389	0.0949	15.57	15.42	15
0.305	0.2358	0.0924	16.34	16.33	16
0.305	0.2302	0.08855	17.78	17.78	17.5
0.305	0.2241	0.0844	19.37	19.32	19

* The standard addition method to estimate holdup [Gomez et al., 1995] involves a comparison between two conductivity cells. One is a simple open flow cell which measures the conductance of a dispersion of electrolyte solution, and a non conductive dispersed phase. One form of the Maxwell model is:

$$\varepsilon = \{1 - (\kappa_d/\kappa_l)\}/\{1 + 0.5\,(\kappa_d/\kappa_l)\}$$

The other cell contains a non conducting solid of known volume (i.e. holdup). Thus, as the dispersion flows through, the appropriate form of Maxwell's model is:

$$\varepsilon + \varepsilon_{st} = \{1 - (\kappa_{dst}/\kappa_l)\}/\{1 + 0.5\,(\kappa_{dst}/\kappa_l)\}$$

where ε_{sp} and κ_{dsp} are the holdup of the added solid, and the conductivity of the dispersion measured in this cell - the standard addition cell.

Inspecting these equations, it is noted that there are two unknowns: ε and κ_l. Since, these two equations are independent, because they are related to two different cells, they can be solved for the unknown quantities.

Although both approaches (phase separation method, and standard addition method) appear possible, the selected through out this work is based on phase separation.

APPENDIX 5

Table 5.1. Data to define discharge coefficient for different orifice size in the syphon cell.

Orifice d, mm	Cell height (h_o), m	dis. vel., m/s	$\sqrt{2 g h_o}$	C_d, disc. coefficient	Q, cm^3/s	cell vel., cm/s
6	0.2	0.413	1.981	0.2084	11.67	1.023
6	0.3	0.501	2.426	0.2066	14.17	1.243
6	0.4	0.594	2.801	0.212	16.79	1.472
6	0.5	0.665	3.132	0.2123	18.8	1.649
5	0.2	0.264	1.981	0.133	5.17	0.453
5	0.3	0.324	2.426	0.1336	6.36	0.558
5	0.4	0.373	2.801	0.1331	7.32	0.642
5	0.5	0.413	3.132	0.132	8.12	0.711
4	0.2	0.21	1.981	0.1058	2.63	0.23
4	0.3	0.252	2.426	0.1037	3.16	0.277
4	0.4	0.29	2.801	0.1035	3.64	0.319
4	0.5	0.323	3.132	0.103	4.05	0.355
3	0.2	0.129	1.981	0.0649	0.91	0.079
3	0.3	0.158	2.426	0.065	1.11	0.097
3	0.4	0.182	2.801	0.065	1.29	0.112
3	0.5	0.202	3.132	0.0646	1.43	0.125

Table 5.2. Conductivity/conductance data for the open and syphon flow cells.

κ liquid, mS/cm	K open cell, mS	K syphon cell, mS
0.30295	3.7003	0.2451
0.6556	7.994	0.5578
0.8424	10.2383	0.7044
0.70995	8.6417	0.6078
0.61105	7.4341	0.5323
0.6365	7.7818	0.551
0.6967	8.5046	0.599
0.80205	9.8018	0.6862
0.8883	10.864	0.751
0.96515	11.8165	0.8147
1.0217	12.4545	0.8589
1.3561	16.6443	1.114
2.05	24.5586	1.5856
2.757	32.8565	2.0709
3.564	42.2705	2.5882
4.777	55.7385	3.3195
6.4	73.9359	4.185

Table 5.3. Experimental data on gas holdup measurements in the 50 cm diameter laboratory flotation column. Two probes are tested. Comparison between gas holdup estimates from pressure and conductivity measurements.

Gas holdup probe I; the system is without frother.

J_{air}, cm/s	$\varepsilon_{pressure}$, %	K_{open}, mS	K_{syphon}, mS	κ_{open}, mS/cm	κ_{syphon}, mS/cm	$\varepsilon_{conductivity}$, %
0	0	3.91	0.26	0.31	0.31	0
0.17	0.31	3.89	0.26	0.31	0.31	0.24
0.25	0.74	3.87	0.26	0.3	0.31	0.58
0.34	1.05	3.86	0.26	0.3	0.31	0.78
0.42	1.57	3.82	0.26	0.3	0.31	1.54
0.51	2.01	3.8	0.26	0.3	0.31	1.74
0.59	2.47	3.78	0.26	0.3	0.31	2.16
0.68	2.98	3.78	0.26	0.3	0.31	2.21
0.76	3.34	3.75	0.26	0.3	0.31	2.62
0.85	3.94	3.7	0.26	0.29	0.31	3.48
1.02	4.65	3.7	0.26	0.29	0.31	3.52
1.19	5.45	3.66	0.26	0.29	0.31	4.3
1.36	6.16	3.62	0.26	0.28	0.31	5.02
1.53	6.83	3.58	0.26	0.28	0.31	5.76
1.7	7.57	3.51	0.26	0.28	0.31	6.93
1.87	8.18	3.49	0.26	0.27	0.31	7.29
2.04	8.55	3.47	0.26	0.27	0.31	7.75
2.21	9.1	3.48	0.26	0.27	0.31	7.51
2.38	9.94	3.39	0.26	0.27	0.31	9.15
2.55	10.62	3.39	0.26	0.27	0.31	9.14

Gas holdup probe II; the system is without frother

J_{air}, cm/s	$\varepsilon_{pressure}$, %	K_{open}, mS	K_{syphon}, mS	κ_{open}, mS/cm	κ_{syphon}, mS/cm	$\varepsilon_{conductivity}$, %
0.17	0.3	6.42	0.49	0.56	0.56	0.08
0.25	0.61	6.41	0.49	0.56	0.56	0.17
0.34	0.92	6.35	0.49	0.55	0.56	0.85
0.42	1.34	6.33	0.49	0.55	0.56	1.07
0.51	1.91	6.3	0.49	0.55	0.56	1.45
0.59	2.18	6.31	0.49	0.55	0.56	1.3
0.68	2.58	6.25	0.49	0.54	0.56	2
0.76	3.09	6.26	0.49	0.54	0.56	1.86
0.85	3.38	6.23	0.49	0.54	0.56	2.22
1.02	4.1	6.13	0.49	0.53	0.56	3.26
1.19	4.8	6.07	0.49	0.53	0.56	3.95
1.36	5.47	6.09	0.49	0.53	0.56	3.78
1.53	6.14	5.89	0.49	0.51	0.56	6.08
1.7	6.78	6.02	0.49	0.52	0.56	4.58
1.87	7.5	5.93	0.49	0.51	0.56	5.59
2.04	8.18	5.9	0.49	0.51	0.56	5.9
2.21	8.83	5.8	0.49	0.5	0.56	7.05
2.38	9.4	5.75	0.49	0.5	0.56	7.63
2.55	10.02	5.7	0.49	0.49	0.56	8.3

Gas holdup probe II; the system contains 20 ppm Dowfroth 250

J_{air}, cm/s	$\varepsilon_{pressure}$, %	K_{open}, mS	K_{syphon}, mS	κ_{open}, mS/cm	κ_{syphon}, mS/cm	$\varepsilon_{conductivity}$, %
0	0	6.4275	0.4851	0.56	0.56	0
0.17	0.5183	6.407	0.4851	0.56	0.56	0.23

0.25	1.301	6.3493	0.4851	0.55	0.56	0.87
0.34	1.9792	6.2959	0.4851	0.55	0.56	1.46
0.42	2.9029	6.1997	0.4851	0.54	0.56	2.54
0.51	3.3748	6.2177	0.4851	0.54	0.56	2.34
0.59	4.5543	6.0402	0.4851	0.52	0.56	4.34
0.68	4.8639	6.0489	0.4851	0.52	0.56	4.24
0.76	6.2686	5.9279	0.4851	0.51	0.56	5.63
0.85	6.8736	5.8721	0.4851	0.51	0.56	6.28
1.02	8.7705	5.7592	0.4851	0.5	0.56	7.59
1.19	10.1972	5.5806	0.4851	0.48	0.56	9.7
1.36	11.3816	5.5087	0.4851	0.47	0.56	10.56
1.53	12.7363	5.4269	0.4851	0.47	0.56	11.55
1.7	14.1166	5.2528	0.4851	0.45	0.56	13.67
1.87	15.5324	5.1846	0.4851	0.44	0.56	14.52
2.04	16.9158	5.0607	0.4851	0.43	0.56	16.06
2.21	18.0849	4.9672	0.4851	0.42	0.56	17.24
2.38	19.6239	4.8526	0.4851	0.41	0.56	18.69
2.55	21.1465	4.6916	0.4851	0.4	0.56	20.77

APPENDIX 6

Table 6.1. Experimental data obtained with the gas holdup probe I in a 50 cm diameter, 4 m height laboratory flotation column. The probe was placed in three radial positions at two meters from the lip of the column. 20 ppm Dowfroth 250 were added. Measurements of gas holdup from pressure and conductivity are presented.

The probe is on the wall of the column.

ε (pressure), %	K open, mS	K syphon, mS	κ open, mS/cm	κ syphon, mS/cm	Jg, cm/s	ε (conduct.), %
0	14.4	1.13	1.09	1.09	0	0
3.07	13.73	1.13	1.04	1.09	0.5	3.14
7.26	12.92	1.13	0.98	1.09	1	7.09
11.48	11.87	1.13	0.9	1.09	1.5	12.43
14.28	11.64	1.13	0.88	1.09	2	13.66
16.88	10.95	1.13	0.83	1.09	2.5	17.38

The probe is between the wall and the centre of the column.

ε (pressure), %	K open, mS	K syphon, mS	κ open, mS/cm	κ syphon, mS/cm	Jg, cm/s	ε (conduct.), %
0	14.4	1.13	1.09	1.09	0	0
3.04	13.75	1.13	1.04	1.09	0.5	3.06
6.85	13.02	1.13	0.98	1.09	1	6.62
10.98	12.06	1.13	0.91	1.09	1.5	11.48
13.59	11.77	1.13	0.89	1.09	2	13.01
16.06	11.25	1.13	0.85	1.09	2.5	15.74

The probe is in the centre of the column.

ε (pressure), %	K open, mS	K syphon, mS	κ open, mS/cm	κ syphon, mS/cm	Jg, cm/s	ε (conduct.), %
0	14.4	1.13	1.09	1.09	0	0
3.07	13.71	1.13	1.04	1.09	0.5	3.22
7.47	12.9	1.13	0.97	1.09	1	7.17

11.47	12.26	1.13	0.93	1.09	1.5	10.43
14.48	11.42	1.13	0.86	1.09	2	14.82
16.87	11.07	1.13	0.84	1.09	2.5	16.72

Table 6.2. Experimental data on gas holdup measurements in a 50 cm diameter, 4 m height, laboratory flotation column. The gas holdup probe II is used. The probe is placed in three radial positions at two meters from the lip of the column. 20 ppm Dowfroth 250 are added. Gas holdup from pressure and conductivity measurements is presented.

The probe is on the wall of the column.

ε (pressure), %	K open, mS	K syphon, mS	κ open, mS/cm	κ syphon, mS/cm	Jg, cm/s	ε (conduct.), %
0	5.35	0.29	1.09	1.09	0	0
3.39	5.06	0.29	1.03	1.09	0.5	3.67
8.12	4.69	0.29	0.96	1.09	1	8.6
11.66	4.39	0.29	0.9	1.09	1.5	12.66
15.45	4.1	0.29	0.84	1.09	2	16.88
19.22	3.87	0.29	0.79	1.09	2.5	20.36

The probe is between the wall and the centre of the column.

ε (pressure), %	K open, mS	K syphon, mS	κ open, mS/cm	κ syphon, mS/cm	Jg, cm/s	ε (conduct.), %
0	5.35	0.29	1.09	1.09	0	0
2.65	5.1	0.29	1.04	1.09	0.5	3.19
7.06	4.75	0.29	0.97	1.09	1	7.69
11.3	4.41	0.29	0.9	1.09	1.5	12.39
14.82	4.23	0.29	0.86	1.09	2	14.93
17.97	3.94	0.29	0.81	1.09	2.5	19.19

The probe is in the centre of the column.

ε (pressure), %	K open, mS	K syphon, mS	κ open, mS/cm	κ syphon, mS/cm	Jg, cm/s	ε (conduct.), %

0	5.42	0.29	1.11	1.11	0	0
2.79	5.08	0.29	1.04	1.11	0.5	4.33
7.04	4.81	0.29	0.98	1.11	1	7.78
11.11	4.51	0.29	0.92	1.11	1.5	11.89
13.71	4.28	0.29	0.87	1.11	2	15.09
16.41	4.11	0.29	0.84	1.11	2.5	17.6

Table 6.3. Experimental data on measurement of gas holdup in a 50 cm diameter, 4 m height, laboratory flotation column as a function of column depth at different air flow rates. The system contains 15 ppm Dowfroth 250. The gas holdup probe II was placed in the centre of the column.

Depth, m	Jg, cm/s	κ open, mS/cm	κ syphon, mS/cm	ε (conductivity), %
1	0	0.252	0.252	0
1	0.34	0.23093	0.252	5.73
2	0.34	0.23093	0.252	5.73
3	0.34	0.23731	0.252	3.96
1	0.42	0.23093	0.252	5.73
2	0.42	0.23731	0.252	3.96
3	0.42	0.24157	0.252	2.79
1	0.59	0.22986	0.252	6.03
2	0.59	0.23306	0.252	5.14
3	0.59	0.23731	0.252	3.96
1	0.68	0.22454	0.252	7.53
2	0.68	0.22774	0.252	6.63
3	0.68	0.22986	0.252	6.03
1	0.76	0.22135	0.252	8.45
2	0.76	0.22454	0.252	7.53

3	0.76	0.2288	0.252	6.33
1	0.85	0.22135	0.252	8.45
2	0.85	0.22029	0.252	8.75
3	0.85	0.22348	0.252	7.84
1	0.93	0.2139	0.252	10.61
2	0.93	0.21709	0.252	9.68
3	0.93	0.22029	0.252	8.75
1	1.02	0.21284	0.252	10.92
2	1.02	0.21922	0.252	9.06
3	1.02	0.21816	0.252	9.37
1	1.27	0.21071	0.252	11.55
2	1.27	0.21177	0.252	11.23
3	1.27	0.21284	0.252	10.92
1	1.7	0.20007	0.252	14.75
2	1.7	0.2022	0.252	14.1
3	1.7	0.20539	0.252	13.14
1	2.12	0.19262	0.252	17.04
2	2.12	0.19794	0.252	15.4
3	2.12	0.1873	0.252	18.71
1	2.55	0.16601	0.252	25.66
2	2.55	0.17878	0.252	21.44
3	2.55	0.1873	0.252	18.71

Table 6.4. Experimental data on gas holdup obtained from a 50 cm diameter, 4 m height, laboratory flotation column with one sparger shut off. The gas holdup probe I was placed at two meters from the column lip. Measurements were done in different radial positions in the column. The time of the rising interface is presented and from that the buoyancy velocity of the swarm is estimated. No frother.

The probe is on the wall in the opposite side to the sparger shut off.

Time, s	κ open, mS/cm	κ syphon, mS/cm	ε (conduct.), %	Buoyan. vel., cm/s	Jg, cm/s	ε (pressure), %
	0.27	0.27	0		0	0
28.1	0.26	0.27	1.81	13.67	0.5	1.5
31.6	0.25	0.27	3.94	11.82	1	3.89
34.11	0.24	0.27	6.36	10.68	1.5	6.18
35.53	0.24	0.27	8.27	10.01	2	8.23
37.84	0.23	0.27	10.86	9.19	2.5	10.23

The probe is between the centre and the wall opposed to the sparger shut off.

Time, s	κ open, mS/cm	κ syphon, mS/cm	ε (conduct.), %	Buoyan. vel., cm/s	Jg, cm/s	ε (pressure), %
	0.27	0.27	0		0	0
28.78	0.26	0.27	1.36	12.07	0.5	1.33
33.39	0.25	0.27	3.79	10.4	1	4.1
37.52	0.25	0.27	5.47	9.26	1.5	6.46
38.9	0.24	0.27	7.17	8.93	2	8.39
40	0.23	0.27	9.64	8.69	2.5	10.34

The probe is in the centre of the column.

Time, s	κ open, mS/cm	κ syphon, mS/cm	ε (conduct.), %	Buoyan. vel., cm/s	Jg, cm/s	ε (pressure), %
	0.27	0.27	0		0	0
30.27	0.26	0.27	1.59	11.47	0.5	1.52
36.31	0.25	0.27	3.85	9.56	1	4.13
38.09	0.25	0.27	5.04	9.12	1.5	6.41
39.43	0.24	0.27	7.17	8.81	2	8.25
41.72	0.23	0.27	8.71	8.33	2.5	10.33

The probe is between the centre and the wall of the sparger shut off.

Time, s	κ open, mS/cm	κ syphon, mS/cm	ε (conduct.), %	Buoyan. vel., cm/s	Jg, cm/s	ε (pressure), %
	0.27	0.27	0		0	0
31.8	0.26	0.27	1.37	10.92	0.5	1.55
36.43	0.26	0.27	2.73	9.53	1	4.12
39.39	0.25	0.27	4.92	8.82	1.5	6.27
40.97	0.24	0.27	6.99	8.47	2	8.27
44.09	0.24	0.27	8.09	7.87	2.5	10.1

The probe is on the wall of the sparger shut off.

Time, s	κ open, mS/cm	κ syphon, mS/cm	ε (conduct.), %	Buoyan. vel., cm/s	Jg, cm/s	ε (pressure), %
	0.27	0.27	0		0	0
35	0.26	0.27	1.05	9.91	0.5	1.49
39.53	0.26	0.27	2.95	8.78	1	4.27
40.97	0.25	0.27	5.37	8.47	1.5	6.43
44.13	0.24	0.27	6.9	7.86	2	8.27
45	0.23	0.27	9.94	7.71	2.5	10.27

Table 6.5. Experimental data on gas holdup. Gas holdup probe I was placed at two meters from the column lip. Gas holdup was measured in the radial direction. The column has two spargers shut off. The system contains 20 ppm Dowfroth 250.

The probe is on the wall opposed to the spargers shut off.

Time, s	κ open, mS/cm	κ syphon, mS/cm	ε (conduct.), %	Buoyan. vel., cm/s	Jg, cm/s	ε (pressure), %
	0.27	0.271	0		0	0
75.79	0.26	0.271	3.16	4.59	0.5	3.68
84.7	0.24	0.271	8.99	4.11	1	9.15

86.78	0.22	0.271	12.18	3.84	1.5	13.16
92.38	0.21	0.271	15.93	3.43	2	17.01
94.74	0.2	0.271	19.77	3.01	2.5	20.43

The probe is between the centre and the wall opposed to the spargers shut off.

Time, s	κ open, mS/cm	κ syphon, mS/cm	ε (conduct.), %	Buoyan. vel., cm/s	Jg, cm/s	ε (pressure), %
	0.27	0.271	0		0	0
69.74	0.26	0.271	2.87	4.06	0.5	3.55
84	0.24	0.271	8.72	3.37	1	8.8
88.19	0.22	0.271	12.62	3.21	1.5	13.37
96	0.21	0.271	16.21	2.95	2	17.15
101.26	0.2	0.271	19.37	2.8	2.5	19.72

The probe is in the centre of the column.

Time, s	κ open, mS/cm	κ syphon, mS/cm	ε (conduct.), %	Buoyan. vel., cm/s	Jg, cm/s	ε (pressure), %
	0.27	0.271	0		0	0
73.56	0.26	0.271	2.7	3.85	0.5	3.45
84	0.24	0.271	7.77	3.37	1	8.83
88.98	0.23	0.271	11.94	3.18	1.5	13.26
96.6	0.21	0.271	16	2.93	2	17.06
94.87	0.2	0.271	19.4	2.98	2.5	20.38

The probe is between the centre and the wall of the spargers shut off.

Time, s	κ open, mS/cm	κ syphon, mS/cm	ε (conduct.), %	Buoyan. vel., cm/s	Jg, cm/s	ε (pressure), %
	0.27	0.271	0		0	0
68	0.26	0.271	2.42	4.16	0.5	3.57
88	0.24	0.271	7.59	3.22	1	8.74
93.66	0.23	0.271	12.32	3.02	1.5	13.56
94.85	0.21	0.271	14.96	2.98	2	16.69
97	0.2	0.271	18.4	2.92	2.5	19.95

The probe is on the wall of the spargers shut off.

Time, s	κ open, mS/cm	κ syphon, mS/cm	ε (conduct.), %	Buoyan. vel., cm/s	Jg, cm/s	ε (pressure), %
	0.27	0.271	0		0	0
76	0.26	0.271	2.14	3.72	0.5	3.66
85.16	0.24	0.271	7.22	3.32	1	8.88
93.5	0.23	0.271	11.65	3.03	1.5	13.43
98	0.21	0.271	15.56	2.89	2	17.06
98.96	0.2	0.271	18.35	2.86	2.5	19.63

Table 6.6. Experimental data on gas holdup in a 50 cm diameter , 4 m height, laboratory flotation column. The column has two spargers shut off. The gas holdup probe I was used. The system is without frother.

The probe is on the wall of the spargers shut off.

Time, s	κ open, mS/cm	κ syphon, mS/cm	ε (conduct.), %	Buoyan. vel., cm/s	Jg, cm/s	ε (pressure), %
	0.27	0.27	0		0	0
37.77	0.27	0.27	1.13	10.21	0.5	1.2
50.54	0.26	0.27	3.69	7.43	1	3.76
55.24	0.25	0.27	5.94	6.32	1.5	6.19
55.59	0.24	0.27	8.09	6.43	2	7.99
57.69	0.23	0.27	10.25	6.06	2.5	9.91

The probe is between the centre and the wall of the spargers shut off.

Time, s	κ open, mS/cm	κ syphon, mS/cm	ε (conduct.), %	Buoyan. vel., cm/s	Jg, cm/s	ε (pressure), %
	0.27	0.27	0		0	0
43.09	0.26	0.27	1	8.1	0.5	1.59
56.13	0.25	0.27	3.01	6.22	1	4.04
57.01	0.24	0.27	5.43	6.12	1.5	6.2

58.86	0.24	0.27	6.02	5.93	2	8.06
62.18	0.24	0.27	7.27	5.61	2.5	989

The probe is in the centre of the column.

Time, s	κ open, mS/cm	κ syphon, mS/cm	ε (conduct.), %0	Buoyan. vel., cm/s	Jg, cm/s	ε (pressure), %
	0.27	0.27	0		0	0
47.79	0.26	0.27	1.13	7.29	0.5	1.49
54.51	0.25	0.27	3.68	6.39	1	3.99
59.2	0.25	0.27	4.77	5.89	1.5	6.24
59.99	0.24	0.27	6.47	5.81	2	8.14
60.88	0.24	0.27	7.62	5.72	2.5	10

The probe is between the centre and the wall opposed to the spargers shut off.

Time, s	κ open, mS/cm	κ syphon, mS/cm	ε (conduct.), %	Buoyan. vel., cm/s	Jg, cm/s	ε (pressure), %
	0.27	0.27	0		0	0
46.98	0.26	0.27	0.99	7.41	0.5	1.41
55.98	0.26	0.27	2.26	6.22	1	4.01
59.03	0.25	0.27	4.83	5.9	1.5	6.36
61.3	0.24	0.27	6.28	5.68	2	8.09
62.88	0.24	0.27	7.87	5.54	2.5	10.05

The probe is on the wall opposed to the spargers shut off.

Time, s	κ open, mS/cm	κ syphon, mS/cm	ε (conduct.), %	Buoyan. vel., cm/s	Jg, cm/s	ε (pressure), %
	0.27	0.27	0		0	0
47.2	0.26	0.27	0.78	7.38	0.5	1.58
53.9	0.26	0.27	2.55	6.46	1	4.15
58.31	0.25	0.27	5	5.97	1.5	6.29
62.02	0.24	0.27	6.56	5.61	2	8.32
65.83	0.23	0.27	8.6	5.29	2.5	10.18

Table 6.7. Experimental data on gas holdup in a 50 cm diameter, 4 m height, laboratory flotation column. The column is baffled into four quadrants with vertical cruciform baffles. Two spargers are below each quadrant. In the first quadrant two spargers are shut off. The data compares the system without frother and with 15 ppm Dowfroth 250. The gas holdup probe I is used.

No frother.

The probe is in the first quadrant.

ε (pressure), %	κ open, mS/cm	κ syphon, mS/cm	ε (conduct.), %	Jg, cm/s
0	0.27	0.27	0	0
2.04	0.27	0.27	0.82	0.5
3.83	0.26	0.27	2.88	1
5.98	0.25	0.27	4.83	1.5
7.36	0.24	0.27	7.05	2
8.74	0.23	0.27	9.29	2.5

The probe is in the second quadrant.

ε (pressure), %	κ open, mS/cm	κ syphon, mS/cm	ε (conduct.), %	Jg, cm/s
0	0.27	0.27	0	0
1.28	0.26	0.27	1.62	0.5
4.06	0.24	0.27	7.42	1
6.3	0.23	0.27	10.52	1.5
7.7	0.22	0.27	13.03	2
9.59	0.21	0.27	15.46	2.5

The probe is in the third quadrant.

ε (pressure), %	κ open, mS/cm	κ syphon, mS/cm	ε (conduct.), %	Jg, cm/s
0	0.27	0.27	0	0
1.43	0.27	0.27	1.19	0.5
4.37	0.26	0.27	3.85	1
6.46	0.24	0.27	7.47	1.5
8.44	0.24	0.27	7.09	2
9.74	0.24	0.27	7.31	2.5

The probe is in the fourth quadrant.

ε (pressure), %	κ open, mS/cm	κ syphon, mS/cm	ε (conduct.), %	Jg, cm/s
0	0.27	0.27	0	0
1.17	0.26	0.27	1.78	0.5
3.47	0.26	0.27	2.45	1
5.43	0.26	0.27	3.61	1.5
6.94	0.25	0.27	5.16	2
8.41	0.24	0.27	6.44	2.5

15 ppm Dowfroth 250.

The probe is in the first quadrant.

ε (pressure), %	κ open, mS/cm	κ syphon, mS/cm	ε (conduct.), %	Jg, cm/s
0	0.27	0.27	0	0
3.33	0.25	0.27	3.17	0.5
8.04	0.24	0.27	7.21	1
11.79	0.23	0.27	9.93	1.5
16.36	0.21	0.27	15.46	2
17.91	0.2	0.27	16.99	2.5

The probe is in the second quadrant.

ε (pressure), %	κ open, mS/cm	κ syphon, mS/cm	ε (conduct.), %	Jg, cm/s
0	0.27	0.27	0	0
3.11	0.26	0.27	2.13	0.5
7.69	0.24	0.27	7.58	1
11.99	0.22	0.27	12.73	1.5
16.03	0.2	0.27	17.98	2
17.63	0.19	0.27	20.04	2.5

The probe is in the third quadrant.

ε (pressure), %	κ open, mS/cm	κ syphon, mS/cm	ε (conuct.), %	Jg, cm/s
0	0.27	0.27	0	0
3.14	0.25	0.27	3.2	0.5

7.84	0.24	0.27	7.4	1
12.22	0.22	0.27	11.68	1.5
15.47	0.22	0.27	13.58	2
19.11	0.2	0.27	17.63	2.5

The probe is in the fourth quadrant.

ε (pressure), %	κ open, mS/cm	κ syphon, mS/cm	ε (conduct.), %	Jg, cm/s
0	0.27	0.27	0	0
2.89	0.26	0.27	1.75	0.5
7.9	0.24	0.27	6.28	1
12.05	0.23	0.27	9.21	1.5
15.03	0.22	0.27	11.66	2
17.32	0.21	0.27	13.87	2.5

Table 6.8. Experimental gas holdup data collected with the probe I in a 50 cm diameter, 4 m height, laboratory flotation column (air-water). Different radial positions at two meters from the column lip. The system is with 10 ppm Dowfroth 250. The velocity as the bubble swarm interface is moving is estimated from the pressure and conductivity readings with respect to time.

The probe is in the centre of the column.

Time, s	κ open, mS/cm	κ syphon, mS/cm	ε (conduct.), %	Buoyan. vel., cm/s	Jg, cm/s	ε (pressure), %
	1.1	1.1	0		0	0
43.6	1.05	1.1	2.76	7.1	0.5	2.54
48.5	0.98	1.1	7.38	6.38	1	7.45
47.67	0.93	1.1	10.57	6.49	1.5	11.24
48.1	0.88	1.1	14.25	6.43	2	12.65
48.7	0.87	1.1	15.01	6.35	2.5	15.84

The probe is between the centre and the wall of the column.

Time, s	κ open, mS/cm	κ syphon, mS/cm	ε (conduct.), %	Buoyan. vel., cm/s	Jg, cm/s	ε (pressure), %
	1.1	1.1	0		0	0
44.6	1.05	1.1	3.15	6.93	0.5	2.98
48.9	0.98	1.1	7.43	6.33	1	7.42
49.13	0.92	1.1	11.33	6.3	1.5	11.61
48.95	0.89	1.1	13.45	6.32	2	13.56
49.16	0.85	1.1	16.11	6.29	2.5	16.17

The probe is on the wall of the column.

Time, s	κ open, mS/cm	κ syphon, mS/cm	ε (conduct.), %	Buoyan. vel., cm/s	Jg, cm/s	ε (pressure), %
	1.1	1.1	0		0	0
44.8	1.05	1.1	3.02	6.9	0.5	3.18
47.7	0.97	1.1	8.06	6.48	1	7.64
48.34	0.91	1.1	11.78	6.39	1.5	11.03
48.08	0.88	1.1	14.44	6.43	2	14.35
48.55	0.83	1.1	17.58	6.37	2.5	16.57

Table 6.9. Experimental data on gas holdup measurements in a 50 cm diameter, 4 m height, laboratory flotation column. The column is without baffles and it compares the effect of addition of 20 ppm Dowfroth 250. The gas holdup probe I is placed in the centre of the column at 2 m from the lip.

The system does not contain frother.

Jg, cm/s	ε (pressure), %	κ open, mS/cm	κ syphon, mS/cm	ε (conductivity), %
0	0	0.56	0.56	0
0.17	0.3	0.56	0.56	0.08
0.25	0.61	0.56	0.56	0.17
0.34	0.92	0.55	0.56	0.85

0.42	1.34	0.55	0.56	1.07
0.51	1.91	0.55	0.56	1.45
0.59	2.18	0.55	0.56	1.3
0.68	2.58	0.54	0.56	2
0.76	3.09	0.54	0.56	1.86
0.85	3.38	0.54	0.56	2.22
1.02	4.1	0.53	0.56	3.26
1.19	4.8	0.53	0.56	3.95
1.36	5.47	0.53	0.56	3.78
1.53	6.14	0.51	0.56	6.08
1.7	6.78	0.52	0.56	4.58
1.87	7.5	0.51	0.56	5.59
2.04	8.18	0.51	0.56	5.9
2.21	8.83	0.5	0.56	7.05
2.38	9.4	0.5	0.56	7.63
2.55	10.08	0.49	0.56	8.3

The system contains 20 ppm Dowfroth 250.

Jg, cm/s	ε (pressure), %	κ open, mS/cm	κ syphon, mS/cm	ε (conductivity), %
0	0	0.56	0.56	0
0.17	0.518	0.56	0.56	0.23
0.25	1.3	0.55	0.56	0.87
0.34	1.98	0.55	0.56	1.46
0.42	2.9	0.54	0.56	2.54
0.51	3.37	0.54	0.56	2.34
0.59	4.55	0.52	0.56	4.34
0.68	4.86	0.52	0.56	4.24
0.76	6.26	0.51	0.56	5.63
0.85	6.87	0.51	0.56	6.28
1.02	8.77	0.5	0.56	7.59
1.19	10.19	0.48	0.56	9.7

1.36	11.38	0.47	0.56	10.56
1.53	12.73	0.47	0.56	11.55
1.7	14.11	0.45	0.56	13.67
1.87	15.53	0.44	0.56	14.52
2.04	16.91	0.43	0.56	16.06
2.21	18.08	0.42	0.56	17.24
2.38	19.62	0.41	0.56	18.69
2.55	21.14	0.4	0.56	20.77

Table 6.10. Experimental data of gas holdup measurements in a 50 cm diameter, 4 m height, laboratory flotation column. The gas holdup probe II is placed at two meters from the lip of the column; measurements were done radially.

The probe is on the wall of the column.

κ open, mS/cm	κ syphon, mS/cm	ε (conductivity), %	Jg, cm/s	ε (pressure), %
1.07	1.07	0	0	0
1.05	1.07	1.46	0.5	1.72
1	1.07	4.84	1	4.43
0.95	1.07	7.27	1.5	6.98
0.92	1.07	9.54	2	8.64
0.9	1.07	11.45	2.5	10.47

The probe is between the wall and the centre of the column.

κ open, mS/cm	κ syphon, mS/cm	ε (conductivity), %	Jg, cm/s	ε (pressure), %
1.07	1.07	0	0	0
1.04	1.07	2.07	0.5	1.8
0.97	1.07	6.46	1	4.31
0.97	1.07	6.71	1.5	6.99
0.93	1.07	9.22	2	8.99
0.88	1.07	12.42	2.5	11.07

The probe is in the centre of the column.

κ open, mS/cm	κ syphon, mS/cm	ε (conductivity), %	Jg, cm/s	ε (pressure), %
1.07	1.07	0	0	0
1.03	1.07	2.65	0.5	1.81
0.98	1.07	5.92	1	4.38
0.95	1.07	7.59	1.5	6.99
0.92	1.07	10.15	2	9.05
0.89	1.07	11.89	2.5	11.46

Table 6.11. Experimental data on gas holdup measurements in air-water systems. The gas holdup probe II is used in a 10 cm diameter laboratory flotation column. Comparison between counter- and co-current flow. The terms Jg, Jf, Jo, and Jt are the air, water-feed, water-overflow, and water-tailings velocity (referred to the column cross section area).

The system is co-current, without frother.

κ open, mS/cm	κ syphon, mS/cm	ε (conduct.), %	Jg, cm/s	Jf, cm/s	Jo, cm/s	Jt, cm/s
0.264	0.264	0	0	0.29	0.29	_
0.26	0.264	0.952	0.21	0.29	0.29	_
0.256	0.264	2.08	0.42	0.29	0.29	_
0.252	0.264	3.11	0.84	0.29	0.29	_
0.238	0.264	6.62	1.27	0.29	0.29	_
0.229	0.264	9.03	1.69	0.29	0.29	_
0.223	0.264	10.88	2.12	0.29	0.29	_
0.216	0.264	12.75	2.54	0.29	0.29	_

The system is counter-current, without frother.

κ open, mS/cm	κ syphon, mS/cm	ε (conduct.), %	Jg, cm/s	Jf, cm/s	Jo, cm/s	Jt, cm/s
0.273	0.273	0	0	0.35	0.2	0.091

0.27	0.273	0.69	0.21	0.35	0.2	0.091
0.267	0.273	1.5	0.42	0.35	0.2	0.091
0.252	0.273	5.07	0.84	0.35	0.2	0.091
0.25	0.273	5.63	1.27	0.35	0.2	0.091
0.235	0.273	9.64	1.69	0.35	0.2	0.091
0.223	0.273	12.91	2.12	0.35	0.2	0.091
0.211	0.273	16.28	2.54	0.35	0.2	0.091

The system is co-current, with 5 ppm Dowfroth 250.

κ open, mS/cm	κ syphon, mS/cm	ε (conduct.), %	Jg, cm/s	Jf, cm/s	Jo, cm/s	Jt, cm/s
0.276	0.276	0	0	0.29	0.29	_
0.261	0.276	3.64	0.21	0.29	0.29	_
0.249	0.276	6.68	0.42	0.29	0.29	_
0.228	0.276	12.15	0.84	0.29	0.29	_
0.214	0.276	16.07	1.27	0.29	0.29	_
0.2	0.276	20.13	1.69	0.29	0.29	_
0.185	0.276	24.42	2.12	0.29	0.29	_
0.174	0.276	28.05	2.54	0.29	0.29	_

The system is counter-current, with 5 ppm Dowfroth 250.

κ open, mS/cm	κ syphon, mS/cm	ε (conduct.), %	Jg, cm/s	Jf, cm/s	Jo, cm/s	Jt, cm/s
0.284	0.284	0	0	0.289	0.179	0.11
0.264	0.284	4.56	0.21	0.289	0.179	0.11
0.256	0.284	6.68	0.42	0.289	0.179	0.11
0.235	0.284	12.18	0.84	0.289	0.179	0.11
0.215	0.284	17.39	1.27	0.289	0.179	0.11
0.198	0.284	22.24	1.69	0.289	0.179	0.11
0.183	0.284	26.66	2.12	0.289	0.179	0.11
0.173	0.284	29.93	2.54	0.289	0.179	0.11

The system is in co-current, with 10 ppm Dowfroth 250.

κ open, mS/cm	κ syphon, mS/cm	ε (conduct.), %	Jg, cm/s	Jf, cm/s	Jo,cm/s	Jt, cm/s
0.282	0.282	0	0	0.289	0.289	_
0.267	0.282	3.56	0.21	0.289	0.289	_
0.256	0.282	6.16	0.42	0.289	0.289	_
0.233	0.282	12.19	0.84	0.289	0.289	_
0.218	0.282	16.34	1.27	0.289	0.289	_
0.199	0.282	21.59	1.69	0.289	0.289	_
0.183	0.282	26.44	2.12	0.289	0.289	_

The system is counter-current, with 10 ppm Dowfroth 250.

κ open, mS/cm	κ syphon, mS/cm	ε (conduct.), %	Jg, cm/s	Jf, cm/s	Jo, cm/s	Jt, cm/s
0.285	0.285	0	0	0.289	0.179	0.11
0.264	0.285	4.8	0.21	0.289	0.179	0.11
0.252	0.285	7.82	0.42	0.289	0.179	0.11
0.232	0.285	13.02	0.84	0.289	0.179	0.11
0.209	0.285	19.49	1.27	0.289	0.179	0.11
0.189	0.285	25.04	1.69	0.289	0.179	0.11
0.17	0.285	30.87	2.12	0.289	0.179	0.11

The system is co-current, with 15 ppm Dowfroth 250.

κ open, mS/cm	κ syphon, mS/cm	ε (conduct.), %	Jg, cm/s	Jf, cm/s	Jo, cm/s	Jt, cm/s
0.258	0.258	0	0	0.289	0.289	_
0.245	0.258	3.29	0.21	0.289	0.289	_
0.232	0.258	6.75	0.42	0.289	0.289	_
0.21	0.258	12.99	0.84	0.289	0.289	_
0.196	0.258	17.13	1.27	0.289	0.289	_
0.181	0.258	22.01	1.69	0.289	0.289	_
0.167	0.258	26.37	2.12	0.289	0.289	_

The system is counter-current, with 15 ppm Dowfroth 250.

κ open, mS/cm	κ syphon, mS/cm	ε (conduct.), %	Jg, cm/s	Jf, cm/s	Jo cm/s	Jt, cm/s
0.276	0.276	0	0	0.287	0.175	0.112
0.256	0.276	4.77	0.21	0.287	0.175	0.112
0.244	0.276	7.99	0.42	0.287	0.175	0.112
0.221	0.276	14.12	0.84	0.287	0.175	0.112
0.201	0.276	19.67	1.27	0.287	0.175	0.112
0.186	0.276	24.24	1.69	0.287	0.175	0.112
0.162	0.276	31.81	2.12	0.287	0.175	0.112

The system is co-current, with 20 ppm Dowfroth 250.

κ open, mS/cm	κ syphon, mS/cm	ε (conduct.), %	Jg, cm/s	Jf, cm/s	Jo, cm/s	Jt, cm/s
0.279	0.279	0	0	0.287	0.287	_
0.26	0.279	4.46	0.21	0.287	0.287	_
0.25	0.279	7.15	0.42	0.287	0.287	_
0.222	0.279	14.55	0.84	0.287	0.287	_
0.203	0.279	19.76	1.27	0.287	0.287	_
0.186	0.279	24.91	1.69	0.287	0.287	_

The system is counter-current, with 20 ppm Dowfroth 250.

κ open, mS/cm	κ syphon, mS/cm	ε (conduct.), %	Jg, cm/s	Jf, cm/s	Jo, cm/s	Jt, cm/s
0.279	0.279	0	0	0.287	0.175	0.112
0.264	0.279	3.4	0.21	0.287	0.175	0.112
0.248	0.279	7.54	0.42	0.287	0.175	0.112
0.225	0.279	13.57	0.84	0.287	0.175	0.112
0.201	0.279	20.28	1.27	0.287	0.175	0.112
0.169	0.279	30.24	1.69	0.287	0.175	0.112

Table 6.12. Experimental data on gas holdup measurements in three phase silica-water-air systems. Experimental systems contain 5% v/v silica. The gas holdup probe II was used in a 10 cm diameter laboratory flotation column.

5% silica; no frother.

K open, mS	K syphon, mS	Q air, l/minute	ε (slurry displ.), %	ε (conduct.), %
1.3	0.075	0	0	0
1.28	0.075	2	1	1.03
1.25	0.075	4	2.5	2.6
1.2	0.075	6	5.2	5.26
1.14	0.075	8	8.3	8.56
1.1	0.075	10	10.9	10.81
1.05	0.075	12	13.6	13.7

5% silica; 5 ppm Dowfroth 250.

K open, mS	K syphon, mS	Q air, l/minute	ε (slurry displ.), %	ε (conduct.), %
1.3	0.076	1	0.72	1.24
1.26	0.076	2	3.1	3.3
1.18	0.076	4	7.8	7.54
1.13	0.076	6	11.1	10.29
1.09	0.076	8	12.8	12.54
1.01	0.076	10	18.2	17.19
0.99	0.076	12	18.5	18.13

5% silica; 10 ppm Dowfroth 250.

K open, mS	K syphon, mS	Q air, l/minute	ε (slurry displ.), %	ε (conduct.), %
1.2	0.077	1	7.1	7.6
1.17	0.077	2	9.3	9.21
0.97	0.077	4	20.3	20.62
0.778	0.077	6	33.4	32.82

5% silica; 15 ppm Dowfroth 250.

K open, mS	K syphon, mS	Q air, l/minute	ε (slurry displ.), %	ε (conduct.), %
1.26	0.076	1	3.9	4.45
1.15	0.076	2	9.7	10.3
0.93	0.076	4	22.9	23.06
0.72	0.076	6	37.3	36.77

5% silica; 20 ppm Dowfroth 250.

K open, mS	K syphon, mS	Q air, l/minute	ε (slurry displ.), %	ε (conduct.), %
1.26	0.0758	1	4.8	5.36
1.14	0.0758	2	12.9	11.72
0.91	0.0758	4	26.4	25.08

Table 6.13. Experimental data on gas holdup measurements in three phase silica-water-air systems. Silica content was varied between 10% and 30% v/v containing 20 ppm Dowfroth 250. Gas holdup is also estimated from slurry displacement.

10% silica.

κ open, mS/cm	κ syphon, mS/cm	ε (conduct.), %	ε (slurry displ.), %	Jg, cm/s
0.2706	0.2707	0.021	0.42	0.21
0.2536	0.2707	4.27	5.6	0.42
0.2008	0.2707	18.82	20.8	0.84
0.1479	0.2707	35.59	38.1	1.27

15% silica.

κ open, mS/cm	κ syphon, mS/cm	ε (conduct.), %	ε (slurry displ.), %	Jg, cm/s
0.2676	0.268	0.086	1.2	0.21
0.2431	0.268	6.38	7.7	0.42
0.1966	0.268	19.48	21.6	0.84
0.1162	0.268	46.52	47.1	1.27

20% silica.

κ open, mS/cm	κ syphon, mS/cm	ε (conduct.), %	ε (slurry displ.), %	Jg, cm/s
0.2659	0.266	0.009	2.4	0.21
0.238	0.266	7.25	10.5	0.42
0.1824	0.266	23.38	25.2	0.84
0.1211	0.266	44.35	46.6	1.27

25% silica.

κ open, mS/cm	κ syphon, mS/cm	ε (conduct.), %	ε (slurry displ.), %	Jg, cm/s
0.2608	0.261	0.028	3.2	0.21
0.2378	0.261	6.09	9.2	0.42
0.1807	0.261	22.83	25.5	0.84

30% silica.

κ open, mS/cm	κ syphon, mS/cm	ε (conduct.), %	ε (slurry displ.), %	Jg, cm/s
0.2558	0.256	0.048	4.5	0.21
0.2325	0.256	6.29	10.6	0.42
0.1733	0.256	24.11	27.9	0.84

Table 6.14. Experimental data on gas holdup. Comparison between co-, and counter-current flow in a 10 cm diameter flotation column. Three phase silica-water-air system. The slurry contains 30% silica and 20 ppm Dowfroth 250. Jg is maintained at 0.8 cm/s. The gas holdup probe II was used.

Counter-current.

κ open, mS/cm	κ syphon, mS/cm	ε (conduct.), %	J slurry, cm/s	J overflow, cm/s	J tailings, cm/s
0.198	0.278	21.04	0.21	0.13	0.07
0.194	0.278	22.16	0.23	0.15	0.07
0.189	0.278	23.86	0.27	0.19	0.07
0.185	0.278	24.94	0.31	0.23	0.07

0.184	0.278	25.2	0.35	0.27	0.07

Co-current.

κ open, mS/cm	κ syphon, mS/cm	ε (conduct.), %	J slurry, cm/s	J overflow, cm/s	J tailings, cm/s
0.194	0.278	22.16	0.21	0.21	_
0.1971	0.278	21.47	0.23	0.23	_
0.1969	0.278	21.53	0.27	0.27	_
0.1971	0.278	21.47	0.31	0.31	_
0.1973	0.278	21.41	0.35	0.35	_

Table 6.15. Experimental data on gas holdup measurements in three phase carbon-water-air systems. Gas holdup probe II was used in a 10 cm diameter laboratory flotation column. The system contains 5% v/v solids.

No frother.

κ open, mS/cm	κ syphon, mS/cm	ε (conductivity), %	ε (slurry displ.), %	Jg, cm/s
1.058	1.058	0	0	0
1.045	1.054	0.58	0.6	0.21
1.064	1.075	0.71	0.8	0.42
1.031	1.084	3.28	3.6	0.84
1.054	1.088	2.06	2	1.27
1.015	1.092	4.83	5	1.69
0.98	1.1	7.13	7.5	2.12

20 ppm Dowfroth 250.

κ open, mS/cm	κ syphon, mS/cm	ε (conductivity), %	ε (slurry displ.), %	Jg, cm/s
1.026	1.026	0	0	0
1.022	1.026	0.303	0.5	0.21
1.001	1.026	1.68	2	0.42
0.982	1.026	2.92	3.4	0.84

0.947	1.026	5.29	5.7	1.27
0.886	1.026	9.52	9.9	1.69
0.875	1.026	10.35	11	2.12
0.805	1.026	15.49	16	2.54

Table 6.16 Experimental data on gas holdup measurements. The experiment shows the effect of wash water distribution on the gas holdup. The gas holdup probe II was placed in a 16 cm diameter flotation column. The column is divided in two sections by a vertical baffle. Wash water is placed only over one of the sections of the column. The terms "in" and "out" mean in the quadrant under wash water, and with no wash water, respectively.

Time, s	κ open (in), mS/cm	κ syphon (in), mS/cm	κ open (out), mS/cm	κ syphon (out), mS/cm	ε (in), %	ε (out), %
0	0.2945	0.3816	0.2604	0.3834	16.45	23.93
5	0.2971	0.3816	0.2746	0.3834	15.93	20.88
10	0.2931	0.3816	0.2815	0.383	16.75	19.37
15	0.2954	0.3816	0.2806	0.383	16.28	19.55
20	0.3036	0.3816	0.2803	0.3816	14.61	19.4
25	0.2945	0.3816	0.2855	0.3816	16.45	18.33
30	0.2923	0.3816	0.2891	0.3816	16.92	17.56
35	0.2965	0.3816	0.2871	0.3816	16.05	17.98
40	0.2991	0.3816	0.2817	0.3816	15.53	19.38
45	0.298	0.3816	0.2809	0.3816	15.76	19.49
50	0.2951	0.3793	0.2846	0.3816	15.98	18.79
55	0.2963	0.3816	0.286	0.3816	16.1	18.21
60	0.2963	0.3816	0.286	0.3816	16.1	18.21
65	0.2971	0.3816	0.2832	0.3816	15.93	18.81
70	0.2954	0.3816	0.2834	0.3834	16.28	19.03
75	0.2857	0.3816	0.2909	0.3834	18.27	17.49
80	0.2815	0.3816	0.2954	0.3834	19.16	16.56

85	0.282	0.3816	0.2957	0.3834	18.76	16.22
90	0.2823	0.3798	0.2914	0.3816	18.63	17.59
95	0.282	0.3793	0.2886	0.3816	19.04	17.89
100	0.2803	0.3816	0.2832	0.3816	19.4	19.36
105	0.2766	0.3816	0.2817	0.3816	20.18	19.66
110	0.2729	0.3816	0.2817	0.3816	20.96	19.66
115	0.2718	0.3816	0.2792	0.3816	21.21	20.19
120	0.2738	0.3816	0.2826	0.3848	20.79	19.41
125	0.2741	0.3816	0.2886	0.3844	20.72	18.25
130	0.2735	0.3816	0.2888	0.3852	20.85	18.19
135	0.2735	0.3816	0.2866	0.3848	20.85	18.59
140	0.2721	0.3816	0.284	0.3852	21.15	19.19

APPENDIX 7

Table 7.1. INCO-Matte Separation Plant column 2. Experimental data on gas holdup measurements using the gas holdup probe II. The system is under operating conditions (i.e. air flow rate = 314 m^3/h). The probe is placed in the quandrants at different depths. The conductivity of the clear liquid from the collection zone was 2.5 mS/cm.

First quadrant.

column depth, m	κ syphon, mS/cm	κ open, mS/cm	ε (conductivity), %
8.53	1.9202	1.422	18.93
7.92	1.919	45451	17.55
7.32	1.9174	1.4341	18.34
6.71	1.913	1.4238	18.64
6.1	1.9033	1.4361	17.82
5.49	1.8937	1.3793	19.91
4.88	1.8832	1.3689	20.03
4.27	1.8744	1.3652	19.91
3.66	1.8611	1.3085	21.97
3.05	1.8506	1.2568	23.95
2.44	1.8498	1.3145	21.35
1.83	1.8426	1.2239	25.21
1.22	1.8365	1.1685	27.59
0.61	1.8265	1.1498	28.18

Second quadrant.

column depth, m	κ syphon, mS/cm	κ open, mS/cm	ε (conductivity), %
8.53	1.9347	1.3683	21.63
7.92	1.9267	1.3847	20.69
7.32	1.9299	1.3559	22.01
6.71	1.9166	1.3605	21.42
6.1	1.9126	1.2801	24.78

5.49	1.9114	1.3548	21.5
4.88	1.9062	1.3639	20.95
4.27	1.905	1.3219	22.72
3.66	1.8977	1.2594	25.25
3.05	1.8933	1.1965	27.97
2.44	1.8808	1.2026	27.32
1.83	1.8643	1.2182	26.12
1.22	1.8603	1.1844	27.56
0.61	1.8506	1.1646	28.2

Third quadrant.

column depth, m	κ syphon, mS/cm	κ open, mS/cm	ε (conductivity), %
8.53	1.9548	1.5376	15.32
7.92	1.9556	1.4764	17.79
7.32	1.9512	1.4472	18.84
6.71	1.944	1.489	16.92
6.1	1.9307	1.48	16.88
5.49	1.9202	1.4412	18.14
4.88	1.9102	1.4702	16.63
4.27	1.9058	1.4622	16.82
3.66	1.8977	1.4	19.14
3.05	1.8877	1.3398	21.42
2.44	1.8824	1.3033	22.85
1.83	1.874	1.2766	23.78
1.22	1.8675	1.2077	26.7
0.61	1.8555	1.1452	29.25

Fourth quadrant.

column depth, m	κ syphon, mS/cm	κ open, mS/cm	ε (conductivity), %
8.53	1.9777	1.4192	20.78
7.92	1.9749	1.4185	20.73

7.32	1.9713	1.3428	23.78
6.71	1.9641	1.393	21.46
6.1	1.9548	1.3919	21.24
5.49	1.948	1.3486	22.86
4.88	1.9472	1.3201	24.05
4.27	1.9432	1.4133	19.99
3.66	1.9206	1.3327	22.73
3.05	1.8981	1.2649	25.02
2.44	1.882	1.3605	20.35
1.83	1.8679	1.2435	25.08
1.22	1.884	1.2969	23.18
0.61	1.8555	1.2048	26.47

Table 7.1. INCO Matte Separation Plant column 2. Test data on gas holdup; operating conditions; air flow rate = 314 m^3/h; gas holdup probe II was used in each quadrant.

First quadrant.

column depth, m	κ syphon, mS/cm	κ open, mS/cm	ε (conductivity), %
8.53	1.4213	1.109	15.81
7.92	1.4164	1.06	18.3
7.32	1.416	1.0779	17.29
6.71	1.4135	1.0412	19.25
6.1	1.4111	1.0773	17.12
5.49	1.4025	1.0394	18.89
4.88	1.3955	0.9907	21.41
4.27	1.3902	1.0051	20.34
3.66	1.3869	0.9619	22.75
3.05	1.3844	0.9519	23.25
2.44	1.3795	0.9596	22.59

1.83	1.3775	0.9968	20.29
1.22	1.375	0.9129	25.23
0.61	1.3746	0.9006	25.97

Second quadrant.

column depth, m	κ syphon, mS/cm	κ open, mS/cm	ε (conductivity), %
8.53	1.3742	1.0509	17.02
7.92	1.3734	1.05	17.03
7.32	1.3697	1.057	16.47
6.71	1.368	1.061	16.12
6.1	1.3643	1.029	17.79
5.49	1.3586	1.0028	19.13
4.88	1.3586	1.0273	17.69
4.27	1.3495	1.0056	18.57
3.66	1.3417	0.9546	21.28
3.05	1.3323	0.9324	22.23
2.44	1.3335	0.9387	21.9
1.83	1.3401	0.9141	23.7
1.22	1.3446	0.9106	24.11
0.61	1.3438	0.8743	26.36

Third quadrant.

column depth, m	κ syphon, mS/cm	κ open, mS/cm	ε (conductivity), %
8.53	1.4135	1.0263	20.1
7.92	1.425	1.0586	18.75
7.32	1.4311	1.0235	20.98
6.71	1.4324	1.0063	22.01
6.1	1.4381	1.0683	18.75
5.49	1.4365	0.9938	22.89
4.88	1.4365	0.946	25.69
4.27	1.4381	1.0402	20.32

3.66	1.4483	1.0411	20.68
3.05	1.4491	1.0008	23
2.44	1.4487	0.9832	23.99
1.83	1.4365	0.9769	23.87
1.22	1.4377	0.9746	24.06
0.61	1.4377	0.5042	55.24

Fourth quadrant.

column depth, m	κ syphon, mS/cm	κ open, mS/cm	ε (conductivity), %
8.53	1.5348	1.2182	14.77
7.92	1.5433	1.1941	16.31
7.32	1.5449	1.1833	16.93
6.71	1.5482	1.1747	17.49
6.1	1.5482	1.1768	17.38
5.49	1.5474	1.1707	17.66
4.88	1.5417	1.1714	17.41
4.27	1.5388	1.2043	15.63
3.66	1.5315	1.1294	19.18
3.05	1.5388	1.1741	17.16
2.44	1.5437	1.1121	20.56
1.83	1.547	1.0689	22.97
1.22	1.5413	1.0897	21.65
0.61	1.5258	0.5166	56.56

Table 7.3. INCO Matte Separation Plant column 3. Gas holdup measurements in two phase air-batch water conditions; the gas holdup probe I is placed at the centre of the column; measurements were done at different depths and air flow rates. Also two portable pressure tranmitters are used.

Air flow rate: 90 m^3/h.

column depth, m	κ syphon, mS/cm	κ open, mS/cm	ε (conductivity), %	ε (pressure), %
7.62	0.4215	0.4207	0.14	0.09
7.01	0.4219	0.4173	0.73	0.5
6.4	0.4222	0.4185	0.58	0.4
5.79	0.4225	0.4168	0.9	0.7
5.18	0.4225	0.4194	0.49	0.6
4.57	0.4225	0.419	0.56	0.4
3.96	0.4225	0.4172	0.85	1
3.35	0.4228	0.4136	1.46	1.1
2.74	0.4228	0.4147	1.28	1.6
2.13	0.423	0.4114	1.85	2.1
1.52	0.4229	0.4122	1.69	2
0.91	0.4231	0.413	1.61	2.4
0.3	0.4276	0.4066	3.32	3
0	0.4294	0.4087	3.26	2.98

Air flow rate: 180 m^3/h

column depth, m	κ syphon, mS/cm	κ open, mS/cm	ε (conductivity), %	ε (pressure), %
7.62	0.4348	0.3989	5.66	4.32
7.01	0.4343	0.3934	6.48	5
6.4	0.4334	0.389	7.07	6.9
5.79	0.4325	0.388	7.09	7
5.18	0.4129	0.3829	4.97	5.8
4.57	0.4123	0.3771	5.87	6.3
3.96	0.4116	0.373	6.45	5.67
3.35	0.4097	0.3699	6.7	5.9

2.74	0.4093	0.3649	7.49	8
2.13	0.4097	0.3624	8.01	10
1.52	0.4091	0.357	8.87	9.54
0.91	0.4093	0.3547	9.29	8.4
0.3	0.4116	0.3503	10.44	10.1
0	0.4122	0.345	11.48	11.5

Air flow rate: 180 m^3/h.

column depth, m	κ syphon, mS/cm	κ open, mS/cm	ε (conductivity), %	ε (pressure), %
8.05	0.3781	0.3452	5.97	4.6
7.45	0.3765	0.3491	4.97	4.7
6.85	0.3753	0.3352	7.38	6.2
6.25	0.3736	0.3341	7.3	6.98
5.64	0.3723	0.3274	8.38	7.3
5.03	0.3717	0.3259	8.57	7.7
4.42	0.3708	0.3228	9.01	10.3
3.83	0.3705	0.3234	8.84	9.2
3.23	0.3978	0.3213	13.7	13.2
2.62	0.3973	0.3161	14.63	14.5
2.02	0.3971	0.3148	14.84	13
1.42	0.3969	0.3106	15.63	14
0.82	0.3972	0.3056	16.67	14.5
0.22	0.4015	0.297	19	18.6

Air flow rate: 118 m^3/h.

column depth, m	κ syphon, mS/cm	κ open, mS/cm	ε (conductivity), %	ε (pressure), %
7.92	0.2128	0.2094	1.1	0.6
7.32	0.2141	0.2055	2.7	2.5
6.71	0.2153	0.2033	3.77	2.98
6.1	0.2151	0.1997	4.89	3.79
5.49	0.2154	0.1989	5.25	5.13

4.88	0.22	0.1964	7.41	7.7
4.27	0.225	0.198	8.33	8.6
3.66	0.2249	0.1983	8.23	8.67
3.05	0.2249	0.1946	9.42	9.21
2.44	0.2252	0.1974	8.56	8.1
1.83	0.2253	0.19	11.01	10
1.22	0.2254	0.1934	9.93	9.9
0.61	0.2255	0.1954	9.31	8.74
0	0.2258	0.2103	4.66	6.35

Air flow rate: 240 m^3/h.

column depth, m	κ syphon, mS/cm	κ open, mS/cm	ε (conductivity), %	ε (pressure), %
7.92	0.226	0.202	7.35	7
7.32	0.2257	0.197	8.83	8
6.71	0.2253	0.1948	9.45	9
6.1	0.225	0.1945	9.46	9.5
5.49	0.2246	0.1896	10.93	10.82
4.88	0.2242	0.1891	10.99	10.9
4.27	0.2236	0.1839	12.58	11.3
3.66	0.223	0.1779	14.45	13.98
3.05	0.2223	0.1826	12.65	13.5
2.44	0.2215	0.1792	13.6	14.23
1.83	0.2209	0.1695	16.81	18.34
1.22	0.2202	0.1724	15.61	17.92
0.61	0.2195	0.17	16.23	15.78
0	0.2189	0.1685	16.6	16.5

Air flow rate: 301 m^3/h.

column depth, m	κ syphon, mS/cm	κ open, mS/cm	ε (conductivity), %	ε (pressure), %
7.9	0.2164	0.1847	10.25	8.3
7.32	0.2155	0.1819	10.96	9.5

6.71	0.215	0.1804	11.33	10.45
6.1	0.2144	0.1727	13.86	14.7
5.49	0.2139	0.1698	14.78	15.96
4.88	0.2135	0.1667	15.76	16.75
4.27	0.213	0.1636	16.74	16.58
3.66	0.2124	0.1536	20.32	18.3
3.05	0.212	0.1612	17.35	18.3
2.44	0.2114	0.1562	19.05	19.5
1.83	0.2108	0.148	22.04	23
1.22	0.2103	0.1581	18.05	17.3
0.61	0.21	0.1537	6219	20.32
0	0.2096	0.1463	22.39	22.43

Air flow rate: 340 m^3/h.

column depth, m	κ syphon, mS/cm	κ open, mS/cm	ε (conductivity), %	ε (pressure), %
7.92	0.3558	0.2802	15.26	15.2
7.32	0.3544	0.272	16.8	15.2
6.71	0.3531	0.2714	16.71	15.8
6.1	0.3523	0.2594	19.27	17.59
5.49	0.3501	0.256	19.67	17.88
4.88	0.3496	0.2521	20.48	20.1
4.27	0.3489	0.2368	23.99	24.6
3.66	0.3481	0.2353	24.23	24.3
3.05	0.3483	0.2361	24.06	23.78
2.44	0.3485	0.2319	25.1	25.07
1.83	0.3486	0.2236	27.15	25.3
1.22	0.3505	0.2212	28.02	26.8
0.61	0.3517	0.2223	27.95	24.98
0	0.3617	0.2114	32.14	30.7

Table 7.4. INCO-Matte Separation Plant column 3. Gas holdup measurements in batch-water conditions; the gas holdup probe I was used in the centre and at the wall of the column; air flow rate was varied.

Air flow rate: 340 m^3/h; the probe is in the centre.

column depth, m	κ syphon, mS/cm	κ open, mS/cm	ε (conductivity), %
7.92	0.208	0.1726	12.05
7.32	0.206	0.1699	12.58
6.71	0.206	0.1726	11.48
6.1	0.206	0.1644	14.43
5.49	0.205	0.1558	17.58
4.88	0.205	0.1556	17.56
4.27	0.205	0.1518	18.95
3.66	0.204	0.1511	19.1
3.05	0.204	0.1395	23.69
2.44	0.204	0.1437	21.88
1.83	0.204	0.1457	20.97
1.22	0.203	0.1345	25.47
0.61	0.203	0.1455	20.87
0	0.202	0.1421	22.17

Air flow rate: 240 m^3/h; the probe is at the wall.

column depth, m	κ syphon, mS/cm	κ open, mS/cm	ε (conductivity), %
7.92	0.201	0.1752	9.14
7.32	0.201	0.1698	10.96
6.71	0.2	0.1656	12.41
6.1	0.198	0.16164	13.06
5.49	0.198	0.1616	13.19
4.88	0.199	0.1567	15.4
4.27	0.199	0.1456	19.75
3.66	0.198	0.1504	17.69
3.05	0.198	0.1393	21.95

2.44	0.198	40.14	21.5
1.83	0.197	0.1343	23.94
1.22	0.194	0.1445	18.73
0.61	0.197	0.1389	21.99
0	0.198	0.1348	23.48

Air flow rate: 180 m^3/h; the probe is in the centre.

column depth, m	κ syphon, mS/cm	κ open, mS/cm	ε (conductivity), %
7.92	0.215	0.1954	6.43
7.32	0.215	0.1883	8.78
6.71	0.215	0.1882	8.78
6.1	0.215	0.1931	7.09
5.49	0.228	0.187	13.01
4.88	0.228	0.1849	13.63
4.27	0.223	0.1806	13.65
3.66	0.223	0.1788	14.2
3.05	0.223	0.1775	14.73
2.44	0.223	0.1825	12.99
1.83	0.223	0.1766	14.89
1.22	0.223	0.1791	13.99
0.61	0.223	0.1739	15.76
0	0.223	0.1674	18.01

Air flow rate: 180 m^3/h; the probe is at the wall.

column depth, m	κ syphon, mS/cm	κ open, mS/cm	ε (conductivity), %
7.92	0.217	0.2014	5.11
7.32	0.217	0.196	6.78
6.71	0.217	0.1899	8.74
6.1	0.217	0.1921	7.95
5.49	0.217	0.1898	9
4.88	0.218	0.1859	10.44

4.27	0.217	0.188	9.56
3.66	0.218	0.1863	10.19
3.05	0.218	0.1852	10.69
2.44	0.219	0.1762	14.06
1.83	0.219	0.1773	13.72
1.22	0.2174	0.1711	15.3
0.61	0.2173	0.174	14.25

Air flow rate: 90 m^3/h; the probe is in the centre.

column depth, m	κ syphon, mS/cm	κ open, mS/cm	ε (conductivity), %
7.92	0.23	0.2185	3.6
7.32	0.23	0.2137	5.11
6.71	0.23	0.2112	5.76
6.1	0.23	0.2105	6.01
5.49	0.23	0.2111	5.84
4.88	0.23	0.2084	6.64
4.27	0.23	0.2075	6.9
3.66	0.23	0.208	6.8
3.05	0.23	0.2057	7.46
2.44	0.23	0.2058	7.45
1.83	0.23	0.2066	7.12
1.22	0.23	0.2056	7.41
0.61	0.23	0.2033	8.09
0	0.23	0.2018	8.54

Air flow rate: 90 m^3/h; the probe is at the wall.

column depth, m	κ syphon, mS/cm	κ open, mS/cm	ε (conductivity),%
7.92	0.23	0.2142	4.81
7.32	0.23	0.2122	5.38
6.71	0.23	0.2095	6.26
6.1	0.23	0.207	6.65

5.49	0.23	0.2059	7.14
4.88	0.23	0.2054	7.3
4.27	0.23	0.2048	7.56
3.66	0.23	0.2035	7.87
3.05	0.23	0.2011	8.58
2.44	0.23	0.2027	8.03
1.83	0.23	0.2024	8.11
1.22	0.23	0.2033	7.8
0.61	0.23	0.2014	8.51
0	0.23	0.2047	7.49

Table 7.5. INCO-Matte Separation Plant column 3. Gas holdup measurements under normal operating conditions; gas holdup probe I and II were used in the centre of the column.

Gas holdup probe II; air flow rate 213 m^3/h.

column depth, m	κ syphon, mS/cm	κ open, mS/cm	ε (conductivity), %
7.92	1.19	0.9445	14.55
7.32	1.19	0.9177	16.29
6.71	1.19	0.9278	15.62
6.1	1.19	0.9266	15.7
5.49	1.19	0.9376	15.22
4.88	1.19	0.9235	16.11
4.27	1.19	0.9152	16.76
3.66	1.19	0.9251	16.43
3.05	1.19	0.8935	18.8
2.44	1.19	0.9021	18.02
1.83	1.19	0.8907	18.51
1.22	1.19	0.877	19.35

0.61	1.19	0.8637	20.08
0	1.19	0.8505	21.06

Gas holdup probe I; air flow rate 217 m^3/h.

column depth, m	κ syphon, mS/cm	κ open, mS/cm	ε (conductivity), %
7.92	1.27	1.014	14.56
7.32	1.21	0.9838	13.57
6.71	1.21	0.9701	14.41
6.1	1.21	0.9778	13.83
5.49	1.21	0.9685	14.41
4.88	1.21	0.9506	15.48
4.27	1.21	0.9514	15.34
3.66	1.21	0.9461	15.61
3.05	1.21	0.9264	16.89
2.44	1.2	0.9039	18.07
1.83	1.2	0.882	19.29
1.22	1.2	0.8655	20.37
0.61	1.19	0.8555	20.42

Table 7.6. INCO-Matte Separation Plant column 3. Gas holdup measurements in three radial positions: in the centre; in the midway between the wall and the centre; and at the wall of the column. Gas holdup probe II was used. The column was run under normal operating conditions. Air flow rate was 220 m^3/h.

The probe was in the centre of the column.

column depth, m	κ syphon, mS/cm	κ open, mS/cm	ε (conductivity), %
8.53	1.75	1.383	15.36
7.92	1.75	1.3695	15.83
7.32	1.75	1.3182	18.07
6.71	1.75	1.3594	16.11

6.1	1.74	1.327	17.45
5.49	1.73	1.3147	17.69
4.88	1.73	1.3195	17.31
4.27	1.73	1.2528	20.27
3.66	1.72	1.2755	19.02
3.05	1.71	1.2144	21.64
2.44	1.7	1.179	33.07
1.83	1.7	1.1491	24.43
1.22	1.7	1.1503	24.17
0.61	1.69	1.1567	23.69
0	1.69	1.1533	25.49

The probe was in the midway between the centre and the wall of the column.

column depth, m	κ syphon, mS/cm	κ open, mS/cm	ε (conductivity), %
8.53	1.8	1.4168	15.29
7.92	1.79	1.3734	16.96
7.32	1.79	1.3522	17.75
6.71	1.78	1.3644	16.97
6.1	1.78	1.4016	15.27
5.49	1.77	1.3129	18.91
4.88	1.76	1.3112	18.59
4.27	1.75	1.3332	17.36
3.66	1.74	1.2909	19.04
3.05	1.71	1.2783	18.52
2.44	1.73	1.2591	19.99
1.83	1.72	1.1922	22.96
1.22	1.72	1.2261	21.11
0.61	1.71	1.1852	22.8
0	1.73	0.6776	50.83

The probe was at the wall of the column.

column depth, m	κ syphon, mS/cm	κ open, mS/cm	ε (conductivity), %
8.53	1.87	1.5417	12.75
7.92	1.87	1.5046	14.1
7.32	1.87	1.5268	13.3
6.71	1.87	1.532	13
6.1	1.87	1.5356	12.83
5.49	1.87	1.5323	12.89
4.88	1.87	1.5178	13.54
4.27	1.87	1.4974	14.24
3.66	1.87	1.4954	14.33
3.05	1.86	1.477	14.85
2.44	1.85	1.4346	16.19
1.83	1.85	1.4147	17.04
1.22	1.84	1.4404	15.78
0.61	1.74	0.5563	58.77
0	1.64	0.1569	86.32

Table 7.7. INCO-Matte Separation Plant column 4. The column is run under water-batch conditions. Probe I is placed in two opposed quadrants at 5 m from the lip of the column. Air flow rate is varied.

First quadrant.

Jg, cm/s	κ syphon, mS/cm	κ open, mS/cm	ε (conductivity), %
0.75	0.495	0.4227	3.15
1.5	0.495	0.4416	7.56
3	0.495	0.3859	15.95
3.75	0.495	0.3183	27.1

Third quadrant.

Jg, cm/s	κ syphon, mS/cm	κ open, mS/cm	ε (conductivity), %
0.75	0.495	0.4648	4.26
1.5	0.495	0.4451	7.05
3	0.495	0.3749	17.68
3.75	0.495	0.3401	23.37

Table 7.8. INCO-Matte Separation Plant column 4. Normal operating conditions: measurement of gas holdup in two opposed quadrants. Gas holdup probe I is placed at 5 m from the lip of the column. Air flow rate is kept at Jg = 3.7 cm/s.

First quadrant.

Time, minutes	κ syphon, mS/cm	κ open, mS/cm	ε (conductivity), %
20	1.528	0.9071	31.15
30	1.5252	0.9281	30.02
40	1.5259	0.9211	30.45
50	1.5265	0.9222	30.4
60	1.5267	0.9175	30.68
70	1.5269	0.9185	30.63

Third quadrant.

Time, minutes	κ syphon, mS/cm	κ open, mS/cm	ε (conductivity), %
20	1.5271	0.9462	29.04
30	1.5294	0.9552	28.61
40	1.5302	0.9648	28.09
50	1.5321	0.9598	28.45
60	1.5348	0.9836	27.2

Table 7.9. INCO-Matte Separation Plant column 4. Gas holdup measurements using the gas holdup probe II. The column was run at normal operating conditions: Jg = 3.4 cm/s. Gas holdup was measured at 5 m from the lip of the column in the four quadrants of the baffled section.

First quadrant.

time, s	κ syphon, mS/cm	κ open, mS/cm	ε (conductivity), %
60	1.511	1.0318	23.65
120	1.51	1.0406	23.08
180	1.513	1.0279	23.95
240	1.512	1.0419	23.14
300	1.512	1.035	23.52

Second quadrant.

time, s	κ syphon, mS/cm	κ open, mS/cm	ε (conductivity), %
60	1.582	1.033	26.17
120	1.582	1.0772	23.81
180	1.583	1.051	25.26
240	1.584	1.0544	25.1
300	1.586	1.061	24.8

Third quadrant.

time, s	κ syphon, mS/cm	κ open, mS/cm	ε (conductivity), %
60	1.607	1.0963	23.71
120	1.607	1.0891	24.09
180	1.607	1.0971	23.67
240	1.606	1.0857	24.24
300	1.607	1.1068	23.18

Fourth quadrant.

time, s	κ syphon, mS/cm	κ open, mS/cm	ε (conductivity), %
60	1.615	1.1227	22.63
120	1.615	1.1155	23
180	1.614	1.1157	22.95

240	1.614	1.1203	22.72
300	1.614	1.0969	23.91

Table 7.10. INCO-Matte Separation Plant column 4. Gas holdup measurements under normal operating conditions. Probe II is placed in two positions in each quadrant, i.e. at 4.8 m from the lip of the column (inside the baffled section = in), and at 1.8 m from the lip of the column (above the baffles = out). Jg = 3.7 cm/s.

First quadrant.

time, s	κ syphon in, mS/cm	κ open in, mS/cm	ε (conduct.) in, %	κ syphon out, mS/cm	κ open out, mS/cm	ε (conduct.) out, %
60	1.806	1.1637	26.91	1.846	1.195	26.65
120	1.801	1.1749	26.22	1.845	1.1987	26.46
180	1.809	1.1681	26.79	1.844	1.1899	26.82
240	1.804	1.1632	26.88	1.847	1.1935	26.74
300	1.805	1.1356	28.21	1.85	1.2138	25.9

Second quadrant.

time, s	κ syphon in, mS/cm	κ open in, mS/cm	ε (conduct.) in, %	κ syphon out, mS/cm	κ open out, mS/cm	ε (conduct.) out, %
60	1.873	1.3399	20.98	1.899	1.2286	26.69
120	1.878	1.3247	21.8	1.884	1.2151	26.84
180	1.878	1.4045	18.35	1.883	1.2084	27.13
240	1.878	1.3251	21.78	1.881	1.1894	27.95
300	1.88	1.383	19.35	1.882	1.1888	27.99

Third quadrant.

time, s	κ syphon in, mS/cm	κ open in, mS/cm	ε (conduct.) in, %	κ syphon out, mS/cm	κ open out, mS/cm	ε (conduct.) out, %
60	1.912	1.376	20.62	1.923	1.2231	27.63
120	1.912	1.4022	19.51	1.927	1.2184	27.96
180	1.912	1.3858	20.2	1.933	1.2203	28.04

240	1.913	1.3979	19.72	1.929	1.2049	28.62
300	1.915	1.3754	20.73	1.93	1.2137	28.25

Fourth quadrant.

time, s	κ syphon in, mS/cm	κ open in, mS/cm	ε (conduct.) in, %	κ syphon out, mS/cm	κ open out, mS/cm	ε (conduct.) out, %
60	1.948	1.3676	22.05	1.95	1.2539	27.01
120	1.951	1.3829	21.51	1.946	1.2556	26.84
180	1.951	1.3735	21.9	1.954	1.2702	26.41
240	1.949	1.3664	22.15	1.95	1.2747	26.11
300	1.952	1.3775	21.76	1.948	1.2858	25.57

Table 7.11. INCO-Matte Separation Plant column 4. Gas holdup measurements under normal operating conditions. The gas holdup probe II was used in each quadrant at different depths. Jg = 3.7 cm/s.

First quadrant.

column depth, m	κ syphon, mS/cm	κ open, mS/cm	ε (conductivity), %
7.9	1.862	1.3349	20.85
7.3	1.864	1.308	22.09
6.7	1.859	1.3096	21.88
6	1.853	1.2591	23.94
5.4	1.845	1.2713	23.14
4.8	1.838	1.2351	24.57
4.2	1.833	1.2236	24.93
3.6	1.834	1.2201	25.15
3	1.821	1.1885	26.21
2.4	1.822	1.1738	26.93
1.8	1.818	1.1004	30.32
1.2	0.358	0.2407	froth

0.6	0.329	0.1491	froth
0	0.269	0.1293	froth

Second quadrant.

column depth, m	κ syphon, mS/cm	κ open, mS/cm	ε (conductivity), %
7.9	1.892	1.4503	16.89
7.3	1.882	1.3536	20.66
6.7	1.877	1.3122	21.91
6	1.868	1.2834	23.3
5.4	1.861	1.2813	23.19
4.8	1.858	1.2763	23.31
4.2	1.853	1.2565	24.05
3.6	1.852	1.2414	24.7
3	1.85	1.2418	24.62
2.4	1.845	1.1795	27.34
1.8	1.841	1.1391	29.13
1.2	1.841	0.7874	froth
0.6	0.334	0.1575	froth
0	0.294	0.1388	froth

Third quadrant.

column depth, m	κ syphon, mS/cm	κ open, mS/cm	ε (conductivity), %
7.9	1.942	1.4192	19.73
7.3	1.931	1.4384	18.59
6.7	1.924	1.3958	20.16
6	1.916	1.3917	20.09
5.4	1.903	1.3805	20.17
4.8	1.9	1.3338	22.07
4.2	1.895	1.3137	22.8
3.6	1.893	1.2858	23.96
3	1.888	1.2578	25.05

2.4	1.885	1.2171	26.79
1.8	1.882	1.1472	29.95
1.2	1.37	0.2223	froth
0.6	0.36	0.1509	froth
0	0.32	0.1337	froth

Fourth quadrant.

column depth, m	κ syphon, mS/cm	κ open, mS/cm	ε (conductivity), %
7.9	1.961	1.5207	16.18
7.3	1.966	1.4023	21.14
6.7	1.958	1.4483	19.01
6	1.954	1.3723	22.03
5.4	1.956	1.3992	20.96
4.8	1.946	1.3912	21
4.2	1.944	1.3395	23.15
3.6	1.944	1.3134	24.27
3	1.942	1.2836	25.49
2.4	1.94	1.2619	26.4
1.8	1.936	1.2232	28
1.2	1.942	0.5315	froth
0.6	0.384	0.1534	froth
0	0.29	0.1366	froth

IMAGE EVALUATION
TEST TARGET (QA-3)

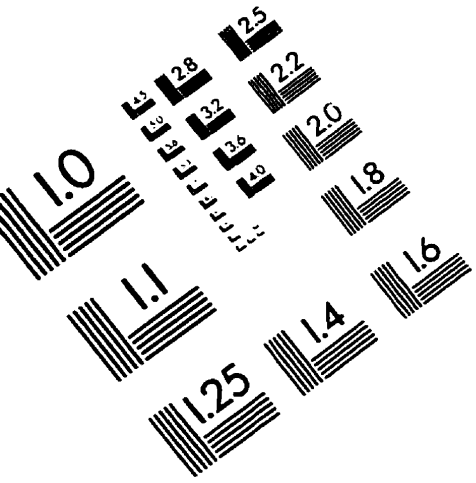

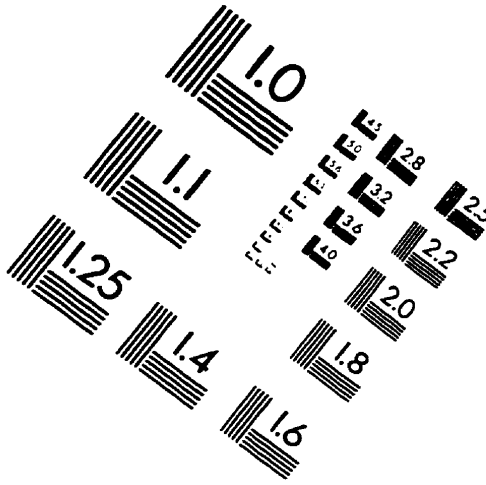

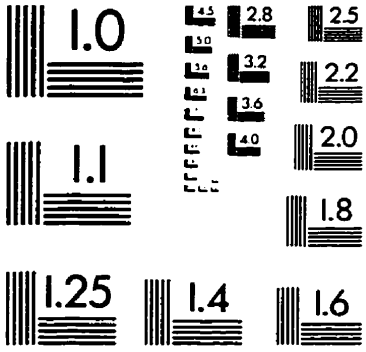

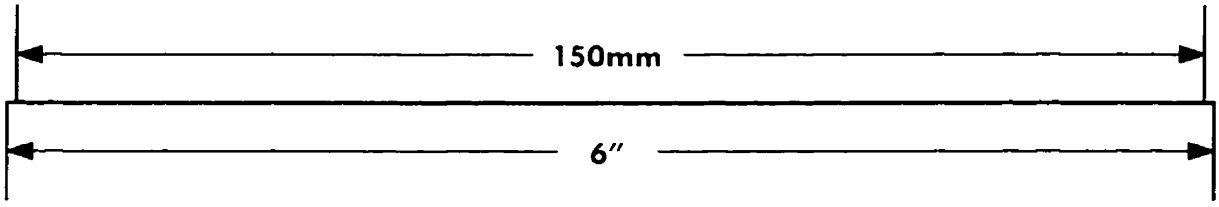

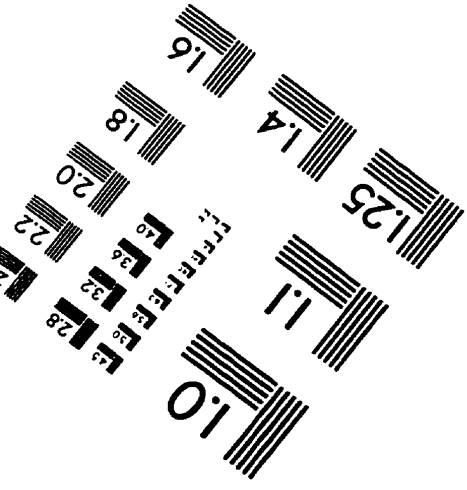

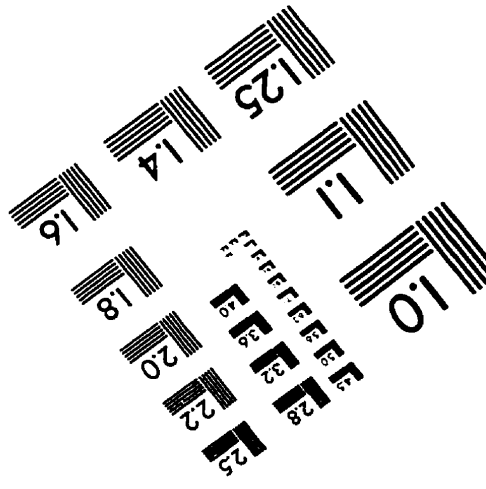

APPLIED IMAGE, Inc
1653 East Main Street
Rochester, NY 14609 USA
Phone: 716/482-0300
Fax: 716/288-5989